Akademia Górniczo-Hutnicza im. Stanisława Staszica w Krakowie

DZIEDZINA NAUK ŚCISŁYCH I PRZYRODNICZYCH

DYSCYPLINA NAUKI FIZYCZNE

ROZPRAWA DOKTORSKA

Zastosowanie nowoczesnych metod spektroskopowych do oceny wpływu diety ketogenicznej stosowanej w okresie ciąży na rozwój układu nerwowego potomstwa

Autor: Marzena Rugieł

Promotor rozprawy: dr hab. inż. Joanna Chwiej, prof. AGH
Drugi promotor: prof. dr hab. Zuzanna Setkowicz-Janeczko

Praca wykonana:
Akademia Górniczo-Hutnicza im. Stanisława Staszica w Krakowie
Wydział Fizyki i Informatyki Stosowanej
Katedra Fizyki Medycznej i Biofizyki

Kraków, Maj 2026

Oświadczenie autora rozprawy:

Oświadczam, świadom odpowiedzialności karnej za poświadczenie nieprawdy, że niniejszą pracę doktorską wykonałam osobiście i samodzielnie i nie korzystałam ze źródeł innych niż wymienione w pracy.

data, podpis autora

Oświadczenie promotorów rozprawy:

Niniejsza rozprawa jest gotowa do oceny przez recenzentów.

data, podpis pierwszego promotora rozprawy

data, podpis drugiego promotora rozprawy

Niniejsza praca została częściowo sfinansowana przez: (1) Ministerstwo Nauki i Szkolnictwa Wyższego, (2) fundusz badań statutowych nr N18/DBS/000018 Pracowni Neuropatologii Doświadczalnej Instytutu Zoologii i Badań Biomedycznych Uniwersytetu Jagiellońskiego oraz (3) ze środków przyznanych Akademii Górniczo-Hutniczej w Krakowie na realizację projektu „Inicjatywa Doskonałości – Uczelnia Badawcza" (Działanie 4: System grantów uczelnianych na prace badawcze realizowane z udziałem doktorantów, PL-Joanna Chwiej; Minigrant dla młodych naukowców i doktorantów, Marzena Rugieł).

Zaprezentowane wyniki uzyskano z wykorzystaniem mikroskopu ramanowskiego WITec Alpha300R zakupionego w ramach projektu „Inicjatywa Doskonałości – Uczelnia Badawcza" przyznanego Akademii Górniczo-Hutniczej w Krakowie.

Składam serdeczne podziękowania za przyznane stypendium, które umożliwiło mi realizację badań oraz rozwój naukowy w trakcie studiów doktoranckich, dzięki wsparciu finansowemu Narodowego Centrum Nauki w ramach projektu nr UMO-2020/38/E/ST4/00197.

Pragnę serdeczne podziękować Pani dr hab. inż. Joannie Chwiej za szansę podjęcia interdyscyplinarnych studiów doktoranckich oraz za otoczenie mnie opieką naukową. Jestem ogromnie wdzięczna za Pani gotowość do dzielenia się rozległą wiedzą – zarówno merytoryczną, jak i tą wynikającą z życiowego doświadczenia. Dziękuję również za możliwość uczestniczenia w ciekawych projektach naukowych, konferencjach i stażach, dzięki którym mogłam się rozwijać. Doceniam czas, który poświęciła Pani na wspólne planowanie badań oraz rozmowy o ich wynikach. Dziękuję też za nieustanne wsparcie, zrozumienie, życzliwość i wszystkie dobre słowa, które dodawały mi motywacji na każdym etapie pracy.

Chciałabym podziękować Pani prof. Zuzannie Setkowicz-Janeczko za umożliwienie mi podjęcia interdyscyplinarnej tematyki badań oraz za wprowadzenie mnie w praktyczny wymiar pracy naukowej od strony biologicznej. Jestem wdzięczna za czas poświęcony na realizację kluczowych etapów badań, a także za Pani zaangażowanie i wsparcie. Doceniam wszystkie cenne uwagi dotyczące uzyskiwanych wyników oraz życzliwą, sprzyjającą współpracy atmosferę.

Bardzo dziękuję Pani dr hab. Katarzynie Marzec, za możliwość udziału w projekcie naukowym, który poszerzył moje naukowe horyzonty, za dzielenie się wiedzą i doświadczeniem.

Podziękowania kieruję również do dr inż. Agnieszki Dróżdż za dyskusje dotyczące prowadzonych badań oraz ich wyników.

Dziękuję również Pani dr inż. Katarzynie Matusiak za życzliwość oraz miłą atmosferę pracy.

Dziękuję mgr Kamilowi Kawoniowi za liczne rozmowy o nauce i życiu, wspólne rozpracowywanie działania mikroskopów, pomoc w zrozumieniu biologicznych aspektów uzyskanych wyników, za wspólne przejście przez studia i wspólnie spędzony czas.

Pragnę podziękować pracownikom linii FLUO synchrotronu KARA za przeprowadzenie pomiarów. Szczególne podziękowania kieruję do dr inż. Mateusza Czyżyckiego za zaangażowanie w prowadzone badania oraz udzieloną pomoc i wartościowe wskazówki.

Dziękuję również mgr Wojciechowi Kośkowi i mgr Zuzannie Rauk za wsparcie w opiece nad zwierzętami.

Chciałabym podziękować również mgr Aleksandrze Wilk za liczne dyskusje nie tylko o nauce i za wspólnie spędzony czas.

Dziękuję również mgr Marioli Kukule za czas spędzony wspólnie na pomiarach mikroskopowych i konferencji, za liczne rozmowy i śmiech, dzięki którym czas na analizowaniu wyników upływał szybciej i w miłej atmosferze.

Dziękuję dr Karolinie Olbrich, dr Natalii Janik-Olchawie, mgr Mateuszowi Gala, dr Annie Ryś, dr Natalii Wilkosz, dr Marcie Sałudze i dr Katarzynie Bułat - za liczne rozmowy, wsparcie oraz tworzenie życzliwej i przyjaznej atmosfery zarówno na Uczelni, jak i poza nią. Składam także podziękowania wszystkim pracownikom i doktorantom Katedry Fizyki Medycznej i Biofizyki za życzliwość oraz pomoc okazywaną w trakcie realizacji studiów doktoranckich.

Chciałabym serdecznie podziękować mojej Rodzinie, Bliskim i Przyjaciołom, za wsparcie w realizacji doktoratu, słowa otuchy w chwili zwątpienia i za liczne pytania i zainteresowanie prowadzonymi przeze mnie badaniami.

Spis treści

1. Streszczenie

Leczenie padaczki u kobiet ciężarnych stanowi istotne wyzwanie kliniczne, przede wszystkim ze względu na teratogenne działanie większości leków przeciwpadaczkowych, które mogą niekorzystnie wpływać na rozwój układu nerwowego płodu. W związku z brakiem terapii całkowicie bezpiecznych w okresie ciąży, prowadzone są intensywne badania nad alternatywnymi strategiami terapeutycznymi, w tym nad wykorzystaniem diety ketogenicznej (KD), która wykazuje wysoką skuteczność w leczeniu padaczki lekoopornej u dzieci i dorosłych.

W ramach badań realizowanych w niniejszej rozprawie doktorskiej zastosowano nowoczesne techniki spektroskopowe, takie jak mikrospektroskopia w podczerwieni z transformacją Fouriera (FTIRM), mikroskopia Ramana (RM) oraz mikroskopia fluorescencji rentgenowskiej ze wzbudzeniem promieniowaniem synchrotronowym (micro-SR-XRF), w celu oceny anomalii biomolekularnych w ośrodkowym układzie nerwowym potomstwa samic poddanych KD w czasie ciąży. Analizy przeprowadzono w 2., 6., 14., 30. i 60. dniu życia postnatalnego zwierząt. Dla każdej z zastosowanych metod instrumentalnych opracowano optymalne procedury przygotowania próbek oraz zoptymalizowano warunki pomiarowe, umożliwiające minimalizację niepożądanych zjawisk fizycznych wpływających na jakość uzyskiwanych danych.

Badania techniką FTIRM wykazały, że w mózgach 14-dniowego potomstwa płci męskiej wzrasta względna zawartość związków zawierających grupy karbonylowe w korze mózgowej oraz warstwach komórkowych formacji hipokampa, a także spada zawartość lipidów i zmienia się ich struktura w istocie białej. Ponadto powierzchnia torebki wewnętrznej (obszar istoty białej) była istotnie mniejsza w porównaniu do grupy kontrolnej. U 60-dniowych samców prenatalnie eksponowanych na KD stwierdzono dalsze obniżenie parametrów biochemicznych związanych z lipidami, co może świadczyć o zaburzeniach metabolizmu lipidów, funkcji oligodendrocytów lub procesów mielinizacji.

Dodatkowo w obszarach formacji hipokampa i kory mózgowej tej grupy zwierząt wykryto wtrącenia bogate w kreatynę i cholesterol, potwierdzone w badaniach ramanowskich. Analiza ilościowa wykazała istotny wzrost powierzchni wtrąceń cholesterolowych w grupie ketogenicznej, podczas gdy dla kreatyny zaobserwowano trend wzrostowy. Może to odzwierciedlać niekorzystne skutki zmienionego metabolizmu energetycznego i/lub mechanizmy neuroadaptacyjne. W przeciwieństwie do samców, potomstwo płci żeńskiej nie wykazywało długofalowych zmian biochemicznych w mózgu, co może być związane z protekcyjnym działaniem estrogenów regulujących metabolizm kreatyny, funkcje mitochondrialne oraz homeostazę lipidową.

Topograficzna analiza pierwiastkowa przeprowadzona techniką micro-SR-XRF dla 30- i 60-dniowego potomstwa płci męskiej wykazała zmniejszenie powierzchni obszarów mózgu o podwyższonej zawartości fosforu i siarki, odpowiadających strukturom istoty białej, co wskazuje na zaburzenia struktury i integralności mieliny. Wyniki te są spójne z obserwacjami uzyskanymi wcześniej przy użyciu FTIRM.

Podsumowując, zastosowane techniki spektroskopowe umożliwiły szczegółową ocenę składu biochemicznego i pierwiastkowego mózgu potomstwa matek karmionych dietą standardową i ketogeniczną, wskazując na potencjalny, zależny od wieku i płci, wpływ KD stosowanej w ciąży na rozwój ośrodkowego układu nerwowego.

2. Abstract

The treatment of epilepsy in pregnant women represents a major clinical challenge, primarily due to the teratogenic effects of most antiepileptic drugs, which may adversely affect fetal nervous system development. In the absence of therapies that are fully safe during pregnancy, intensive research is being conducted on alternative treatment strategies, including the ketogenic diet (KD), which has demonstrated high efficacy in the management of drug-resistant epilepsy in both children and adults.

This doctoral dissertation employed advanced spectroscopic techniques—Fourier-transform infrared microspectroscopy (FTIRM), Raman microscopy (RM), and synchrotron radiation based X-ray fluorescence microscopy (micro-SR-XRF)—to evaluate biomolecular alterations in the central nervous system of offspring born to females maintained on a KD during pregnancy. Analyses were performed on postnatal days 2, 6, 14, 30, and 60. For each analytical method, optimized sample preparation protocols and measurement conditions were developed to minimize physical artifacts and ensure high data quality.

FTIRM analysis revealed an increased relative abundance of carbonyl-containing compounds in the cerebral cortex and hippocampal cell layers of 14-day-old male offspring, accompanied by a reduction in lipid content and alterations in lipid structure within the white matter. In addition, the area of the internal capsule was significantly reduced compared to controls. In 60-day-old males prenatally exposed to KD, further decreases in lipid-related biochemical parameters were observed, suggesting impairments in lipid metabolism, oligodendrocyte function, or myelination processes.

Additionally, in the hippocampal and cortical regions of this group of animals, inclusions rich in creatine and cholesterol were detected and confirmed by Raman spectroscopy. Quantitative analysis demonstrated a significant increase in the area of cholesterol inclusions in the ketogenic group, while an increasing trend was observed for creatine. This may reflect adverse effects of altered energy metabolism and/or neuroadaptive mechanisms. In contrast to males, female offspring did not exhibit long-term biochemical changes in the brain, which may be related to the protective effects of estrogens regulating creatine metabolism, mitochondrial function, and lipid homeostasis.

Elemental mapping using micro-SR-XRF in 30- and 60-day-old male offspring demonstrated a reduction in the area of brain regions with elevated phosphorus and sulfur levels corresponding to white matter structures, indicating compromised myelin integrity. These findings are consistent with FTIRM results.

In conclusion, the applied spectroscopic approaches enabled a comprehensive biochemical and elemental characterization of the brains of offspring from mothers fed standard and ketogenic diets, revealing a potential age- and sex-dependent impact of maternal KD during pregnancy on central nervous system development.

3. Układ rozprawy

Na rozprawę doktorską składają się dwa opublikowane artykuły naukowe [A1,A2] oraz jeden manuskrypt [M1], który w momencie złożenia pracy znajduje się w recenzji w czasopiśmie ACS Chemical Neuroscience (po pierwszej recenzji i po rewizji manuskryptu zgodnie z zaleceniami recenzentów). Prace poświęcone są zastosowaniu nowoczesnych metod spektroskopowych do oceny składu biochemicznego i pierwiastkowego mózgu w modelu biologicznym służącym do badania wpływu diety ketogenicznej stosowanej w okresie ciąży na rozwój układu nerwowego potomstwa.

A1. Marzena Rugiel, Zuzanna Setkowicz-Janeczko, Wojciech Kosiek, Zuzanna Rauk, Kamil Kawon, Joanna Chwiej, *Does Ketogenic Diet Used in Pregnancy Affect the Nervous System Development in Offspring? - FTIR Microspectroscopy Study*, ACS Chem Neurosci 14 (2023) 2775–2791.

A2. Marzena Rugieł, Zuzanna Setkowicz, Mateusz Czyzycki, Rolf Simon, Tilo Baumbach, Joanna Chwiej, *Element Changes Occurring in Brain Point at the White Matter Abnormalities in Rats Exposed to the Ketogenic Diet During Prenatal Life*, ACS Chem Neurosci 15 (2024) 3932-3944.

M1. Marzena Rugiel, Zuzanna Setkowicz, Agnieszka Drozdz, Aleksandra Wilk, Zofia Brylowska, Joanna Chwiej, *Fourier Transform Infrared Imaging Supported by Raman Spectroscopy Reveals Biochemical Changes in Adult Rat Brains Following Prenatal Exposure to a Ketogenic Diet*, (w recenzji w czasopismie ACS Chemical Neuroscience).

4. Wprowadzenie

Leczenie pacjentek w ciąży, cierpiących na padaczkę jest szczególnie trudne, ponieważ większość dostępnych leków przeciwdrgawkowych ma działanie teratogenne. Ich stosowanie w krytycznych fazach rozwoju płodu może prowadzić do przemijających lub długotrwałych działań niepożądanych ze strony układu nerwowego potomstwa, obejmujących anomalie anatomiczne i behawioralne [1,2]. Ze względu na brak bezpiecznych dla kobiet w ciąży leków przeciwpadaczkowych, trwają poszukiwania nowych środków farmakologicznych i alternatywnych terapii, które przyniosą korzyści zarówno matce, jak i będą bezpieczne dla potomstwa. Jedną z możliwości może być zastosowanie diety ketogenicznej (ang. *ketogenic diet*, KD), która jest z powodzeniem stosowana w leczeniu różnych rodzajów padaczki (w tym padaczki lekoopornej) u niemowląt, dzieci i dorosłych [3–5].

KD charakteryzuje się wysokim spożyciem tłuszczu, umiarkowaną ilością białka oraz znacznym ograniczeniem węglowodanów, co prowadzi do istotnej zmiany metabolizmu energetycznego i wykorzystania ciał ketonowych zamiast glukozy jako podstawowego źródła energii [4,6]. W warunkach niskiego spożycia węglowodanów organizm pozyskuje energię głównie z utleniania kwasów tłuszczowych, czego efektem jest zwiększona produkcja acetylo-CoA – kluczowego substratu ketogenezy zachodzącej w wątrobie. W procesie tym powstaje kwas acetooctowy, który może następnie ulegać spontanicznej dekarboksylacji do acetonu lub enzymatycznej redukcji do β-hydroksymaślanu (BHB) [7]. Wzmożona produkcja ciał ketonowych (BHB, acetooctanu i acetonu) prowadzi do stanu ketozy, charakteryzującego się podwyższonym stężeniem tych związków w organizmie. Ciała ketonowe są transportowane z krwią do tkanek obwodowych, w tym do mózgu, gdzie przenikają przez barierę krew–mózg za pośrednictwem transporterów monokarboksylanów. Dzięki temu mogą stanowić alternatywne źródło energii dla komórek nerwowych, zwłaszcza w warunkach ograniczonej dostępności glukozy [8,9]. Co więcej, ze względu na wysoką efektywność energetyczną stanowią nawet bardziej wydajne źródło energii niż glukoza, a ich obecność zwiększa stosunek ATP/ADP oraz rezerwy energetyczne mózgu [10–12].

Odżywianie matki w okresie ciąży ma istotny wpływ na rozwój oraz zdrowie płodu zarówno po urodzeniu, jak i w wieku dorosłym, gdyż wpływa na to co i w jakiej ilości przenika przez łożysko [13,14]. Jest ono związane z indukowaniem zmian epigenetycznych u płodu oraz z procesami programowania metabolicznego, które mogą determinować funkcjonowanie organizmu na późniejszych etapach życia [13,15,16]. Z tego względu kluczowe jest określenie bezpieczeństwa stosowania różnych modeli żywieniowych w kontekście prawidłowego rozwoju płodu. Badania kliniczne dotyczące stosowania KD w czasie ciąży u ludzi są bardzo ograniczone. Dostępna literatura obejmuje głównie opisy pojedynczych przypadków klinicznych [17,18] oraz prace przeglądowe i analizy obserwacyjne, najczęściej rozpatrujące KD w szerszym kontekście diet o ograniczonej podaży węglowodanów u kobiet ciężarnych [13].

Badania na modelach zwierzęcych wskazują na potencjalny wpływ KD stosowanej w okresie prenatalnym na rozwój potomstwa, chociaż wyniki te nie są spójne. Prenatalna ekspozycja na KD u gryzoni wykazuje wieloaspektowe skutki, obejmujące zarówno zmiany neuroanatomiczne, jak i funkcjonalne [19–21]. Stwierdzono m.in. względne zmniejszenie objętości kory mózgowej, formacji hipokampa, ciała modzelowatego, strzępków i komór bocznych, przy jednoczesnym względnym zwiększeniu objętości podwzgórza i rdzenia przedłużonego, co sugeruje zróżnicowaną preferencję wykorzystania ketonów jako źródła energii w rozwoju prenatalnym przez różne rejony mózgu [21]. Ponadto KD wiąże się ze zmniejszonym spożyciem białka, co w modelach zwierzęcych powoduje trwałe lub odwracalne zmiany anatomiczne i funkcjonalne mózgu potomstwa oraz opóźnienia w pojawianiu się odruchów [22,23]. Wyniki te wskazują, że efekty KD mogą być modulowane zarówno przez dostępność makroskładników, jak i przez mechanizmy metaboliczne związane z transportem składników odżywczych przez łożysko oraz regionalne różnice w metabolizmie energetycznym rozwijającego się mózgu. Niektóre badania donoszą, że ekspozycja na dietę wysokotłuszczową ograniczona do okresu ciąży może mieć korzystny wpływ na zdrowie mózgu potomstwa w późniejszym życiu, obejmujący poprawę uczenia

się i pamięci oraz zmniejszenie nasilenia markerów neurodegeneracji. Wyniki te podkreślają, że wpływ diety matki ma charakter zależny od kontekstu i może różnić się w zależności od czasu ekspozycji, składu diety oraz płci potomstwa [24]. Rozbieżności obserwowane w literaturze, dotyczące m.in. masy ciała, struktury mózgu oraz parametrów rozwoju neurologicznego potomstwa, podkreślają konieczność dalszych badań nad mechanizmami molekularnymi i metabolicznymi odpowiedzialnymi za wpływ KD na rozwój ośrodkowego układu nerwowego.

Współczesne badania biologiczne i biomedyczne coraz częściej wykorzystują metody analityczne pozwalające na szybką, nieinwazyjną i wieloparametryczną charakteryzację próbek biologicznych. Wśród nich szczególne miejsce zajmują metody spektroskopii wibracyjnej, które umożliwiają uzyskanie informacji o składzie biochemicznym, strukturze molekularnej oraz zmianach konformacyjnych biomolekuł bez konieczności stosowania znaczników czy skomplikowanej preparatyki próbki. Najważniejsze z nich to spektroskopia w podczerwieni z transformacją Fouriera (ang. *Fourier transform infrared spectroscopy*, FTIRS) oraz spektroskopia ramanowska (ang. *Raman spectroscopy*, RS), w których oddziaływanie promieniowania elektromagnetycznego z molekułami w próbce pozwala na uzyskanie widm oscylacyjnych, które dostarczają informacji o strukturze chemicznej badanego materiału. Obie techniki mogą być zintegrowane z mikroskopią optyczną (mikrospektroskopia FTIR oraz mikroskopia ramanowska), co umożliwia jednoczesne uzyskanie informacji morfologicznej i chemicznej na temat analizowanego materiału. Takie połączenie pozwala na selektywną analizę mikroobszarów próbki, zwiększając rozdzielczość przestrzenną oraz umożliwiając mapowanie zmian biochemicznych w obrębie pojedynczych komórek i struktur tkankowych.

Mikrospektroskopia FTIR (FTIRM) jest techniką analityczną opartą na absorpcji promieniowania podczerwonego przez drgające wiązania chemiczne w cząsteczkach. Zjawisko zachodzi wtedy, gdy energia padającego na próbkę promieniowania podczerwonego odpowiada energii drgań wiązań chemicznych obecnych w cząsteczkach. Ponieważ różne grupy funkcyjne zawierają charakterystyczne układy wiązań chemicznych, absorbują promieniowanie w specyficznych zakresach liczby falowej. Dzięki temu widmo FTIR dostarcza informacji o obecności określonych grup funkcyjnych i składzie chemicznym próbki, tworząc jej unikalny „odcisk palca" (fingerprint). W podczerwieni widoczne są te drgania, dla których w wyniku pochłonięcia energii zachodzą zmiany momentu dipolowego wiązania lub grupy atomów [25]. Dlatego też w widmach absorpcyjnych z zakresu podczerwieni intensywne są pasma pochodzące od drgań grup polarnych (np. OH, NH, >C=O).

W próbkach biologicznych szczególne znaczenie ma pasmo amidu I (1600-1690 cm^{-1}), związane głównie z drganiami rozciągającymi wiązania C=O w grupach amidowych (wiązaniach peptydowych) białek i stanowiące czuły marker ich konformacji. Informacje dotyczące struktury drugorzędowej białek uzyskuje się, na przykład, poprzez analizę pasm przypisywanych α-helisie (~1658 cm^{-1}) oraz β-kartce (~1635 cm^{-1}) [26,27]. Istotny wkład do widma w zakresie 2800-3050 cm^{-1} wnoszą drgania rozciągające wiązań C–H w grupach $–CH_2$ i $–CH_3$, obecnych w wielu biomolekułach, jednak dominująco pochodzących od lipidów [28,29]. W obrębie tego zakresu pasma ~2955 cm^{-1} i ~2924 cm^{-1} są przypisywane nasyconym kwasom tłuszczowym. Z kolei pasmo około 3012 cm^{-1} przypisywane jest drganiom rozciągającym =C–H, charakterystycznym dla nienasyconych kwasów tłuszczowych, co umożliwia ocenę stopnia nienasycenia lipidów [28]. W widmach obserwuje się również pasma związane z obecnością grup fosforanowych (~1080 oraz 1240 cm^{-1}), wynikające z drgań odpowiednio symetrycznych i asymetrycznych wiązań $–PO^{2-}$, charakterystycznych dla kwasów nukleinowych oraz fosfolipidów [28,29]. Pasmo w okolicy ~1740 cm^{-1} związane jest z drganiami rozciągającymi wiązania C=O w związkach zawierających grupy karbonylowe, przy czym w materiałach biologicznych dominujący wkład w tym zakresie pochodzi od grup estrowych lipidów, takich jak triglicerydy, fosfolipidy oraz estry cholesterolu [30,31]. Należy jednak podkreślić, że przypisanie pasm w widmach tkanek biologicznych ma charakter przybliżony, ponieważ obserwowane sygnały stanowią superpozycję wkładów pochodzących od różnych grup funkcyjnych obecnych w wielu klasach biomolekuł.

Do głównych zalet FTIRS należą: krótki czas akwizycji widma wynikający z jednoczesnej rejestracji całego zakresu liczb falowych (tzw. przewaga Fellgetta, efekt multiplexowy), co prowadzi do poprawy stosunku sygnału do szumu w porównaniu do metod dyspersyjnych [32,33]. Dodatkowo zastosowanie interferometru Michelsone'a zapewnia wysoką przepuszczalność układu optycznego (tzw. przewaga Jacquinota, efekt throughput), wynikającą z braku szczelin ograniczających natężenie promieniowania, co przekłada się na większą czułość pomiaru [32,33]. Kolejną zaletą jest wysoka dokładność wyznaczania liczb falowych (przewaga Connesa), wynikająca z zastosowania stabilnego lasera referencyjnego do kontroli przesunięcia zwierciadła interferometru [32]. FTIRS nie wymaga znakowania próbek, umożliwia analizę materiałów w różnych stanach skupienia (ciała stałe, ciecze oraz próbki półstałe), a także charakteryzuje się niewielkimi wymaganiami dotyczącymi przygotowania próbek [34–36]. Dodatkowo pozwala na jednoczesne uzyskanie informacji jakościowej oraz półilościowej dotyczącej składu chemicznego badanych materiałów i cechuje się wysoką powtarzalnością pomiarów [35–37]. Wadami tej techniki są m.in. silna absorpcja wody w zakresie średniej podczerwieni oraz ograniczona dyfrakcyjnie rozdzielczość przestrzenna (w porównaniu z technikami ramanowskimi) [38–40]. W FTIRM materiałów biologicznych rejestrowane widma mogą ulegać zniekształceniom na skutek efektów fizycznych związanych z oddziaływaniem promieniowania z heterogeniczną strukturą próbki. Szczególne znaczenie ma rozproszenie Mie'go oraz jego rezonansowa forma (RMieS), wynikające z porównywalności długości fali promieniowania podczerwonego i rozmiarów struktur komórkowych, co prowadzi m.in. do zaburzeń linii bazowej oraz zmian kształtu i położenia pasm, zwłaszcza pasma amidu I [41–43]. Dodatkowo w pomiarach transfleksyjnych może występować efekt fali stojącej pola elektrycznego, związany z interferencją promieniowania odbitego od podłoża i niejednorodności próbki, powodujący odstępstwa od prawa Lamberta-Beera [44]. Niezależnie od tych efektów interpretację widm utrudnia również nakładanie się pasm absorpcyjnych pochodzących od różnych grup funkcyjnych obecnych w złożonych układach biologicznych [39].

Mikroskopia ramanowska (RM) opiera się na zjawisku nieelastycznego rozpraszania światła, znanego jako efekt Ramana [45,46]. W wyniku oddziaływania monochromatycznego promieniowania (najczęściej laserowego) z cząsteczką dochodzi do zmiany energii fotonów, odpowiadającej energiom drgań molekularnych. W widmie ramanowskim rejestrowane są przesunięcia ramanowskie, odpowiadające różnicy energii pomiędzy promieniowaniem padającym a rozproszonym [45,46]. Intensywność pasm zależy od zmian polaryzowalności cząsteczki podczas drgań [47]. W widmach Ramana intensywne są pasma drgań niepolarnych ugrupowań homojądrowych (C=C, N–N, S–S). Podobnie jak w FTIRM w materiałach biologicznych RM umożliwia identyfikację składu chemicznego badanych materiałów (w tym detekcję białek, lipidów, kwasów nukleinowych i metabolitów komórkowych), oraz analizę ich struktury molekularnej [46]. Technika ta charakteryzuje się wysoką selektywnością chemiczną wynikającą z czułości na drgania cząsteczkowe, szczególnie związane z wiązaniami niepolarnymi i symetrycznymi [47]. Istotną zaletą RM jest możliwość prowadzenia pomiarów z wysoką rozdzielczością przestrzenną (poniżej 1 μm), co pozwala na analizę mikro- i nanoskali obszarów próbki [47,48]. Dodatkowo, dzięki zastosowaniu konfiguracji konfokalnej, możliwe jest uzyskiwanie informacji przestrzennych nie tylko w dwóch wymiarach (mapowanie powierzchni), ale również w trzecim wymiarze (profilowanie głębokości) [47,49]. Technika ta umożliwia pomiary w środowisku wodnym oraz nie wymaga skomplikowanego przygotowania próbek ani ich znakowania, co czyni ją metodą nieniszczącą i potencjalnie *in vivo* [49,50]. Do ograniczeń RM należy natomiast niska wydajność procesu rozpraszania (słaby sygnał), możliwość występowania fluorescencji maskującej widmo oraz ryzyko lokalnego przegrzewania próbki w wyniku absorpcji promieniowania laserowego [46,51,52]. Dodatkowym ograniczeniem jest stosunkowo długi czas akwizycji danych, co sprawia, że technika ta jest mniej efektywna w przypadku szybkiego mapowania dużych obszarów i jest szczególnie przydatna do analizy małych, wybranych fragmentów próbki [53].

FTIRM i RM dostarczają informacji o tych samych drganiach molekularnych, jednak opierają się na różnych mechanizmach fizycznych i regułach wyboru. W konsekwencji

niektóre drgania cząsteczki są silnie aktywne w podczerwieni, ale słabe w widmie ramanowskim i odwrotnie. W badaniach komórek i tkanek połączenie obu metod umożliwia jednoczesną analizę zmian w białkach, lipidach i kwasach nukleinowych, co ma istotne znaczenie w badaniach z wykorzystaniem materiału biologicznego. Komplementarne zastosowanie obu technik zwiększa wiarygodność interpretacji danych, umożliwia pełniejszą charakterystykę chemiczną próbki, pozwala na lepsze rozróżnianie zmian patologicznych w tkankach i zwiększa czułość diagnostyczną w badaniach biomedycznych.

Oprócz analizy zmian w zakresie składu i struktury biomolekuł, które można badać za pomocą technik wibracyjnych takich jak FTIRM czy RM, bardzo istotne jest także określenie składu pierwiastkowego badanych próbek. W tym kontekście szczególnie przydatna jest metoda fluorescencji rentgenowskiej (ang. *X-ray fluorescence*, XRF), należąca do grupy technik analizy pierwiastkowej i umożliwiająca szybkie jakościowe oraz ilościowe oznaczanie pierwiastków w materiale biologicznym [54]. Metoda ta opiera się na zjawisku fluorescencji rentgenowskiej, polegającym na emisji charakterystycznego promieniowania wtórnego przez atomy wzbudzone promieniowaniem pierwotnym [54,55]. Gdy próbka zostaje naświetlona promieniowaniem rentgenowskim o energii przewyższającej energię wiązania elektronów na wewnętrznych powłokach atomowych, może dojść do wybicia elektronu i powstania wakansu elektronowego [56]. Stan ten jest nietrwały, dlatego atom dąży do jego zapełnienia poprzez przejście elektronu z wyższego poziomu energetycznego na niższy, czemu może towarzyszyć emisja fotonu promieniowania rentgenowskiego o energii charakterystycznej dla danego pierwiastka [55,57]. Widmo XRF przedstawia rozkład intensywności emitowanego promieniowania rentgenowskiego w funkcji energii fotonów. Położenie charakterystycznych pików emisyjnych umożliwia identyfikację pierwiastków obecnych w próbce, natomiast ich intensywność stanowi podstawę do oceny ich względnej lub bezwzględnej zawartości [55,57].

Jedną z odmian metody XRF jest technika synchrotronowej fluorescencji rentgenowskiej (ang. *synchrotron X-ray fluorescence*, SR-XRF) wykorzystująca promieniowanie synchrotronowe jako źródło promieniowania wzbudzającego. Promieniowanie takie stanowi wyjątkowo korzystne źródło wzbudzenia w spektroskopii i mikroskopii XRF ze względu na swoją bardzo wysoką jasność, dużą intensywność, szeroki i ciągły zakres energii oraz bardzo małą naturalną rozbieżność wiązki [58–60]. Właściwości te umożliwiają precyzyjny dobór energii promieniowania wzbudzającego do krawędzi absorpcji analizowanych pierwiastków i zwiększenie wydajności wzbudzenia fluorescencji oraz ograniczenie wpływu sygnału tła. Dodatkowo, wysoka stabilność i naturalna kolimacja wiązki pozwalają na jej skuteczne ogniskowanie do rozmiarów mikro- lub nanometrowych z wykorzystaniem nowoczesnych układów optycznych, takich jak soczewki refrakcyjne czy zwierciadła Kirkpatricka–Baez'a [54,58,61]. Dzięki temu SR-XRF umożliwia prowadzenie nieniszczącej, dwuwymiarowej analizy wielopierwiastkowej z bardzo wysoką czułością oraz rozdzielczością przestrzenną [62–64]. Metoda ta jest szczególnie przydatna do oznaczania pierwiastków śladowych i śledzenia ich lokalnego rozmieszczenia w materiale biologicznym [63,64]. Dodatkowymi zaletami SR-XRF są krótki czas pomiaru, brak konieczności stosowania znaczników chemicznych oraz stosunkowo proste przygotowanie próbek [63,64]. W wariancie mikroskopii SR-XRF (micro-SR-XRF) możliwa jest szczegółowa analiza niewielkich obszarów, pojedynczych komórek, a nawet struktur subkomórkowych, co czyni tę technikę niezwykle użytecznym narzędziem do badań przestrzennego rozmieszczenia, akumulacji i transportu pierwiastków w układach biologicznych [65]. Do ograniczeń tej metody należy mniejsza czułość dla pierwiastków lekkich, potrzeba odpowiedniego przygotowania próbki w przypadku próbek wilgotnych lub bardzo nieregularnych, a także jej ograniczona dostępność oraz wysokie koszty sprzętu i jego utrzymania, który wymaga stosowania promieniowania rentgenowskiego, co wiąże się z koniecznością przestrzegania procedur bezpieczeństwa [63,66].

Zastosowanie w pracy doktorskiej zarówno technik opartych na spektroskopii wibracyjnej, jak i micro-SR-XRF pozwala na uzyskanie komplementarnych informacji o badanym materiale biologicznym. FTIRM i RM umożliwia ocenę składu biochemicznego, organizacji molekularnej oraz zmian strukturalnych zachodzących w tkankach na poziomie biomolekuł, takich jak białka, lipidy, kwasy nukleinowe czy metabolity. Z kolei micro-SR-

XRF dostarcza informacji o jakościowym i ilościowym składzie pierwiastkowym oraz przestrzennym rozmieszczeniu pierwiastków, w tym biopierwiastków i metali śladowych, których obecność może zmieniać się na skutek przebieg procesów fizjologicznych oraz patologicznych i wpływać na funkcjonowanie komórek, tkanek i całego organizmu.

Połączenie tych metod umożliwia kompleksową charakterystykę badanych próbek, obejmującą zarówno poziom molekularny, jak i pierwiastkowy. Takie podejście pozwala nie tylko na dokładniejszą interpretację obserwowanych zmian biochemicznych i strukturalnych, ale również na identyfikację potencjalnych zależności pomiędzy składem pierwiastkowym a właściwościami biomolekularnymi tkanek. W kontekście niniejszej pracy doktorskiej zastosowanie komplementarnych technik spektroskopowych znacząco zwiększa wartość poznawczą prowadzonych badań, umożliwiając bardziej wszechstronną ocenę wpływu KD stosowanej w okresie ciąży na rozwój układu nerwowego potomstwa.

5. Cele i zakres pracy

Głównym celem badań prowadzonych w ramach niniejszej rozprawy doktorskiej była ocena wpływu KD stosowanej w okresie ciąży na rozwój układu nerwowego potomstwa. Analizę przeprowadzono poprzez ocenę różnic w składzie biochemicznym i pierwiastkowym mózgu zwierząt, których matki w czasie ciąży były karmione KD, w porównaniu z potomstwem pochodzącym z grupy kontrolnej. W badaniach zastosowano nowoczesne metody instrumentalne, takie jak FTIRM, RM oraz micro-SR-XRF.

W ramach pracy sformułowano następujące szczegółowe cele badawcze:

1. Optymalizacja warunków pomiarowych oraz identyfikacja czynników mogących wpływać na jakość i wiarygodność wyników uzyskiwanych z zastosowaniem wybranych technik spektroskopowych w analizowanym modelu badawczym, obejmujących FTIRM, RM oraz micro-SR-XRF.
2. Ocena zmian w przestrzennym rozmieszczeniu oraz względnej zawartości głównych makromolekuł biologicznych w wybranych obszarach mózgu szczurów, indukowanych prenatalną ekspozycją na KD, z wykorzystaniem FTIRM i RM.
3. Analiza zmian w przestrzennym rozmieszczeniu oraz zawartości wybranych pierwiastków w mózgu szczurów zachodzących w następstwie prenatalnej ekspozycji na KD, z zastosowaniem micro-SR-XRF.
4. Ocena wpływu prenatalnej ekspozycji na KD na rozwój układu nerwowego potomstwa w zależności od etapu rozwoju postnatalnego.
5. Ocena wpływu prenatalnej ekspozycji na KD na rozwój układu nerwowego potomstwa w zależności od płci potomstwa.

Zakres niniejszej rozprawy doktorskiej obejmuje:

1. Sformułowanie hipotezy badawczej i studia literaturowe dot. tematyki rozprawy.
2. Opracowanie planu badawczego i przeprowadzenie eksperymentu na zwierzętach.
3. Zapoznanie z metodami preparatyki próbek zwierzęcych oraz przygotowanie preparatów do badań spektroskopowych.
4. Opanowanie techniki pracy z mikroskopem podczerwieni Nicolet™ iN10 MX i mikroskopem ramanowskim Witec alpha 300R, optymalizacja warunków pomiarowych pod kątem pomiarów próbek tkanki.
5. Opanowanie obsługi oprogramowania oraz procedur analizy danych spektroskopowych, a także zaznajomienie się z podstawami wybranych metod analizy chemometrycznej.
6. Wykonanie pomiarów i analiza rozmieszczenia głównych makromolekuł biologicznych w tkance mózgowej metodą FTIRM i RM.
7. Analiza dystrybucji pierwiastków w mózgu szczurów metodą micro-SR-XRF.
8. Porównanie wpływu działania KD na układ nerwowy potomstwa w zależności od jego rozwoju postnatalnego i płci.

6. Materiały i metody

Hodowlę zwierząt oraz wszystkie związane z nią procedury przeprowadzono w Pracowni Neuropatologii Doświadczalnej w Instytucie Zoologii i Badań Biomedycznych Uniwersytetu Jagiellońskiego. Wszystkie eksperymenty zostały zatwierdzone przez Pierwszą Lokalną Komisję Etyczną ds. Doświadczeń na Zwierzętach w Krakowie (pozwolenie nr 122/2015) i zrealizowane zgodnie z krajowymi oraz międzynarodowymi przepisami dotyczącymi dobrostanu zwierząt, a także w oparciu o wytyczne ARRIVE dotyczące raportowania badań na zwierzętach.

Badaniem objęto potomstwo szczurów szczepu Wistar, których matki w okresie ciąży były utrzymywane na KD (grupy eksperymentalne) lub standardowej diecie laboratoryjnej (grupy kontrolne). W badaniu wykorzystano karmę ketogeniczną z długołańcuchowymi kwasami tłuszczowymi (ssniff EF R/M z 80% zawartością tłuszczu) oraz standardową dietę laboratoryjną w postaci Labofeed (Morawski). Wybrana KD charakteryzuje się wysokim współczynnikiem ketogenicznym (KR), czyli stosunkiem masowym tłuszczów do sumy białek i węglowodanów. W okresie laktacji samice z grup kontrolnych kontynuowały dietę standardową, natomiast w grupach eksperymentalnych KD zastąpiono dietą standardową drugiego dnia po porodzie. Po narodzinach określano płeć potomstwa, a zwierzęta każdej płci losowo przypisywano do grup różniących się czasem perfuzji i pobrania próbek. Liczba osobników w każdej grupie eksperymentalnej wynosiła od pięciu do sześciu. Mózgi pobierano w 2., 6., 14., 30. i 60. dniu życia, a wybrane punkty czasowe odpowiadały kluczowym procesom zachodzącym w mózgu szczura w okresie jego rozwoju postnatalnego.

W 2., 6., 14., 30. i 60. dniu życia po urodzeniu (w zależności od grupy) szczury znieczulano Morbitalem (Biowet) i perfundowano dożylnie roztworem soli fizjologicznej. Następnie mózgi wyjmowano, głęboko zamrażano w ciekłym azocie i cięto kriomikrotomem na skrawki zawierające grzbietową część formacji hipokampa. Skrawki o grubości 12 µm umieszczano na szkiełkach z CaF_2 w celu analizy metodami FTIRM i RM, natomiast skrawki o grubości 20 µm przenoszono na folie Ultralene do badań przy użyciu micro-SR-XRF.

W celu zbadania zmian w zawartości głównych makromolekuł biologicznych w mózgach potomstwa, w pracach A1 i M1 zastosowano FTIRM, dodatkowo w pracy M1 zastosowano RM, jako metodę komplementarną. Pomiary z wykorzystaniem FTIRM przeprowadzono w Laboratorium Biospektroskopii Atomowej i Molekularnej Wydziału Fizyki i Informatyki Stosowanej Akademii Górniczo-Hutniczej im. Stanisława Staszica w Krakowie. Wykonano je w trybie transmisyjnym z użyciem mikroskopu podczerwieni Thermo Scientific Nicolet iN10 MX (Thermo Fisher Scientific, USA) wyposażonego w ceramiczne źródło promieniowania podczerwonego, interferometr Michelsona oraz detektor MCT chłodzony ciekłym azotem. Uzupełniające pomiary ramanowskie przeprowadzono również w Laboratorium Biospektroskopii Atomowej i Molekularnej. Dokonano ich przy użyciu konfokalnego mikroskopu ramanowskiego WITec Alpha300R (WITEC GmbH, Niemcy) wyposażonego w laser 532 nm, obiektyw powietrzny 100× (Zeiss EC Epiplan-Neofluar, NA = 0,9) oraz spektrometr UHTS 300 z siatką dyfrakcyjną o gęstości 600 rowków/mm.

Do przeprowadzenia topograficznej i ilościowej analizy pierwiastkowej mózgu zwierząt badanych w artykule A2 zastosowano metodę micro-SR-XRF. Tkanki skanowano na linii badawczej FLUO zainstalowanej w synchrotronie KARA (wcześniej ANKA) w Karlsruhe (Niemcy). Energia wzbudzającej wiązki promieniowania rentgenowskiego wynosiła 17 keV, a jej wymiary 200 µm × 200 µm. Stosunkowo duża wiązka promieniowania umożliwiła rastrowe skanowanie wycinków tkanek obejmujących całe obszary badanego mózgu, z krokiem 200 µm w obu kierunkach i czasem akwizycji pojedynczego widma XRF wynoszącym 10 s.

7. Streszczenia artykułów wchodzących w skład rozprawy

Artykuł A1:

„Does Ketogenic Diet Used in Pregnancy Affect the Nervous System Development in Offspring? - FTIR Microspectroscopy Study"

W pracy [A1] zastosowana została FTIRM do identyfikacji potencjalnych anomalii w zawartości i strukturze głównych makrocząsteczek biologicznych występujących w mózgu potomstwa szczurów płci męskiej, których matki były karmione KD w czasie ciąży. W badaniu skupiono się na okresie intensywnego rozwoju mózgu po urodzeniu, dlatego do eksperymentu włączono zwierzęta w wieku 2, 6 i 14 dni rozwoju postnatalnego. Analizie poddano całe przekroje poprzeczne mózgu obejmujące grzbietową część formacji hipokampa. W badaniu uwzględniono poziom biocząsteczek, takich jak białka, lipidy, związki zawierające grupy fosforanowe i karbonylowe, a także cholesterol i jego estry. Ponadto analizowano zmiany w strukturze białek i lipidów. W celu określenia istotności statystycznej obserwowanych różnic pomiędzy grupą eksperymentalną i kontrolną zastosowano test *U* Manna-Whitneya.

Przeprowadzone mapowanie chemiczne oraz dalsza analiza półilościowa i statystyczna wykazały, że stosowanie KD w czasie ciąży zasadniczo nie prowadzi do istotnych anomalii biochemicznych w mózgu 2- i 6-dniowych szczurów. Wyjątkiem była zwiększona względna (w odniesieniu do białek) zawartość związków zawierających grupy fosforanowe w istocie białej oraz korze mózgowej 2-dniowych szczurów narażonych prenatalnie na KD. Zmiany te mogą odzwierciedlać różnice w poziomie kwasów nukleinowych, fosfolipidów lub stopniu ufosforylowania innych związków, a także w zawartości węglowodanów w tkance mózgowej [67–69]. Brak wyraźnych różnic w kolejnych dniach rozwoju może być związany z dynamicznymi zmianami metabolizmu energetycznego we wczesnym okresie życia, kiedy dostępność glukozy w mózgu noworodków jest ograniczona, a ważnym źródłem energii pozostają ciała ketonowe [70,71].

Więcej różnic stwierdzono w mózgach 14-dniowego potomstwa matek karmionych KD. Obejmowały one wzrost względnego poziomu związków zawierających grupy karbonylowe w korze mózgowej oraz w warstwach komórkowych formacji hipokampa (warstwie komórek wielokształtnych i molekularnej). Zmiany te można wiązać ze zwiększoną akumulacją związków lipidowych zawierających grupy karbonylowe, estrów cholesterolu lub ciał ketonowych. Ciała ketonowe powstające w wątrobie w wyniku β-oksydacji kwasów tłuszczowych mogą łatwo przekraczać barierę krew-mózg oraz barierę łożyskową, osiągając w organizmie płodu poziomy zbliżone do obserwowanych u matki [72,73]. Niedojrzały mózg wykazuje również zwiększoną zdolność do ich wychwytu i wykorzystania w procesach metabolicznych [70,74].

Istotne zmiany zaobserwowano także w obrębie struktur istoty białej mózgu 14-dniowych szczurów narażonych prenatalnie na KD. Stwierdzono zmniejszenie powierzchni torebki wewnętrznej, obniżenie względnej zawartości lipidów w innych obszarach istoty białej, takich jak ciało modzelowate, oraz zmiany w strukturze lipidów.

Uzyskane wyniki wskazują, że prenatalna ekspozycja na KD może wpływać na metabolizm wybranych biocząsteczek w mózgu rozwijającego się potomstwa, przy czym charakter tych zmian zależy od etapu rozwoju postnatalnego. Możliwe jest również, że obserwowane efekty są częściowo związane z procesami kompensacyjnymi zachodzącymi w organizmie matki po zakończeniu stosowania KD i powrocie do diety standardowej po porodzie.

Artykuł A2:

„Element Changes Occurring in Brain Point at the White Matter Abnormalities in Rats Exposed to the Ketogenic Diet During Prenatal Life"

Celem pracy [A2] była identyfikacja topograficznych oraz ilościowych zmian w rozmieszczeniu pierwiastków w mózgach potomstwa wynikających ze stosowania KD przez matkę w okresie ciąży. Aby go zrealizować, porównano potomstwo płci męskiej samic żywionych w czasie ciąży KD lub standardową dietą laboratoryjną. Analizie poddano szczury w wieku 2, 6, 14, 30 i 60 dni, co umożliwiło monitorowanie zmian pierwiastkowych

oraz ocenę ich dynamiki i trwałości w trakcie rozwoju postnatalnego. Mapowanie pierwiastkowe wycinków mózgu przeprowadzono z wykorzystaniem techniki micro-SR-XRF, która jest nieniszczącą i wysoce czułą techniką analizy wielopierwiastkowej. Zastosowane warunki eksperymentalne pozwoliły na określenie przestrzennego rozkładu oraz akumulacji fosforu (P), siarki (S), potasu (K), wapnia (Ca), żelaza (Fe) i cynku (Zn) w analizowanych obszarach tkanek.

Topograficzna analiza mózgów potomstwa matek karmionych KD w czasie ciąży oraz odpowiednich osobników kontrolnych wykazała potencjalny wpływ takiego sposobu żywienia na poziomy niektórych pierwiastków, szczególnie P i S. W przypadku najstarszego potomstwa zaobserwowano istotne zmniejszenie powierzchni obszarów mózgu charakteryzujących się zwiększoną zawartością tych pierwiastków, które histologicznie odpowiadają strukturom istoty białej. Podobną zależność obserwowano wcześniej w odniesieniu do przestrzennego rozkładu lipidów w mózgach 14-dniowego potomstwa matek karmionych dietą wysokotłuszczową. Ponieważ istota biała składa się głównie z aksonów otoczonych osłonką mielinową, bogatą w lipidy takie jak sfingomielina czy cholesterol [75–79], obserwowane zmiany w dystrybucji P i lipidów mogą wskazywać na zaburzenia akumulacji sfingomieliny oraz potencjalne zmiany w strukturze i integralności mieliny.

Analiza topograficzna wykazała również zmiany w rozmieszczeniu innych pierwiastków w zależności od etapu rozwoju postnatalnego. W przypadku S i K ich zawartość pozostawała względnie stabilna w początkowych etapach rozwoju mózgu, natomiast wyraźniejsze zmiany obserwowano około 30. dnia życia zwierząt. Kolokalizacja obszarów o podwyższonej zawartości S ze strukturami istoty białej może być związana z obecnością sulfatydów - sulfoglikolipidów będących ważnym składnikiem osłonek mielinowych i odgrywających istotną rolę w utrzymaniu ich prawidłowej struktury oraz funkcji [80–82].

Ilościowa analiza pierwiastkowa wykazała również przejściowe obniżenie poziomu Fe w prążkowiu i istocie białej 30-dniowych szczurów narażonych prenatalnie na KD. Zjawisko to nie było obserwowane u starszych, 60-dniowych zwierząt, co wskazuje na jego przejściowy charakter. Żelazo jest pierwiastkiem niezbędnym dla prawidłowego funkcjonowania układu nerwowego, uczestniczącym m.in. w syntezie neuroprzekaźników oraz procesie mielinizacji [83].

Najbardziej dynamiczne zmiany w trakcie rozwoju postnatalnego zaobserwowano w przypadku Zn. W mózgach młodych szczurów eksponowanych prenatalnie na KD stwierdzono przejściowo zwiększoną akumulację tego pierwiastka w obrębie formacji hipokampa, szczególnie w 6. i 14. dniu życia. Zjawisko to może wskazywać na intensyfikację procesów reorganizacji tkanki nerwowej w tym obszarze mózgu.

Uzyskane wyniki wskazują, że stosowanie KD przez matki w okresie ciąży może wpływać na dystrybucję i poziom wybranych pierwiastków w mózgu rozwijającego się potomstwa płci męskiej, prowadząc m.in. do zmian topograficznych w obrębie struktur istoty białej.

Manuskrypt M1:

„*Fourier Transform Infrared Imaging Supported by Raman Spectroscopy Reveals Biochemical Changes in Adult Rat Brains Following Prenatal Exposure to a Ketogenic Diet*".

Celem pracy [M1] było wykorzystanie FTIRM i RM do zbadania potencjalnych zmian biochemicznych w mózgach potomstwa matek narażonych na KD w okresie prenatalnym. Niniejsze badanie rozszerza wcześniejszą pracę [A1], uwzględniając zarówno wiek, jak i płeć jako zmienne biologiczne. Wcześniejsze analizy ograniczały się do samców we wczesnych stadiach rozwoju postnatalnego (2., 6. i 14. dzień życia). W pracy [M1] uwzględniono również samice w analogicznych stadiach rozwoju, a ponadto zbadano zarówno samce, jak i samice w 30. i 60. dniu życia, co odpowiada późnemu okresowi młodzieńczemu oraz wczesnej dorosłości. Tak zaprojektowany eksperyment umożliwił ocenę długofalowego, zależnego od płci wpływu prenatalnej ekspozycji na KD na skład biomolekularny tkanki mózgowej.

Zastosowanie komplementarnych technik spektroskopowych – FTIRM oraz RM – pozwoliło na szczegółową charakterystykę zmian w zawartości i strukturze głównych biocząsteczek w mózgu. Analizy spektroskopowe ujawniły zmiany zależne od regionu

mózgu, wieku oraz płci zwierząt, dotyczące przede wszystkim metabolizmu lipidów oraz związków zawierających grupy fosforanowe, które stanowią istotne składniki błon komórkowych i osłonek mielinowych. Najbardziej wyraźne zmiany biochemiczne stwierdzono u 60-dniowych samców prenatalnie eksponowanych na KD. W obrębie formacji hipokampa oraz kory mózgowej wykryto ogniskowe wtrącenia bogate w kreatynę i/lub cholesterol, przy czym analiza ilościowa wykazała istotny wzrost powierzchni wtrąceń cholesterolowych w grupie ketogenicznej, podczas gdy dla kreatyny zaobserwowano trend wzrostowy. Zjawisko to może odzwierciedlać zaburzenia metabolizmu energetycznego komórek nerwowych lub stanowić przejaw procesów adaptacyjnych związanych z metabolicznym „prekondycjonowaniem" mózgu w warunkach zwiększonej dostępności lipidów i ciał ketonowych. Kreatyna pełni kluczową rolę w utrzymaniu homeostazy energetycznej komórki poprzez udział w układzie kreatyna/fosfokreatyna/kinaza kreatynowa (Cr/PhCr/CK), który wspomaga szybką regenerację ATP w tkankach o dużym zapotrzebowaniu na energię, takich jak mózg [84,85], natomiast cholesterol jest istotnym składnikiem błon biologicznych oraz osłonek mielinowych [86]. W niektórych przypadkach obserwowano współwystępowanie depozytów obu związków, co może wskazywać na ich częściowo powiązane tło metaboliczne. U tych samych samców stwierdzono również obniżenie wielu parametrów biochemicznych związanych z lipidami, szczególnie w obrębie ciała modzelowatego. Zmiany te mogą świadczyć o zmniejszonej zawartości lipidów lub modyfikacjach ich struktury, co potencjalnie wskazuje na zaburzenia funkcjonowania oligodendrocytów oraz dynamiki mielinizacji. Wyniki te są zgodne z wcześniejszymi obserwacjami dotyczącymi zmian w rozmieszczeniu pierwiastków (P i S) związanych z mieliną w mózgach zwierząt narażonych prenatalnie na KD.

W przeciwieństwie do samców, u samic zmiany biochemiczne miały bardziej przejściowy charakter. Najbardziej widoczne były u 30-dniowych osobników i obejmowały spadki parametrów lipidowych w niektórych warstwach formacji hipokampa oraz w obrębie torebki wewnętrznej. Jednocześnie w korze mózgowej, ciele modzelowatym oraz wybranych warstwach formacji hipokampa obserwowano podwyższone wskaźniki związane z obecnością grup fosforanowych. W wieku 60 dni większość tych różnic ulegała jednak normalizacji, co może wskazywać na stabilizację metaboliczną na późniejszych etapach rozwoju postnatalnego. Brak podobnych zmian u dorosłych samic może być związany z działaniem czynników zależnych od płci. Estrogeny regulują metabolizm kreatyny, wspierają funkcjonowanie mitochondriów, modulują homeostazę lipidów oraz wykazują właściwości neuroprotekcyjne [87–89], co może łagodzić zaburzenia metaboliczne indukowane prenatalną ekspozycją na KD.

Uzyskane wyniki wskazują, że prenatalna ekspozycja na KD może prowadzić do złożonych, zależnych od płci i wieku zmian biochemicznych w rozwijającym się mózgu potomstwa. Szczególnie widoczne są one u młodych dorosłych samców i mogą dotyczyć metabolizmu lipidów, procesów mielinizacji oraz mechanizmów regulujących gospodarkę energetyczną komórek nerwowych.

8. Dyskusja wyników

Celem niniejszej pracy była kompleksowa ocena wpływu prenatalnej ekspozycji na KD na rozwój oraz właściwości biochemiczne mózgu potomstwa szczurów. W badaniach wykorzystano zestaw komplementarnych metod analitycznych, obejmujących FTIRM, RM oraz mikroskopię fluorescencji rentgenowskiej ze wzbudzeniem synchrotronowym. Zastosowanie tych technik umożliwiło szczegółową analizę zmian molekularnych i pierwiastkowych w tkance mózgowej na różnych etapach rozwoju postnatalnego oraz ocenę ich przestrzennego rozmieszczenia w obrębie wybranych struktur mózgu, w tym formacji hipokampa, kory mózgowej oraz obszarów istoty białej. Uzyskane wyniki wskazują, że KD stosowana w okresie ciąży może prowadzić do złożonych, zależnych od wieku, regionu mózgu oraz płci potomstwa zmian biochemicznych i strukturalnych w rozwijającym się układzie nerwowym.

Pierwszy etap badań, opisany w pracy [A1], dotyczył analizy wczesnych zmian molekularnych zachodzących w mózgach młodych samców w pierwszych tygodniach życia (2., 6. i 14. dzień po urodzeniu). Analiza map chemicznych uzyskanych metodą FTIRM wykazała, że w początkowym okresie rozwoju postnatalnego różnice między potomstwem samic żywionych dietą standardową i ketogeniczną są stosunkowo niewielkie. W mózgach dwudniowych i sześciodniowych samców nie obserwowano wyraźnych różnic w ogólnym rozmieszczeniu głównych biomolekuł, takich jak białka, lipidy czy węglowodany. Analiza statystyczna, obejmująca między innymi analizę głównych składowych (ang. *principal components analysis*, PCA), również nie wykazała wyraźnej separacji pomiędzy widmami zmierzonymi dla mózgów zwierząt z grupy kontrolnej i eksperymentalnej. Pomimo ogólnego podobieństwa obserwowano jednak pewne subtelne różnice biochemiczne. U dwudniowych szczurów, których matki były żywione KD w czasie ciąży, stwierdzono zwiększoną wartość stosunku intensywności pasm 1080 cm^{-1}/1658 cm^{-1} w ciele modzelowatym, a także podwyższoną względną intensywność pasma 1240 cm^{-1}/1658 cm^{-1} w korze. Pasma te są związane z obecnością grup fosforanowych w cząsteczkach takich jak kwasy nukleinowe czy fosfolipidy, a także mogą odzwierciedlać zmiany w stopniu fosforylacji niektórych biomolekuł, w tym węglowodanów i glikoprotein [68,69]. Wzrost intensywności pasma przy 1080 cm^{-1} może również wskazywać na zmiany w metabolizmie węglowodanów lub w poziomie glukozy w tkance mózgowej. Warto podkreślić, że w początkowym okresie życia dostępność glukozy w mózgu noworodków jest stosunkowo ograniczona, ponieważ transport tego substratu przez barierę krew-mózg jest wówczas jeszcze słabo rozwinięty [70]. W związku z tym rozwijający się mózg wykorzystuje w większym stopniu alternatywne źródła energii, w tym ciała ketonowe [70].

W późniejszym etapie rozwoju, szczególnie w czternastym dniu życia, zaobserwowano wyraźniejsze zmiany w składzie biochemicznym mózgu męskiego potomstwa samic żywionych KD. Analiza map chemicznych uzyskanych techniką FTIRM wykazała zwiększoną względną intensywność pasma 1740 cm^{-1} w korze mózgowej oraz w wybranych warstwach formacji hipokampa. Pasmo to jest charakterystyczne dla grup karbonylowych obecnych w estrach lipidowych, takich jak estry cholesterolu czy niektóre fosfolipidy, a także może być związane z obecnością ciał ketonowych. Obserwowany wzrost intensywności tego pasma może więc wskazywać na zwiększoną akumulację lipidów lub metabolitów lipidowych w tkance mózgowej młodych zwierząt. Wynik ten jest zgodny z faktem, że ciała ketonowe, powstające w wyniku metabolizmu kwasów tłuszczowych w wątrobie, mogą łatwo przenikać przez barierę krew-mózg oraz przez łożysko, osiągając w krążeniu płodowym poziomy zbliżone do obserwowanych u matki [72]. Mózg noworodków i młodych zwierząt charakteryzuje się wysoką zdolnością do wykorzystania ciał ketonowych jako substratów energetycznych oraz prekursorów biosyntetycznych [70,74,90]. Związki te mogą być wykorzystywane nie tylko jako źródło energii, lecz także w syntezie lipidów, w tym cholesterolu oraz innych składników błon komórkowych i osłonek mielinowych [91].

Pomimo zwiększonej dostępności substratów lipidowych u męskiego potomstwa samic karmionych KD analiza struktur istoty białej wykazała jednak pewne nieoczekiwane zmiany w ich morfologii i składzie. Jakościowa analiza map chemicznych przedstawiających względną zawartość lipidów (2800-3000 cm^{-1}/1658 cm^{-1}, 2924 cm^{-1}/1658 cm^{-1}), cholesterolu i jego estrów (1480 cm^{-1}/1658 cm^{-1}), a także zmiany w strukturze lipidów

(2924 cm^{-1}/2955 cm^{-1}), ujawniła mniejszą powierzchnię obszaru torebki wewnętrznej w przypadku 14-dniowych zwierząt. Znaczenie wspomnianego efektu potwierdziła dalsza półilościowa analiza biochemiczna oraz wyniki testu *U* Manna-Whitneya, które wykazały również niższą względną zawartość lipidów i ich nieprawidłowości strukturalne dla innego obszaru istoty białej, a mianowicie ciała modzelowatego. Wyniki te mogą wskazywać, że prenatalna ekspozycja na KD wpływa na procesy mielinizacji zachodzące w rozwijającym się mózgu. Jest to szczególnie istotne, ponieważ mielina stanowi strukturę bogatą w lipidy, a jej prawidłowe tworzenie jest kluczowe dla sprawnego przewodzenia impulsów nerwowych. Wydaje się zatem, że mimo zwiększonej dostępności lipidów wykorzystywanych jako źródło energii oraz do procesów biosyntezy w organizmie potomstwa, ich metabolizm w rozwijającym się mózgu może być odmiennie regulowany, co wpływa na dynamikę tworzenia osłonek mielinowych.

Istotnym uzupełnieniem tych obserwacji była analiza składu pierwiastkowego mózgu szczurów płci męskiej na różnych etapach rozwoju postnatalnego z wykorzystaniem mikroskopii fluorescencji rentgenowskiej [A2]. Badania te wykazały, że zawartość P w mózgu szczura wzrasta przede wszystkim pomiędzy czternastym a trzydziestym dniem życia, co odzwierciedla intensywne procesy wzrostu i dojrzewania tkanki nerwowej. U młodych zwierząt prenatalnie eksponowanych na KD obserwowano tendencję do wyższej akumulacji P w pierwszych dwóch tygodniach życia, natomiast u osobników dorosłych zależność ta ulegała odwróceniu. Szczególnie interesującym wynikiem było zmniejszenie powierzchni obszarów mózgu o wysokiej zawartości P oraz S u 30- i 60-dniowych potomków samic żywionych KD w czasie ciąży. Obszary te odpowiadają histologicznie strukturom istoty białej, która składa się z pęczków włókien nerwowych. Włókna te to głównie aksony otoczone osłonkami mielinowymi bogatymi w lipidy tj. galaktocerebrozyd, sulfatydy, sfingomielina i cholesterol [78,79,81,82]. Ponieważ zarówno fosfor, jak i siarka są ważnymi składnikami cząsteczek takich jak sfingomielina czy sulfatydy, obserwowane zmiany mogą wskazywać na potencjalne zaburzenia struktury lub integralności osłonek mielinowych. Mielina odgrywa kluczową rolę w funkcjonowaniu układu nerwowego, umożliwiając szybkie przewodzenie impulsów nerwowych oraz zwiększając efektywność energetyczną neuronów [77,79]. Ponadto komórki glejowe tworzące osłonki mielinowe zapewniają aksonom wsparcie metaboliczne i ochronę strukturalną [92]. W związku z tym wszelkie zmiany w strukturze mieliny mogą potencjalnie wpływać na funkcjonowanie sieci neuronalnych, procesy poznawcze oraz zachowanie [93,94].

Analiza map pierwiastkowych wykazała również dynamiczne zmiany związane z rozwojem mózgu. Szczególnie interesujące wyniki uzyskano w przypadku cynku. Najniższy poziom tego pierwiastka obserwowano w mózgach sześciodniowych zwierząt, po czym jego zawartość stopniowo wzrastała w kolejnych etapach rozwoju, zarówno u zwierząt prenatalnie eksponowanych na KD, jak i ich odpowiedników z grupy kontrolnej. U potomstwa matek karmionych KD stwierdzono wyższą akumulację cynku w formacji hipokampa w pierwszych tygodniach życia. Cynk odgrywa istotną rolę w wielu procesach neuronalnych, w tym w modulacji transmisji synaptycznej, funkcjonowaniu receptorów glutaminergicznych oraz w regulacji procesów plastyczności synaptycznej [95]. Zwiększona akumulacja tego pierwiastka w formacji hipokampa może wskazywać na intensyfikację procesów reorganizacji tkanki nerwowej, takich jak przebudowa połączeń synaptycznych czy zmiany w unerwieniu GABA-ergicznym.

W dalszej części badań skupiono się na analizie długofalowych konsekwencji prenatalnej ekspozycji na KD, ze szczególnym uwzględnieniem różnic zależnych od płci. Kluczowe znaczenie miało tu zastosowanie dwóch komplementarnych technik: FTIRM oraz RM [M1]. Interesujące wyniki uzyskano dla sześćdziesięciodniowych samców. W ich mózgach zidentyfikowano wyraźne depozyty zawierające kreatynę oraz cholesterol, zlokalizowane głównie w formacji hipokampa i korze mózgowej. Całkowita i względna powierzchnia inkluzji kreatyny wykazywała tendencję wzrostową u dorosłych samców szczurów poddanych prenatalnej ekspozycji na KD, jednak bez istotności statystycznej. W grupie ketogenicznej stwierdzono natomiast istotny statystycznie wzrost zarówno całkowitej, jak i względnej powierzchni inkluzji bogatych w cholesterol w korze mózgowej oraz formacji hipokampa. Kreatyna jest niewielką cząsteczką pełniącą kluczową rolę w

utrzymaniu homeostazy energetycznej komórek [84,85]. W komórkach o wysokim zapotrzebowaniu energetycznym, takich jak neurony, system kreatyna-fosfokreatyna-kinaza kreatynowa umożliwia szybkie buforowanie poziomu ATP oraz transport wysokoenergetycznych grup fosforanowych pomiędzy mitochondriami a miejscami zużycia energii w cytoplazmie [12,85]. Z kolei cholesterol jest jednym z głównych składników błon komórkowych oraz ważnym elementem strukturalnym osłonek mielinowych [86,96]. Współwystępowanie złogów kreatyny i cholesterolu może wskazywać na zaburzenia metabolizmu energetycznego i lipidowego w rozwijającym się mózgu. Jednocześnie nie można wykluczyć, że obserwowane zmiany stanowią adaptacyjną odpowiedź komórek nerwowych na warunki metaboliczne związane z KD. Dieta ta prowadzi bowiem do przesunięcia metabolizmu energetycznego w kierunku zwiększonego wykorzystania kwasów tłuszczowych oraz ciał ketonowych, co może wpływać na równowagę pomiędzy różnymi systemami dostarczania energii w komórkach.

Interesującym aspektem uzyskanych wyników jest również ich zależność od płci potomstwa. W przypadku samic największe różnice pomiędzy grupą kontrolną i eksperymentalną obserwowano w trzydziestym dniu życia. W tym okresie stwierdzono między innymi zmniejszenie niektórych parametrów biochemicznych związanych z zawartością lipidów w wybranych warstwach formacji hipokampa oraz w obrębie torebki wewnętrznej. Jednak w wieku sześćdziesięciu dni większość analizowanych parametrów u samic ulegała stabilizacji i nie różniła się istotnie od wartości obserwowanych w grupie kontrolnej. Może to sugerować istnienie mechanizmów ochronnych związanych z działaniem hormonów płciowych, takich jak estrogeny. Hormony te są znane z licznych właściwości neuroprotekcyjnych, obejmujących modulację metabolizmu lipidów, regulację funkcjonowania mitochondriów oraz wpływ na mechanizmy antyoksydacyjne w komórkach nerwowych [89,97–100]. Estrogeny mogą również wpływać na metabolizm kreatyny oraz na procesy transportu i dystrybucji cholesterolu w organizmie [88,100].

Podsumowując, wyniki przedstawione w niniejszej pracy wskazują, że prenatalna ekspozycja na KD może prowadzić do wielopoziomowych zmian w rozwijającym się mózgu potomstwa. Zmiany te obejmują zarówno metabolizm głównych biomolekuł, takich jak lipidy i węglowodany, jak i dystrybucję pierwiastków niezbędnych dla prawidłowego funkcjonowania układu nerwowego. Wiele z obserwowanych efektów ma charakter zależny od etapu rozwoju oraz regionu mózgu, a część z nich wykazuje również wyraźną zależność od płci. Uzyskane wyniki sugerują, że KD stosowana w czasie ciąży może modulować procesy metaboliczne i strukturalne w rozwijającym się mózgu, wpływając między innymi na dynamikę mielinizacji, reorganizację połączeń neuronalnych oraz mechanizmy utrzymania homeostazy energetycznej. Jednocześnie część obserwowanych zmian może mieć charakter adaptacyjny, odzwierciedlając zdolność rozwijającego się układu nerwowego do przystosowania się do zmienionych warunków metabolicznych.

Istotnym elementem przeprowadzonych badań było zastosowanie komplementarnych technik spektroskopowych, takich jak FTIRM, RM oraz micro-SR-XRF. Metody te umożliwiły uzyskanie szczegółowych informacji zarówno o składzie molekularnym, jak i pierwiastkowym badanej tkanki, a także o ich przestrzennym rozmieszczeniu w obrębie poszczególnych struktur mózgu. Dzięki wysokiej czułości i możliwości prowadzenia analiz bez konieczności stosowania dodatkowych znaczników techniki te pozwoliły na identyfikację subtelnych zmian biochemicznych i strukturalnych zachodzących w rozwijającym się mózgu potomstwa eksponowanego prenatalnie na KD. Zastosowanie podejścia wielotechnicznego umożliwiło uzyskanie komplementarnego obrazu badanych procesów oraz zwiększyło wiarygodność interpretacji uzyskanych wyników, podkreślając istotną rolę metod spektroskopowych w badaniach nad wpływem czynników metabolicznych na rozwój układu nerwowego.

9. Podsumowanie

W ramach niniejszej rozprawy doktorskiej zbadano zmiany biochemiczne oraz pierwiastkowe zachodzące w mózgach potomstwa szczurów, których matki w okresie ciąży były żywione KD. W tym celu zastosowano nowoczesne techniki spektroskopowe, takie jak FTIRM, micro-SR-XRF oraz RM. Badania koncentrowały się nie tylko na analizie zmian molekularnych i pierwiastkowych w tkance mózgowej, lecz również na optymalizacji warunków pomiarowych oraz ograniczeniu potencjalnych efektów niepożądanych i artefaktów, które mogą pojawiać się podczas analizy tkanek. Szczególną uwagę poświęcono ocenie przydatności wybranych metod instrumentalnych do kompleksowej charakterystyki zmian biochemicznych i strukturalnych zachodzących w rozwijającym się układzie nerwowym.

W szczególności:

1. Wykorzystano FTIRM w celu uzyskania map chemicznych badanych tkanek, umożliwiających identyfikację globalnych różnic biomolekularnych pomiędzy grupami eksperymentalnymi i kontrolnymi 2-, 6- i 14-dniowych samców oraz dalszą analizę zmian w wybranych obszarach mózgu. Zastosowanie tej techniki pozwoliło na wykazanie zwiększonej względnej intensywności pasma 1740 cm^{-1}, charakterystycznego dla grup karbonylowych, w korze mózgowej oraz w wybranych warstwach formacji hipokampa u 14-dniowych samców eksponowanych prenatalnie na KD. Jednocześnie zaobserwowano obniżenie względnej zawartości lipidów w obszarach istoty białej tych zwierząt [praca A1].
2. Mapy biochemiczne uzyskane metodą FTIRM, przedstawiające rozkład pasm charakterystycznych dla lipidów, zestawiono z obrazami mikroskopowymi analizowanych przekrojów mózgu. Takie podejście umożliwiło wykazanie zmniejszenia powierzchni torebki wewnętrznej u 14-dniowych samców poddanych prenatalnej ekspozycji na KD [A1].
3. Za pomocą techniki micro-SR-XRF wykazano różnice w składzie oraz rozmieszczeniu pierwiastków w mózgu pomiędzy zwierzętami z grup eksperymentalnych i kontrolnych. W szczególności stwierdzono zmniejszenie powierzchni obszarów mózgu o wysokiej zawartości fosforu oraz siarki u 30- i 60-dniowych potomków samic żywionych KD w czasie ciąży. Zauważono ponadto, że obszary te odpowiadają histologicznie strukturom istoty białej, która zbudowana jest ze skupisk włókien nerwowych, przede wszystkim aksonów otoczonych osłonkami mielinowymi bogatymi w lipidy [A2].
4. Przeanalizowano zmiany w zawartości i rozmieszczeniu pierwiastków zachodzące w trakcie rozwoju postnatalnego w zależności od stosowanej prenatalnie diety. Najbardziej dynamiczne zmiany zaobserwowano w przypadku cynku. Ponadto u młodych osobników eksponowanych prenatalnie na KD stwierdzono wyższą akumulację tego pierwiastka w formacji hipokampa w pierwszych tygodniach życia. Zjawisko to powiązano z intensyfikacją procesów reorganizacji tkanki nerwowej, takich jak przebudowa połączeń synaptycznych czy zmiany w unerwieniu GABA-ergicznym [A2].
5. Przeanalizowano długofalowe zmiany biochemiczne zachodzące w rozwijającym się mózgu szczura po prenatalnej ekspozycji na KD z wykorzystaniem FTIRM i RM. Najbardziej wyraźne zmiany zaobserwowano u 60-dniowych samców, u których w obrębie formacji hipokampa i kory mózgowej stwierdzono obecność wtrąceń bogatych w kreatynę i cholesterol oraz obniżenie parametrów związanych z lipidami. Zjawiska te powiązano z zaburzeniami metabolizmu energetycznego oraz zmianami w procesach mielinizacji i neuroadaptacji [M1].
6. Przeanalizowano zależne od płci różnice w odpowiedzi mózgu na prenatalną ekspozycję na KD. U 30-dniowych samic stwierdzono przejściowe, regionowo specyficzne zmiany w profilu lipidowym i parametrach fosforanowych, które w dużej mierze ulegały normalizacji do 60. dnia życia. W przeciwieństwie do samców nie obserwowano wtrąceń kreatyny ani cholesterolu, co powiązano z neuroprotekcyjnym działaniem estrogenów oraz ich wpływem na homeostazę energetyczną i lipidową [M1].

10. Bibliografia

[1] M. Kellogg, K.J. Meador, Neurodevelopmental Effects of Antiepileptic Drugs, Neurochem. Res. 42 (2017) 2065–2070. https://doi.org/10.1007/s11064-017-2262-4.

[2] K.J. Meador, D.W. Loring, Developmental effects of antiepileptic drugs and the need for improved regulations, Neurology 86 (2016) 297–306. https://doi.org/10.1212/WNL.0000000000002119.

[3] D.R. Nordli, M.M. Kuroda, J. Carroll, D.Y. Koenigsberger, L.J. Hirsch, H.J. Bruner, W.T. Seidel, D.C. De Vivo, Experience With the Ketogenic Diet in Infants, Pediatrics 108 (2001) 129–133. https://doi.org/10.1542/peds.108.1.129.

[4] T.J.W. McDonald, M.C. Cervenka, Ketogenic Diet Therapies for Seizures and Status Epilepticus, Semin. Neurol. 40 (2020) 719–729. https://doi.org/10.1055/s-0040-1719077.

[5] M.A. Mady, E.H. Kossoff, A.L. McGregor, J.W. Wheless, P.L. Pyzik, J.M. Freeman, The Ketogenic Diet: Adolescents Can Do It, Too, Epilepsia 44 (2003) 847–851. https://doi.org/10.1046/j.1528-1157.2003.57002.x.

[6] M.A. McNally, A.L. Hartman, Ketone bodies in epilepsy, J. Neurochem. 121 (2012) 28–35. https://doi.org/10.1111/j.1471-4159.2012.07670.x.

[7] W. Kosiek, Z. Rauk, P. Szulc, A. Cichy, M. Rugieł, J. Chwiej, K. Janeczko, Z. Setkowicz, Ketogenic diet impairs neurological development of neonatal rats and affects biochemical composition of maternal brains: evidence of functional recovery in pups, Brain Struct. Funct. 227 (2022) 1099–1113. https://doi.org/10.1007/s00429-021-02450-1.

[8] N.J. Jensen, H.Z. Wodschow, M. Nilsson, J. Rungby, Effects of Ketone Bodies on Brain Metabolism and Function in Neurodegenerative Diseases, Int. J. Mol. Sci. 21 (2020) 8767. https://doi.org/10.3390/ijms21228767.

[9] J. Huffman, E.H. Kossoff, State of the ketogenic diet(s) in epilepsy, Curr. Neurol. Neurosci. Rep. 6 (2006) 332–340. https://doi.org/10.1007/s11910-006-0027-6.

[10] A.L. Hartman, M. Gasior, E.P.G. Vining, M.A. Rogawski, The Neuropharmacology of the Ketogenic Diet, Pediatr. Neurol. 36 (2007) 281–292. https://doi.org/10.1016/j.pediatrneurol.2007.02.008.

[11] S. Masino, M. Kawamura Jr., C. Wasser, L. Pomeroy, D. Ruskin, Adenosine, Ketogenic Diet and Epilepsy: The Emerging Therapeutic Relationship Between Metabolism and Brain Activity, Curr. Neuropharmacol. 7 (2009) 257–268. https://doi.org/10.2174/157015909789152164.

[12] A. Skoczen, Z. Setkowicz, K. Janeczko, Ch. Sandt, F. Borondics, J. Chwiej, The influence of high fat diets with different ketogenic ratios on the hippocampal accumulation of creatine – FTIR microspectroscopy study, Spectrochim. Acta A Mol. Biomol. Spectrosc. 184 (2017) 13–22. https://doi.org/10.1016/j.saa.2017.04.085.

[13] A. Miłosz, J. Michalczyk, I. Morawik, K. Długoborska, M. Gesek, Possible impact of use of a ketogenic diet in pregnancy on the fetus: Review of animal and human studies, NFS Journal 38 (2025) 100212. https://doi.org/10.1016/j.nfs.2025.100212.

[14] T. Jansson, T.L. Powell, Role of the placenta in fetal programming: underlying mechanisms and potential interventional approaches, Clin. Sci. 113 (2007) 1–13. https://doi.org/10.1042/CS20060339.

[15] S.E. Cusick, M.K. Georgieff, The Role of Nutrition in Brain Development: The Golden Opportunity of the "First 1000 Days," J. Pediatr. 175 (2016) 16–21. https://doi.org/10.1016/j.jpeds.2016.05.013.

[16] S. Lacagnina, The Developmental Origins of Health and Disease (DOHaD), Am. J. Lifestyle Med. 14 (2020) 47–50. https://doi.org/10.1177/1559827619879694.

[17] E.J.T.M. van der Louw, T.J. Williams, B.J. Henry-Barron, J.F. Olieman, J.J. Duvekot, M.J. Vermeulen, N. Bannink, M. Williams, R.F. Neuteboom, E.H. Kossoff, C.E.

Catsman-Berrevoets, M.C. Cervenka, Ketogenic diet therapy for epilepsy during pregnancy: A case series, Seizure 45 (2017) 198–201. https://doi.org/10.1016/j.seizure.2016.12.019.

[18] J. Kramer, L. Smith, Ketogenic Diet in Glut 1 Deficiency Through the Life Cycle: Pregnancy to Neonate to Preschooler, Child Neurol. Open 8 (2021). https://doi.org/10.1177/2329048X211034655.

[19] D. Sussman, M. van Eede, M.D. Wong, S.L. Adamson, M. Henkelman, Effects of a ketogenic diet during pregnancy on embryonic growth in the mouse, BMC Pregnancy Childbirth 13 (2013) 109. https://doi.org/10.1186/1471-2393-13-109.

[20] D. Sussman, J. Germann, M. Henkelman, Gestational ketogenic diet programs brain structure and susceptibility to depression & anxiety in the adult mouse offspring, Brain Behav. 5 (2015). https://doi.org/10.1002/brb3.300.

[21] D. Sussman, J. Ellegood, M. Henkelman, A gestational ketogenic diet alters maternal metabolic status as well as offspring physiological growth and brain structure in the neonatal mouse, BMC Pregnancy Childbirth 13 (2013) 198. https://doi.org/10.1186/1471-2393-13-198.

[22] A.K.F. Soares, R.G.S. Guerra, M.L. de Castro, A. Amancio-dos-Santos, R.C.A. Guedes, J.E. Cabral-Filho, J.A. Costa, M. do C. Medeiros, Somatic and reflex development in suckling rats: effects of mother treatment with ketogenic diet associated with lack of protein, Nutr. Neurosci. 12 (2009) 260–266. https://doi.org/10.1179/147683009X423427.

[23] M. del C. Rodriguez-Perez, F. De Vicente-Perez, G. Gomez-Jarabo Garcia, Effects of protein malnutrition and the administration of cortisol on the reflexologic development in rats, Behav. Neural Biol. 58 (1992) 165–170. https://doi.org/10.1016/0163-1047(92)90412-W.

[24] A. Di Meco, D. Praticò, Early-life exposure to high-fat diet influences brain health in aging mice, Aging Cell 18 (2019). https://doi.org/10.1111/acel.13040.

[25] D.L.; Pavia, G.M.; Lampman, G.S.; Kriz, J.R. Vyvyan, Introduction to spectroscopy, 5th ed., CENGAGE Learning, 2013.

[26] Q. Wang, A. Kretlow, M. Beekes, D. Naumann, L. Miller, In situ characterization of prion protein structure and metal accumulation in scrapie-infected cells by synchrotron infrared and X-ray imaging, Vib. Spectrosc. 38 (2005) 61–69. https://doi.org/10.1016/j.vibspec.2005.02.023.

[27] A. Barth, Infrared spectroscopy of proteins, Biochimica et Biophysica Acta (BBA) - Bioenergetics 1767 (2007) 1073–1101. https://doi.org/10.1016/j.bbabio.2007.06.004.

[28] B.H. Stuart, Infrared Spectroscopy: Fundamentals and Applications, Wiley, 2004. https://doi.org/10.1002/0470011149.

[29] S. Caine, P. Heraud, M.J. Tobin, D. McNaughton, C.C.A. Bernard, The application of Fourier transform infrared microspectroscopy for the study of diseased central nervous system tissue, Neuroimage 59 (2012) 3624–3640. https://doi.org/10.1016/j.neuroimage.2011.11.033.

[30] I. Dreissig, S. Machill, R. Salzer, C. Krafft, Quantification of brain lipids by FTIR spectroscopy and partial least squares regression, Spectrochim. Acta A Mol. Biomol. Spectrosc. 71 (2009) 2069–2075. https://doi.org/10.1016/j.saa.2008.08.008.

[31] Z. Movasaghi, S. Rehman, Dr.I. ur Rehman, Fourier Transform Infrared (FTIR) Spectroscopy of Biological Tissues, Appl. Spectrosc. Rev. 43 (2008) 134–179. https://doi.org/10.1080/05704920701829043.

[32] P.R. Griffiths, J.A. de Haseth, Fourier Transform Infrared Spectrometry, Wiley, 2007. https://doi.org/10.1002/047010631X.

[33] M.C.A. and J.W.B. Sumner P. Davis, Fourier Transform Spectrometry, Elsevier, 2001. https://doi.org/10.1016/B978-0-12-042510-5.X5000-8.

[34] Y. Gong, X. Chen, W. Wu, Application of fourier transform infrared (FTIR) spectroscopy in sample preparation: Material characterization and mechanism investigation, Advances in Sample Preparation 11 (2024) 100122. https://doi.org/10.1016/j.sampre.2024.100122.

[35] Y. Tkachenko, P. Niedzielski, FTIR as a Method for Qualitative Assessment of Solid Samples in Geochemical Research: A Review, Molecules 27 (2022) 8846. https://doi.org/10.3390/molecules27248846.

[36] P.A. Valente, S.I. Mota, A. Teixeira, E. Ferreiro, H. Sarmento, I. Cipriano, J.R. Campos, L. Rama, P.J. Oliveira, Fourier Transform Infrared (FTIR) Spectroscopy as a Tool to Characterize Exercise and Physical Activity: A Systematic Review, Sports Medicine 55 (2025) 459–472. https://doi.org/10.1007/s40279-024-02139-5.

[37] M. Al-Kelani, N. Buthelezi, Advancements in medical research: Exploring Fourier Transform Infrared (FTIR) spectroscopy for tissue, cell, and hair sample analysis, Skin Research and Technology 30 (2024). https://doi.org/10.1111/srt.13733.

[38] R.A. Shaw, H.H. Mantsch, Infrared Spectroscopy in Clinical and Diagnostic Analysis, in: Encyclopedia of Analytical Chemistry, Wiley, 2000. https://doi.org/10.1002/9780470027318.a0106.

[39] M.J. Baker, J. Trevisan, P. Bassan, R. Bhargava, H.J. Butler, K.M. Dorling, P.R. Fielden, S.W. Fogarty, N.J. Fullwood, K.A. Heys, C. Hughes, P. Lasch, P.L. Martin-Hirsch, B. Obinaju, G.D. Sockalingum, J. Sulé-Suso, R.J. Strong, M.J. Walsh, B.R. Wood, P. Gardner, F.L. Martin, Using Fourier transform IR spectroscopy to analyze biological materials, Nat. Protoc. 9 (2014) 1771–1791. https://doi.org/10.1038/nprot.2014.110.

[40] M. Diem, A. Mazur, K. Lenau, J. Schubert, B. Bird, M. Miljković, C. Krafft, J. Popp, Molecular pathology *via* IR and Raman spectral imaging, J. Biophotonics 6 (2013) 855–886. https://doi.org/10.1002/jbio.201300131.

[41] B. Mohlenhoff, M. Romeo, M. Diem, B.R. Wood, Mie-Type Scattering and Non-Beer-Lambert Absorption Behavior of Human Cells in Infrared Microspectroscopy, Biophys. J. 88 (2005) 3635–3640. https://doi.org/10.1529/biophysj.104.057950.

[42] M. Romeo, B. Mohlenhoff, M. Diem, Infrared micro-spectroscopy of human cells: Causes for the spectral variance of oral mucosa (buccal) cells, Vib. Spectrosc. 42 (2006) 9–14. https://doi.org/10.1016/j.vibspec.2006.04.009.

[43] M.J. Romeo, M. Diem, Infrared spectral imaging of lymph nodes: Strategies for analysis and artifact reduction, Vib. Spectrosc. 38 (2005) 115–119. https://doi.org/10.1016/j.vibspec.2005.03.009.

[44] T.G. Mayerhöfer, J. Popp, The electric field standing wave effect in infrared transflection spectroscopy, Spectrochim. Acta A Mol. Biomol. Spectrosc. 191 (2018) 283–289. https://doi.org/10.1016/j.saa.2017.10.033.

[45] R.R. Jones, D.C. Hooper, L. Zhang, D. Wolverson, V.K. Valev, Raman Techniques: Fundamentals and Frontiers, Nanoscale Res. Lett. 14 (2019) 231. https://doi.org/10.1186/s11671-019-3039-2.

[46] A. V. Vlasov, N.L. Maliar, S. V. Bazhenov, E.I. Nikelshparg, N.A. Brazhe, A.D. Vlasova, S.D. Osipov, V. V. Sudarev, Y.L. Ryzhykau, A.O. Bogorodskiy, E. V. Zinovev, A. V. Rogachev, I. V. Manukhov, V.I. Borshchevskiy, A.I. Kuklin, J. Pokorný, O. Sosnovtseva, G. V. Maksimov, V.I. Gordeliy, Raman Scattering: From Structural Biology to Medical Applications, Crystals (Basel). 10 (2020) 38. https://doi.org/10.3390/cryst10010038.

[47] S.G.D.G. Paul Rostron, Raman Spectroscopy, Review, International Journal of Engineering and Technical Research 6 (2016) 50–64.

[48] K. Eberhardt, C. Stiebing, C. Matthäus, M. Schmitt, J. Popp, Advantages and limitations of Raman spectroscopy for molecular diagnostics: an update, Expert Rev. Mol. Diagn. 15 (2015) 773–787. https://doi.org/10.1586/14737159.2015.1036744.

[49] S. Gomes da Costa, A. Richter, U. Schmidt, S. Breuninger, O. Hollricher, Confocal Raman microscopy in life sciences, Morphologie 103 (2019) 11–16. https://doi.org/10.1016/j.morpho.2018.12.003.

[50] L. Ahlinder, S. Wiklund Lindström, C. Lejon, P. Geladi, L. Österlund, Noise Removal with Maintained Spatial Resolution in Raman Images of Cells Exposed to Submicron Polystyrene Particles, Nanomaterials 6 (2016) 83. https://doi.org/10.3390/nano6050083.

[51] S. Pimenta, J.H. Correia, Biomedical Applications of Raman Spectroscopy: A Review, Photochem 5 (2025) 29. https://doi.org/10.3390/photochem5040029.

[52] J. Li, J. Huang, S. Naz, Y. Zhan, L. Zheng, Effect of measurement parameters and laser-induced heating on the Raman measurement of aerosol powders, Talanta 301 (2026) 129259. https://doi.org/10.1016/j.talanta.2025.129259.

[53] C. Krafft, Raman Spectroscopy and Microscopy of Cells and Tissues, in: Encyclopedia of Biophysics, Springer Berlin Heidelberg, Berlin, Heidelberg, 2013: pp. 2178–2185. https://doi.org/10.1007/978-3-642-16712-6_121.

[54] W. Xu, Z. Du, S. Liu, Y. Zhu, C. Xiao, A. Marcelli, Perspectives of XRF and XANES Applications in Cryospheric Sciences Using Chinese SR Facilities, Condens. Matter 3 (2018) 29. https://doi.org/10.3390/condmat3040029.

[55] R. Jenkins, X-Ray Fluorescence Spectrometry, Wiley, 1999. https://doi.org/10.1002/9781118521014.

[56] K.W. Jones, B.M. Gordon, A.L. Hanson, W.M. Kwiatek, J.G. Pounds, X-ray fluorescence with synchrotron radiation, Ultramicroscopy 24 (1988) 313–328. https://doi.org/10.1016/0304-3991(88)90318-X.

[57] B. Beckhoff, habil. B. Kanngießer, N. Langhoff, R. Wedell, H. Wolff, eds., Handbook of Practical X-Ray Fluorescence Analysis, Springer Berlin Heidelberg, Berlin, Heidelberg, 2006. https://doi.org/10.1007/978-3-540-36722-2.

[58] P.J. Potts, A.T. Ellis, M. Holmes, P. Kregsamer, C. Streli, M. West, P. Wobrauschek, X-ray fluorescence spectrometry, J. Anal. At. Spectrom. 15 (2000) 1417–1442. https://doi.org/10.1039/b005284l.

[59] P.M. Kopittke, T. Punshon, D.J. Paterson, R. V. Tappero, P. Wang, F.P.C. Blamey, A. van der Ent, E. Lombi, Synchrotron-Based X-Ray Fluorescence Microscopy as a Technique for Imaging of Elements in Plants, Plant Physiol. 178 (2018) 507–523. https://doi.org/10.1104/pp.18.00759.

[60] N.P. Edwards, S.M. Webb, C.M. Krest, D. van Campen, P.L. Manning, R.A. Wogelius, U. Bergmann, A new synchrotron rapid-scanning X-ray fluorescence (SRS-XRF) imaging station at SSRL beamline 6-2, J. Synchrotron Radiat. 25 (2018) 1565–1573. https://doi.org/10.1107/S1600577518010202.

[61] C. Vanhoof, A. Cross, U.E.A. Fittschen, L. Vincze, Atomic spectrometry update: review of advances in X-ray fluorescence spectrometry, J. Anal. At. Spectrom. 40 (2025) 2275–2289. https://doi.org/10.1039/D5JA90030A.

[62] R. Ortega, P. Cloetens, G. Devès, A. Carmona, S. Bohic, Iron Storage within Dopamine Neurovesicles Revealed by Chemical Nano-Imaging, PLoS One 2 (2007) e925. https://doi.org/10.1371/journal.pone.0000925.

[63] M.J. Pushie, N.J. Sylvain, H. Hou, M.J. Hackett, M.E. Kelly, S.M. Webb, X-ray fluorescence microscopy methods for biological tissues, Metallomics 14 (2022). https://doi.org/10.1093/mtomcs/mfac032.

[64] M.J. Pushie, M.E. Kelly, M.J. Hackett, Direct label-free imaging of brain tissue using synchrotron light: a review of new spectroscopic tools for the modern neuroscientist, Analyst 143 (2018) 3761–3774. https://doi.org/10.1039/C7AN01904A.

[65] K.G. Slepchenko, S. Chen, K.L. Corbin, R.A. Colvin, C.S. Nunemaker, The use of synchrotron X-ray fluorescent imaging to study distribution and content of elements in chemically fixed single cells: a case study using mouse pancreatic beta-cells, Metallomics 15 (2023). https://doi.org/10.1093/mtomcs/mfad006.

[66] Y. Yang, M. Chen, A Review of Application of Synchrotron-Based X-Ray Techniques in Sulfide Mineral (Bio)leaching, Mineral Processing and Extractive Metallurgy Review 47 (2026) 444–470. https://doi.org/10.1080/08827508.2025.2507874.

[67] J. Chwiej, J. Dulinska, K. Janeczko, P. Dumas, D. Eichert, J. Dudala, Z. Setkowicz, Synchrotron FTIR micro-spectroscopy study of the rat hippocampal formation after pilocarpine-evoked seizures, J. Chem. Neuroanat. 40 (2010) 140–147. https://doi.org/10.1016/j.jchemneu.2010.03.008.

[68] M. Diem, S. Boydston-White, L. Chiriboga, Infrared spectroscopy of cells and tissues: shining light onto a novel subject, Appl. Spectrosc. 53 (1999) 148–161. https://doi.org/10.1366/0003702991946712.

[69] J. Liquier, R. Taillandier, Infrared spectroscopy of nucleic acids, in Infrared Spectroscopy of Biological Molecules, Wiley-Liss, New York, 1996.

[70] A. Nehlig, Age-dependent pathways of brain energy metabolism: the suckling rat, a natural model of the ketogenic diet, Epilepsy Res. 37 (1999) 211–221. https://doi.org/10.1016/S0920-1211(99)00073-X.

[71] M.L. Prins, J.H. Matsumoto, The collective therapeutic potential of cerebral ketone metabolism in traumatic brain injury, J. Lipid Res. 55 (2014) 2450–2457. https://doi.org/10.1194/jlr.R046706.

[72] E. Herrera, D. Gómez-Coronado, M.A. Lasunción, Lipid Metabolism in Pregnancy, Neonatology 51 (1987) 70–77. https://doi.org/10.1159/000242635.

[73] J. Chwiej, A. Skoczen, K. Janeczko, J. Kutorasinska, K. Matusiak, H. Figiel, P. Dumas, C. Sandt, Z. Setkowicz, The biochemical changes in hippocampal formation occurring in normal and seizure experiencing rats as a result of a ketogenic diet, Analyst 140 (2015) 2190–2204. https://doi.org/10.1039/C4AN01857E.

[74] A. Nehlig, A. Pereira de Vasconcelos, Glucose and ketone body utilization by the brain of neonatal rats, Prog. Neurobiol. 40 (1993) 163–220. https://doi.org/10.1016/0301-0082(93)90022-K.

[75] H.-G. Bae, T.K. Kim, H.Y. Suk, S. Jung, D.-G. Jo, White matter and neurological disorders, Arch. Pharm. Res. 43 (2020) 920–931. https://doi.org/10.1007/s12272-020-01270-x.

[76] S. Safaiyan, S. Besson-Girard, T. Kaya, L. Cantuti-Castelvetri, L. Liu, H. Ji, M. Schifferer, G. Gouna, F. Usifo, N. Kannaiyan, D. Fitzner, X. Xiang, M.J. Rossner, M. Brendel, O. Gokce, M. Simons, White matter aging drives microglial diversity, Neuron 109 (2021) 1100-1117.e10. https://doi.org/10.1016/j.neuron.2021.01.027.

[77] I.A. McKenzie, D. Ohayon, H. Li, J. Paes de Faria, B. Emery, K. Tohyama, W.D. Richardson, Motor skill learning requires active central myelination, Science (1979). 346 (2014) 318–322. https://doi.org/10.1126/science.1254960.

[78] A. Kister, I. Kister, Overview of myelin, major myelin lipids, and myelin-associated proteins, Front. Chem. 10 (2023). https://doi.org/10.3389/fchem.2022.1041961.

[79] R. Chrast, G. Saher, K.-A. Nave, M.H.G. Verheijen, Lipid metabolism in myelinating glial cells: lessons from human inherited disorders and mouse models, J. Lipid Res. 52 (2011) 419–434. https://doi.org/10.1194/jlr.R009761.

[80] T. Takahashi, T. Suzuki, Role of sulfatide in normal and pathological cells and tissues, J. Lipid Res. 53 (2012) 1437–1450. https://doi.org/10.1194/jlr.R026682.

[81] M. Pintado-Sierra, I. García-Álvarez, A. Bribián, E.M. Medina-Rodríguez, R. Lebrón-Aguilar, L. Garrido, F. de Castro, A. Fernández-Mayoralas, J.E. Quintanilla-López, A comprehensive profiling of sulfatides in myelin from mouse brain using liquid chromatography coupled to high-resolution accurate tandem mass spectrometry, Anal. Chim. Acta 951 (2017) 89–98. https://doi.org/10.1016/j.aca.2016.11.054.

[82] H. Baba, T. Ishibashi, The Role of Sulfatides in Axon–Glia Interactions, in: 2019: pp. 165–179. https://doi.org/10.1007/978-981-32-9636-7_11.

[83] N. Zhang, X. Yu, J. Xie, H. Xu, New Insights into the Role of Ferritin in Iron Homeostasis and Neurodegenerative Diseases, Mol. Neurobiol. 58 (2021) 2812–2823. https://doi.org/10.1007/s12035-020-02277-7.

[84] D.A. Bonilla, R.B. Kreider, J.R. Stout, D.A. Forero, C.M. Kerksick, M.D. Roberts, E.S. Rawson, Metabolic Basis of Creatine in Health and Disease: A Bioinformatics-Assisted Review, Nutrients 13 (2021) 1238. https://doi.org/10.3390/nu13041238.

[85] S. Singh, A.K. Dash, Creatine Monohydrate, in: 2009: pp. 1–35. https://doi.org/10.1016/S1871-5125(09)34001-7.

[86] J. Guo, S. Chen, Y. Zhang, J. Liu, L. Jiang, L. Hu, K. Yao, Y. Yu, X. Chen, Cholesterol metabolism: physiological regulation and diseases, MedComm (Beijing). 5 (2024). https://doi.org/10.1002/mco2.476.

[87] R.H. Knopp, X. Zhu, Multiple Beneficial Effects of Estrogen on Lipoprotein Metabolism, J. Clin. Endocrinol. Metab. 82 (1997) 3952–3954. https://doi.org/10.1210/jcem.82.12.4472.

[88] A.E. Smith-Ryan, H.E. Cabre, J.M. Eckerson, D.G. Candow, Creatine Supplementation in Women's Health: A Lifespan Perspective, Nutrients 13 (2021) 877. https://doi.org/10.3390/nu13030877.

[89] J.R. Rettberg, J. Yao, R.D. Brinton, Estrogen: A master regulator of bioenergetic systems in the brain and body, Front. Neuroendocrinol. 35 (2014) 8–30. https://doi.org/10.1016/j.yfrne.2013.08.001.

[90] M.S. Patel, O.E. Owen, DEVELOPMENT AND REGULATION OF LIPID SYNTHESIS FROM KETONE BODIES BY RAT BRAIN, J. Neurochem. 28 (1977) 109–114. https://doi.org/10.1111/j.1471-4159.1977.tb07715.x.

[91] A.A.M. Morris, Cerebral ketone body metabolism, J. Inherit. Metab. Dis. 28 (2005) 109–121. https://doi.org/10.1007/s10545-005-5518-0.

[92] A.S. Saab, K.-A. Nave, Myelin dynamics: protecting and shaping neuronal functions, Curr. Opin. Neurobiol. 47 (2017) 104–112. https://doi.org/10.1016/j.conb.2017.09.013.

[93] C.M. Filley, R.D. Fields, White matter and cognition: making the connection, J. Neurophysiol. 116 (2016) 2093–2104. https://doi.org/10.1152/jn.00221.2016.

[94] S. Bells, J. Lefebvre, G. Longoni, S. Narayanan, D.L. Arnold, E.A. Yeh, D.J. Mabbott, White matter plasticity and maturation in human cognition, Glia 67 (2019) 2020–2037. https://doi.org/10.1002/glia.23661.

[95] J. Chwiej, M. Palczynska, A. Skoczen, K. Janeczko, J. Cieslak, R. Simon, Z. Setkowicz, Elemental changes of hippocampal formation occurring during postnatal brain development, Journal of Trace Elements in Medicine and Biology 49 (2018) 1–7. https://doi.org/10.1016/j.jtemb.2018.04.030.

[96] A. Zampelas, E. Magriplis, New Insights into Cholesterol Functions: A Friend or an Enemy?, Nutrients 11 (2019) 1645. https://doi.org/10.3390/nu11071645.

[97] C.M. Klinge, Estrogenic control of mitochondrial function, Redox Biol. 31 (2020) 101435. https://doi.org/10.1016/j.redox.2020.101435.

[98] S. Arnold, M.B. Victor, C. Beyer, Estrogen and the regulation of mitochondrial structure and function in the brain, J. Steroid Biochem. Mol. Biol. 131 (2012) 2–9. https://doi.org/10.1016/j.jsbmb.2012.01.012.

[99] C.M. Klinge, Estrogens regulate life and death in mitochondria, J. Bioenerg. Biomembr. 49 (2017) 307–324. https://doi.org/10.1007/s10863-017-9704-1.

[100] B.T. Palmisano, L. Zhu, J.M. Stafford, Role of Estrogens in the Regulation of Liver Lipid Metabolism, in: 2017: pp. 227–256. https://doi.org/10.1007/978-3-319-70178-3_12.

11. Publikacje spoza rozprawy

1. Aleksandra Wilk, Natalia Wilkosz, Marzena Rugiel, Marta Saluga, Kamil Kawon, Tetiana Stepanenko, Katarzyna Bulat, Aleksandra Wajda, Michał Szuwarzynski, Anna Zajaczkowska, Anna Morgunowicz, Grzegorz Chodaczek, Víctor Navarro-Esteve, David Perez-Guaita, Joanna Chwiej, Katarzyna M. Marzec, *Next-generation diabetes diagnostics: spectrochemical staging of red blood cells using vibrational spectroscopy*, Journal of Advanced Research, 2026.
2. Aleksandra Wilk, Karolina W. Łakomy, Zuzanna Setkowicz, Karol Szary, Regina Stachura, Katarzyna M. Marzec, Marzena Rugieł, Joanna Chwiej, *Elemental and biomolecular changes in serum as indicators of SPION action in the body: analysis using TXRF, FTIR and Raman spectroscopy*, Scientific Reports, 15(1), artykuł 45585, s. 1-12 (2025).
3. Agnieszka Dróżdż, Dominika Kubera, Alina Olender, Wojciech Dabrowski, Magdalena Szukala, Sylwia Wosko, Joanna Chwiej, Marzena Rugieł, Kamil Kawoń, Mariusz Gagoś, *ATR-FTIR spectroscopic markers indicating drug resistance in selected Candida strains*, Scientific Reports, 15(18130), s. 1-15 (2025).
4. Aleksandra Wilk, Zuzanna Setkowicz, Katarzyna Matusiak, Eva Margui Grabulosa, Marzena Rugieł, Paula Kasprzyk, Agnieszka Dróżdż, Joanna Chwiej, *Sex-dependent differences in the elemental composition of internal organs determined via total reflection X-ray fluorescence and inductively coupled plasma optical emission spectroscopy*, Biomedicines, 12(2774), s. 1-15 (2024).
5. Marzena Rugieł, Natalia Janik-Olchawa, Julia Kowalczyk, Karolina Pomorska, Maciej Sitarz, Ewelina Bik, Daniel Horak, Michal Babic, Zuzanna Setkowicz, Joanna Chwiej, *Raman microscopy allows to follow internalization, subcellular accumulation and fate of iron oxide nanoparticles in cells*, Spectrochimica Acta Part A: Molecular and Biomolecular Spectroscopy, 323(124888), s. 1-11 (2024).
6. Kamil Kawoń, Marzena Rugieł, Zuzanna Setkowicz, Katarzyna Matusiak, Aldona Kubala-Kukuś, Ilona Stabrawa, Karol Szary, Zuzanna Rauk, Joanna Chwiej, *Ketogenic diet influence on the elemental homeostasis of internal organs is gender dependent*, Scientific Reports, 13(18448), s. 1-11 (2023).
7. Wojciech Kosiek, Zuzanna Rauk, Piotr Szulc, Anna Cichy, Marzena Rugieł, Joanna Chwiej, Krzysztof Janeczko, Zuzanna Setkowicz, *Ketogenic diet impairs neurological development of neonatal rats and affects biochemical composition of maternal brains: evidence of functional recovery in pups*, Brain Structure & Function, 227(3), s. 1099-1113 (2022).
8. Marzena Rugieł, Zuzanna Setkowicz, Agnieszka Drozdz, Krzysztof Janeczko, Justyna Kutorasińska, Joanna Chwiej, *The use of Fourier transform infrared microspectroscopy for the determination of biochemical anomalies of the hippocampal formation characteristic for the kindling model of seizures*, ACS Chemical Neuroscience, 12(24), s. 4564-4579 (2021).

12. Lista wystąpień konferencyjnych wygłoszonych osobiście

1. Marzena Rugieł, Zuzanna Setkowicz, Mateusz Czyżycki, Wojciech Kosiek, Zuzanna Rauk, Rolf Simon, Tilo Baumbach, Joanna Chwiej, SR-XRF microscopy in the study of the impact of ketogenic diet used during pregnancy on the nervous system of offspring, European conference on X-Ray Spectrometry: EXRS 2024, National Centre for Scientific Research "Demokritos", Ateny, Grecja, 24-28 czerwca 2024, plakat.
2. Marzena Rugieł, Zuzanna Setkowicz-Janeczko, Mateusz Czyżycki, Wojciech Kosiek, Zuzanna Rauk, Rolf Simon, Tilo Baumbach, Joanna Chwiej, The use of synchrotron X-ray fluorescence microscopy to assess the elemental composition of the brain of rats exposed to the ketogenic diet during prenatal life, International Conference on Development and Applications of Nuclear Technologies NUTECH 2023, Akademia Górniczo-Hutnicza im. Stanisława Staszica w Krakowie, Kraków, Polska, 20-22 września 2023, prezentacja ustna.
3. Marzena Rugieł, Wojciech Kosiek, Zuzanna Rauk, Zuzanna Setkowicz, Joanna Chwiej, The influence of the ketogenic diet used in pregnancy on the nervous system development in offspring - spectroscopic study, HERCULES European School 2023, European Synchrotron Radiation Facility (ESRF), Grenoble, Francja, 9 marca 2023, plakat.
4. Marzena Rugieł, Wojciech Kosiek, Zuzanna Rauk, Zuzanna Setkowicz, Joanna Chwiej, The influence of ketogenic diet used in pregnancy on the nervous system development in offspring - FTIR microspectroscopy study, XVIth International Conference on Molecular Spectroscopy ICMS 2022, Akademia Górniczo-Hutnicza im. Stanisława Staszica w Krakowie, Szczawnica, Polska, 11-14 września 2022, prezentacja ustna.
5. Marzena Rugieł, Wojciech Kosiek, Zuzanna Rauk, Zuzanna Setkowicz, Joanna Chwiej, The use of biospectroscopic methods for evaluation of the influence of ketogenic diet used in pregnancy on the nervous system development in offspring, 1st Interdisciplinary annual PhD conference on Material Science and Innovative Technologies, Łukasiewicz Research Network - Krakow Institute of Technology, Kraków, Polska, 19-20 maja 2022, prezentacja ustna.
6. Marzena Rugieł, Agnieszka Dróżdż, Justyna Kutorasińska, Zuzanna Setkowicz, Joanna Chwiej, The molecular changes appearing in the hippocampal formation as a result of repetitive electrical stimulation: FTIR microspectroscopy study, 11th International Conference on Advanced Vibrational Spectroscopy (ICAVS 11), Jagiellonian University in Krakow, Kraków, Polska, 23-26 sierpnia 2021, plakat.
7. Marzena Rugieł, Justyna Kutorasińska, Agnieszka Dróżdż, Zuzanna Setkowicz, Joanna Chwiej, The use of FTIR microspectroscopy for the investigation of molecular changes in the hippocampal formation after repetitive electrical stimulation, XXII Polish Conference on Biocybernetics and Biomedical Engineering (PCBBE), Committee of Biocybernetics and Biomedical Engineering of the Polish Academy of Sciences, Polish Society of Biomedical Engineering, Warszawa, Polska, 19-21 maja 2021, plakat.

13. Lista współautorskich wystąpień konferencyjnych

1. Joanna Chwiej, Karolina Olbrich, Marzena Rugieł, Kamil Kawoń, Aleksandra Wilk, Aldona Kubala-Kukuś, Agnieszka Dróżdż, Katarzyna Matusiak, Zuzanna Setkowicz, From bulk to spatial insight: TXRF and micro-XRF in biomedical investigations, TXRF 2025: 20th international conference on Total Reflection X-ray Fluorescence analysis and related methods, Uniwersytet Jana Kochanowskiego w Kielcach, Kielce, Polska, 9-12 września 2025.
2. Zuzanna Prus, Klaudia Szkadłubowicz, Joanna Mikusińska, Xymena Badura, Jagoda Worek, Kamil Kawoń, Marzena Rugieł, Joanna Chwiej, Katarzyna Styszko, Małgorzata Wilk, The effect of hydrothermal carbonization of sewage sludge on microplastic behaviour, CYPRUS 2025: 12th international conference on Sustainable Solid Waste Management, National Technical University of Athens, Pafos, Cypr, 25-28 czerwca 2025.
3. Zuzanna Prus, Klaudia Szkadłubowicz, Joanna Mikusińska, Jagoda Worek, Xymena Badura, Marzena Rugieł, Kamil Kawoń, Joanna Chwiej, Katarzyna Styszko, Małgorzata Wilk, Investigating the impact of hydrothermal carbonization on microplastic contamination in biosolids, HTC 2025: 4th International Symposium on Hydrothermal Carbonization, Louisiana State University, Nowy Orlean, Luizjana, USA, 21-24 stycznia, 2025.
4. Karolina W. Łakomy, Aleksandra Wilk, Zuzanna Setkowicz, Karol Szary, Ilona Stabrawa, Marzena Rugieł, Joanna Chwiej, Metody spektroskopowe w badaniach zmian pierwiastkowych i molekularnych osocza wywołanych podaniem superparamagnetycznych nanocząstek tlenków żelaza o potencjale teranostycznym - [Spectroscopic methods in the study of elemental and molecular changes in plasma induced by the administration of superparamagnetic iron oxide nanoparticles with theranostic potential], 18 kongres Polskiego Towarzystwa Fizyki Medycznej, Polskie Towarzystwo Fizyki Medycznej, Poznań, Polska, 19-21 września 2024.
5. Joanna Chwiej, Marzena Rugieł, Kamil Kawoń, Katarzyna Matusiak, Aldona Kubala-Kukuś, Ilona Stabrawa, Karol Szary, Zuzanna Rauk, Zuzanna Setkowicz, Mikrospektroskopia atomowa i molekularna w badaniach bezpieczeństwa i potencjału terapeutycznego diety ketogenicznej - [Atomic and molecular microspectroscopy in studies of the safety and therapeutic potential of the ketogenic diet], 18 kongres Polskiego Towarzystwa Fizyki Medycznej, Polskie Towarzystwo Fizyki Medycznej, Poznań, Polska, 19–21 września 2024.
6. Karolina Papacz, Magdalena Wytrwał, Ewa Ocłoń, Jolanta Gol, Aleksandra Wilk, Marzena Rugieł, Joanna Chwiej, Microplastics influence on human lung cells - subcellular identification of particles with the use of Raman spectroscopy, XXVIII ICORS: 28th International Conference on Raman Spectroscopy, Rzym, Włochy, 28 lipca - 2 sierpnia 2024.
7. Kamil Kawoń, Natalia Wilkosz, Marzena Rugieł, Aleksandra Wilk, Marta Saługa, Katarzyna Bułat, Tetiana Stepanenko, Joanna Chwiej, Katarzyna Marzec, Raman spectroscopy and associated techniques reveals abnormalities in RBC membranes in diabetic mice, XXVIII ICORS: 28th International Conference on Raman Spectroscopy, Rzym, Włochy, 28 lipca - 2 sierpnia 2024.
8. Kamil Kawoń, Zuzanna Setkowicz, Marzena Rugieł, Zuzanna Rauk, Mateusz Czyżycki, Ilaria Carlomango, Giuliana Aquilanti, Joanna Chwiej, Spectroscopic methods in the study of the effect of the ketogenic diet on glial scar development in terms of time and gender, JS2024: 5th Jagiellonian Symposium on Advances in particle physics and medicine, Uniwersytet Jagielloński, Kraków, Polska, 29 czerwca – 7 lipca 2024.
9. Jolanta Gol, Zuzanna Setkowicz, Aleksandra Wilk, Marzena Rugieł, Joanna Chwiej, Infrared microspectroscopy in the study of biodistribution, kinetics and fate of microplastics in the body, ESAS 2024: European Symposium on Analytical Spectrometry, Centrum Nauk Biologiczno-Chemicznych Uniwersytetu Warszawskiego, Warszawa, Polska, 24–28 czerwca 2024.
10. Joanna Chwiej, Karolina Olbrich, Aleksandra Wilk, Kamil Kawoń, Marzena Rugieł, Aldona Kubala-Kukus, Dariusz Banaś, Eva Margui, Ramón Fernández-Ruiz, Katarzyna Matusiak, Paweł Wróbel, Zuzanna Setkowicz, The total reflection X-ray fluorescence applications

in biomedical research, EXRS 2024 : European conference on X-Ray Spectrometry, National Centre for Scientific Research "Demokritos", Ateny, Grecja, 24-28 czerwca 2024.

11. Marzena Rugieł, Madalena Wytrwał, Mariola Kukuła, Daria Oczkiewicz, Karolina Lechowicz, Ewa Ocłoń, Joanna Chwiej, Microplastics toxicity in vitro studies - subcellular identification of particles with the use of Raman spectroscopy, 19th confocal Raman imaging symposium, WITec GmbH, Ulm, Niemcy, 25-27 września, 2023.
12. Aleksandra Wilk, Zuzanna Setkowicz-Janeczko, Katarzyna Matusiak, Marzena Rugieł, Zuzanna Rauk, Paula Kasprzyk, Joanna Chwiej, Assessment of gender differences in elemental composition of chosen organs by the means of TXRF and ICP-based techniques, International Conference on Development and Applications of Nuclear Technologies NUTECH 2023, Akademia Górniczo-Hutnicza im. Stanisława Staszica w Krakowie, Kraków, Polska, 20-22 września 2023.
13. Kamil Kawoń, Marzena Rugieł, Aldona Kubala-Kukuś, Katarzyna Matusiak, Ilona Stabrawa, Karol Szary, Zuzanna Setkowicz, Zuzanna Rauk, Joanna Chwiej, TXRF study of ketogenic diet influence on the elemental composition of selected rat organs, International Conference on Development and Applications of Nuclear Technologies NUTECH 2023, Akademia Górniczo-Hutnicza im. Stanisława Staszica w Krakowie, Kraków, Polska, 20-22 września 2023.
14. Joanna Chwiej, Natalia Janik-Olchawa, Agnieszka Dróżdż, Aleksandra Wajda, Maciej Sitarz, Daniel Horak, Michal Babic, Jolanta Gol, Zuzanna Setkowicz-Janeczko, Aleksandra Wilk, Marzena Rugieł, Katarzyna Matusiak, Christoph Sandt, Ferenc Borondics, Magdalena Wytrwał-Sarna, Methods of vibrational microspectroscopy for the assessment of the internalization, biodistribution, fate and toxicity of nano- and microparticles at in vitro and in vivo conditions, ICAVS-12: 12th International Conference on Advanced Vibrational Spectroscopy, Uniwersytet Jagielloński, Kraków, Polska, 27 sierpnia - 1 września 2023.
15. Joanna Chwiej, Karolina Płaneta, Agnieszka Dróżdż, Katarzyna Matusiak, Marzena Rugieł, Aldona Kubala-Kukus, Mateusz Czyżycki, Rolf Simon, Tilo Baumbach, Zuzanna Setkowicz, The use of X-ray fluorescence based methods for the study of pathological processes occurring in living organism, EXRS 2022: European conference on X-Ray Spectrometry, University of Antwerp, Brugia, Belgia, 26 czerwca - 1 lipca 2022.

14. Staże, naukowe wyjazdy zagraniczne i inna aktywność naukowa

1. Udział w zimowej szkole pt. „Advanced Techniques for the Analysis of Novel Materials Strategic for Sustainability Transitions: I. Bioplasticss”, Piza, Włochy, 27.01-03.02.2024, w ramach projektu: Działanie 4. Projektu IDUB AGH (kierownik grantu dr hab. inż. Joanna Chwiej, prof. Uczelni).
2. Udział w realizacji grantu pomiarowego z wykorzystaniem promieniowania synchrotronowego w Elettra Sincrotrone Trieste, zakwalifikowanego do finansowania przez IAEA, Triest, Włochy, 26.11-03.12.2023 (kierownik grantu dr hab. inż. Joanna Chwiej, prof. Uczelni).
3. Udział w sympozjum „19th Confocal Raman Imaging Symposium 2023”, WITec GmbH, Ulm, Niemcy, 25.09-27.09.2023, w ramach projektu: Działanie 4. Projektu IDUB AGH (kierownik grantu dr hab. inż. Joanna Chwiej).
4. Udział w warsztatach „STAT-IR”, SOLEIL Synchrotron, Paryż, Francja, 15.10-18.10.2023, w ramach projektu: Działanie 4. Projektu IDUB AGH (kierownik grantu dr hab. inż. Joanna Chwiej, prof. Uczelni).
5. Udział w HERCULES European School 2023, Grenoble, Francja, Universiste Grenoble Alpes, 26.02-01.04.2023, w ramach projektu: Działanie 4. Projektu IDUB AGH (kierownik grantu dr hab. inż. Joanna Chwiej, prof. Uczelni).
6. Organizacja 17. Kongresu Polskiego Towarzystwa Fizyki Medycznej, Kraków, 30.09-02.10.2022, Akademia Górniczo-Hutnicza im. Stanisława Staszica w Krakowie.
7. Udział w warsztatach „Vienna-Budapest Joint Training School”, TU Wien, Atominstitut Radiation physics X-ray physics, Wiedeń, Austria, 06-08.07.2022, w ramach programu COST Action CA18130 - European Network for Chemical Elemental Analysis by Total Reflection X-Ray Fluorescence.

15. Projekty naukowe

1. Udział w projekcie realizowanym w ramach NCN Sonata BIS 10 pt. *„Spectroscopic and microscopic techniques in nano-probing, modeling and recognition of interactions between erythrocytes and vascular endothelial cells at the molecular level”*, nr UMO-2020/38/E/ST4/00197, 07.2023 – 09.2025 (kierownik dr hab. Katarzyna Marzec, prof. Uczelni).
2. Udział w projekcie realizowanym w ramach Działania 4. (System grantów uczelnianych na prace badawcze realizowane z udziałem doktorantów) Inicjatywa Doskonałości Uczelnia Badawcza AGH pt. *„Wpływ materiału rdzenia na toksyczność/biokompatybilność in vivo magnetycznych nanocząstek tlenków żelaza o potencjale teranostycznym”*, 2022-2024 (kierownik dr hab. inż. Joanna Chwiej, prof. Uczelni).
3. Realizacja minigrantu dla młodych naukowców i doktorantów ramach Działania 4. (System grantów uczelnianych na prace badawcze realizowane z udziałem doktorantów) Inicjatywa Doskonałości Uczelnia Badawcza AGH pt. *„Ocena wpływu diety ketogenicznej stosowanej w okresie ciąży na postnatalny rozwój układu nerwowego potomstwa – badania z użyciem biospektroskopii atomowej i cząsteczkowej oraz zaawansowanych technik analizy danych wielowymiarowych”*, 1.10.2021-31.08.2022 (kierownik minigrantu mgr inż. Marzena Rugieł).
4. Udział w grancie pomiarowym w KARA Synchrotron (Karlsruhe Institute of Technology, Karlsruhe, Niemcy) pt. *„Element anomalies in brains of the rat progeny fed with ketogenic drugs during pregnancy”*, nr A2021-031-019293, 03-09.2021 r. finansowanym z subwencji.

16. Oświadczenia współautorów publikacji

Autorzy (alfabetycznie)	A1	A2	M1
Baumbach Tilo		+	
Bryłowska Zofia			+
Chwiej Joanna	+	+	+
Czyżycki Mateusz		+	
Dróżdż Agnieszka			+
Kawoń Kamil	+		
Kosiek Wojciech	+		
Rauk Zuzanna	+		
Rugieł Marzena	+	+	+
Setkowicz Zuzanna	+	+	+
Simon Rolf		+	
Wilk Aleksandra			+

Karlsruhe,
10.02.2026

.....
(Place and date)

Prof. Dr. Tilo Baumbach
(Professional title, name and surname)

Karlsruhe Institute of Technology
Institute for Photon Science and Synchrotron Radiation
(Institution)

Hermann-von-Helmholtz-Platz 1
76344 Eggenstein-Leopoldshafen, Germany
(Address)

CO-AUTHOR CONFIRMATION

As a co-author of the publication entitled:

"Element Changes Occurring in Brain Point at the White Matter Abnormalities in Rats Exposed to the Ketogenic Diet During Prenatal Life" (ACS Chem Neurosci, 2024)

Hereby, I declare that my contribution to the above-mentioned paper was to grant a beamtime at the beamline FLUO at the KIT Synchrotron Light Source.

I declare that a separatable part of the above-mentioned paper demonstrates the individual contribution from **Marzena Rugieł** in developing research concept, conducting the experiment as well as analyzing and interpreting the results. I give my permission for the above-mentioned paper to be submitted by **Marzena Rugieł** as a part of her doctoral dissertation in the form of a thematically coherent of papers published in scientific journals.

Kraków 27.04.2026
(miejscowość, data)

Zofia Bryłowska
(imię i nazwisko)

Wydział Fizyki i Informatyki Stosowanej
Akademia Górniczo-Hutnicza
im. Stanisława Staszica w Krakowie
(instytucja)
al. Adama Mickiewicza 30, 30-059 Kraków
(adres)

OŚWIADCZENIE

Jako współautor pracy pod tytułem:

"Fourier Transform Infrared Imaging Supported by Raman Spectroscopy Reveals Biochemical Changes in Adult Rat Brains Following Prenatal Exposure to a Ketogenic Diet" (w recenzji w czasopismie ACS Chemical Neuroscience),

oświadczam, że mój wkład w powstanie ww. pracy obejmował współudział w opracowaniu metodologii, prowadzeniu badań oraz walidacji otrzymanych wyników.

Oświadczam, że samodzielna oraz możliwa do wyodrębnienia część ww. pracy wykazuje indywidualny wkład mgr inż. **Marzeny Rugieł** przy opracowaniu koncepcji badań, przeprowadzeniu części eksperymentalnej, analizie i interpretacji wyników niniejszej pracy. Jednocześnie wyrażam zgodę na przedłożenie ww. pracy przez mgr inż. **Marzenę Rugieł** jako część rozprawy doktorskiej w formie spójnego tematycznie zbioru artykułów opublikowanych w czasopismach naukowych.

[redacted]

04.05.2026 Kraków
(miejscowość, data)

Dr hab. inż. Joanna Chwiej, prof. AGH
(tytuł zawodowy, imię i nazwisko)

Wydział Fizyki i Informatyki Stosowanej
Akademia Górniczo-Hutnicza
im. Stanisława Staszica w Krakowie
(instytucja)
al. Adama Mickiewicza 30, 30-059 Kraków
(adres)

OŚWIADCZENIE

Jako współautor prac pod tytułem:

1. "Does Ketogenic Diet Used in Pregnancy Affect the Nervous System Development in Offspring? - FTIR Microspectroscopy Study" (ACS Chemical Neuroscience, 2023),
2. "Element Changes Occurring in Brain Point at the White Matter Abnormalities in Rats Exposed to the Ketogenic Diet During Prenatal Life" (ACS Chemical Neuroscience, 2024),
3. "Fourier Transform Infrared Imaging Supported by Raman Spectroscopy Reveals Biochemical Changes in Adult Rat Brains Following Prenatal Exposure to a Ketogenic Diet" (w recenzji w czasopismie ACS Chemical Neuroscience),

oświadczam, że mój wkład w powstanie ww. prac obejmował:

- udział w opracowaniu koncepcji i metodologii badań,
- nadzór nad realizacją badań,
- udział w przygotowaniu manuskryptów oraz odpowiedzi dla recenzentów.

Oświadczam, że samodzielna oraz możliwa do wyodrębnienia część ww. pracy wykazuje indywidualny wkład mgr inż. **Marzeny Rugieł** przy opracowaniu koncepcji badań, przeprowadzeniu części eksperymentalnej, analizie i interpretacji wyników niniejszej pracy. Jednocześnie wyrażam zgodę na przedłożenie ww. pracy przez mgr inż. **Marzenę Rugieł** jako część rozprawy doktorskiej w formie spójnego tematycznie zbioru artykułów opublikowanych w czasopismach naukowych.

[redacted]

Hamburg,
12.01.2026

.....
(Place and date)

Dr. Mateusz Czyżycki
(Professional title, name and surname)

Karlsruhe Institute of Technology
Institute for Photon Science and Synchrotron Radiation
(Institution)

Hermann-von-Helmholtz-Platz 1
76344 Eggenstein-Leopoldshafen, Germany
(Address)

CO-AUTHOR CONFIRMATION

As a co-author of the publication entitled:

"Element Changes Occurring in Brain Point at the White Matter Abnormalities in Rats Exposed to the Ketogenic Diet During Prenatal Life" (ACS Chem Neurosci, 2024),

Hereby, I declare that my contribution to the above-mentioned paper consisted of conducting the experiment at the beamline FLUO at the KIT Synchrotron Light Source and revising the manuscript.

I declare that a separatable part of the above-mentioned paper demonstrates the individual contribution from **Marzena Rugieł** in developing research concept, conducting the experiment as well as analyzing and interpreting the results. I give my permission for the above-mentioned paper to be submitted by **Marzena Rugieł** as a part of her doctoral dissertation in the form of a thematically coherent of papers published in scientific journals.

Kraków, 23.04.2026
(miejscowość, data)

Dr inż. Agnieszka Dróżdż
(tytuł zawodowy, imię i nazwisko)

Wydział Fizyki i Informatyki Stosowanej
Akademia Górniczo-Hutnicza
im. Stanisława Staszica w Krakowie
(instytucja)
al. Adama Mickiewicza 30, 30-059 Kraków
(adres)

OŚWIADCZENIE

Jako współautor pracy pod tytułem:

"Fourier Transform Infrared Imaging Supported by Raman Spectroscopy Reveals Biochemical Changes in Adult Rat Brains Following Prenatal Exposure to a Ketogenic Diet" (w recenzji w czasopismie ACS Chemical Neuroscience),

oświadczam, że mój wkład w powstanie ww. pracy obejmował współudział w opracowaniu metodologii, prowadzeniu badań oraz walidacji otrzymanych wyników.

Oświadczam, że samodzielna oraz możliwa do wyodrębnienia część ww. pracy wykazuje indywidualny wkład mgr inż. **Marzeny Rugieł** przy opracowaniu koncepcji badań, przeprowadzeniu części eksperymentalnej, analizie i interpretacji wyników niniejszej pracy. Jednocześnie wyrażam zgodę na przedłożenie ww. pracy przez mgr inż. **Marzenę Rugieł** jako część rozprawy doktorskiej w formie spójnego tematycznie zbioru artykułów opublikowanych w czasopismach naukowych.

[redacted]

Kraków, 08.04.2026
(miejscowość, data)

Mgr Kamil Kawoń
(tytuł zawodowy, imię i nazwisko)

Wydział Fizyki i Informatyki Stosowanej
Akademia Górniczo-Hutnicza
im. Stanisława Staszica w Krakowie
(instytucja)

al. Adama Mickiewicza 30, 30-059 Kraków
(adres)

OŚWIADCZENIE

Jako współautor pracy pod tytułem:

"Does Ketogenic Diet Used in Pregnancy Affect the Nervous System Development in Offspring? - FTIR Microspectroscopy Study" (ACS Chemical Neuroscience, 2023),

oświadczam, że mój wkład w powstanie ww. pracy obejmował wsparcie w pomiarach i analizie oraz rewizję pierwotnej wersji manuskryptu.

Oświadczam, że samodzielna oraz możliwa do wyodrębnienia część ww. pracy wykazuje indywidualny wkład mgr inż. **Marzeny Rugieł** przy opracowaniu koncepcji badań, przeprowadzeniu części eksperymentalnej, analizie i interpretacji wyników niniejszej pracy. Jednocześnie wyrażam zgodę na przedłożenie ww. pracy przez mgr inż. **Marzenę Rugieł** jako część rozprawy doktorskiej w formie spójnego tematycznie zbioru artykułów opublikowanych w czasopismach naukowych.

Skorzyszyn 10.04.2026
(miejscowość, data)

Mgr inż. Wojciech Kosiek
(tytuł zawodowy, imię i nazwisko)

Instytut Zoologii i Badań Biomedycznych
Uniwersytet Jagielloński
(instytucja)
Gronostajowa 9, 30-387, Kraków
(adres)

OŚWIADCZENIE

Jako współautor pracy pod tytułem:

"Does Ketogenic Diet Used in Pregnancy Affect the Nervous System Development in Offspring? - FTIR Microspectroscopy Study" (ACS Chemical Neuroscience, 2023),

oświadczam, że mój wkład w powstanie ww. pracy obejmował wsparcie w przeprowadzeniu eksperymentu na zwierzętach.

Oświadczam, że samodzielna oraz możliwa do wyodrębnienia część ww. pracy wykazuje indywidualny wkład mgr inż. **Marzeny Rugieł** przy opracowaniu koncepcji badań, przeprowadzeniu części eksperymentalnej, analizie i interpretacji wyników niniejszej pracy. Jednocześnie wyrażam zgodę na przedłożenie ww. pracy przez mgr inż. **Marzenę Rugieł** jako część rozprawy doktorskiej w formie spójnego tematycznie zbioru artykułów opublikowanych w czasopismach naukowych.

[redacted]

Kraków, 08.04.2026
(miejscowość, data)

Mgr Zuzanna Rauk
(tytuł zawodowy, imię i nazwisko)

Instytut Zoologii i Badań Biomedycznych
Uniwersytet Jagielloński
(instytucja)
Gronostajowa 9, 30-387, Kraków
(adres)

OŚWIADCZENIE

Jako współautor pracy pod tytułem:

"Does Ketogenic Diet Used in Pregnancy Affect the Nervous System Development in Offspring? - FTIR Microspectroscopy Study" (ACS Chemical Neuroscience, 2023),

oświadczam, że mój wkład w powstanie ww. pracy obejmował wsparcie w przeprowadzeniu eksperymentu na zwierzętach.

Oświadczam, że samodzielna oraz możliwa do wyodrębnienia część ww. pracy wykazuje indywidualny wkład mgr inż. **Marzeny Rugieł** przy opracowaniu koncepcji badań, przeprowadzeniu części eksperymentalnej, analizie i interpretacji wyników niniejszej pracy. Jednocześnie wyrażam zgodę na przedłożenie ww. pracy przez mgr inż. **Marzenę Rugieł** jako część rozprawy doktorskiej w formie spójnego tematycznie zbioru artykułów opublikowanych w czasopismach naukowych.

Kraków, 05.05.26 r.
(miejscowość, data)

Mgr inż. Marzena Rugieł
(tytuł zawodowy, imię i nazwisko)

Wydział Fizyki i Informatyki Stosowanej
Akademia Górniczo-Hutnicza
im. Stanisława Staszica w Krakowie
(instytucja)
al. Adama Mickiewicza 30, 30-059 Kraków
(adres)

OŚWIADCZENIE

Jako współautor prac pod tytułem:

1. "Does Ketogenic Diet Used in Pregnancy Affect the Nervous System Development in Offspring? - FTIR Microspectroscopy Study" (ACS Chemical Neuroscience, 2023),
2. "Element Changes Occurring in Brain Point at the White Matter Abnormalities in Rats Exposed to the Ketogenic Diet During Prenatal Life" (ACS Chemical Neuroscience, 2024),
3. "Fourier Transform Infrared Imaging Supported by Raman Spectroscopy Reveals Biochemical Changes in Adult Rat Brains Following Prenatal Exposure to a Ketogenic Diet" (w recenzji w czasopismie ACS Chemical Neuroscience),

oświadczam, że mój wkład w powstanie ww. prac obejmował

1. Udział w opracowaniu koncepcji i metodologii badań, przygotowanie próbek, wykonanie pomiarów, przeprowadzenie analiz, dyskusję wyników, walidację, przygotowanie tekstu publikacji;

2. Udział w opracowaniu koncepcji i metodologii badań, przygotowanie próbek, przeprowadzenie analiz, dyskusję wyników, walidację, przygotowanie tekstu publikacji;

3. Udział w opracowaniu koncepcji i metodologii badań, przygotowanie próbek, wykonanie pomiarów, przeprowadzenie analiz, dyskusję wyników, walidację, przygotowanie tekstu publikacji;

Oświadczam także, że samodzielna oraz możliwa do wyodrębnienia część ww. prac wykazuje mój indywidualny wkład przy opracowaniu koncepcji badań, przeprowadzeniu części eksperymentalnej, analizie i interpretacji wyników niniejszych prac.

[redacted]

Kraków 28 04 26

Prof. dr hab. Zuzanna Setkowicz-Janeczko
(tytuł zawodowy, imię i nazwisko)

Instytut Zoologii i Badań Biomedycznych
Uniwersytet Jagielloński
(instytucja)
Gronostajowa 9, 30-387, Kraków
(adres)

OŚWIADCZENIE

Jako współautor prac pod tytułem:

1. "Does Ketogenic Diet Used in Pregnancy Affect the Nervous System Development in Offspring? - FTIR Microspectroscopy Study" (ACS Chemical Neuroscience, 2023),
2. "Element Changes Occurring in Brain Point at the White Matter Abnormalities in Rats Exposed to the Ketogenic Diet During Prenatal Life" (ACS Chemical Neuroscience, 2024),
3. "Fourier Transform Infrared Imaging Supported by Raman Spectroscopy Reveals Biochemical Changes in Adult Rat Brains Following Prenatal Exposure to a Ketogenic Diet" (w recenzji w czasopismie ACS Chemical Neuroscience),

oświadczam, że mój wkład w powstanie ww. prac obejmował oświadczam, że mój wkład w powstanie ww. prac obejmował przeprowadzenie części eksperymentu na zwierzętach oraz twórczą dyskusję manuskryptów.

Oświadczam, że samodzielna oraz możliwa do wyodrębnienia część ww. pracy wykazuje indywidualny wkład mgr inż. **Marzeny Rugieł** przy opracowaniu koncepcji badań, przeprowadzeniu części eksperymentalnej, analizie i interpretacji wyników niniejszej pracy. Jednocześnie wyrażam zgodę na przedłożenie ww. pracy przez mgr inż. **Marzenę Rugieł** jako część rozprawy doktorskiej w formie spójnego tematycznie zbioru artykułów opublikowanych w czasopismach naukowych.

[redacted]

Karlsruhe
05.02.2026

.....
(Place and date)

Dr. Rolf Simon
(Professional title, name and surname)

Karlsruhe Institute of Technology
Institute for Photon Science and Synchrotron Radiation
(Institution)

Hermann-von-Helmholtz-Platz 1
76344 Eggenstein-Leopoldshafen, Germany
(Address)

CO-AUTHOR CONFIRMATION

As a co-author of the publication entitled:

"Element Changes Occurring in Brain Point at the White Matter Abnormalities in Rats Exposed to the Ketogenic Diet During Prenatal Life" (ACS Chem Neurosci, 2024),

Hereby, I declare that my contribution to the above-mentioned paper was to prepare the beamline FLUO at the KIT Synchrotron Light Source.

I declare that a separatable part of the above-mentioned paper demonstrates the individual contribution from **Marzena Rugieł** in developing research concept, conducting the experiment as well as analyzing and interpreting the results. I give my permission for the above-mentioned paper to be submitted by **Marzena Rugieł** as a part of her doctoral dissertation in the form of a thematically coherent of papers published in scientific journals.

Kraków, 28/04/2026
(miejscowość, data)

Mgr inż. Aleksandra Wilk
(tytuł zawodowy, imię i nazwisko)

Wydział Fizyki i Informatyki Stosowanej
Akademia Górniczo-Hutnicza
im. Stanisława Staszica w Krakowie
(instytucja)
al. Adama Mickiewicza 30, 30-059 Kraków
(adres)

OŚWIADCZENIE

Jako współautor pracy pod tytułem:

"Fourier Transform Infrared Imaging Supported by Raman Spectroscopy Reveals Biochemical Changes in Adult Rat Brains Following Prenatal Exposure to a Ketogenic Diet" (w recenzji w czasopismie ACS Chemical Neuroscience),

oświadczam, że mój wkład w powstanie ww. pracy obejmował wsparcie w badaniach oraz rewizję pierwotnej wersji manuskryptu.

Oświadczam, że samodzielna oraz możliwa do wyodrębnienia część ww. pracy wykazuje indywidualny wkład mgr inż. **Marzeny Rugiel** przy opracowaniu koncepcji badań, przeprowadzeniu części eksperymentalnej, analizie i interpretacji wyników niniejszej pracy. Jednocześnie wyrażam zgodę na przedłożenie ww. pracy przez mgr inż. **Marzenę Rugiel** jako część rozprawy doktorskiej w formie spójnego tematycznie zbioru artykułów opublikowanych w czasopismach naukowych.

[redacted]

17. Oryginalne wersje publikacji stanowiących podstawę rozprawy doktorskiej

A1. Marzena Rugiel, Zuzanna Setkowicz-Janeczko, Wojciech Kosiek, Zuzanna Rauk, Kamil Kawon, Joanna Chwiej, *Does Ketogenic Diet Used in Pregnancy Affect the Nervous System Development in Offspring? - FTIR Microspectroscopy Study*, ACS Chem Neurosci 14 (2023) 2775–2791.

Suplement do pracy A1

A2. Marzena Rugieł, Zuzanna Setkowicz, Mateusz Czyzycki, Rolf Simon, Tilo Baumbach, Joanna Chwiej, *Element Changes Occurring in Brain Point at the White Matter Abnormalities in Rats Exposed to the Ketogenic Diet During Prenatal Life*, ACS Chem Neurosci 15 (2024) 3932-3944.

Suplement do pracy A2

M1. Marzena Rugiel, Zuzanna Setkowicz, Agnieszka Drozdz, Aleksandra Wilk, Zofia Brylowska, Joanna Chwiej, *Fourier Transform Infrared Imaging Supported by Raman Spectroscopy Reveals Biochemical Changes in Adult Rat Brains Following Prenatal Exposure to a Ketogenic Diet*, (w recenzji w czasopismie ACS Chemical Neuroscience).

Suplement do pracy M1

ACS Chemical Neuroscience

pubs.acs.org/chemneuro Research Article

Does Ketogenic Diet Used in Pregnancy Affect the Nervous System Development in Offspring?—FTIR Microspectroscopy Study

Marzena Rugiel,[§] Zuzanna Setkowicz-Janeczko,[§] Wojciech Kosiek, Zuzanna Rauk, Kamil Kawon, and Joanna Chwiej*

Cite This: *ACS Chem. Neurosci.* 2023, 14, 2775−2791 Read Online

ACCESS | Metrics & More | Article Recommendations | Supporting Information

ABSTRACT: Anti-seizure medications used during pregnancy may have transient or long-lasting impact on the nervous system of the offspring. Therefore, there is a great need to search for alternative therapies for pregnant women suffering from seizures. One of the solutions may be the use of the ketogenic diet (KD), which has been successfully applied as a treatment of drug-resistant epilepsy in children and adults. However, the risks associated with the use of this dietary therapy during pregnancy are unknown and more investigation in this area is needed. To shed some light on this problem, we attempted to determine the potential abnormalities in brain biomolecular composition that may occur in the offspring after the prenatal exposure to KD. To achieve this, the female Wistar rats were, during pregnancy, fed with either ketogenic or standard laboratory diet, and for further studies, their male offspring at 2, 6, or 14 days of age were used. Fourier transform infrared microspectroscopy was applied for topographic and quantitative analysis of main biological macromolecules (proteins, lipids, compounds containing phosphate and carbonyl groups, and cholesterol) in brain samples. Performed chemical mapping and further semi-quantitative and statistical analysis showed that the use of the KD during pregnancy, in general, does not lead to the brain biochemical anomalies in 2 and 6 days old rats. The exception from this rule was increased relative (comparing to proteins) content of compounds containing phosphate groups in white matter and cortex of 2 days old rats exposed prenatally to KD. Greater number of abnormalities was found in brains of the 14 days old offspring of KD-fed mothers. They included the increase of the relative level of compounds containing carbonyl groups (in cortex as well as multiform and molecular cells of the hippocampal formation) as well as the decrease of the relative content of lipids and their structural changes (in white matter). What is more, the surface of the internal capsule (structure of the white matter) determined for this age group was smaller in animals subjected to prenatal KD exposure. The observed changes seem to arise from the elevated exposition to ketone bodies during a fetus life and the disturbance of lipid metabolism after prenatal exposure to the KD. These changes may be also associated with the processes of compensation of mother organism, which slowly began to make up for the deficiencies in carbohydrates postpartum.

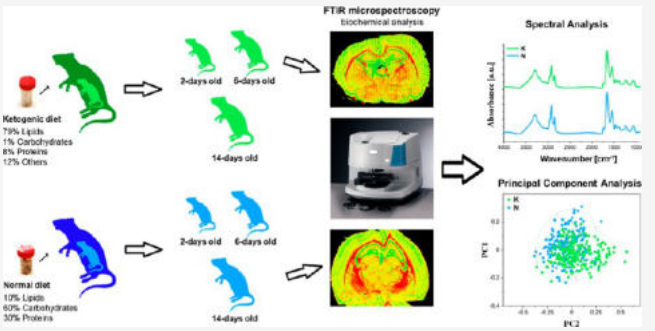

KEYWORDS: *ketogenic diet, pregnancy, brain development, Fourier transform infrared microspectroscopy, biochemical analysis, principal component analysis (PCA)*

INTRODUCTION

Treatment of patients with epilepsy during pregnancy is challenging because most of the available anticonvulsant drugs are teratogenic. Their use in critical stages of fetal development may lead to transient or long-term side effects in the nervous system of the offspring that involve anatomical and behavioral anomalies.[1,2] Because of the fact that antiepileptic medicines that are safe for pregnant women have not been found so far, the search for new pharmacological agents and alternative therapies that will both benefit the mother and be safe for the offspring is ongoing. One of the possibilities may be the utilization of a ketogenic diet (KD), which has been successfully used in the treatment of various type of epilepsy (including drug-resistant epilepsy) in infants, children, and adults.[3−7]

KD is a high-fat and low-carbohydrate diet that goal is to imitate a beneficial effects of fasting but without depriving the organism calories demanded to metabolism.[4,8] During KD, fat intake should be around 80% of total caloric consumption, thus changing the main energy source for metabolism from

Received: May 18, 2023
Accepted: July 5, 2023
Published: July 20, 2023

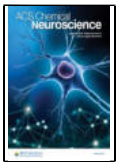

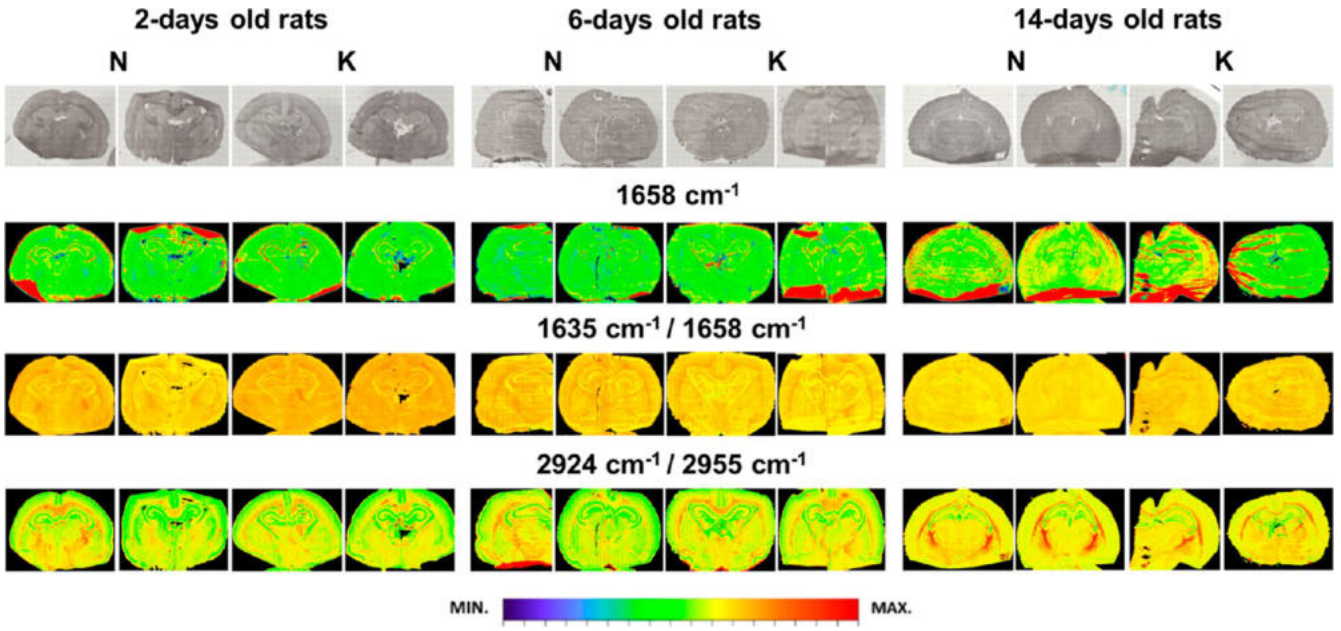

Figure 1. Exemplary chemical maps presenting the distributions of the amide I band as well as the ratios of absorbance at the wavenumbers of 1635 and 1658 cm^{-1} and 2924 and 2955 cm^{-1}, obtained for the brain samples taken from 2, 6, and 14 days old rats, which during prenatal life were exposed to the ketogenic (K) and normal (N) diets. Additionally, in the first row, the microscopic views of the scanned tissue areas are shown. For better visualization of anatomical details in brain sections, the reader is referred to Figures S1−S3 of the Supporting Information.

carbohydrates to fats and inducing ketone body production in the liver.[4,9,10] Acetoacetate, which spontaneously converts into acetone, and β-hydroxybutyrate are the ketone bodies (KBs) produced from fatty acids in the liver which during KD become the major source of energy for the central nervous system, replacing glucose.[4,10] KBs are able to cross the blood−brain barrier through monocarboxylate transporters (MCTs) of endothelial cells and astroglia.[11] However, the mechanism of KD action in patients with drug-resistant epilepsy is not fully understood.[12] The diet is supposed to act on many levels of nerve cells function, including the influence on the neuronal metabolism and excitability.[7] Its effectiveness in reducing the frequency of epileptic episodes may be associated with the increased availability of ketone bodies, the elevated concentration of free fatty acids and a decreased content of glucose in the blood and cerebrospinal fluid, which may have an anticonvulsant effect.[6,7] Other studies pointed out that KB also exert a direct inhibitory effect on the vesicular glutamate transport[13] and have an influence on neurotransmitter release and ATP sensitive potassium channels.[14]

There is a lack of medical data on the risks of using KD during pregnancy in humans.[15] According to our best knowledge, there are only two publications documenting the pregnancy of women treated with KD.[16,17] In the first article, a case of 19 year-old woman with glucose transporter type 1 deficiency syndrome (Glut1DS) treated with KD before and during gestation was presented.[16] Her child, also fed with KD as a neonate, was monitored for the next 5 years later and described as an asymptomatic and excelling developmentally.[16] The second article included two case reports using KD therapy for epilepsy during pregnancy.[17] The authors of the cited paper claim that non-pharmacological epilepsy therapies, including KD, may be effective during pregnancy. However, they also highlight the necessity of further patient and offspring monitoring to identify potential long term side effects of the dietary therapies.[17] The results of research based on the animal models have shown that the prenatal exposure to KD may cause the disruptions in the embryotic organ growth of rodents, lead to neuroanatomical changes and influence the behavior of offspring later in life.[18−20] According to Sussman et al. the brain is the organ especially susceptible to the changes influenced by KD and the possible anomalies include the relative reduction of the cortex, hippocampus, corpus callosum, fimbria, and the lateral ventricles and a relative increase of the hypothalamus and medulla volume.[20] As reported by the mentioned study, the observed abnormalities may be the consequence of certain brain regions preferences for ketones utilization during prenatal development and increased efficiency of energy production from them.[20] KD is also associated with the reduced protein intake. The lack of these macromolecules during pregnancy in rats reveal in persistent or reversible anatomical and functional changes to the brain of their pups, and may lead to the delay in the appearance of reflexes.[21,22] There is also a number of studies showing that a mother nutrition during pregnancy, especially high-fat diet, may affect the development of the progeny.[23−25] The numerous papers report negative effects of the exposure to such a diet at the prenatal stage.[26−30] However, there is also study suggesting that in utero exposure to high-fat diet may play a protective role for offspring brain health later in the adulthood.[31]

The methods of vibrational spectroscopy have not been used so far to image biochemical changes occurring in the brain as a result of prenatal exposure to KD in any of the animal models. In the present study, due to its many advantages, Fourier transform infrared (FTIR) microspectroscopy was applied. The method allows to obtain high quality molecular spectra (high signal to noise ratio and good spectral resolution) of various biological systems.[32] Because of high speed of data acquisition, it is possible to examine relatively large areas of samples and/or increase the statistics of examined cases what is very important in biomedical research. Another benefit of

https://doi.org/10.1021/acschemneuro.3c00331
ACS Chem. Neurosci. 2023, 14, 2775−2791

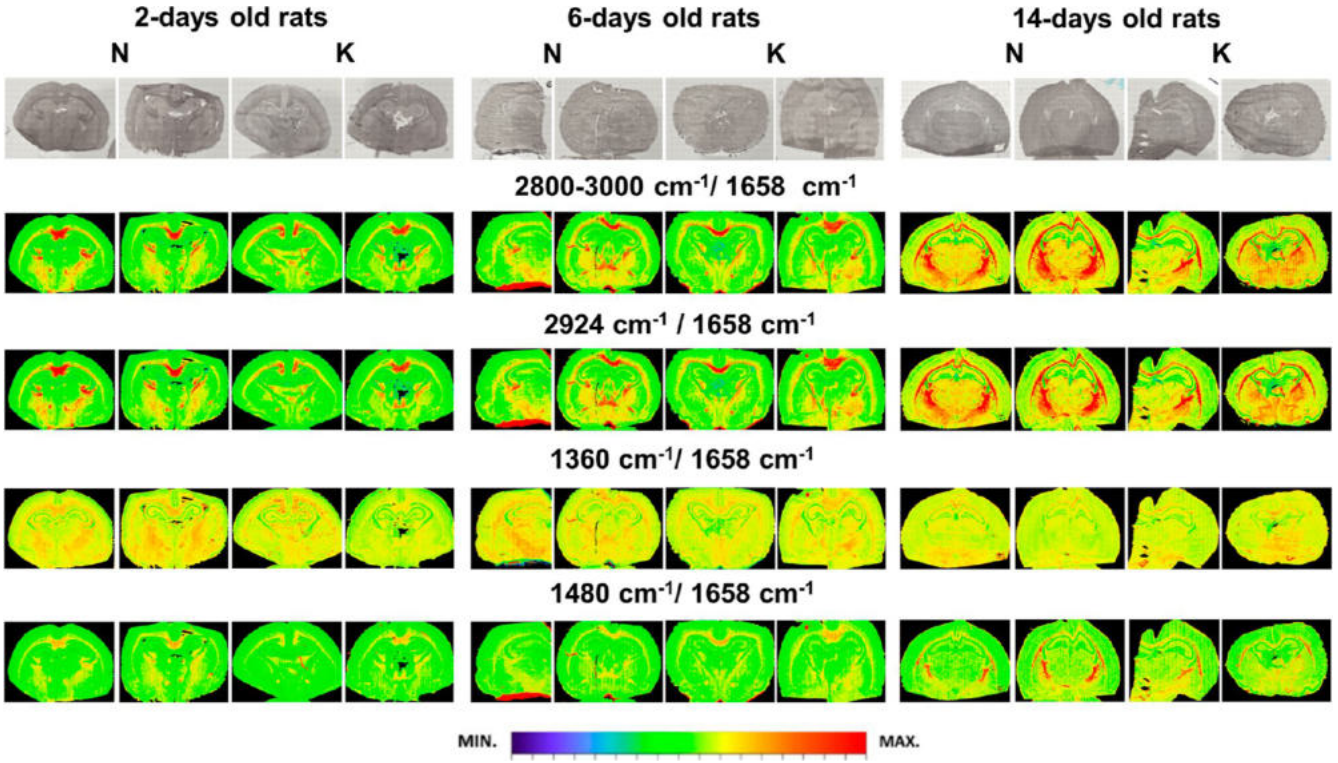

Figure 2. Exemplary chemical maps presenting the distributions of the relative (comparing to amide I band) intensity of selected absorption bands (2924, 1360, and 1480 cm^{-1}) and the lipid massif (2800−3000 cm^{-1}) for brain samples taken from 2, 6, and 14 days old rats, which during prenatal life were exposed to the ketogenic (K) and normal (N) diets. Additionally, in the first row, the microscopic views of the scanned tissue areas are shown.

FTIR microspetroscopy is the possibility of utilization, depending on the type of examined sample, of different measurement modes (transmission, transflection, and attenuated total reflection).[32] Thanks to the combination with optical microscopy, FTIR microspectroscopy allows to identify microscopic details in the sample, simultaneously providing the information concerning the presence of particular functional groups, bonding types or molecular conformations in the examined area.[32−34] What is more, it is non-invasive method and require only small amounts of material and minimum sample preparation.[32−34]

In our research, FTIR microspectroscopy was applied to identify the potential anomalies in the content and structure of main biological macromolecules that occur in the brain of the progeny of rats fed with KD during pregnancy. The levels of the biomolecules such as proteins, lipids, compounds containing phosphate and carbonyl groups, cholesterol, and its esters were included in the study. What is more, the changes in the structure of proteins and lipids were analyzed. In the study, we were focused on the period of intensive brain postnatal development and, therefore, the animals at the age of 2, 6, and 14 days old were included in the experiment.

RESULTS

To answer the question whether prenatal exposition to KD modifies the content and structure of biological macromolecules within the white matter, brain cortex, and hippocampal cellular layers, the biochemical composition of these areas was compared for offspring of females fed during pregnancy with ketogenic (K group) and normal (N group) diet. The performed comparisons included the qualitative analysis of chemical maps presenting the distribution of the absorption bands characteristic for the main biomolecules, as well as the evaluation of the spectral differences between the examined animal populations. Moreover, the semi-quantitative biochemical analysis based on absolute and relative intensities of selected absorption bands was done and statistical relevance of the observed differences between experimental groups and appropriate controls was verified with the Mann−Whitney *U* test.

Chemical Mapping. *Distribution of Proteins and Structural Changes of Proteins and Lipids.* As one can see from Figure 1, the chemical maps presenting the distribution of the amide I band intensity (1658 cm^{-1}) within examined brain slices did not show the differences in proteins accumulation between the rats from K and N groups at any stages of their postnatal development. Therefore, in the further study, the intensity of this band was applied as normalizing parameter when relative content of examined biomolecules in the tissue was calculated.

Also, for the ratio of the absorbance at the wavenumbers of 1635 and 1658 cm^{-1}, which is used to identify the changes in the relative secondary structure of proteins, none differences between experimental and control groups were noticed. The chemical maps imaged the ratio of the intensity of the bands at the wavenumbers of 2924 and 2955 cm^{-1} did not point at the existence of the anomalies in the structure of lipids in the 2 and 6 days old offspring of females fed with KD. For 14 days old rats, however, some differences in the surface of brain areas characterized by an elevated ratio of these lipid bands intensity were found. As one can see from Figure 1, the mentioned region is localized under the hippocampal formation and

https://doi.org/10.1021/acschemneuro.3c00331
ACS Chem. Neurosci. 2023, 14, 2775−2791

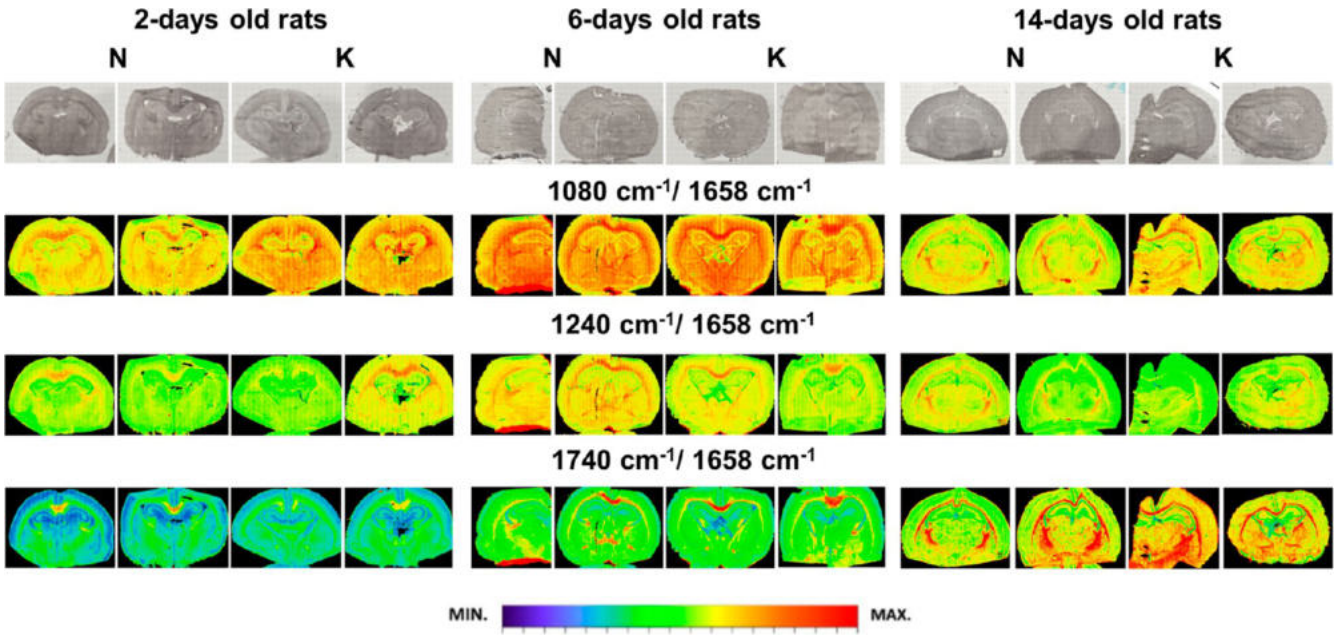

Figure 3. Exemplary chemical maps presenting the distributions of the relative (comparing to amide I band) intensity of 1080, 1240, and 1740 cm^{-1} absorption bands for brain samples taken from 2, 6, and 14 days old rats, which during prenatal life were exposed to the ketogenic (K) and normal (N) diets. Additionally, in the first row, the microscopic views of the scanned tissue areas are shown.

corresponds to the area of internal capsule and its surface is noticeably larger for animals from N comparing to K group.

The developmental changes observed in the offspring of females fed with ketogenic and standard diets were similar and included an increase in the intensity of the amide I band and the ratio of the examined lipid bands between the 6th and 14th days of rat postnatal life.

Distribution of Lipids, Cholesterol and Its Esters. The chemical maps obtained for 2 and 6 days old rats (Figure 2) did not show any general differences in the relative content of lipids (2800−3000/1658 and 2924/1658 cm^{-1}) as well as cholesterol and its esters (1360/1658 and 1480/1658 cm^{-1}) between the experimental groups and appropriate controls. However, for 14 days old rats, the area of internal capsule was significantly smaller for experimental group comparing to the control one and characterized by lower values of parameters describing the relative content of lipids as well as cholesterol and its esters. Moreover, as it can be seen in Figure 2, the relative content of the mentioned biomolecules was increasing significantly between 6th and 14th day of postnatal brain development independently on the mother diet.

Accumulation of Compounds Containing Phosphate and Carbonyl Groups. As one can see from the Figure 3, the general increase in the ratio of bands 1080/1658 cm^{-1} was found for 2 days old rats exposed in prenatal life to the KD. The similar relation was observed for the relative intensity of the band 1740 cm^{-1} originating from compounds containing carbonyl groups, but only in the case of 14 days old rats and, especially, for the area of the brain cortex.

Taking into account the stage of brain development, independently on the animal group (N or K), the highest relative intensity of the bands at 1080 and 1240 cm^{-1} was noticed for 6 days old rats. In turn, the intensity ratio of bands at 1740 and 1658 cm^{-1} showed gradual increase from 2nd until the 14th day of postnatal life.

Principal Component Analysis. In order to check potential biochemical abnormalities which may appear in the offspring of KD-fed females, the recorded spectral data were subjected to PCA. This advanced statistical method was used, separately, for IR spectra measured in the area of corpus callosum and brain cortex as well as in four cellular layers of hippocampal formation (granular, pyramidal, multiform, and molecular layer). The average spectra, their second derivatives and the results of PCA carried out on the second derivative spectra subjected to vector normalization are presented in the Figures 4, 5, and 6 for the 2, 6, and 14 days old rats, respectively. The performed PCA showed, for all examined brain regions and cellular layers as well as any stages of postnatal development, that the absorption spectra recorded for animals from experimental and control groups did not differ significantly. As the analysis took into account all the components of the collected IR spectra, its results suggest that there are no global quantitative biomolecular differences between the offspring of females fed during pregnancy with ketogenic and normal diets.

Mann−Whitney U Test. The next step of the study was semi-quantitative analysis of the spectral data. For each animal, the absolute or relative mean intensities of the chosen absorption bands (Table 3) in the areas/cellular layers of interest were calculated. The intensities were calculated as integrated peak areas. The obtained results are compared in Figures 7−9, presenting the minimum and maximum values as well as medians of the biochemical parameters determined for particular experimental groups (K_2, K_6, and K_14) and appropriate controls (N_2, N_6, and N_14).

To verify if KD used during prenatal life modifies the content and structure of biomolecules within the brains of the offspring, the semi-quantitative data were subjected to the statistical analysis with the use of the Mann−Whitney *U* test. The statistically significant differences found between experimental groups and controls were marked with stars in Figures 7−9.

None statistically relevant differences in the biomolecular composition of examined areas/cellular layers were found for the group of 6 days old rats. Such differences, however, were

https://doi.org/10.1021/acschemneuro.3c00331
ACS Chem. Neurosci. 2023, 14, 2775−2791

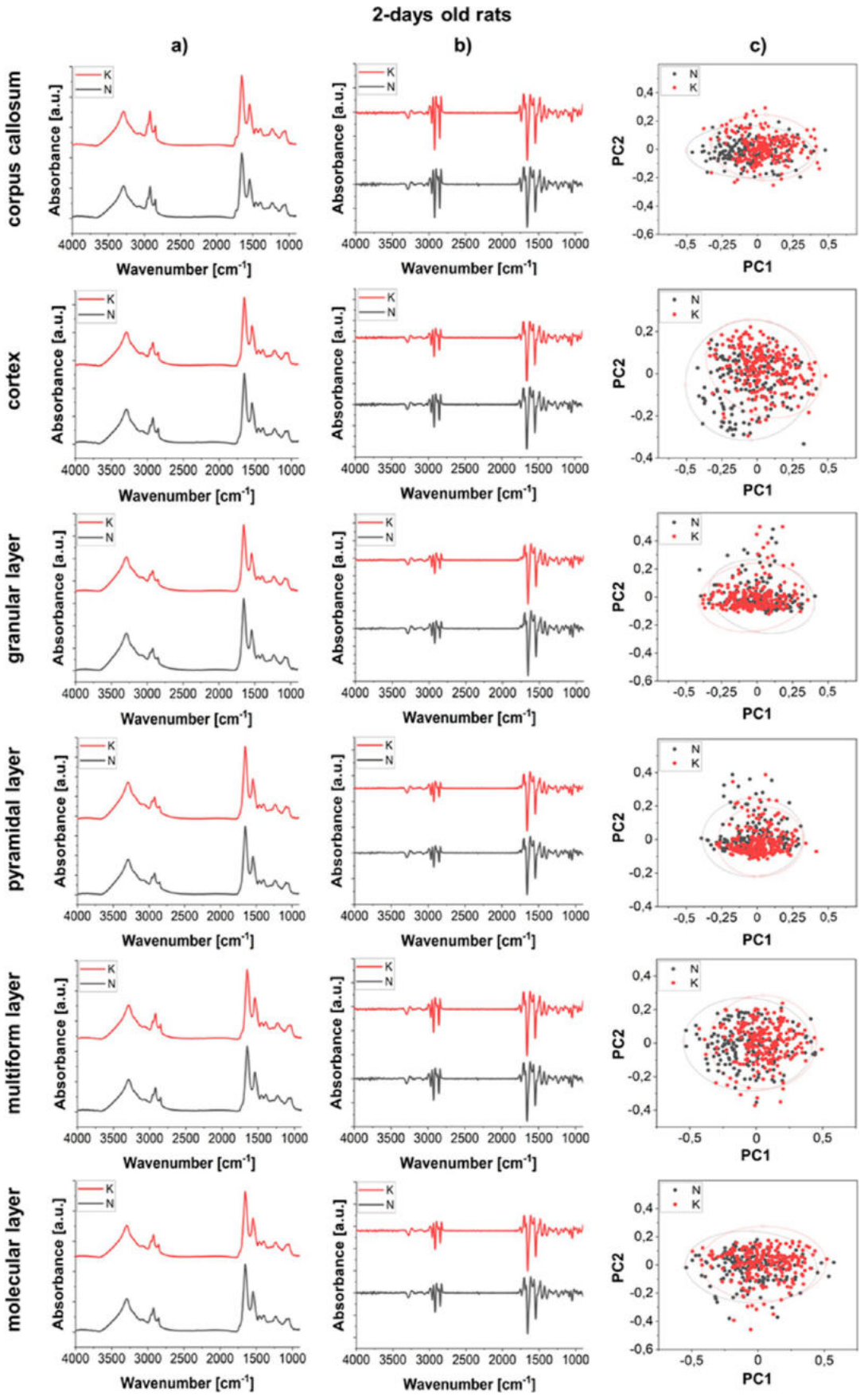

Figure 4. Comparison of the average spectra (column a) and the second derivative spectra (column b) obtained for corpus callosum, cerebral cortex, and hippocampal cellular layers (granular, pyramidal, multiform, and molecular) for 2 days old offspring of females fed with the KD (red) and standard laboratory diet (black). The results of PCA done on the second derivatives of vector-normalized spectra are shown in the column c.

https://doi.org/10.1021/acschemneuro.3c00331
ACS Chem. Neurosci. 2023, 14, 2775−2791

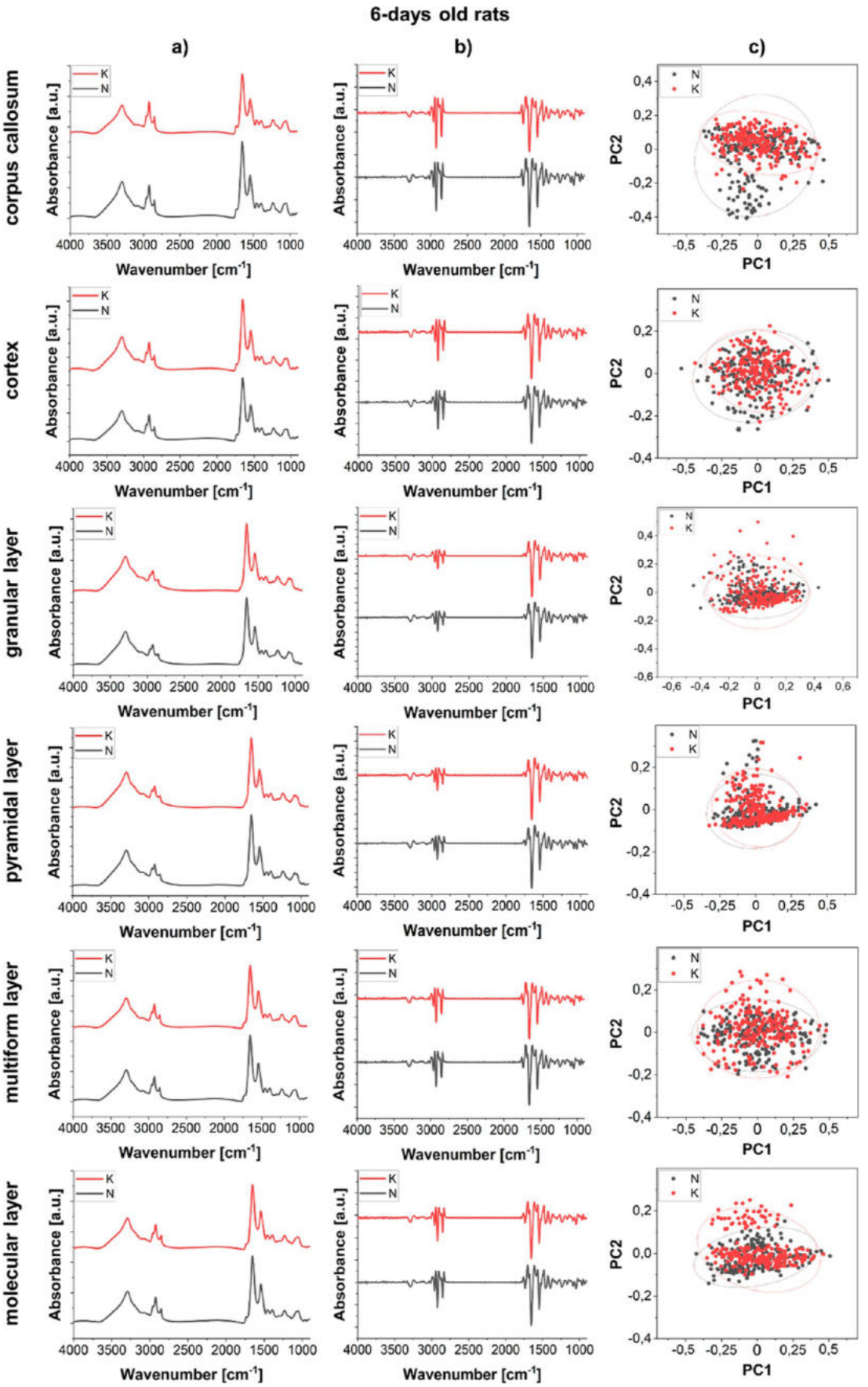

https://doi.org/10.1021/acschemneuro.3c00331
ACS Chem. Neurosci. 2023, 14, 2775−2791

Figure 5. continued

Figure 5. Comparison of the average spectra (column a) and the second derivative spectra (column b) obtained for corpus callosum, cerebral cortex, and hippocampal cellular layers (granular, pyramidal, multiform, and molecular) for 6 days old offspring of females fed with the KD (red) and standard laboratory diet (black). The results of PCA done on the second derivatives of vector-normalized spectra are shown in the column c.

detected in the part of white matter called corpus callosum in the case of 14 days old animals fed prenatally with KD. As one can see in Figures 7 and 8, they included the diminished relative intensities of lipid bands (2800−3000/1658 and 2924/1658 cm^{-1}) and structural changes of these biomolecules (2924/2955 cm^{-1}). For the same age group, higher relative content of compounds containing carbonyl groups (1740/1658 cm^{-1}) in cortex and two cellular layers of hippocampus (multiform and molecular) was also found (Figure 9), what confirmed the prior results of the topographic biomolecular analysis. As it can be seen in Figure 9, the performed statistical analysis allowed also to find the differences in the accumulation of biomolecules between 2 days old offspring of females fed with ketogenic and normal diet. The rats representing the experimental group showed higher relative content of compounds containing phosphate groups in corpus callosum (1080/1658 cm^{-1}) and cortex (1240/1658 cm^{-1}) comparing to the appropriate control group.

Relative Surfaces of the Internal Capsule Region. The results of chemical mapping performed for lipid bands showed that the surface of internal capsule (structure of the white matter) is smaller for the 14 days old offspring of females fed with KD than with normal one. To confirm this result the relative, comparing to the whole brain slice, surface of the area was determined for each animal. This was done on the basis of the chemical maps presenting the following biochemical parameters: 2800−3000/1658, 2924/1658, 2924/2955, and 1480/1658 cm^{-1}. To estimate the surface of the internal capsule and whole brain slice, ImageJ software (version 1.52a) was applied. The calculated relative surfaces were subjected to statistical evaluations with the use of the Mann−Whitney *U* test to verify the relevance of the differences between experimental animals and the appropriate controls. As one can see from Figure 10, the performed statistical analysis confirmed the prior qualitative observations done on the basis of the chemical mapping results.

DISCUSSION

In the present study, FTIR microspectroscopy was, for the first time, used to assess biochemical changes, which may occur in the nervous system of the offspring as an effect of maternal KD. The chemical mapping was performed on the whole brain slices which included the dorsal part of the hippocampal formation.

Analysis of chemical maps obtained for 2 and 6 days old animals, mothers of which were fed with normal or KD during pregnancy, generally did not show the differences in the accumulation and structure of examined biomolecules. The only exception from this observation concerned the ratio of 1080/1658 cm^{-1} bands intensity for 2 days old rats. Namely, the mentioned biochemical parameter presented higher values in case of the offspring of females fed during pregnancy with ketogenic chow. PCA did not show the relevance of the differences between the spectra recorded within the examined areas and cellular layers for experimental animals and the appropriate controls. Nonetheless, further semi-quantitative biochemical analysis and the results of Mann−Whitney *U* test confirmed the increase of the relative intensity of 1080 cm^{-1} absorption band for corpus callosum in case of 2 days old rats exposed prenatally to KD. What is more, a similar relation was detected for the relative intensity of the band at 1240 cm^{-1} within the brain cortex. The intensity of the bands at 1240 and 1080 cm^{-1} is related to the accumulation of the compounds containing phosphate groups, including nucleic acids, phospholipids, and may be the source of the information about the differences in the degree of phosphorylation of carbohydrates or glycoproteins.[35−37] The band at 1080 cm^{-1} is characteristic also for carbohydrates, and the changes in its intensity may reflect the fluctuations in the tissue glucose levels. The females fed during pregnancy with KD, on the 2nd day after delivery started to obtain standard chow which significantly increased the availability of carbohydrates for them. The change of mother diet, however, does not seem to be able to elevate immediately the brain glucose levels of the offspring. Especially, that maternal milk is always rich in fats and the transport capacity of glucose through the blood−brain barrier is poor at the beginning of the postnatal life.[38] Later, glucose availability in pups organism is progressively increasing due to both the increased expression of cerebral glucose transporters and the intensified activity of glycolytic enzymes. The final "adult" levels of glucose metabolic rates are achieved on the 30th day of postnatal life.[39]

Chemical mapping showed general elevated relative level of 1740 cm^{-1} band intensity for 14 days old rats from K group. The detailed semi-quantitative and statistical analysis confirmed these qualitative observations for cortex and two cellular layers of hippocampal formation (multiform and molecular). Because the levels of proteins did not differ between the experimental and control groups, the observed changes are associated with the increased accumulation of compounds containing carbonyl groups, such as phospholipids, cholesterol esters, and ketone bodies. Although lipids themselves have difficulties crossing the placenta, they can, indirectly, simplify the transport of other substances to the fetus.[40] During KD, free fatty acids present in the blood are carried to the liver where, in the process of β-oxidation, are degraded what leads to the production of KB: acetoacetate, acetone, and β-hydroxybutyrate.[41−44] All KB can more easily, comparing to glucose, cross the blood−brain barrier and therefore, they may be observed in the nervous tissue of KD fed animals.[42,44] The literature evidence indicates, moreover, that KB circulating in the maternal blood can easily cross the placenta and reach the same levels as those in maternal plasma.[40] The immature brain is able to take up KB from two to three times more efficiently than the mature one and use them for energy metabolism and lipid as well amino acid biosynthesis.[38,45−47] Our earlier study carried out on adults male Wistar rats showed increased intensity of the band at 1740 cm^{-1} in hippocampal formation of animals fed with KD.[42] On the other hand, we did not notice an elevated level of this band in the females fed with KD 2 days postpartum, although the level of β-hydroxybutyrate in

https://doi.org/10.1021/acschemneuro.3c00331
ACS Chem. Neurosci. 2023, 14, 2775−2791

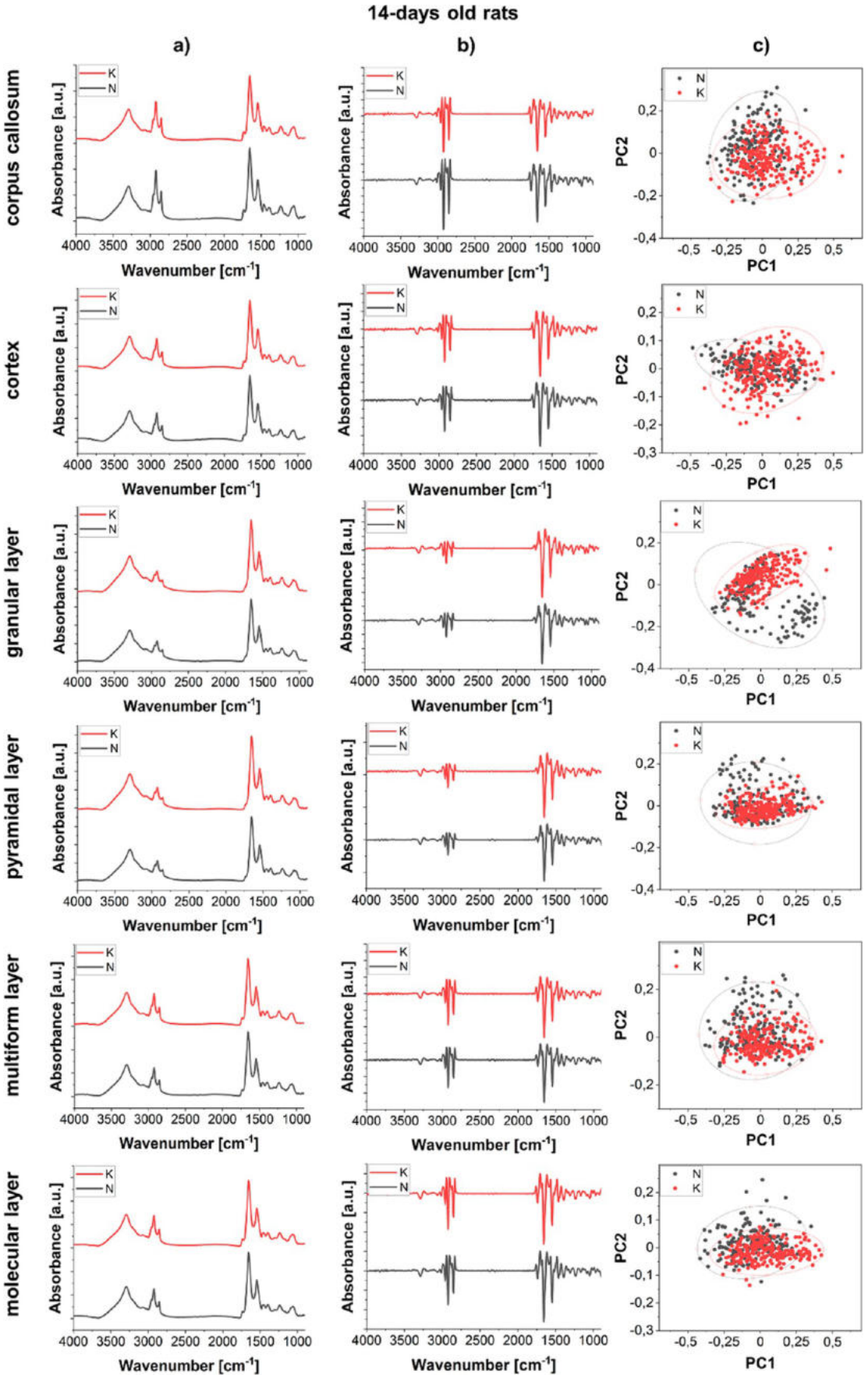

https://doi.org/10.1021/acschemneuro.3c00331
ACS Chem. Neurosci. 2023, 14, 2775−2791

Figure 6. continued

Figure 6. Comparison of the average spectra (column a) and the second derivative spectra (column b) obtained for corpus callosum, cerebral cortex, and hippocampal cellular layers (granular, pyramidal, multiform, and molecular) for 14 days old offspring of females fed with the KD (red) and standard laboratory diet (black). The results of PCA done on the second derivatives of vector-normalized spectra are shown in the column c.

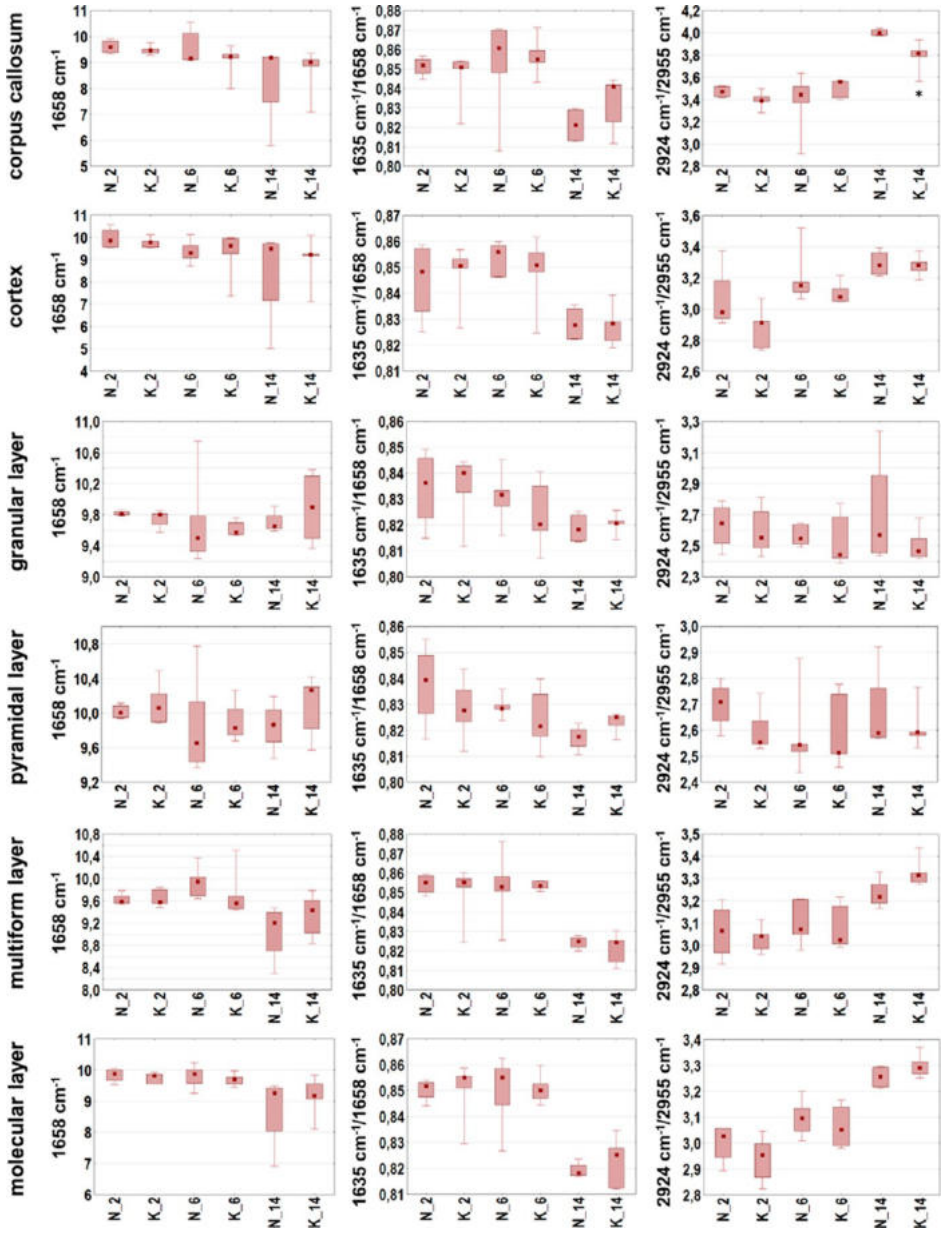

Figure 7. Box-and-whisker plots presenting the spread of the biochemical parameters values (integrated band areas or their ratios) in corpus callosum, cortex, and four hippocampal layers (granular, pyramidal, multiform, and molecular) for experimental and control rats (K and N groups, respectively) at examined stages of postnatal development (2, 6, and 14 days of life). Statistically significant differences (Mann−Whitney *U* test, 95% confidence level) between experimental groups and appropriate controls were marked with *.

their blood was significantly higher both on the day of fertilization as well as on 4th, 15th, and 20th gestational day.[10]

Some crucial observations have been done for the area of white matter of 14 days old offspring of rats fed prenatally with KD. The qualitative analysis of chemical maps showing the relative content of lipids (2800−3000/1658, 2924/1658 cm^{-1}), cholesterol, and its esters (1480/1658 cm^{-1}), as well as the changes in the lipid structure (2924/2955 cm^{-1}), revealed smaller surface of the internal capsule area in the case of the offspring of KD-fed females. The relevance of the mentioned effect was confirmed by the further semi-quantitative biochemical analysis and the results of the Mann−Whitney *U* test, which showed also lower relative content of lipids and their structural abnormalities for other white matter area, namely, corpus callosum. The results obtained are quite surprising taking into account the fact that lipids are the main energy source during KD. What is more, the accumulation of fatty acids in the brain of animals from the K

https://doi.org/10.1021/acschemneuro.3c00331
ACS Chem. Neurosci. 2023, 14, 2775−2791

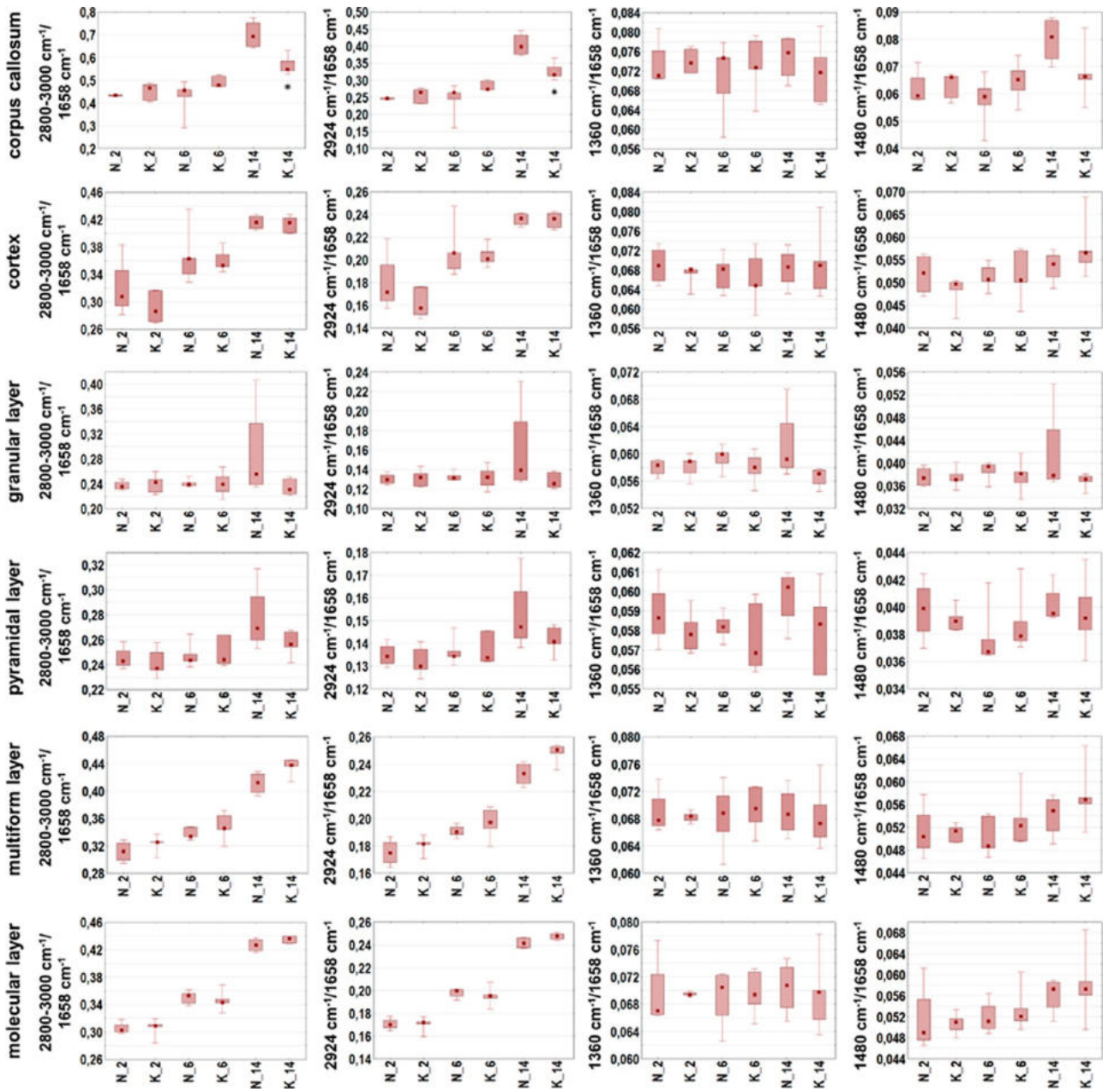

Figure 8. Box-and-whisker plots presenting the spread of the biochemical parameters values (integrated band areas or their ratios) in corpus callosum, cortex, and four hippocampal layers (granular, pyramidal, multiform, and molecular) for experimental and control rats (K and N groups, respectively) at examined stages of postnatal development (2, 6, and 14 days of life). Statistically significant differences (Mann−Whitney *U* test, 95% confidence level) between experimental groups and appropriate controls were marked with *.

group should be greater, with the elevated level of the 1740 cm^{-1}. This absorption band is associated with KB, which are the precursors for the synthesis of lipids (mainly cholesterol) and amino acids, especially in the neonatal period.[48] They also constitute the substrates in the myelination process.[48] Therefore, one might expect that their elevated availability should rather lead to the increased area of the structures of the white matter. On the other hand, cerebral KB metabolism is regulated by the permeability of the blood−brain barrier (BBB), which in rats, increases during the suckling term, even if mothers did not obtain special, high-fat diet during pregnancy.[48] According to the study of Gjedde and Crone (1975), the BBB contains a transporter for short-chain monocarboxylic acids, such as KB and lactates.[49] Shortly after birth, the brain temporarily uses lactate as a source of metabolic substrates, followed by the suckling period in which metabolism is dependent mostly on ketones.[39] During lactation, the offspring has higher circulating ketone levels, elevated amount of the BBB transporters, and greater enzymatic activities of some ketone metabolizing enzymes.[39] In rat brain, changes in the three mitochondrial enzymes of KB utilization (3-hydroxybutyrate dehydrogenase, succinyl-CoA 3-oxoacid CoA transferase, and mitochondrial acetoacetyl-CoA thiolase) associated to the age are present.[48,50] Activity of these enzymes is relatively low at birth but steadily elevates through the lactation to a maximum at the time of weaning—about 21 days from delivery.[48,50] Reassuming, the changes in these enzyme activity are simultaneous to the changes in BBB

https://doi.org/10.1021/acschemneuro.3c00331
ACS Chem. Neurosci. 2023, 14, 2775−2791

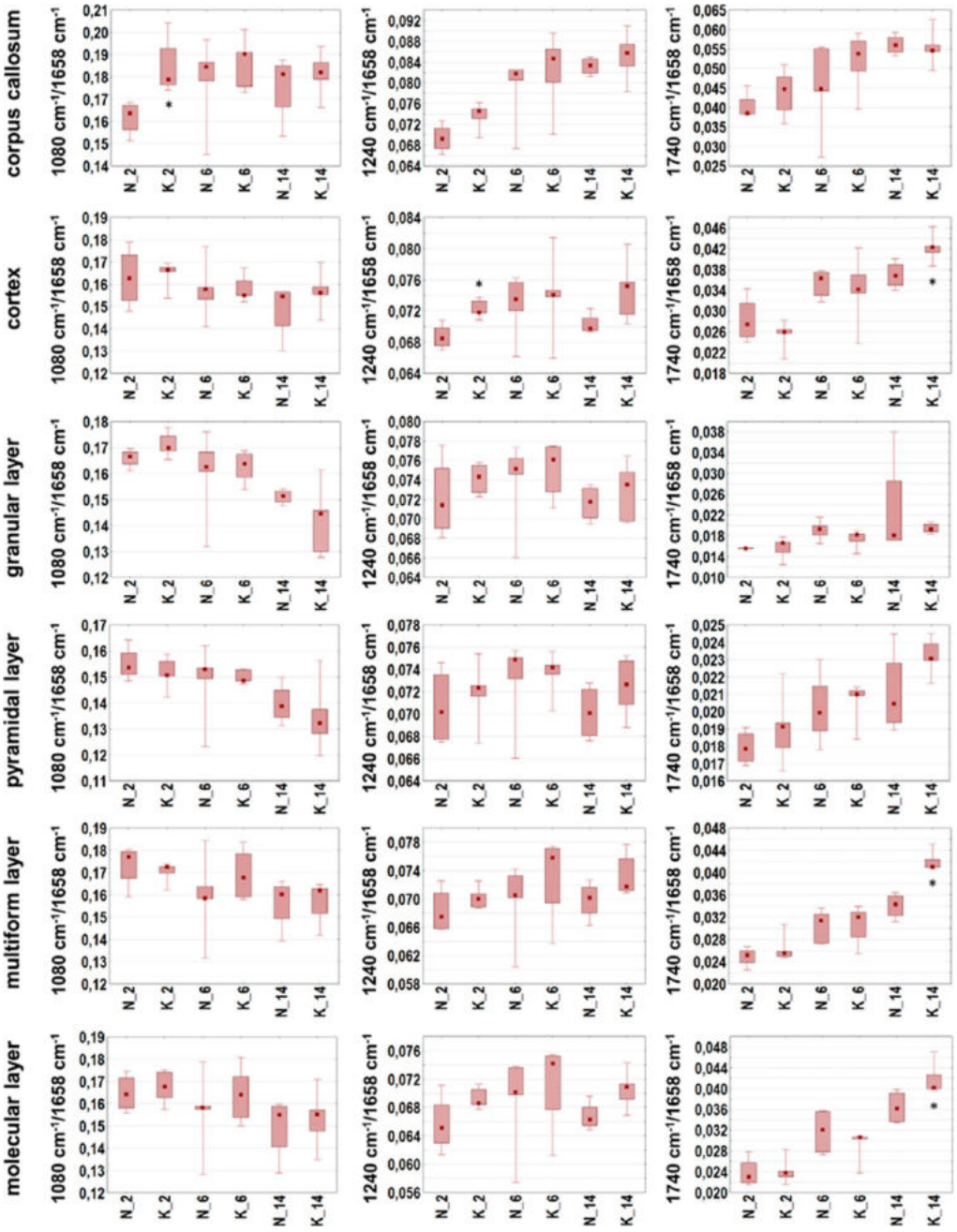

Figure 9. Box-and-whisker plots presenting the spread of the biochemical parameters values (integrated band areas or their ratios) in corpus callosum, cortex, and four hippocampal layers (granular, pyramidal, multiform, and molecular) for experimental and control rats (K and N groups, respectively) at examined stages of postnatal development (2, 6, and 14 days of life). Statistically significant differences (Mann−Whitney *U* test, 95% confidence level) between experimental groups and appropriate controls were marked with *.

permeability for KB and they together enable the brain to use the high levels of KB circulating in the blood during the suckling period.[48] In turn, the cytoplasmic enzymes of cerebral KB metabolism—acetoacetyl-CoA synthetase and cytoplasmic acetoacetyl-CoA thiolase—show the opposite changes in the activity with the development. The activity of both enzymes is the highest at birth and falls gradually to 25−50% of the initial value in adult rats.[48,50,51] The mentioned cytoplasmic enzymes are used for the synthesis of lipids, particularly cholesterol, which is necessary for the process of myelination.[48] Myelination starts in rat at birth and lowers considerably by the age of 30 days, correlating with the changes in the cytoplasmic enzymes activity.[48]

In the case of females, which additionally receive KD during feeding their offspring, the mentioned relations may be intensified and lead to metabolic acidosis. This may connect not only with the developmental brain disorders leading to worse performance of neurodevelopmental reflexes but also with the body mass reduction and the delayed muscle development.[10,18] In our study, the mothers of rats from K groups were fed with KD only during gestation and then since 2nd day postpartum, during suckling term, they obtained the normal diet. Taking into account this fact and the above-presented considerations, our outcomes may testify about the process of compensation occurring in mothers organisms. When they started to obtain the normal diet with the standard

https://doi.org/10.1021/acschemneuro.3c00331
ACS Chem. Neurosci. 2023, 14, 2775−2791

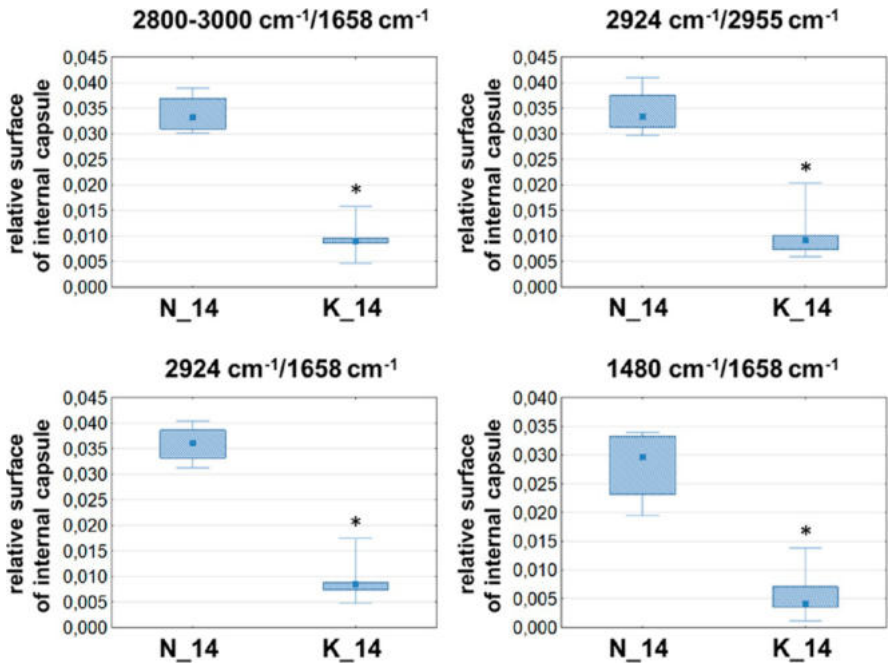

Figure 10. Box-and-whisker plots presenting the spread of the relative surface of the internal capsule for 14 days old experimental and control rats (K and N groups, respectively). Statistically significant differences (Mann−Whitney *U* test, 95% confidence level) between groups were marked with *.

amount of carbohydrates, their organisms slowly began to replenish with the deficiencies of these compounds, leaving KB to the young rats as the main source of the energy for the metabolism.

It is also worth mentioning here, that at the beginning of postnatal life, the offspring of mothers fed with KD during pregnancy had significantly lower body mass what was described in details in our previous work.[10] When, on the 2nd day postpartum, in KD-fed mothers, normal diet was introduced, and their progeny began to rebuilt the body mass very quickly. Although on the 6th day of postnatal life body mass was still significantly lower comparing to control group, the differences between the experimental and control group were much less pronounced. On the 14th day after birth, the offspring showed complete restoration of their body mass.[10] This is particularly interesting considering the fact that we have noticed an inverse relation in the biochemical changes in the brains of the experimental animals: almost none of the abnormalities were detected in 2 and 6 days old animals that were just regaining body weight, while some differences were evident in the 14 days old rats.

Taking into account the developmental changes in the relative intensity of the 1080 cm^{-1} band, it was the highest on the 6th day of postnatal life for both experimental and control animals with no significant differences between them. Also the relative intensity of the band at 1740 cm^{-1} changed during postnatal development but it gradually increased until the 14th day of animal life. Reassuming, the cerebral accumulation of the carbohydrates and KB changes together with the brain development and depends on the diet of mother during pregnancy. This study should be continued. Especially, the adult offspring of KD-treated pregnant females should be examined to verify if observed biochemical alterations are of temporary or permanent nature.

LIMITATIONS OF THE STUDY

This study and conclusions resulting from it have some limitations, which we would like to discuss in this chapter.

Interpretation of Measured Biochemical Parameters. FTIR microspectroscopy is based on the absorption of IR radiation by the vibrating molecules. The functional groups are the parts of the molecules that determine their major properties. Each functional group has its own discrete vibrational energy which depends on the atoms present in it, type, and strength of bonds. The vibrations are unique to particular functional groups and, therefore, can be used to identify molecules. FTIR microspectroscopy provides information on a wide range of molecular classes, such as lipids, proteins, carbohydrates, and others. Although these biomolecules have individual spectral signatures, which are called "finger prints", absorption bands tend to overlap if the biomolecules have common molecular vibrational modes. Because of that, the use of integrated bands or their ratios to estimate the content and structural anomalies of biomolecules in tissues is complicated. As such analysis indirectly inform about the presence and distribution of biological macromolecules, it is called "semi-quantitative". The tissues may be also very complex and heterogeneous which causes that the interpretation of their IR absorption spectra may be in some cases ambiguous.

The interpretation of tissue IR spectra in this study was done according to the established knowledge based on many previously published papers confirming the usefulness of FTIR microscopy for the biomolecular analysis of such type of samples. According to the work of Kneipp et al., the band at 1600−1700 cm^{-1}, called amide I band, provides information about proteins accumulation and, what is more, it is their conformation-sensitive.[52] Other studies have reported that vibrational frequencies characteristic for α-helices and β-sheets occur, respectively, at the wavenumbers of approximately 1655 and 1630 cm^{-1} and, therefore, the ratio of the absorbance at

https://doi.org/10.1021/acschemneuro.3c00331
ACS Chem. Neurosci. 2023, 14, 2775−2791

these wavenumbers may provide information about structural changes/abnormalities of proteins.[53,54] In turn, the spectral range of 2800−3000 cm^{-1} is dominated by the absorption bands connected with the asymmetric and symmetric C−H stretching vibrations of the CH_2 and CH_3 groups of fatty acids.[52,55−57] The compounds containing carbonyl groups may be recognized in the IR spectrum by the band found at the wavenumber of 1740 cm^{-1} and characterisic for C=O stretching vibrations.[58,59] At lower wavenumbers (1000−1300 cm^{-1}) spectrum is dominated by P=O stretching vibrational modes of compounds containing phosphate groups such as phospholipids and nucleic acids and also characteristic vibrations of DNA/RNA backbone and carbohydrate structures (C−O stretching vibrations).[33,52,54,60] The most complex spectral region is the wavenumber range of 1360−1480 cm^{-1}, which contains information about the presence of fatty acids, cholesterol, and its esters.[33,60] The tentative assignment of the vibrational modes and biomolecules to the band frequencies present in the IR spectra measured in nervous tissue are shown in Tables 2 and 3.

Small Number of Animals Used in the Study. Another limitation of this study is small number of animal used in the experiment (five rats per group). Scientific research should be carried out in accordance to 3Rs which provides a clear set of directions for improving the welfare of experimental animals and enables improving scientific results.[61] Especially important are rules associated with the minimization of animals suffering and reduction in the number of animals used to obtain comparable level of information as in the larger groups. In such a case, however, the use of parametric tests that require normal distribution of variables in population is not recommended. That is why non-parametric Mann−Whitney *U* test was applied in the study to verify the statistical significance of the differences between experimental groups and appropriate controls.

Statistical Analysis. The Mann−Whitney *U* test with 95% confidence interval was applied here to verify the statistical significance of biomolecular and morphological differences between experimental groups and appropriate controls. The choice of the nonparametric statistical test was dictated by the fact that our data might have not fulfill the assumptions about normality, homoscedasticity and linearity, which are necessary for the use of parametric one. The Mann−Whitney *U* test is the most commonly used alternative for the two-sample Student *t*-test. The typically used significance levels for the *U* test, are analogical as in case of parametric tests, namely, 0.01, 0.05, or 0.1.

Perme and Manevski showed the alternative to the Mann−Whitney *U* test based on the degree of the variable distributions overlap and proposed several algorithms for the construction of the confidence interval for this method including the Newcombe's 5th or DeLong method.[62] Although both algorithms seem promising, they are based on a parametric approach to variance estimation and, what is more, may be inadequate in case of small sample sizes. Another problem is that this attitude is still rarely used for reporting the confidence intervals and it would be difficult to compare our results with the experimental results of other research groups.

CONCLUSIONS

The results presented in this study confirmed the usefulness of FTIR microspectroscopy in the investigation of the influence of KD used during pregnancy on the biochemical status of the nervous system of the offspring. The topographic analysis of chemical maps showed that the distribution and accumulation of biomolecules in brains of young rats depend both on the stage of postnatal development and the female diet during pregnancy. The offspring of females subjected to KD presented the differences in the relative levels of the bands at 1080 and 1740 cm^{-1} which point at the alterations in the distribution of KB and glucose in their brains. What is more, it was stated that the KD treatment during fetus life may lead to the decrease in the size of internal capsule of progeny and the changes in the relative level and structure of lipids in white matter. FTIR microspectroscopy turned out to be extremely helpful in assessing the biochemical composition of the tested samples. However, new light on the obtained results could be shed by the data concerning the elemental anomalies occurring in the changed tissue areas as well as more detailed, carried out with better spatial resolution, and biomolecular analysis.

MATERIALS AND METHODS

Animals. The animal husbandry and all procedures associated with them were carried out in the Department of Experimental Neuropathology (Institute of Zoology and Biomedical Research of Jagiellonian University) in accordance with the permission no. 122/2015 of the First Local Ethical Committee and with the international standards. In the experiment, the offspring (at the age: 2, 6, and 14 days of the postnatal life) of the rats fed with the ketogenic or standard diet during pregnancy were used. To control fertilization, 2

Table 1. Content of Main Nutrients (% of the Dry Mass) in the Ketogenic and Standards Laboratory Diet

nutrient	KD	standard diet
lipids	79	10
carbohydrates	1	60
proteins	8	30
others	12	0

Table 2. Tentative Assignments of the Band Frequencies Characteristic for IR Spectra Measured in the Nervous Tissue[42,52−54,60,66]

frequency [cm^{-1}]	assignment
~2954	CH_3 asymmetric stretching (saturated fatty acids)
~2924	CH_2 asymmetric stretching (saturated fatty acids)
~2870	CH_3 symmetric stretching (saturated fatty acids)
~2852	CH_2 symmetric stretching (saturated fatty acids)
~1730	C=O stretching (phospholipids, cholesterol ester)
~1640−1653	C=O stretching, C−N stretching, N−H bending (proteins, sphingolipids)
~1545−1567	N−H bending, C−N stretching (proteins, sphingolipids)
~1460−1473	CH_2 scissoring, CH_3 asymmetric bending (fatty acids)
~1443	CH_2 (cyclic) scissoring (cholesterol, cholesterol ester)
~1378−1381	CH_3 symmetric bending (fatty acids)
~1365	CH_2 symmetric bending (fatty acids)
~1200−1400	C−N stretching, N−H bending, C=O stretching, O=C−N bending (proteins)
~1228−1244	PO_2 asymmetric stretching (nucleic acids, phospholipids)
~1170	CO−O−C asymmetric stretching (phospholipids)
~1084−1089	PO_2 symmetric stretching (nucleic acids, phospholipids)

https://doi.org/10.1021/acschemneuro.3c00331
ACS Chem. Neurosci. 2023, 14, 2775−2791

Table 3. Examined Biochemical Parameters[67,68]

absorption band/ratio of absorption bands	biochemical parameter
1658 cm^{-1}	amide I band, distribution of proteins
1635/1658 cm^{-1}	structural changes of proteins (β-sheet to α-helix ratio)
2924/2955 cm^{-1}	structural changes of lipids
2800−3000/1658 cm^{-1}	distribution of lipids (lipid massif) in relation to proteins
2924/1658 cm^{-1}	distribution of lipids in relation to proteins
1240/1658 cm^{-1}	distribution of compounds containing phosphate groups in relation to proteins
1080/1658 cm^{-1}	distribution of compounds containing phosphate groups in relation to proteins
1740/1658 cm^{-1}	distribution of compounds containing carbonyl groups in relation to proteins
1360/1658 cm^{-1}	distribution of lipids, cholesterol and its esters in relation to proteins
1480/1658 cm^{-1}	distribution of lipids, cholesterol and its esters in relation to proteins

month old female Wistar rats were placed in one cage with males during the night and in the morning, those sperm-positive females were set in a separate cages for the period of pregnancy. Pregnant rats were randomly divided into two groups. The first one remained on the standard laboratory diet whilst the second was fed with KD. Both diets were continued during the whole gestation. In turn, during the lactation period both groups obtained standard laboratory diet which, in the case of the previously KD fed females, was introduced 2 days after labor. The pregnant rats had the access to food and water ad libitum, and the mass of the consumed chow was controlled three times a week. Once a week, the females were weighed and the levels of the ketone bodies and glucose were measured in their blood.

Postpartum, the gender of the offspring was identified and afterward the animals of each sex were randomly divided into groups differing in the times of the perfusion and the collection of samples. The number of rats was five per each experimental group. The brains were taken from them on the 2nd, 6th, and 14th day of life, and the chosen periods correspond to the key processes occurring in the rat brain during its postnatal development.

Ketogenic and Standard Laboratory Diet. In the study, we used KD with long-chain fatty acids (ssniff EF R/M with 80% Fat) and the standard laboratory diet in the form of Labofeed (Morawski). The selected KD is characterized with high ketogenic ratio (KR), which is the mass ratio of fats to proteins and carbohydrates.[63] The choice of a high KR diet is related to the fact, that it is usually more efficient in the seizure control.[64,65] The comparison of the content of main nutrients in the dry mass of the used ketogenic and standard chow is done in Table 1.

Sample Preparation. On the 2, 6, or 14 days of postnatal life rats were deeply anesthetized with Morbital (Biowet) and perfused with physiological saline solution of high analytical quality. The brains were excised and deeply frozen in liquid nitrogen. Twelve micrometer thick slices with the dorsal part of the hippocampal formation were cut using cryomicrotome and placed on sample carriers made of CaF_2, and dedicated to measurements with FTIR microspectroscopy in the transmission mode.

IR Data Collection. The biochemical analysis of brain samples was performed using FTIR microspectroscopy. The measurements were performed at the Faculty of Physics and Applied Computer Science of the AGH University of Science and Technology (Krakow, Poland). Thermo Scientific Nicolet iN10 MX infrared microscope, equipped with a ceramic radiation source, was used for the study. For faster scanning of samples and chemical imaging, the ultrafast mapping system and a linear array of mercury cadmium telluride (MCT) detectors were used. In turn, the single spectra from areas of interest were recorded with the point MCT detector. The samples deposited on CaF_2 slides were analyzed in transmission mode with a spatial resolution of around 25 μm. The spectra were recorded for the wavenumber range 4000−900 cm^{-1} with spectral resolution set to 8 cm^{-1}. 32 scans were averaged per both sample and background spectrum. The data acquisition as well as spectral analysis were performed with OMNIC Picta software (version 8.1).

Topographic and Semi-Quantitative Biochemical Analysis, Statistical Evaluation of the Results. The topographic analysis of the main biological macromolecules in the brain was based on the chemical mapping of their absorption bands or the ratios of their absorption bands. For this purpose OMNIC Picta software (version 8.1) was used. The two-dimensional chemical maps were generated by imaging of the area of one peak or the area ratio of two peaks, including trapezoidal baseline correction. In one case, for the wavenumber region between 2800 and 3000 cm^{-1}, we did not examine the intensity of the bands, but the integrated absorbance within this particular wavenumber range. The mentioned spectral range, called lipid massif, includes a few absorption bands specific to lipids. Also, in this case, trapezoidal baseline correction was applied. In Table 2, the tentative assignments of the band frequencies characteristic for IR spectra measured in nervous tissue are shown. In

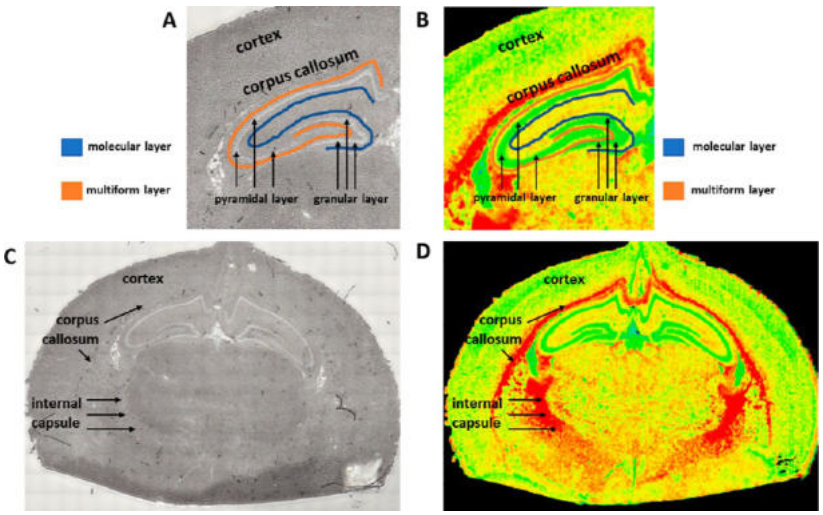

Figure 11. Localization of the areas (two structures of white matter, namely, corpus callosum and internal capsule, and cortex) and cellular layers (granular, pyramidal molecular, and multiform layer) of interest, presented in the microscopic images (A,C) and chemical maps (B,D) showing the distribution of lipids for the selected sample of the brain.

https://doi.org/10.1021/acschemneuro.3c00331
ACS Chem. Neurosci. 2023, 14, 2775−2791

turn, the characteristics of the absorption bands and the ratios of absorption bands examined in this study are presented in Table 3.

For the statistical evaluation of the spectral data and identification of the potential differences between experimental and control groups, the principal component analysis (PCA) and Mann−Whitney *U* test were utilized. At first, important brain regions including brain cortex, corpus callosum (structure of the white matter), and four cellular layers of hippocampal formation, namely, granular, pyramidal, multiform and molecular, were localized in each examined tissue slice (Figure 11). Then, with the use of point MCT detector, 100 spectra in the randomly chosen points from the mentioned areas of interest were collected for each animal. For the purposes of PCA of the spectral data the Origin Pro software (version 2020b) was applied. The preprocessing of the spectra included atmospheric and baseline correction as well as vector normalization. The PCA was done based on the second derivative spectra.

In the next step, for each animal and examined area/cellular layer, the absolute and/or relative average intensities of chosen absorption bands (given in Table 3) were calculated. Afterward, the nonparametric Mann−Whitney *U* test was applied to verify the statistical significance of the differences in the obtained biochemical parameters between animals exposed prenatally to KD and the controls at the appropriate stage of postnatal development. For statistical analysis, STATISTICA software (version 14.0.1.25) was used, and the significance level was assumed as 5%. The Mann−Whitney *U* test was also applied in order to confirm the statistical significance of the differences in the relative surface of the internal capsule between experimental groups and appropriate controls.

■ ASSOCIATED CONTENT

Supporting Information

The Supporting Information is available free of charge at https://pubs.acs.org/doi/10.1021/acschemneuro.3c00331.

Microscopic views of the scanned brain tissue areas of 2, 6, and 14 days old animals (PDF)

■ AUTHOR INFORMATION

Corresponding Author

Joanna Chwiej − *Faculty of Physics and Applied Computer Science, AGH University of Krakow, Krakow 30-059, Poland;* orcid.org/0000-0002-3792-7876; Email: joanna.chwiej@fis.agh.edu.pl

Authors

Marzena Rugiel − *Faculty of Physics and Applied Computer Science, AGH University of Krakow, Krakow 30-059, Poland*

Zuzanna Setkowicz-Janeczko − *Institute of Zoology and Biomedical Research, Jagiellonian University, Krakow 31-007, Poland*

Wojciech Kosiek − *Institute of Zoology and Biomedical Research, Jagiellonian University, Krakow 31-007, Poland*

Zuzanna Rauk − *Institute of Zoology and Biomedical Research, Jagiellonian University, Krakow 31-007, Poland*

Kamil Kawon − *Faculty of Physics and Applied Computer Science, AGH University of Krakow, Krakow 30-059, Poland*

Complete contact information is available at: https://pubs.acs.org/10.1021/acschemneuro.3c00331

Author Contributions

§M.R. and Z.S.-J. contributed equally.

Author Contributions

M.R.: conceptualization, methodology, investigation, analysis, validation, writing original draft, and answers to the reviewers' remarks. Z.S.: conceptualization, animal experiment, methodology, resources, investigation, and reviewing manuscript. W.K.: methodology and investigation. Z.R.: methodology and investigation. K.K.: methodology and investigation. J.C.: conceptualization, methodology, resources, validation, supervision, writing original draft, corresponding author, and answers to the reviewers' remarks. M.R. and Z.S. contributed equally.

Notes

The authors declare no competing financial interest.

■ ACKNOWLEDGMENTS

This work was partially financed by the Ministry of Education and Science of Poland and the subvention no. N18/DBS/000018 of the Laboratory of Experimental Neuropathology (Institute of Zoology and Biomedical Research, Jagiellonian University). For the evaluation of tissues morphology, the WITec Alpha300R Raman microscope purchased from the funds granted to the AGH University of Science and Technology in the frame of the "Excellence Initiative-Research University" project was applied. Marzena Rugiel has been partially supported by the program "Excellence Initiative-Research University" for the AGH UST.

■ REFERENCES

(1) Kellogg, M.; Meador, K. J. Neurodevelopmental Effects of Antiepileptic Drugs. *Neurochem. Res.* **2017**, *42*, 2065−2070.

(2) Meador, K. J.; Loring, D. W. Developmental effects of antiepileptic drugs and the need for improved regulations. *Neurology* **2016**, *86*, 297−306.

(3) Nordli, D. R., Jr; Kuroda, M. M.; Carroll, J.; Koenigsberger, D. Y.; Hirsch, L. J.; Bruner, H. J.; Seidel, W. T.; De Vivo, D. C. Experience with the ketogenic diet in infants. *Pediatrics* **2001**, *108*, 129−133.

(4) McDonald, T. J. W.; Cervenka, M. C. Ketogenic Diet Therapies for Seizures and Status Epilepticus. *Semin. Neurol.* **2020**, *40*, 719−729.

(5) Mady, M. A.; Kossoff, E. H.; McGregor, A. L.; Wheless, J. W.; Pyzik, P. L.; Freeman, J. M. The ketogenic diet: adolescents can do it, too. *Epilepsia* **2003**, *44*, 847−851.

(6) Kossoff, E. H.; Rho, J. M. Ketogenic diets: evidence for short- and long-term efficacy. *Neurotherapeutics* **2009**, *6*, 406−414.

(7) D'Andrea Meira, I.; Romão, T. T.; Pires do Prado, H. J.; Krüger, L. T.; Pires, M. E. P.; da Conceição, P. O. Ketogenic Diet and Epilepsy: What We Know So Far. *Front. Neurosci.* **2019**, *29*, 5−15.

(8) McNally, M. A.; Hartman, A. L. Ketone bodies in epilepsy. *J. Neurochem.* **2012**, *121*, 28−35.

(9) Cervenka, M. C.; Kossoff, E. H. Dietary treatment of intractable epilepsy. *Continuum* **2013**, *19*, 756−766.

(10) Kosiek, W.; Rauk, Z.; Szulc, P.; Cichy, A.; Rugieł, M.; Chwiej, J.; Janeczko, K.; Setkowicz, Z. Ketogenic diet impairs neurological development of neonatal rats and affects biochemical composition of maternal brains: evidence of functional recovery in pups. *Brain Struct. Funct.* **2022**, *227*, 1099−1113.

(11) Jensen, N. J.; Wodschow, H. Z.; Nilsson, M.; Rungby, J. Effects of Ketone Bodies on Brain Metabolism and Function in Neurodegenerative Diseases. *Int. J. Mol. Sci.* **2020**, *21*, 8767.

(12) Freeman, J.; Veggiotti, P.; Lanzi, G.; Tagliabue, A.; Perucca, E. The ketogenic diet: from molecular mechanisms to clinical effects. *Epilepsy Res.* **2006**, *68*, 145−180.

(13) Juge, N.; Gray, J. A.; Omote, H.; Miyaji, T.; Inoue, T.; Hara, C.; Uneyama, H.; Edwards, R. H.; Nicoll, R. A.; Moriyama, Y. Metabolic control of vesicular glutamate transport and release. *Neuron* **2010**, *68*, 99−112.

(14) Rho, J. M. How does the ketogenic diet induce anti-seizure effects? *Neurosci. Lett.* **2017**, *637*, 4−10.

(15) Kossoff, E.; Cervenka, M. Ketogenic Dietary Therapy Controversies for Its Second Century. *Epilepsy Curr.* **2020**, *20*, 125−129.

(16) Kramer, J.; Smith, L. Ketogenic Diet in Glut 1 Deficiency Through the Life Cycle: Pregnancy to Neonate to Preschooler. *Child Neurol. Open* **2021**, *8*, 2329048X2110346.
(17) van der Louw, E. J.; Williams, T. J.; Henry-Barron, B. J.; Olieman, J. F.; Duvekot, J. J.; Vermeulen, M. J.; Bannink, N.; Williams, M.; Neuteboom, R. F.; Kossoff, E. H.; Catsman-Berrevoets, C. E.; Cervenka, M. C. Ketogenic diet therapy for epilepsy during pregnancy: A case series. *Seizure* **2017**, *45*, 198−201.
(18) Sussman, D.; van Eede, M.; Wong, M. D.; Adamson, S. L.; Henkelman, M. Effects of a ketogenic diet during pregnancy on embryonic growth in the mouse. *BMC Pregnancy Childbirth* **2013**, *13*, 109.
(19) Sussman, D.; Germann, J.; Henkelman, M. Gestational ketogenic diet programs brain structure and susceptibility to depression & anxiety in the adult mouse offspring. *Brain Behav.* **2015**, *5*, No. e00300.
(20) Sussman, D.; Ellegood, J.; Henkelman, M. A gestational ketogenic diet alters maternal metabolic status as well as offspring physiological growth and brain structure in the neonatal mouse. *BMC Pregnancy Childbirth* **2013**, *13*, 198.
(21) Soares, A. K.; Guerra, R. G.; de Castro, M. L.; Amancio-dos-Santos, A.; Guedes, R. C.; Cabral-Filho, J. E.; Costa, J. A.; Medeiros, M. d. C. Somatic and reflex development in suckling rats: effects of mother treatment with ketogenic diet associated with lack of protein. *Nutr. Neurosci.* **2009**, *12*, 260−266.
(22) Rodriguez-Perez, M. d. C.; Vicente-Perez, F. D.; Gomez-Jarabo Garcia, G. Effects of protein malnutrition and the administration of cortisol on the reflexologic development in rats. *Behav. Neural. Biol.* **1992**, *58*, 165−170.
(23) Lucas, E. S.; Finn, S. L.; Cox, A.; Lock, F. R.; Watkins, A. J. The impact of maternal high fat nutrition on the next generation: food for thought? *J. Physiol. Soc.* **2009**, *587*, 3425−3426.
(24) Howie, G. J.; Sloboda, D. M.; Kamal, T.; Vickers, M. H. Maternal nutritional history predicts obesity in adult offspring independent of postnatal diet. *J. Physiol.* **2009**, *587*, 905−915.
(25) Gluckman, P. D.; Hanson, M. A. The developmental origins of the metabolic syndrome. *Trends Endocrinol. Metab.* **2004**, *15*, 183−187.
(26) Gawlińska, K.; Gawliński, D.; Filip, M.; Przegaliński, E. Relationship of maternal high-fat diet during pregnancy and lactation to offspring health. *Nutr. Rev.* **2020**, *79*, 709−725.
(27) Cortés-Álvarez, N. Y.; Vuelvas-Olmos, C. R.; Pinto-González, M. F.; Guzmán-Muñiz, J.; Gonzalez-Perez, O.; Moy-López, N. A. A high-fat diet during pregnancy impairs memory acquisition and increases leptin receptor expression in the hippocampus of rat offspring. *Nutr. Neurosci.* **2020**, *25*, 146−158.
(28) Hawkes, C. A.; Gentleman, S. M.; Nicoll, J. A.; Carare, R. O. Prenatal high-fat diet alters the cerebrovasculature and clearance of β-amyloid in adult offspring. *J. Pathol.* **2015**, *235*, 619−631.
(29) Ohta, T.; Toriniwa, Y.; Ryumon, N.; Inaba, N.; Hirao, T.; Yamanaka, S.; Maeno, T.; Sakakibara, W.; Sumikawa, M.; Chiba, K.; Nakamura, A.; Miyajima, K.; Fatchiyah, F.; Yamada, T. Maternal high-fat diet promotes onset of diabetes in rat offspring. *Anim. Sci. J.* **2017**, *88*, 149−155.
(30) Wentzel, P.; Eriksson, U. J.; Herrera, E. High-fat diet in pregnant rats and adverse fetal outcome. *Ups. J. Med. Sci.* **2019**, *124*, 125−134.
(31) Di Meco, A.; Praticò, D. Early-life exposure to high-fat diet influences brain health in aging mice. *Aging Cell* **2019**, *18*, No. e13040.
(32) Bunaciu, A. A.; Fleschin, S.; Aboul-Enein, H. Y. Biomedical investigations using Fourier transform-infrared microspectroscopy. *Crit. Rev. Anal. Chem.* **2014**, *44*, 270−276.
(33) Ami, D.; Mereghetti, P.; Leri, M.; Giorgetti, S.; Natalello, A.; Doglia, S. M.; Stefani, M.; Bucciantini, M. A FTIR microspectroscopy study of the structural and biochemical perturbations induced by natively folded and aggregated transthyretin in HL-1 cardiomyocytes. *Sci. Rep.* **2018**, *8*, 12508.
(34) Srisayam, M.; Weerapreeyakul, N.; Barusrux, S.; Tanthanuch, W.; Thumanu, K. Application of FTIR microspectroscopy for characterization of biomolecular changes in human melanoma cells treated by sesamol and kojic acid. *J. Dermatol. Sci.* **2014**, *73*, 241−250.
(35) Chwiej, J.; Dulinska, J.; Janeczko, K.; Dumas, P.; Eichert, D.; Dudala, J.; Setkowicz, Z. Synchrotron FTIR micro-spectroscopy studyof the rat hippocampal formation after pilocarpine-evoked seizures. *J. Chem. Neuroanat.* **2010**, *40*, 140−147.
(36) Diem, M.; Boydston-White, S.; Chiriboga, L. Infrared spectroscopy of cells and tissues: shining light onto a novel subject. *Appl. Spectrosc.* **1999**, *53*, 148A−161A.
(37) Liquier, J.; Taillandier, R. *Infrared Spectroscopy of Nucleic Acids. Infrared Spectroscopy of Biological Molecules*; Wiley-Liss: New York, 1996; pp 131−158.
(38) Nehlig, A. Age-dependent pathways of brain energy metabolism:the suckling rat, a natural model of the ketogenic diet. *Epilepsy Res.* **1999**, *37*, 211−221.
(39) Prins, M. L. Cerebral ketone metabolism during development and injury. *Epilepsy Res.* **2012**, *100*, 218−223.
(40) Herrera, E.; Gomez-Coronado, D.; Lasunción, M. A. Lipid metabolism in pregnancy. *Biol. Neonate* **1987**, *51*, 70−77.
(41) Barry, D.; Ellul, S.; Watters, L.; Lee, D.; Haluska, R., Jr; White, R. The ketogenic diet in disease and development. *Int. J. Dev. Neurosci.* **2018**, *68*, 53−58.
(42) Chwiej, J.; Skoczen, A.; Janeczko, K.; Kutorasinska, J.; Matusiak, K.; Figiel, H.; Dumas, P.; Sandt, C.; Setkowicz, Z. The biochemical changes in hippocampal formation occurring in normal and seizure experiencing rats as a result of a ketogenic diet. *Analyst* **2015**, *140*, 2190−2204.
(43) Politi, K.; Shemer-Meiri, L.; Shuper, A.; Aharoni, S. The ketogenic diet 2011: how it works. *Epilepsy Res. Treat.* **2011**, *2011*, 1−4.
(44) Bough, K. J.; Rho, J. M. Anticonvulsant mechanisms of the ketogenic diet. *Epilepsia* **2007**, *48*, 43−58.
(45) Persson, B.; Settergren, G.; Dahlquist, G. CEREBRAL ARTERIO-VENOUS DIFFERENCE OF ACETOACETATE AND D-β-HYDROXYBUTYRATE IN CHILDREN. *Acta Paediatr. Scand.* **1972**, *61*, 273−278.
(46) Patel, M. S.; Owen, O. E. Development and regulation of lipid synthesis from ketone bodies by rat brain. *J. Neurochem.* **1977**, *28*, 109−114.
(47) Nehlig, A.; Pereira de Vasconcelos, A. Glucose and ketone body utilization by the brain of neonatal rats. *Prog. Neurobiol.* **1993**, *40*, 163−220.
(48) Morris, A. A. Cerebral ketone body metabolism. *J. Inherit. Metab. Dis.* **2005**, *28*, 109−121.
(49) Gjedde, A.; Crone, C. Induction processes in blood-brain transfer of ketone bodies during starvation. *Am. J. Physiol.* **1975**, *229*, 1165−1169.
(50) Middleton, B. The acetoacetyl-coenzyme A thiolases of rat brain and their relative activities during postnatal development. *Biochem. J.* **1973**, *132*, 731−737.
(51) Buckley, B. M.; Williamson, D. H. Acetoacetate and brain lipogenesis: developmental pattern of acetoacetyl-coenzyme A synthetase in the soluble fraction of rat brain (*Short Communication*). *Biochem. J.* **1973**, *132*, 653−656.
(52) Kneipp, J.; Lasch, P.; Baldauf, E.; Beekes, M.; Naumann, D. Detection of pathological molecular alterations in scrapie-infected hamster brain by Fourier transform infrared (FT-IR) spectroscopy. *Biochim. Biophys. Acta, Mol. Basis Dis.* **2000**, *1501*, 189−199.
(53) Miller, L. M.; Wang, Q.; Telivala, T. P.; Smith, R. J.; Lanzirotti, A.; Miklossy, J. Synchrotron-based infrared and X-ray imaging shows focalized accumulation of Cu and Zn co-localized with β-Amyloid deposits in Alzheimer's disease. *J. Struct. Biol.* **2006**, *155*, 30−37.
(54) Kretlow, A.; Wang, Q.; Kneipp, J.; Lasch, P.; Beekes, M.; Miller, L.; Naumann, D. FTIR-microspectroscopy of prion-infected nervous tissue. *Biochim. Biophys. Acta, Biomembr.* **2006**, *1758*, 948−959.

https://doi.org/10.1021/acschemneuro.3c00331
ACS Chem. Neurosci. 2023, 14, 2775−2791

(55) Petibois, C.; Deléris, G. Evidence that erythrocytes are highly susceptible to exercise oxidative stress: FT-IR spectrometric studies at the molecular level. *Cell Biol. Int.* **2005**, *29*, 709−716.
(56) Petibois, C.; Deléris, G. Chemical mapping of tumor progression by FT-IR imaging: towards molecular histopathology. *Trends Biotechnol.* **2006**, *24*, 455−462.
(57) Moggio, M.; Errico, S.; Diano, N.; Lepore, M. FTIR Spectroscopy for Evaluation and Monitoring of Lipid Extraction Efficiency for Murine Liver Tissues Analysis. *Eng. Proc.* **2021**, *10*, 9.
(58) Bujok, J.; Gąsior-Głogowska, M.; Marszałek, M.; Trochanowska-Pauk, N.; Zigo, F.; Pavl'ak, A.; Komorowska, M.; Walski, T. Applicability of FTIR-ATR Method to Measure Carbonyls in Blood Plasma after Physical and Mental Stress. *Biomed. Res. Int.* **2019**, *2019*, 1−9.
(59) Vileno, B.; Jeney, S.; Sienkiewicz, A.; Marcoux, P. R.; Miller, L. M.; Forro, L. Evidence of lipid peroxidation and protein phosphorylation in cells upon oxidative stress photo-generated by fullerols. *Biophys. Chem.* **2010**, *152*, 164−169.
(60) Dreissig, I.; Machill, S.; Salzer, R.; Krafft, C. Quantification of brain lipids by FTIR spectroscopy and partial least squares regression. *Spectrochim. Acta, Part A* **2009**, *71*, 2069−2075.
(61) Hubrecht, R. C.; Carter, E. The 3Rs and Humane Experimental Technique: Implementing Change. *Animals* **2019**, *9*, 754.
(62) Perme, M. P.; Manevski, D. Confidence intervals for the Mann-Whitney test. *Stat. Methods Med. Res.* **2019**, *28*, 3755−3768.
(63) Wirrell, E. C. Ketogenic ratio, calories, and fluids: do they matter? *Epilepsia* **2008**, *49*, 17−19.
(64) Chwiej, J.; Patulska, A.; Skoczen, A.; Matusiak, K.; Janeczko, K.; Ciarach, M.; Simon, R.; Setkowicz, Z. Various ketogenic diets can differently support brain resistance against experimentally evoked seizures and seizure-induced elemental anomalies of hippocampal formation. *J. Trace Elem. Med. Biol.* **2017**, *42*, 50−58.
(65) Hee Seo, J.; Mock Lee, Y.; Soo Lee, J.; Chul Kang, H.; Dong Kim, H. Efficacy and tolerability of the ketogenic diet according to lipid:nonlipid ratios–comparison of 3:1 with 4:1 diet. *Epilepsia* **2007**, *48*, 801−805.
(66) Stuart, B. *Infrared Spectroscopy: Fundamentals and Applications*; John Wiley & Sons Ltd: England, 2004.
(67) Beekes, M.; Lasch, P.; Naumann, D. Analytical applications of Fourier transform-infrared (FT-IR) spectroscopy in microbiology and prion research. *Vet. Microbiol.* **2007**, *123*, 305−319.
(68) Chwiej, J. G.; Ciesielka, S. W.; Skoczen, A. K.; Janeczko, K. J.; Sandt, C.; Planeta, K. L.; Setkowicz, Z. K. Biochemical Changes Indicate Developmental Stage in the Hippocampal Formation. *ACS Chem. Neurosci.* **2019**, *10*, 628−635.

https://doi.org/10.1021/acschemneuro.3c00331
ACS Chem. Neurosci. 2023, 14, 2775−2791

Supporting Information

DOES KETOGENIC DIET USED IN PREGNANCY AFFECT THE NERVOUS SYSTEM DEVELOPMENT IN OFFSPRING? – FTIR MICROSPECTROSCOPY STUDY

Marzena Rugiel[1#], Zuzanna Setkowicz-Janeczko[2#], Wojciech Kosiek[2], Zuzanna Rauk[2], Kamil Kawon[1], Joanna Chwiej[1*]

[1]*Faculty of Physics and Applied Computer Science, AGH University of Krakow, Krakow 30-059, Poland*
[2]*Institute of Zoology and Biomedical Research, Jagiellonian University, Krakow 31-007, Poland*

# equally contributed

* Corresponding author; email address: joanna.chwiej@fis.agh.edu.pl

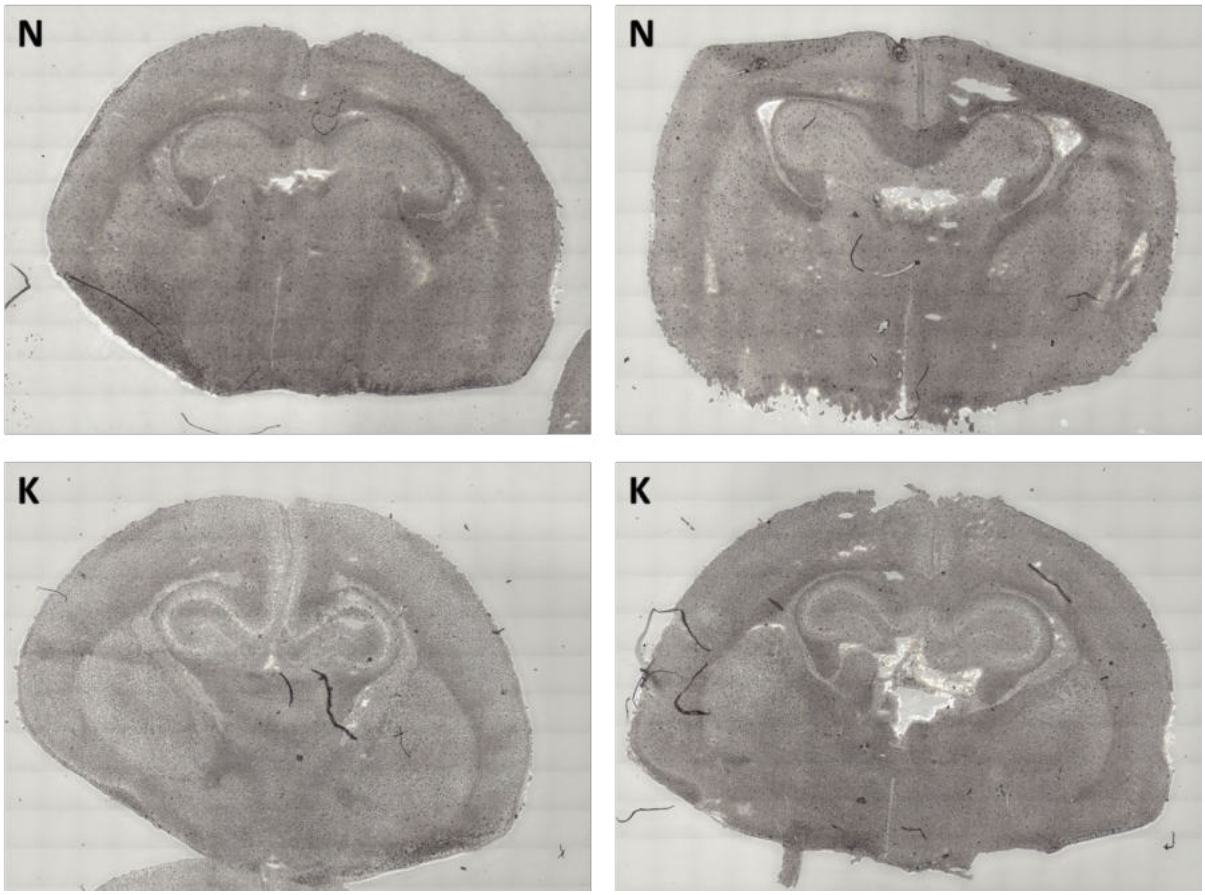

Figure S1. The microscopic views of the scanned brain tissue areas of 2-days old animals.

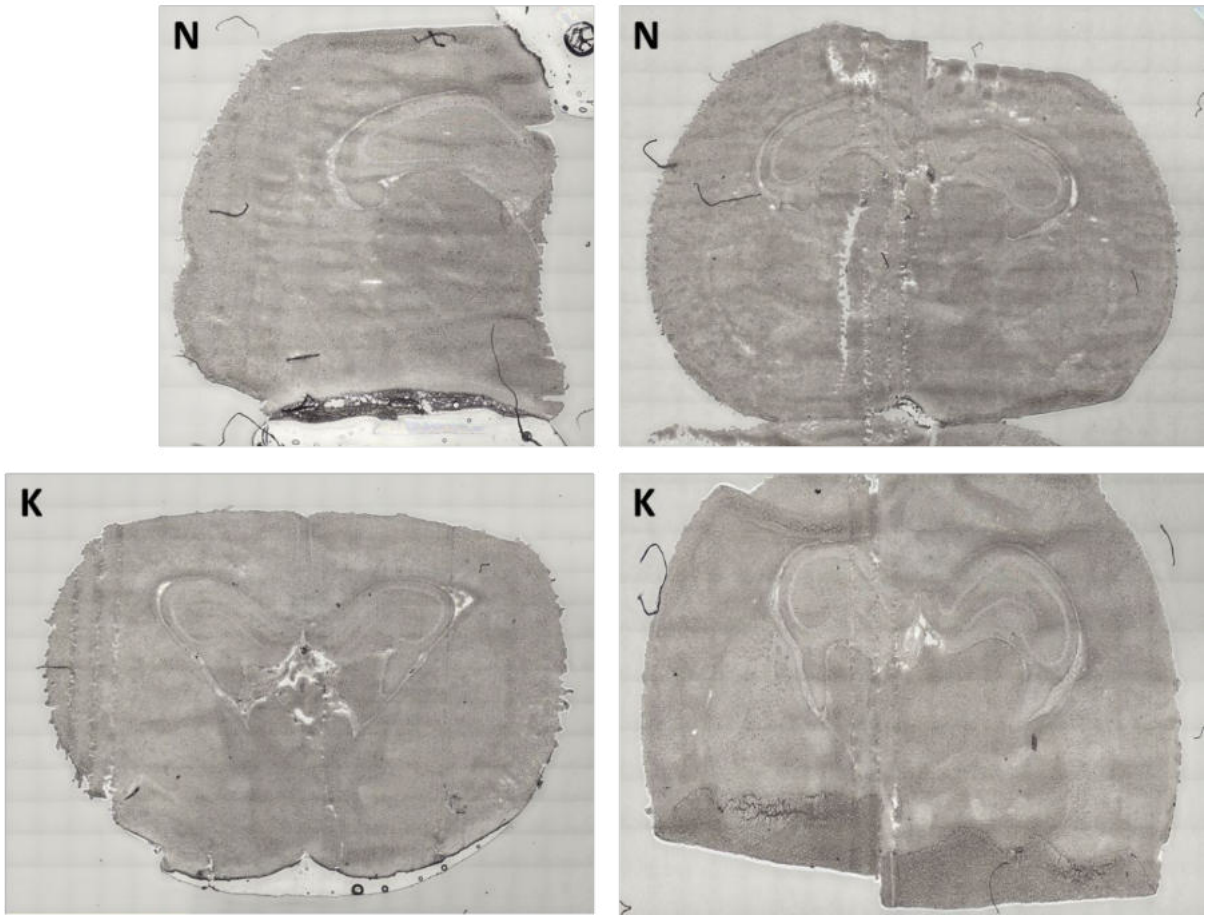

Figure S2. The microscopic views of the scanned brain tissue areas of 6-days old animals.

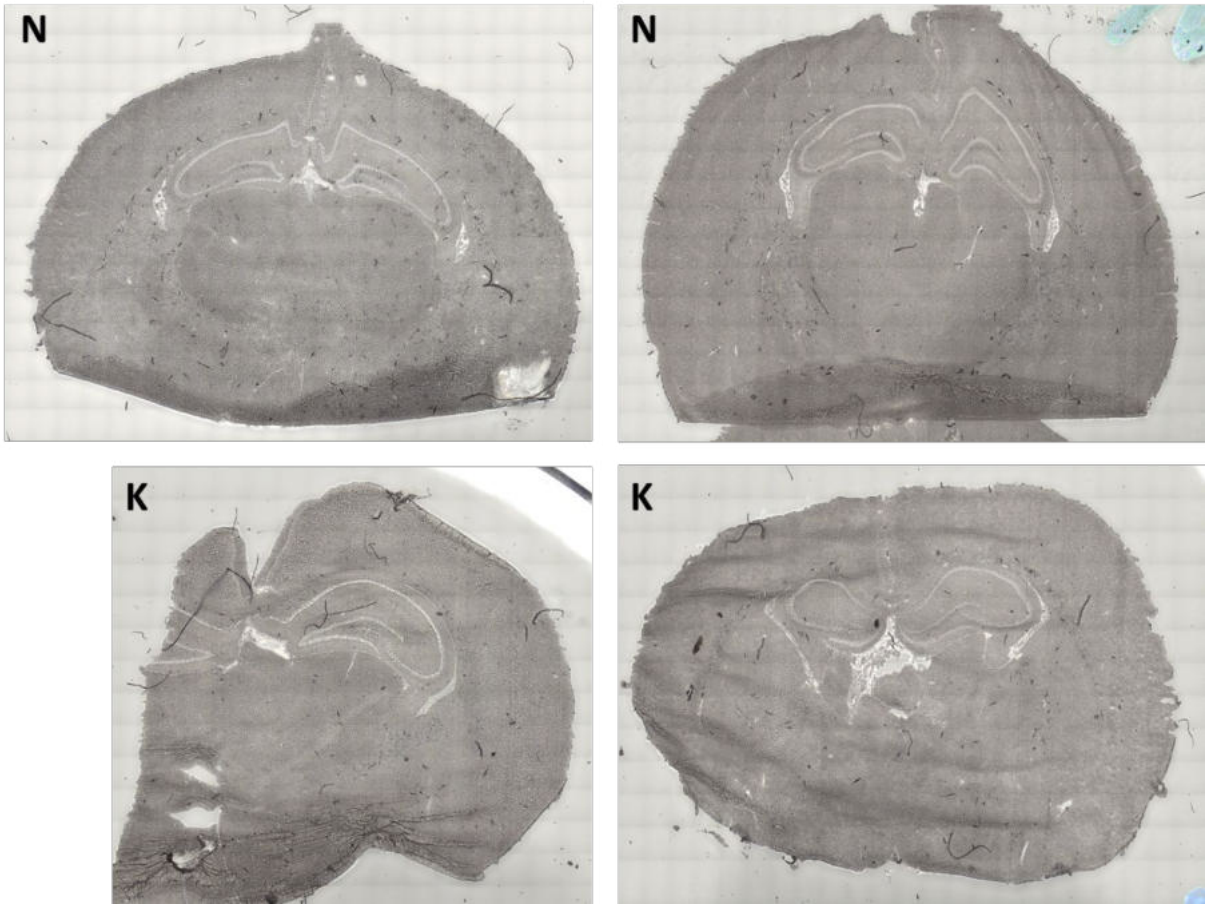

Figure S3. The microscopic views of the scanned brain tissue areas of 14-days old animals.

ACS Chemical Neuroscience

pubs.acs.org/chemneuro
Research Article

Element Changes Occurring in Brain Point at the White Matter Abnormalities in Rats Exposed to the Ketogenic Diet During Prenatal Life

Marzena Rugieł,[#] Zuzanna Setkowicz,[#] Mateusz Czyzycki, Rolf Simon, Tilo Baumbach, and Joanna Chwiej*

Cite This: ACS Chem. Neurosci. 2024, 15, 3932−3944
Read Online

ABSTRACT: A large number of clinical studies demonstrate that the ketogenic diet (KD) may be an effective approach to the reduction of epileptic seizures in children and adults. Such dietary therapy could also help pregnant women with epilepsy, especially since most antiseizure drugs have teratogenic action. However, there is a lack of medical data, considering the safety of using KD during gestation for the progeny. Therefore, we examined the influence of KD used prenatally in rats on the elemental composition of the selected brain regions in their offspring. For this purpose, synchrotron radiation-induced X-ray fluorescence (SR-XRF) microscopy was utilized, and elements such as P, S, K, Ca, Fe, and Zn were determined. Moreover, to verify whether the possible effects of KD are temporary or long-term, different stages of animal postnatal development were taken into account in our experiment. The obtained results confirmed the great applicability of SR-XRF microscopy to track the element changes occurring in the brain during postnatal development as well as those induced by prenatal exposure to the high-fat diet. The topographic analysis of the brains taken from offspring of mothers fed with KD during pregnancy and appropriate control individuals showed a potential influence of such dietary treatment on the brain levels of elements such as P and S. In the oldest progeny, a significant reduction of the surface of brain areas characterized by an increased P and S content, which histologically/morphologically correspond to white matter structures, was noticed. In turn, quantitative elemental analysis showed significantly decreased levels of Fe in the striatum and white matter of 30-day-old rats exposed prenatally to KD. This effect was temporary and was not noticed in adult animals. The observed abnormalities may be related to the changes in the accumulation of sphingomyelin and sulfatides and may testify about disturbances in the structure and integrity of the myelin, present in the white matter.

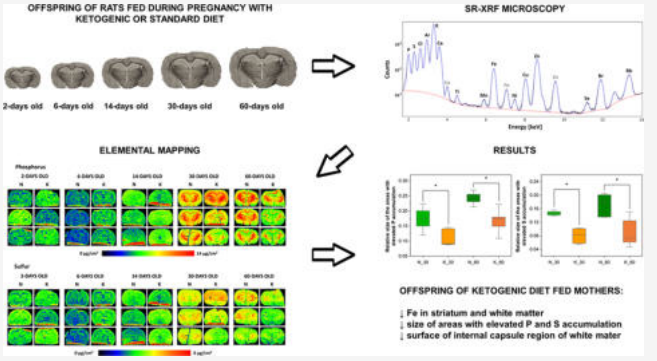

KEYWORDS: *ketogenic diet, synchrotron X-ray fluorescence microscopy, multielement analysis, prenatal exposure, animal models, brain development*

INTRODUCTION

The ketogenic diet (KD) is a dietary therapy characterized by an intake of high fat, usually adequate protein, and always strongly restricted carbohydrate amounts. Its use leads to alteration in the energy metabolism and the use of ketone bodies (KBs), instead of glucose, as a primary energy source.[1−4] During normal glycolysis, when a typical diet is consumed, glucose is converted to pyruvate, which is then transformed into acetyl-CoA.[5] During consumption of KD, when an amount of glucose is limited, the glycolysis process is significantly reduced.[2,6] In this case, fatty acids undergo oxidation, which leads to the production of acetyl-CoA from them.[1,6] This compound takes part in the process of ketogenesis in the liver as a result of which three main KBs, acetone, acetoacetate, and β-hydroxybutyrate,[1,3,6] are produced. Excess acetyl-CoA produced from fats cannot be used in the Krebs cycle; therefore, its remaining amount is converted to acetoacetate.[1,6] In turn, acetoacetate may be spontaneously degraded to acetone or enzymatically converted by β-hydroxybutyrate dehydrogenase to β-hydroxybutyrate.[1,6] Elevated ketone concentrations found in urine or serum testify about the state of ketosis and may be used as a marker of early compliance following dietary initiation.[3,7,8]

Received: May 6, 2024
Revised: October 16, 2024
Accepted: October 16, 2024
Published: October 23, 2024

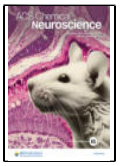

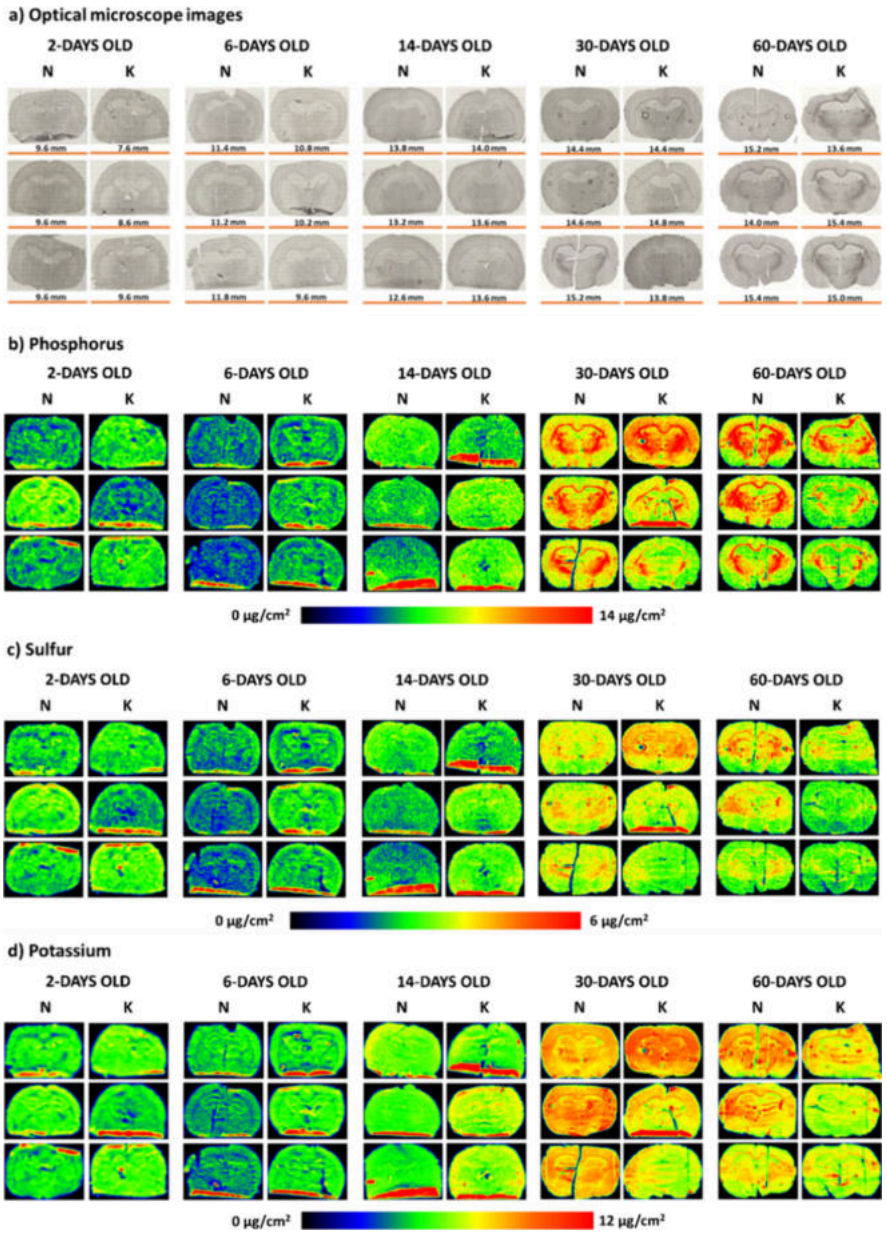

Figure 1. Microscope images (a) and distribution maps of P, S, and K (b–d, respectively) in the representative brain tissue slices taken from the rats of all the examined stages of postnatal development (2-, 6-, 14-, 30-, and 60-days old), the mothers of which were fed during pregnancy with the ketogenic (K) or standard fodder (N). Color scales below the maps express the elemental mass deposits in $\mu g/cm^2$.

Many researchers suggest some therapeutic benefits related to a state of ketosis and point out potential applications of KD for the treatment of a variety of metabolic, oncologic, neurodegenerative, and psychiatric disorders.[9−11] Although KD has been tailored to meet the needs of patients suffering from epilepsy,[3,9] the literature evidence indicates that it can be successfully used to treat obesity,[12] Alzheimer's disease,[13] traumatic brain injury,[14] depression,[15] or Parkinson's disease.[11]

KD has been shown to have positive effects in the case of drug-resistant epilepsy in both children[16,17] and adults.[7,8,18] A particular challenge is still an effective and safe treatment of pregnant women with epilepsy as most of antiseizure drugs are teratogenic.[19] In this case, any alternative treatments for the disease should be considered, and one of them may be KD. First, however, it is necessary to find out how such a dietary therapy may affect a developing fetus. A placenta acts as a filter that allows nutrients to pass from the mother to the fetus's blood.[20] Herrera and Gómez-Coronado[21] pointed out that KBs circulating in the mother's plasma can cross the placenta and reach the same level in the fetus. Furthermore, they may be used for brain lipid synthesis of developing offspring.[21] However, according to our best knowledge, there is still a lack of medical evidence answering the question of whether in the case of higher levels of KBs present in the mother organism, the risk of ketoacidosis in the fetus increases. A case study of two pregnant women suffering from epilepsy, described by van der Louw and Williams,[22] showed no negative impact of prenatal exposure to KD on child health and its nervous system development. The authors of the cited article, however, pointed out that further monitoring of children is warranted to identify possible long-term side effects of the therapy.[22]

https://doi.org/10.1021/acschemneuro.4c00283
ACS Chem. Neurosci. 2024, 15, 3932−3944

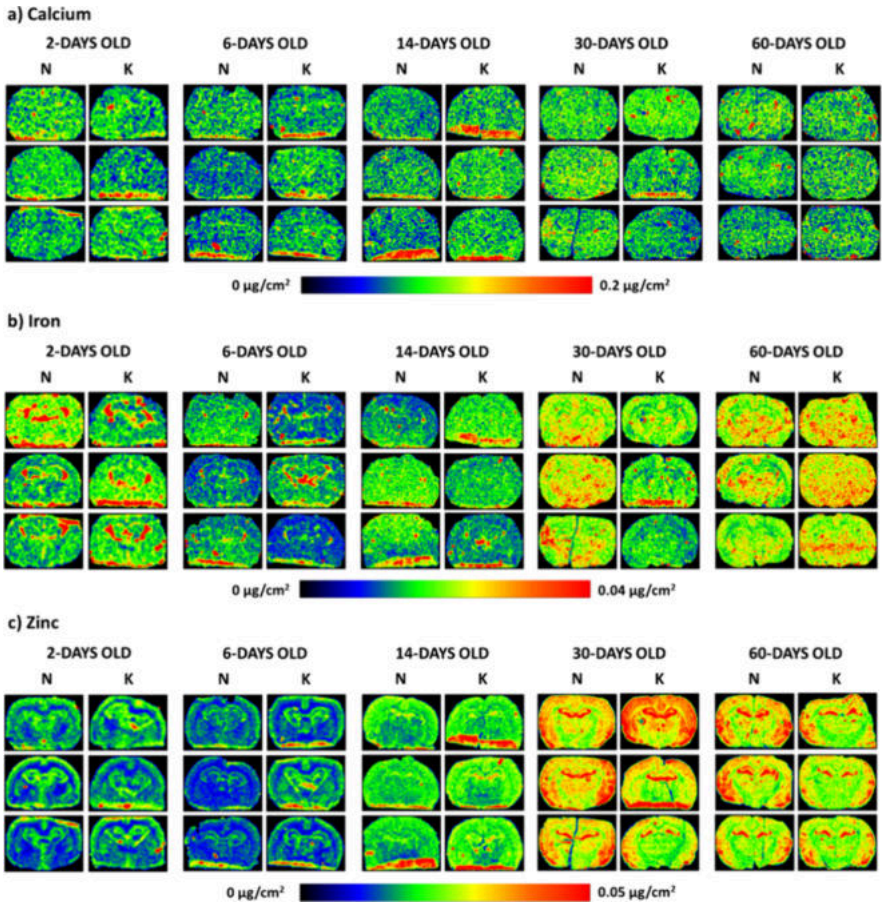

Figure 2. Distribution maps of Ca, Fe, and Zn (a−c, respectively) in the representative brain tissue slices taken from the rats of all the examined stages of postnatal development (2-, 6-, 14-, 30-, and 60-days old), the mothers of which were fed during pregnancy with the ketogenic (K) or standard fodder (N). Color scales below the maps express the element mass deposits in $\mu g/cm^2$.

Conclusions from the animal studies regarding an influence of the high-fat diet used in gestation on pups are not consistent.[9] Discrepancies can be noted, among others, taking into account the body weight of the offspring. Some investigations showed that a maternal high-fat diet before and during pregnancy causes a significant up-regulation of placental nutrient transport and fetal overgrowth both in mice and rats.[23,24] Another study showed that embryos, mothers of which were exposed to the KD diet during pregnancy were volumetrically larger in the middle of gestation, in comparison to their counterparts from the control group and then the volumetric decreases at a later stage were noticed.[25] It has also been reported that such a diet used during pregnancy and early postnatal life may lead to alterations in the neonatal brain structure, including the areas of the cortex, hippocampus, corpus callosum, fimbria, lateral ventricles, hypothalamus, and medulla.[26] The authors suggested that such anomalies could be associated with functional and behavioral changes in later postnatal life.[26] Our previous investigation showed a reduction of the body mass and delays in the neurological development of the offspring from females fed during gestation with KD.[27] However, discontinuation of the high-fat diet and introducing the standard one in mothers at the beginning of lactation resulted in the recovery of weight and neurological function of pups to the normal levels already on the postnatal day 14th.[27]

Our previous studies showed that the spatial distribution and the accumulation of main biological macromolecules within the brain differ between rats fed prenatally with ketogenic and standard laboratory diets.[28] In 14-day-old offspring of KD-fed mothers, an increase in the relative level of compounds containing carbonyl groups as well as a decrease in the relative content of lipids and their structural changes in some areas of the brain were observed.[28] Moreover, the chemical mapping of absorption bands specific to lipids showed that the surface of the internal capsule is smaller for these animals.

This study aims to identify topographic and quantitative elemental anomalies appearing in offspring brains as a result of maternal ketogenic diet (KD) treatment during gestation. To achieve this, we compared the male offspring of the female rats fed during pregnancy either with a ketogenic or standard laboratory diet. The study included the progeny at 2, 6, 14, 30, and 60 days of age, enabling us to monitor the progression of potential elemental changes and determine whether they are temporary or persistent. The elemental mapping of brain slices was performed using synchrotron radiation-induced X-ray fluorescence (SR-XRF) microscopy being a nondestructive, highly sensitive, and relatively fast technique of multielemental analysis. This method has proven to be very useful in our previous research on the epilepsy pathogenesis and progression,[29−32] the neuroprotective and antiseizure effect of KD,[33−35] and the elemental markers of brain injury and glioma development.[36] Element-sensitive hard X-ray imaging, necessary to realize the purposes of the present paper, was conducted at the FLUO beamline[37] of the KIT Synchrotron light source (Karlsruhe, Germany) and the used experimental

https://doi.org/10.1021/acschemneuro.4c00283
ACS Chem. Neurosci. 2024, 15, 3932−3944

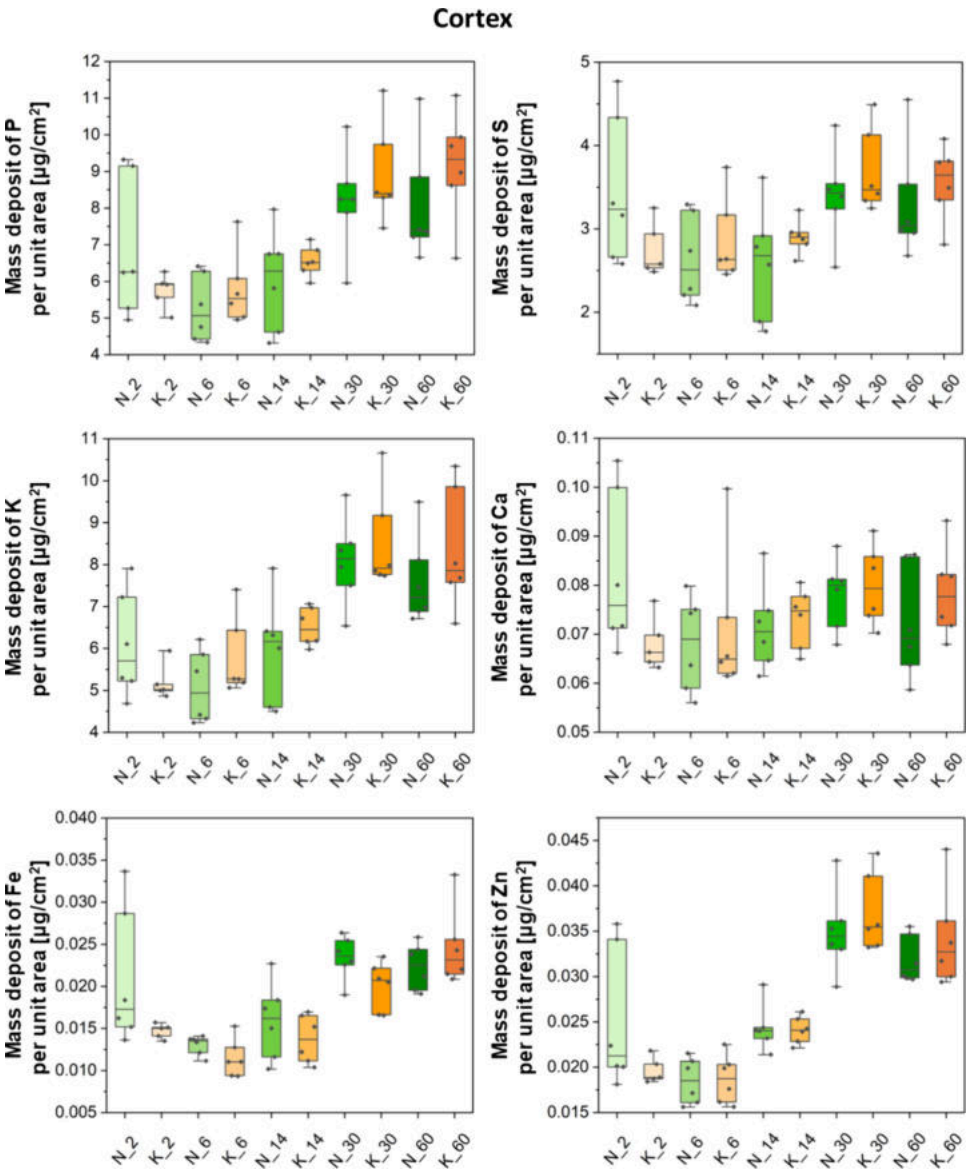

Figure 3. Box-and-whisker plots presenting the median, minimal, and maximal values as well as interquartile spans of the mass deposits of P, S, K, Ca, Fe, and Zn in the cortex determined for the experimental (K) and control (N) groups. The 2-, 6-, 14-, 30-, and 60-days old rats were taken into account in the analysis. No statistically significant differences (Mann−Whitney *U* test, 95% confidence level) were found between the K and N groups of the rats at a given age.

conditions allowed us to track the spatial distribution and accumulation of phosphorus (P), sulfur (S), potassium (K), calcium (Ca), iron (Fe), and zinc (Zn) within the scanned tissue regions.

RESULTS AND DISCUSSION

Considering the safety of the use of KD by pregnant women, it is crucial to determine the potential effects of such dietary treatment on the offspring, among others, on the nervous system. In our previous investigations we focused on checking how KD used during gestation influences the body mass, neurological functions, and general state of pups[27] as well as the distribution, accumulation, and structure of biomolecules in their brains.[28] The purpose of this study was to verify if prenatally used KD has an influence on the topographic and quantitative elemental changes occurring in the offspring's brain with age.

The results of the topographic elemental analysis from mapping the distributions of P, S, K, Ca, Fe, and Zn in the examined brain slices are shown in Figures 1 and 2. Additionally, in Figure 1, optical microscope images showing anatomical features of the examined tissues were presented.

The element distribution maps shown in Figures 1 and 2 indicate that the level of most of the examined elements is higher in the most mature brains (60-day-old animals) than in the initial stages of the postnatal development of the nervous system. The only exception here is Ca, the mass deposit of which, regardless of the mother's diet during pregnancy, does not differ significantly among the rats at various ages. The most dynamic changes in the accumulation of the majority of elements in the brains were observed between the 14th and 30th days of the animals' life. In turn, their lowest levels were found in 6-day-old rats.

A qualitative comparison of the element distribution maps from the offspring of mothers fed prenatally with the ketogenic

https://doi.org/10.1021/acschemneuro.4c00283
ACS Chem. Neurosci. 2024, 15, 3932−3944

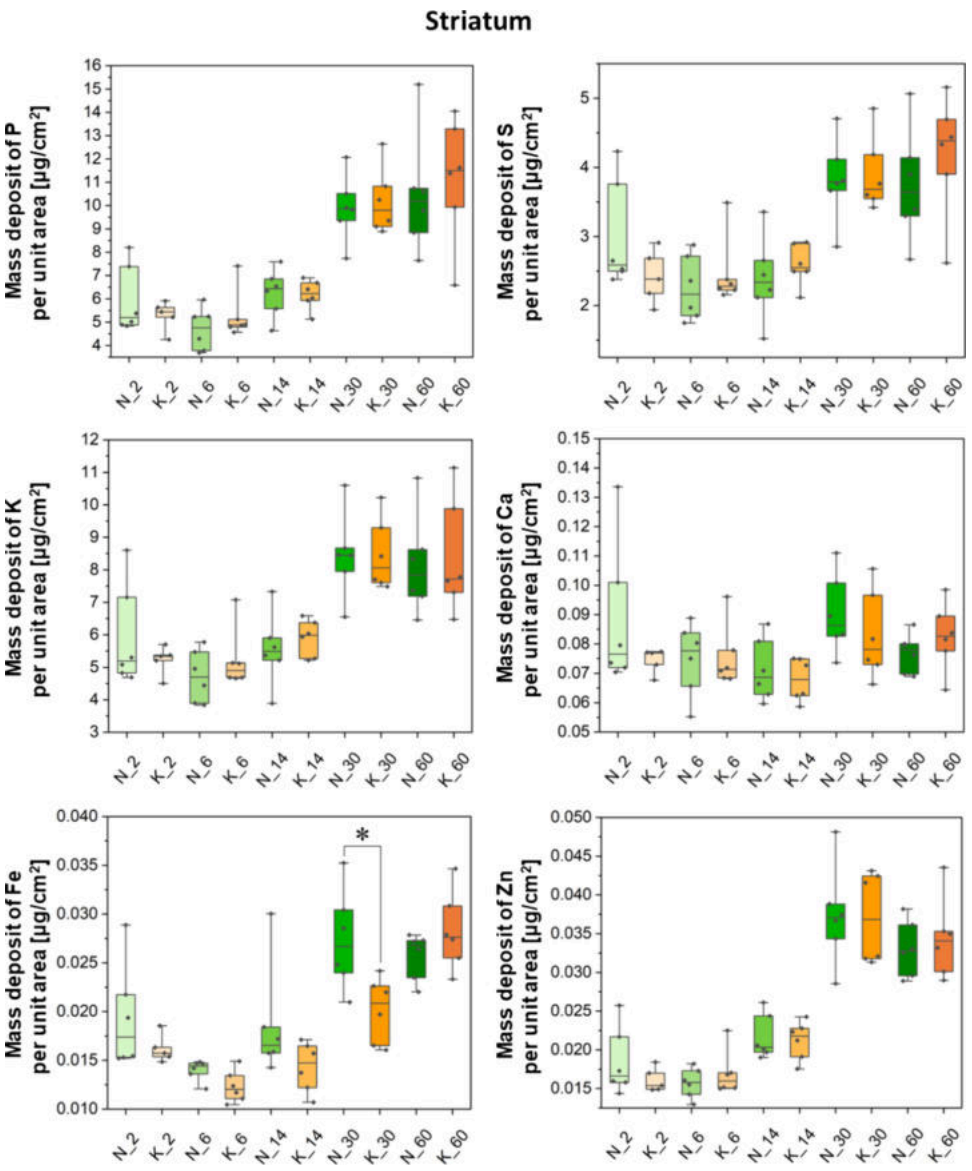

Figure 4. Box-and-whisker plots presenting the median, minimal, and maximal values as well as interquartile spans of the mass deposits of P, S, K, Ca, Fe, and Zn in the striatum determined for the experimental (K) and control (N) groups. The 2-, 6-, 14-, 30-, and 60-day-old rats were taken into account in the analysis. Statistically significant difference(s) (Mann−Whitney *U* test, 95% confidence level) between the K and N groups at a given age was(were) marked with *.

and standard diets indicates an influence of the dietary nutrition used during pregnancy on the level of low-Z elements in the brain. The rats, prenatally exposed to the high-fat diet, at the age of 6 and 14 days seemed to have a higher accumulation of P, S, and K than their corresponding control animals. The opposite tendency for the mentioned elements was observed for the adult (60-day-old) animals. In the 30- and 60-day-old offspring of the mothers fed with KD during pregnancy, a reduction of the surface of brain areas characterized by an increased P and S content, which histologically/morphologically correspond to white matter structures, was noticed. The Fe distribution maps indicated a lower content of this element in the brains of 30-day-old animals whose mothers received high-fat fodder. In turn, Zn distribution maps revealed that the use of KD during pregnancy leads to a temporary increase in the level of this element in the hippocampal formation of the young offspring (6- and 14-day-old).

Besides the topographic analysis giving insight into the global element changes occurring in the brain as a result of postnatal development and prenatally used KD, a more detailed quantitative analysis was performed for the selected brain areas. These were the cortex, striatum, and corpus callosum and, in the case of the older animals, also the internal capsule. Results of quantitative comparisons between the experimental KD-fed groups (K_2, K_6, K_14, K_30, and K_60 where the numbers denote the age) and their corresponding control animals (N_2, N_6, N_14, N_30, and N_60) are shown in a form of box-and-whisker plots in Figures 3−6. Furthermore, to follow the dynamics of elemental changes occurring during postnatal brain development, the statistical significance of the differences in the elemental accumulation between the subsequent time points was verified, and the obtained results are presented in the Supporting Information in Figure S1.

https://doi.org/10.1021/acschemneuro.4c00283
ACS Chem. Neurosci. 2024, 15, 3932−3944

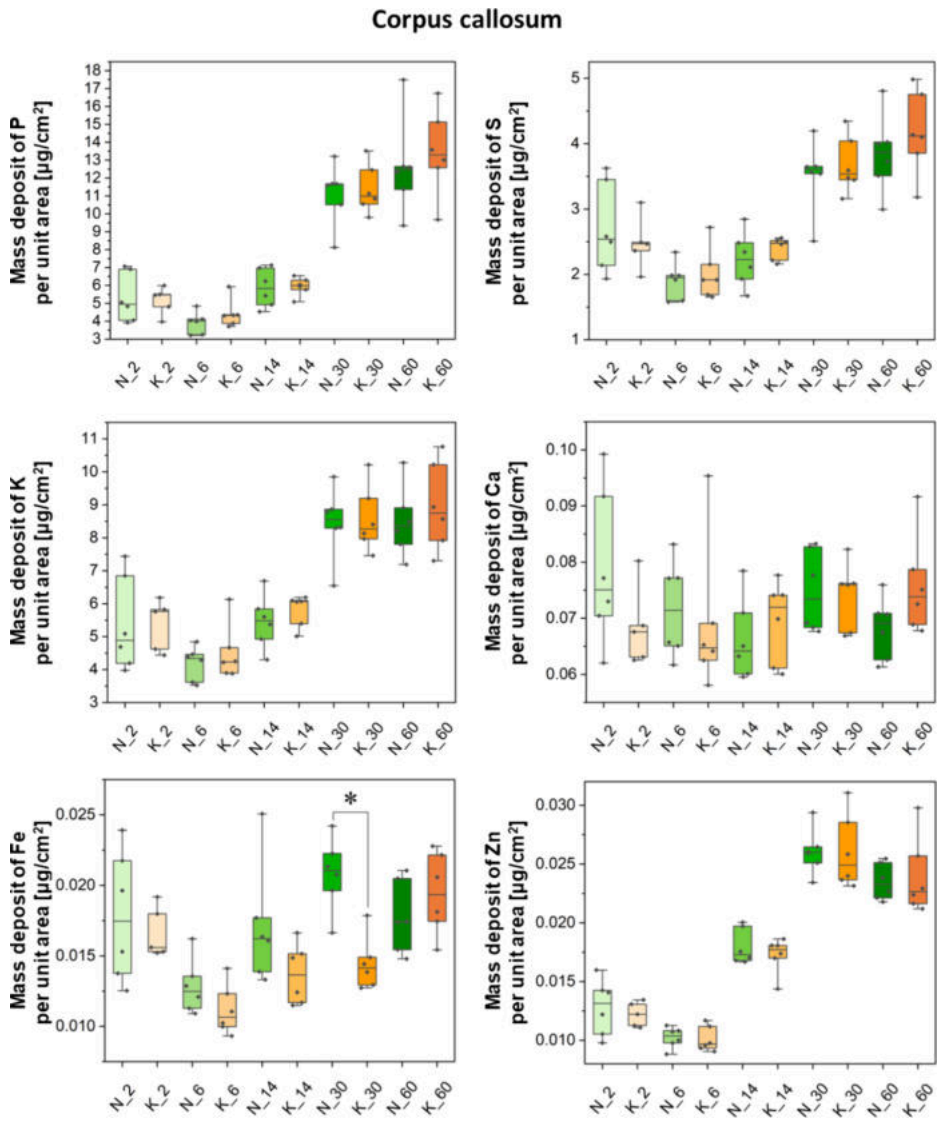

Figure 5. Box-and-whisker plots presenting the median, minimal, and maximal values as well as interquartile spans of the mass deposits of P, S, K, Ca, Fe, and Zn in the corpus callosum determined for the experimental (K) and control (N) groups. The 2-, 6-, 14-, 30-, and 60-day-old rats were taken into account in the analysis. Statistically significant difference(s) (Mann−Whitney *U* test, 95% confidence level) between the K and N groups at a given age was(were) marked with *.

The Mann−Whitney *U* test was performed in order to identify statistically relevant differences in the accumulation of the examined elements in the selected brain areas. Its results showed only some temporary differences in the Fe mass deposits between the experimental and control animals. In 30-day-old rats that were exposed prenatally to the KD, a lower level of Fe in the striatum and in both studied white matter structures (namely, corpus callosum and internal capsule) was noticed. The aforementioned effect, however, was not observed in adult animals.

The previously performed topographic analysis suggested also the existence of the differences in the size of the areas characterized by the increased P and S levels and corresponding to the structures of white matter between the older offspring of mothers fed during pregnancy with the ketogenic and normal diet. Figure 7 presents box-and-whisker plots showing the median, minimal, and maximal values of the relative sizes of the areas characterized by the increased P and S accumulation for the 30- and 60-day-old experimental and control rats (K and N groups, respectively). The method of determining these relative sizes is presented in the Materials and Methods chapter. As one can easily notice in Figure 7, the statistical analysis performed confirmed the prior qualitatively observed differences.

Statistical analysis confirmed that the content of P in rat brains increases mainly between the 14th and 30th days of their postnatal life and it does not change at a later stage of the development. The consumption of KD by mothers during pregnancy seems to affect the level of this element in the brains of the offspring. Qualitative analysis showed that the rats at the age of 6 and 14 days, exposed prenatally to the high-fat diet, showed in general a higher accumulation of P than the corresponding control animals, in turn, the opposite relationship was observed for adult ones. However, the statistical analysis performed for selected brain regions did not reveal any statistically significant differences. Additionally, the subarea highly abundant with P, corresponding morphologically to the white matter, was significantly smaller in the case of the 30-

https://doi.org/10.1021/acschemneuro.4c00283
ACS Chem. Neurosci. 2024, 15, 3932−3944

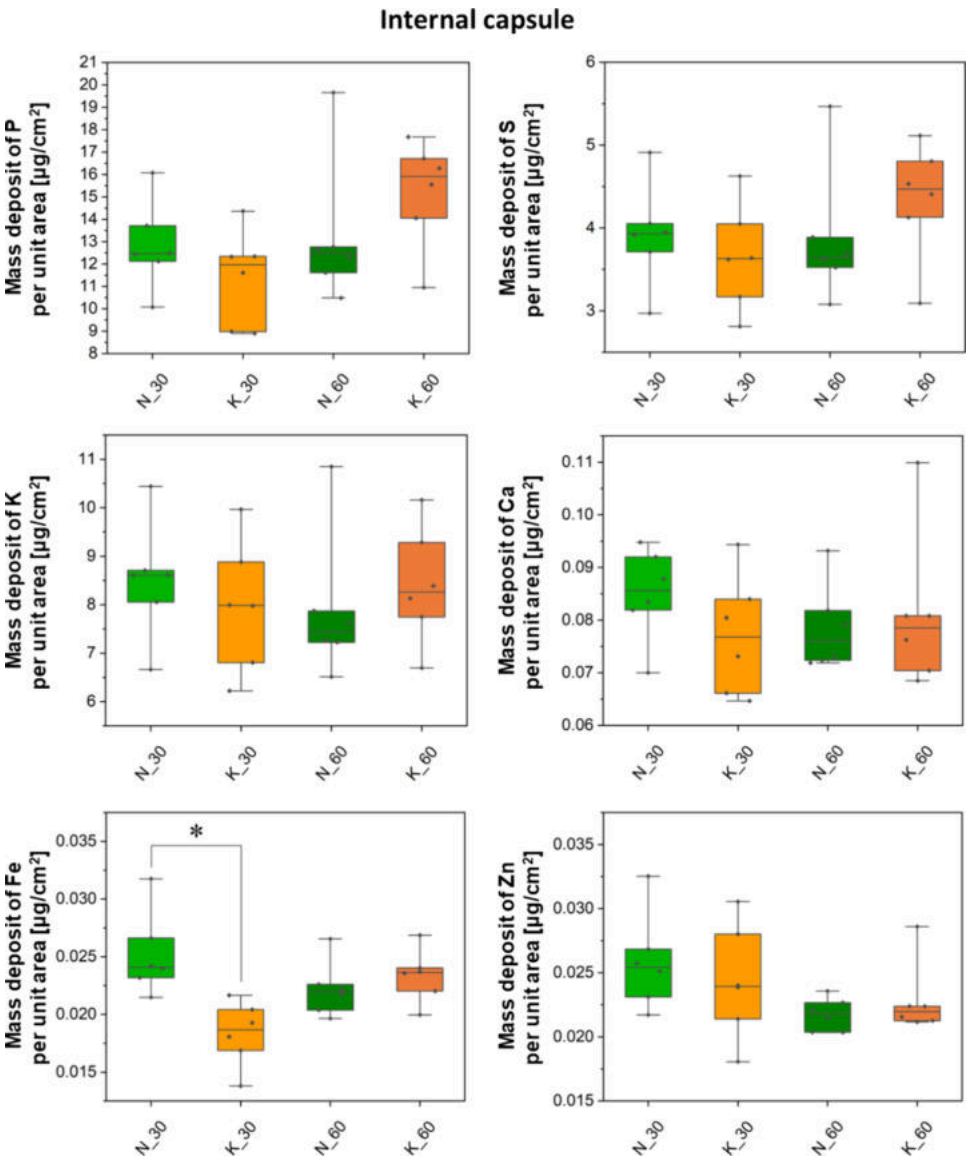

Figure 6. Box-and-whisker plots presenting the median, minimal, and maximal values as well as interquartile spans of the mass deposits of P, S, K, Ca, Fe, and Zn in the internal capsule determined for the experimental (K) and control (N) groups. The 30- and 60-day-old rats were taken into account in the analysis. Statistically significant difference(s) (Mann−Whitney *U* test, 95% confidence level) between the K and N groups at a given age was(were) marked with *.

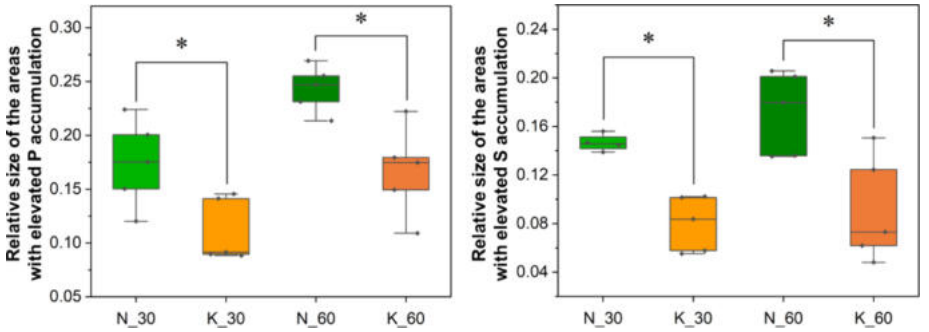

Figure 7. Box-and-whisker plots presenting the median, minimal, and maximal values of the relative sizes of the areas characterized by the increased P and S accumulation for the 30- and 60-day-old experimental and control rats (K and N groups, respectively). Statistically significant difference(s) (Mann−Whitney *U* test, 95% confidence level) between the K and N groups at a given age were marked with *.

and 60-day-old pups of the KD-fed mothers. A similar relationship was also observed in our previous paper[28] with respect to the spatial distribution of lipids in the 14-day-old offspring of high-fat fodder fed rats. The subarea of the brain

https://doi.org/10.1021/acschemneuro.4c00283
ACS Chem. Neurosci. 2024, 15, 3932−3944

characterized by an increased intensity of lipid bands (corresponding to the internal capsule of the white matter) was smaller in animals when the mothers during pregnancy were treated with KD.

The white matter constitutes well-vascularized clusters of nerve fibers. These fibers are mostly axons surrounded by myelin sheaths which, in the brain, are formed by oligodendrocytes.[38−40] Myelin contains 70−85% of lipids and the most abundant of them are galactocerebroside, sphingomyelin (containing predominantly a phosphocholine as a headgroup), and cholesterol.[41,42] The observed in the pups of KD-fed mothers correlated abnormalities in the distributions of P and lipids may mirror the changes in the accumulation of sphingomyelin and, the same, point at the disturbances in the structure and integrity of the myelin. Recently, more and more attention has been focused on the role of myelin in the central nervous system and its most known functions are the acceleration of nerve impulse conduction and increasing energy efficiency in this process.[40,42] Furthermore, myelinating glial cells, such as oligodendrocytes, present in the myelin sheath provide physical and chemical protection to axons, which make them more resistant to damage, but also regulate their ionic environment and fuel their energy demands with metabolites.[43] There is also growing evidence that the myelin sheath provides a trophic support to the axons.[41,44] Facilitating efficient communication between nerve cells, the myelin is crucial for the proper action of the nervous system and it plays a crucial role in cognition, learning, and even human behavior.[40,45,46] However, to check how the observed changes in the white matter structure affect the function of the nervous system or animal behavior, further long-term observation of the offspring is necessary.

The content of S and K remained at a relatively constant level in the initial stages of brain development, and a noticeable change in the accumulation of these elements occurred on the 30th day of animal life. The qualitative topographic analysis showed, moreover, that similarly as in the case of P, the level of S and K presented the opposite pattern of changes induced by prenatal exposure to KD in the case of younger and older animals. One of the reasons for the higher content of low-Z elements in the brains of the younger offspring from the females fed with the high-fat diet could be a higher content of these elements in the KD than in the standard laboratory diet. However, the analysis of the element composition of the fodders performed by us indicates exactly the opposite relationship for P and S, in which the concentration was lower in the high-fat than in the standard diet.[47] The content of K in both diets was at a similar level. However, because of the lower fodder mass consumed by the rats on KD, the intake of K through these animals was smaller compared to that of controls. It also should be noted that in the mothers fed with KD during pregnancy, the standard diet was introduced at 2 days of postpartum and continued during the whole time of lactation, so the potential KD influence would be associated with the period before postpartum.

S is an essential component that influences the function of several bioactive molecules. Sulfatide, a sulfated form of galactocerebroside, is an important sulfoglycolipid found on the extracellular leaflet of myelin.[48,49] Most of the sulfatide in the nervous system is present in myelinating cells, namely oligodendrocytes in the central nerves and Schwann cells in the peripheral ones.[50] The literature evidence points out that these sulfoglycolipids may play an important role in the differentiation of myelinating cells, formation of the paranodal junctions, and general myelin maintenance.[49,51] They are involved in the formation of membrane microdomains (lipid rafts), where together with cholesterol and raft-associated proteins play roles in different myelin functions.[49] Moreover, sulfatides participate in a variety of cellular processes such as protein trafficking, axon-myelin interactions, neural plasticity, and immune response.[52] The research indicates that although the lack of sulfatide does not interfere with the processes related to the myelin formation or cause drastic changes in its structure, it does prevent the maintenance of the normal myelin sheath in adult mice.[53,54] The colocalization, we found in the present paper, between the areas of the increased S content and the structures of the white matter may be a result of the presence of sulfatides from the myelin sheaths. Taking into consideration the above-mentioned dependences, the reduction of this surface in the offspring of the KD-fed mothers may testify about white matter abnormalities.

We noticed a reduction in the level of Fe in the 30-day-old rats, mothers of which were fed with KD during pregnancy. Although excessive Fe accumulation in the brain appears to be much more dangerous than element deficiency, any imbalance in micronutrients should be monitored. On the other hand, the nature of the anomalies, we found in the present paper, seems to be transient as no similar relationship was observed in the older, 60-days-old animals. The research based on animal models showed that adequate Fe levels support the proper neurological and cognitive development while its fetal and neonatal deficiency may reduce the oxidative metabolism in the hippocampus and frontal cortex, increase concentrations of intracellular neuronal glutamate, reduce dopamine distribution in the striatum, and alter the fatty acids and myelin profiles in brains.[55−58] Fe concentration in the brain increases with age, because of the constant intake and the slow exchange of this element during the whole life.[59] Our results collected in the present investigation showed that the level of Fe, for both the experimental and control groups, was the lowest in the 6-day-old animals, and it slowly increased in subsequent time periods.

Fe is a micronutrient that is needed for the proper functioning of the nervous system. It has the ability to cross the blood-brain barrier (BBB) and participate in the generation of neurotransmitters and axonal myelination.[59] Furthermore, various metabolic processes, including the synthesis of DNA, which is crucial for cell division and growth, demand this element.[36,60] Despite the many positive roles of Fe in the nervous system, the element may also be potentially toxic for living cells by catalyzing Fenton's reaction, which leads to the creation of highly reactive hydroxyl radicals, intensifying the effect of the oxidative stress.[31,59] The decreased level of Fe, which we found in the 30-day-old offspring of the high-fat fodder-fed mothers, may be related to the above-mentioned changes, namely, the reduction of the relative surface of the other elements in the white matter in the older rats exposed prenatally to KD. However, at this stage of our investigation, it is not possible to answer the question of whether or not the brain structural changes are induced by the diminished level of the element or if the diminished deposits of Fe are a result of intensified processes of myelination and formation of neural connections.

Among all of the investigated elements, the most dynamic changes during the animal postnatal development were found for Zn. The lowest mass deposit of this element was observed in the brains of the 6-day-old rats. The level of Zn increased

https://doi.org/10.1021/acschemneuro.4c00283
ACS Chem. Neurosci. 2024, 15, 3932−3944

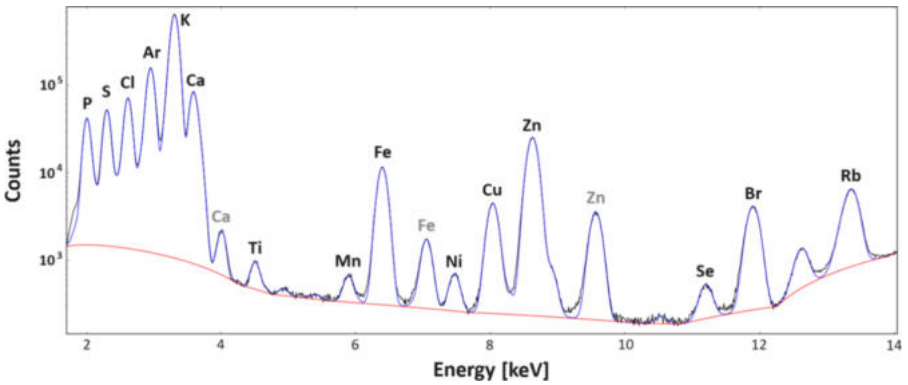

Figure 8. Typical cumulative X-ray fluorescence spectrum (black line) obtained for a brain tissue sample taken from a 60-day-old control rat. The fitted curve and its background are marked with blue and red line, respectively. The analytical Kα lines of the elements were marked in black, while Kβ lines were signed in gray.

during the next two observation periods and then remained at a similar level between the 30th and 60th days of the animal life. The mass deposit of Zn within the hippocampal formation of the control rats diminished between the second and sixth days of postnatal development. Afterward, its level increased to reach the highest quantity in the 60-day-old animals, which is in agreement with our previous study.[61] The comparison between the offspring of the mothers fed during pregnancy with the high-fat and standard fodder showed a higher Zn accumulation in the hippocampus of the 6- and 14-day-old rats prenatally exposed to the KD. The increase of Zn accumulation in particular areas of the brain at the beginning of its development may testify to the reorganization of GABA-ergic innervation, sprouting of mossy fibers, and/or functional changes of nervous tissue.[61] The higher level of the element observed temporarily within the hippocampal formation of the animals exposed prenatally to KD may point to the intensification of the processes of nervous tissue reorganization within this brain area.

Summarizing, elements such as P, S, K, Ca, Fe, and Zn perform many important functions in the brain, so it is important to monitor potential changes in their levels and distributions in the offspring nervous system that may be caused by the use of KD during pregnancy. In this paper, we showed that X-ray fluorescence microscopy can be successfully employed to track the element changes occurring in the brain during its postnatal development as well as those induced by prenatal exposure to high-fat fodder. In view of our present results, KD implemented in mothers influences the element content in the brains of their offspring. Moreover, our investigation showed some topographical abnormalities in the brains of the oldest rats exposed prenatally to KD. For these animals, a reduction of brain area characterized by an increased P and S level and histologically/morphologically corresponding to the structures of white matter were noticed. In order to confirm or exclude different influences of the prenatally used KD on the offspring depending on their gender, it is worth extending the investigation in the future to female pups. Further research on mechanisms of the observed phenomena and their possible health consequences is still necessary in order to increase the chances for the implementation of such dietary treatment of epilepsy in pregnant women.

MATERIALS AND METHODS

Animals. The rats investigated in this study originated from the Laboratory of Experimental Neuropathology at the Institute of

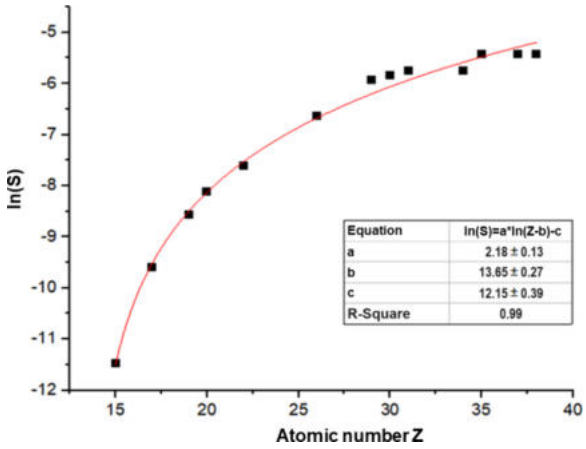

Figure 9. Sensitivity curve calculated on the basis of the micromatter XRF calibration standards.

Zoology and Biomedical Research (Jagiellonian University, Krakow, Poland). A culture of animals as well as all animal-use experiments was also conducted there. This was done in accordance with permission 122/2015 of the First Local Ethical Committee and with international standards. In the study, the male rats of the Wistar strain at different ages, which had been born by females receiving during their gestation the ketogenic or standard diet (experimental and control groups, respectively), were used. Both diets were maintained during the entire period of pregnancy. In the case of the mothers of the control group, the standard laboratory diet was continued during lactation. In turn, in the case of the previously KD-fed females, a normal diet was introduced 2 days after labor. The offspring were nourished with maternal milk until 21 days of postnatal life, after which they were transferred to individual cages and provided with a standard diet. The details of the experiment were described in our previous papers.[27,28] The present study included 5 stages of the offspring development, namely, 2-, 6-, 14-, 30-, and 60-day-old rats, and the typical number of animals in each group was 6.

Ketogenic and Standard Laboratory Diet. KD with long-chain fatty acids (ssniff, EF R/M with 80% Fat) and the standard laboratory diet in the form of Labofeed (Morawski, Inc.) were used in the study. The content of main nutrients (defined by the producers of the fodders) as well as the major, minor, and trace elements (determined by us using the TXRF method) in both diets was presented in our previous works.[28,47]

https://doi.org/10.1021/acschemneuro.4c00283
ACS Chem. Neurosci. 2024, 15, 3932−3944

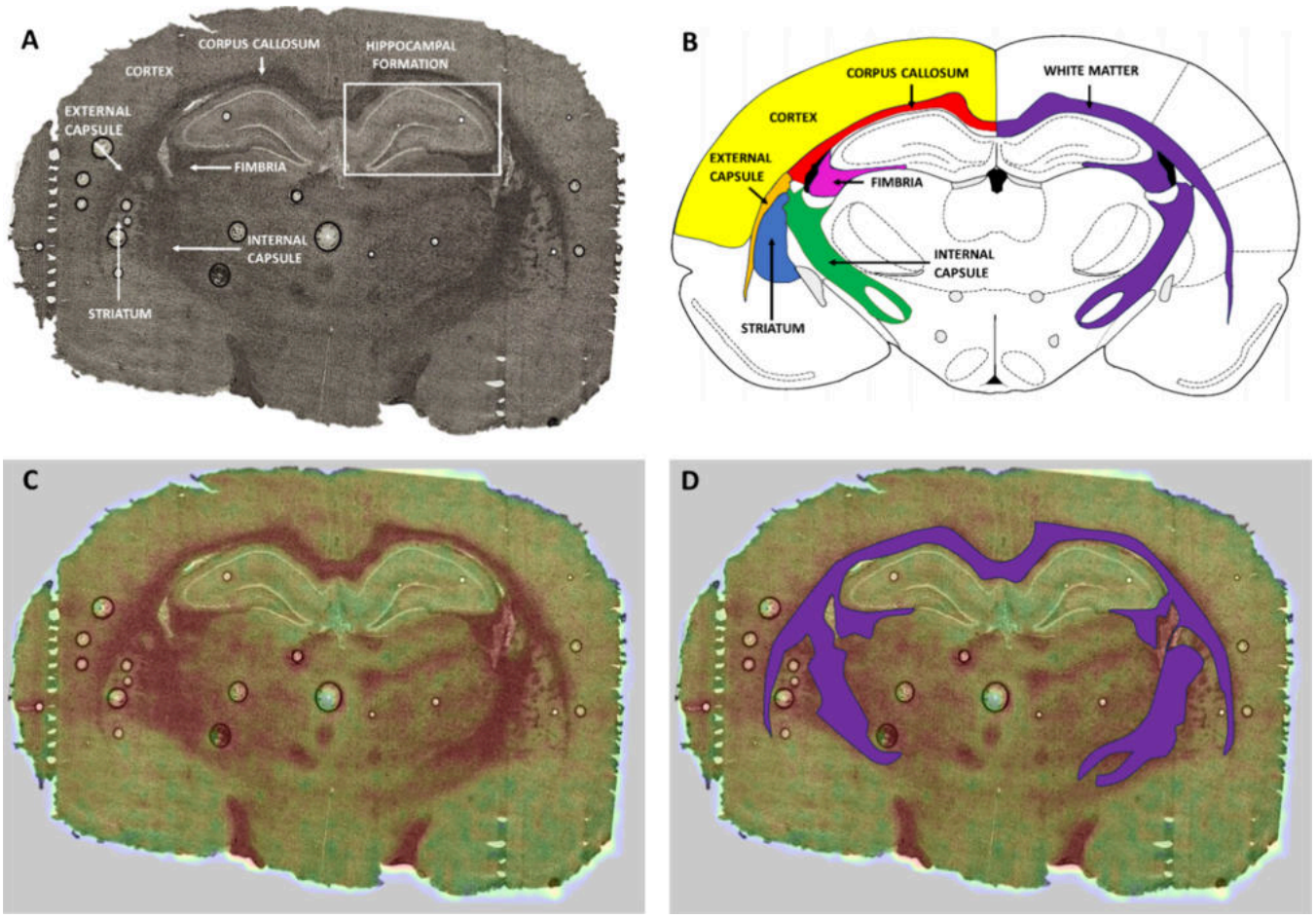

Figure 10. Comparison of the localization of selected regions (cortex, striatum, hippocampal formation and structures of white matter: corpus callosum, fimbria, internal capsule, and external capsule) in the microscopic image of an exemplary brain slice taken from 60-days old rat (A) with the graphics, based on the Paxinos and Watson anatomical atlas,[65] presenting these brain areas in the corresponding coronal diagram (B). Blend of the microscopic image of the brain with the map of P distribution (C) and definition of the region taken into account in calculations of the relative size of the area characterized by the increased P content (D).

Sample Preparation. On the 2nd, 6th, 14th, 30th, and 60th days of postnatal life (depending on the group), the animals were anesthetized with Morbital (Biowet) and perfused with a physiological saline solution of high analytical purity. After that, the brains were extracted from the skulls, deeply frozen in liquid nitrogen, and cut with a cryomicrotome into slices with a thickness of 20 μm. From each brain, the slice containing the dorsal part of the hippocampal formation was taken (Figure 10 A), placed on a stretched Ultralene foil, and freeze-dried.

SR-XRF Element Imaging. To visualize the mass deposits of the elements of our interest within the brain slices and to perform subsequently a topographic and quantitative elemental analysis, SR-XRF microscopy was applied. The brain tissues were scanned at the FLUO beamline installed at the KIT synchrotron light source in Karlsruhe, Germany. The energy of the exciting X-ray beam was 17 keV while its size was 200 μm (v) × 200 μm (h). Such a relatively large X-ray beam was employed for raster scanning of the whole-area tissue slices with a step size of 200 μm in both directions and an acquisition time for a single XRF spectrum of 10 s.

Qualitative, Topographic, and Quantitative Element Analysis. The content of P, S, K, Ca, Fe, and Zn was determined in brain samples. Although, as one can see in Figure 8, other element X-ray lines were also detected in the cumulative XRF spectrum of tissue. Cl was excluded from further analysis because a NaCl solution was used for perfusion. Ar came from the ambient air, as the element imaging was not done in vacuum. In turn, Ti, Mn, and Ni in the cumulative XRF spectrum were of a nontissue but instrumentation origin. The remaining elements (Cu, Se, Br, and Rb), not taken into account in topographic and quantitative analysis, were below the limits of their detection for some of the examined pixels or tissue samples and therefore were not the subject of further analysis.

The two-dimensional topographic analysis of the elements of interest was based on mapping of their mass deposits in brain slices. The mass deposit per unit area of the element (M_T) was calculated for each pixel of the map in accordance with eq 1):

$$M_T = \frac{Y_T}{S \times Y_T^N} \tag{1}$$

M_T is the mass deposit per unit area of the examined element in the tissue sample [μg/cm^2].

Y_T is the net peak area of the $K\alpha$ line of the measured element for the tissue sample [cts].

S is the sensitivity for the measured element [cm^2/μg].

Y_T^N is the incoming X-ray beam normalization for the tissue sample [cts].

The sensitivities S for the measured elements were calculated on the basis of measurements of the Micromatter Technologies Inc. (Surrey, Canada) XRF calibration standards (RbI, Se, Cu, Ti, Fe, CaF_2, GaP, SrF_2, CsBr, ZnTe, and KCl) and using formula 2:

$$S = \frac{Y_S}{M_S \times Y_S^N} \tag{2}$$

https://doi.org/10.1021/acschemneuro.4c00283
ACS Chem. Neurosci. 2024, 15, 3932−3944

Y_S is the net peak area of the $K\alpha$ line of the measured element for the standard sample [cts].

M_S is the mass deposit per unit area of the analyzed element in the standard sample [$\mu g/cm^2$].

Y_S^N is the incoming X-ray beam normalization for the standard sample [cts].

For the XRF spectra normalization an electric charge accumulated within a semiconductor X-ray transparent diode placed upstream of the tissue/standard samples was used. The net peak areas of the $K\alpha$ lines for the selected elements were determined with the PyMca software[62] (version 5.1.2). Once the sensitivities S were calculated, a calibration curve (Figure 9) was fitted according to eq 3 with the use of OriginPro (OriginLab Corporation, Northampton, MA, USA) software.

$$\ln(S) = a \times \ln(Z - b) - c \quad (3)$$

Z is the atomic number of the measured element, a, b, and c are the parameters of the calibration curve.

Once the element mass deposits per unit area for all the pixels of a particular map were calculated, the distributions of P, S, K, Ca, Fe, and Zn were drawn for the examined brain samples. The obtained maps were, then, compared with the corresponding microscopic pictures of the tissues in order to identify in them the important brain regions: cortex, striatum, hippocampal formation, and structures of white matter: corpus callosum, fimbria, internal capsule, and external capsule. For subsequent quantitative analysis, the cortex, striatum, and corpus callosum were selected. These regions were identified even for younger animals, and their size allowed for the collection of the number of data points allowing reliable quantitative analysis. In the case of older rats (30- and 60-day-old), the internal capsule was also included for further analysis as it was well visible in tissues taken for these age groups. In Figure 10 A,B, the localization of the mentioned regions within an exemplary brain slice was compared with the graphics based on the Paxinos and Watson rat brain anatomical atlas.

In order to perform the quantitative element analysis, for each examined slice, the average mass deposits of P, S, K, Ca, Fe, and Zn in the cortex, striatum, and selected structure(s) of the white matter were calculated. The average mass deposits were based on 50 randomly chosen points from particular areas (excluding some artifacts e.g. local contaminations of tissue, air bubbles formed between the tissue and the Utralene foil substrate, and tissue-free places within the scanned areas) and then employed for further statistical analysis. A nonparametric Mann−Whitney U test was applied to verify the significance of the differences between the animals exposed prenatally to KD and controls at the appropriate stage of postnatal development. The nonparametric U test is the right tool for statistical analysis because our data could not meet the assumptions about normality, homoscedasticity, and linearity, which are necessary for the use of parametric test.[63,64] For the statistical analysis, OriginPro software was used, and the significance level was 5%.

The performed topographic analysis suggested the existence of the differences in the size of the areas characterized by the increased P and S levels between the older offspring of mothers fed during pregnancy with a ketogenic and normal diet. Histologically/morphologically these areas correspond to the structures of white matter. To verify this observation, the relative (compared to the whole brain slice) sizes of brain areas showing elevated P and S accumulation and corresponding white matter concentrations were determined. This was done independently for all the animals at the age of 30 and 60 days. Figure 10 C illustrates the methodology used to identify regions with elevated phosphorus and sulfur levels corresponding to white matter, which were included in the quantitative analysis. The sizes of the areas characterized by increased accumulation of mentioned elements as well as the surfaces of entire brain slices were determined with ImageJ software (version 1.52a, NIH, USA). Then, with the Mann−Whitney U test (95% confidence level), the ratios of these surfaces for the experimental and control rats were compared.

■ ASSOCIATED CONTENT

Supporting Information

The Supporting Information is available free of charge at https://pubs.acs.org/doi/10.1021/acschemneuro.4c00283.

(Figure S1) Dynamics of elemental changes occurring in selected brain areas during postnatal development in the offspring of mothers fed during pregnancy with the ketogenic or standard fodder (PDF)

■ AUTHOR INFORMATION

Corresponding Author

Joanna Chwiej − *Faculty of Physics and Applied Computer Science, AGH University of Krakow, Krakow 30-059, Poland;* orcid.org/0000-0002-3792-7876; Email: Joanna.Chwiej@fis.agh.edu.pl

Authors

Marzena Rugieł − *Faculty of Physics and Applied Computer Science, AGH University of Krakow, Krakow 30-059, Poland*

Zuzanna Setkowicz − *Institute of Zoology and Biomedical Research, Jagiellonian University, Krakow 30-387, Poland*

Mateusz Czyzycki − *Institute for Photon Science and Synchrotron Radiation, Karlsruhe Institute of Technology, Eggenstein-Leopoldshafen D-76344, Germany*

Rolf Simon − *Institute for Photon Science and Synchrotron Radiation, Karlsruhe Institute of Technology, Eggenstein-Leopoldshafen D-76344, Germany*

Tilo Baumbach − *Institute for Photon Science and Synchrotron Radiation, Karlsruhe Institute of Technology, Eggenstein-Leopoldshafen D-76344, Germany; Laboratory for Applications of Synchrotron Radiation, Karlsruhe Institute of Technology, Karlsruhe D-76131, Germany*

Complete contact information is available at: https://pubs.acs.org/10.1021/acschemneuro.4c00283

Author Contributions

#M.R. and Z.S. equally contributed to this work.

Author Contributions

M.R. performed methodology, investigation, formal analysis, visualization, and writing−original draft. Z.S. performed conceptualization, methodology, investigation, resource gathering, supervision, and writing−review and editing. M.C. performed methodology, investigation, and writing−review and editing. R.S. performed methodology and resource gathering. T.B. performed methodology and resource gathering. J.C. performed conceptualization, methodology, validation, resource gathering, supervision, and writing−original draft.

Notes

The authors declare no competing financial interest.

■ ACKNOWLEDGMENTS

This work was partially financed by the Ministry of Education and Science of Poland and the statutory research fund no. N18/DBW/000018 of the Laboratory of Experimental Neuropathology (Institute of Zoology and Biomedical Research, Jagiellonian University, Krakow, Poland). For the evaluation of tissue morphology, the WITec Alpha300R Raman microscope purchased from the funds granted to the AGH UST in the frame of the "Excellence Initiative-Research University" project was applied. M.R. has also been partially supported by the

program "Excellence Initiative-Research University" for the AGH UST (Action 4-leader M.R. and Action 4-leader J.C.).

REFERENCES

(1) McNally, M. A.; Hartman, A. L. Ketone bodies in epilepsy. *J. Neurochem* **2012**, *121*, 28−35.
(2) D'Andrea Meira, I.; Romão, T. T.; et al. Ketogenic Diet and Epilepsy: What We Know So Far. *Front Neurosci* **2019**, *13*, 5.
(3) McDonald, T. J. W.; Cervenka, M. C. Ketogenic Diet Therapies for Seizures and Status Epilepticus. *Semin Neurol* **2020**, *40*, 719−729.
(4) Hartman, A. L.; Vining, E. P. G. Clinical Aspects of the Ketogenic Diet. *Epilepsia* **2007**, *48*, 31−42.
(5) Gray, L. R.; Tompkins, S. C.; et al. Regulation of pyruvate metabolism and human disease. *Cell. Mol. Life Sci.* **2014**, *71*, 2577−2604.
(6) Hartman, A. L.; Gasior, M.; et al. The Neuropharmacology of the Ketogenic Diet. *Pediatr Neurol* **2007**, *36*, 281−292.
(7) Payne, N. E.; Cross, J. H.; et al. The ketogenic and related diets in adolescents and adults-A review. *Epilepsia* **2011**, *52*, 1941−1948.
(8) Klein, P.; Tyrlikova, I.; et al. Dietary treatment in adults with refractory epilepsy: A review. *Neurology* **2014**, *83*, 1978−1985.
(9) Barry, D.; Ellul, S.; et al. The ketogenic diet in disease and development. *International Journal of Developmental Neuroscience* **2018**, *68*, 53−58.
(10) Kossoff, E. H.; Hartman, A. L. Ketogenic diets: new advances for metabolism-based therapies. *Curr. Opin Neurol* **2012**, *25*, 173−178.
(11) Barañano, K. W.; Hartman, A. L. The ketogenic diet: Uses in epilepsy and other neurologic illnesses. *Curr. Treat Options Neurol* **2008**, *10*, 410−419.
(12) Yancy, W. S.; Olsen, M. K.; et al. A Low-Carbohydrate, Ketogenic Diet versus a Low-Fat Diet To Treat Obesity and Hyperlipidemia. *Ann. Int. Med.* **2004**, *140*, 769.
(13) Henderson, S. T. Ketone bodies as a therapeutic for Alzheimer's disease. *Neurotherapeutics* **2008**, *5*, 470−480.
(14) Prins, M. L.; Matsumoto, J. H. The collective therapeutic potential of cerebral ketone metabolism in traumatic brain injury. *J. Lipid Res.* **2014**, *55*, 2450−2457.
(15) Murphy, P.; Likhodii, S.; et al. The antidepressant properties of the ketogenic diet. *Biol. Psychiatry* **2004**, *56*, 981−983.
(16) Neal, E. G.; Chaffe, H.; et al. The ketogenic diet for the treatment of childhood epilepsy: a randomised controlled trial. *Lancet Neurol* **2008**, *7*, 500−506.
(17) Hemingway, C.; Freeman, J. M.; et al. The Ketogenic Diet: A 3- to 6-Year Follow-Up of 150 Children Enrolled Prospectively. *Pediatrics* **2001**, *108*, 898−905.
(18) Liu, H.; Yang, Y.; et al. Ketogenic diet for treatment of intractable epilepsy in adults: A meta-analysis of observational studies. *Epilepsia Open* **2018**, *3*, 9−17.
(19) Kellogg, M.; Meador, K. J. Neurodevelopmental Effects of Antiepileptic Drugs. *Neurochem. Res.* **2017**, *42*, 2065−2070.
(20) Jansson, T.; Powell, T. L. Role of the placenta in fetal programming: underlying mechanisms and potential interventional approaches. *Clin Sci.* **2007**, *113*, 1−13.
(21) Herrera, E.; Gómez-Coronado, D.; et al. Lipid Metabolism in Pregnancy. *Neonatology* **2004**, *51*, 70−77.
(22) van der Louw, E. J. T. M.; Williams, T. J.; et al. Ketogenic diet therapy for epilepsy during pregnancy: A case series. *Seizure* **2017**, *45*, 198−201.
(23) Jones, H. N.; Woollett, L. A.; et al. High-fat diet before and during pregnancy causes marked up-regulation of placental nutrient transport and fetal overgrowth in C57/BL6 mice. *FASEB J.* **2009**, *23*, 271−278.
(24) Gaccioli, F.; White, V.; et al. Maternal Overweight Induced by a Diet with High Content of Saturated Fat Activates Placental mTOR and eIF2alpha Signaling and Increases Fetal Growth in Rats1. *Biol. Reprod.* **2013**, *89*, 1.
(25) Sussman, D.; van Eede, M.; Wong, M. D.; Adamson, S. L.; Henkelman, M.; et al. Effects of a ketogenic diet during pregnancy on embryonic growth in the mouse. *BMC Pregnancy Childbirth* **2013**, *13*, 109.
(26) Sussman, D.; Ellegood, J.; Henkelman, M.; et al. A gestational ketogenic diet alters maternal metabolic status as well as offspring physiological growth and brain structure in the neonatal mouse. *BMC Pregnancy Childbirth* **2013**, *13*, 198.
(27) Kosiek, W.; Rauk, Z.; et al. Ketogenic diet impairs neurological development of neonatal rats and affects biochemical composition of maternal brains: evidence of functional recovery in pups. *Brain Struct Funct* **2022**, *227*, 1099−1113.
(28) Rugiel, M.; Setkowicz-Janeczko, Z.; et al. Does Ketogenic Diet Used in Pregnancy Affect the Nervous System Development in Offspring?—FTIR Microspectroscopy Study. *ACS Chem. Neurosci.* **2023**, *14*, 2775−2791.
(29) Chwiej, J.; Winiarski, W.; et al. The role of trace elements in the pathogenesis and progress of pilocarpine-induced epileptic seizures. *Journal of Biological Inorganic Chemistry* **2008**, *13*, 1267−1274.
(30) Chwiej, J.; Dulinska, J.; et al. Variations in elemental compositions of rat hippocampal formation between acute and latent phases of pilocarpine-induced epilepsy: an X-ray fluorescence microscopy study. *JBIC Journal of Biological Inorganic Chemistry* **2012**, *17*, 731−739.
(31) Chwiej, J.; Kutorasinska, J.; et al. Progress of elemental anomalies of hippocampal formation in the pilocarpine model of temporal lobe epilepsy—an X-ray fluorescence microscopy study. *Anal Bioanal Chem.* **2012**, *404*, 3071−3080.
(32) Chwiej, J.; Gabrys, H.; et al. Elemental anomalies in the hippocampal formation after repetitive electrical stimulation: an X-ray fluorescence microscopy study. *JBIC Journal of Biological Inorganic Chemistry* **2014**, *19*, 1209−1220.
(33) Chwiej, J.; Skoczen, A.; et al. The influence of the ketogenic diet on the elemental and biochemical compositions of the hippocampal formation. *Epilepsy & Behavior* **2015**, *49*, 40−46.
(34) Chwiej, J.; Patulska, A.; et al. Elemental changes in the hippocampal formation following two different formulas of ketogenic diet: an X-ray fluorescence microscopy study. *JBIC Journal of Biological Inorganic Chemistry* **2015**, *20*, 1277−1286.
(35) Chwiej, J.; Patulska, A.; et al. Various ketogenic diets can differently support brain resistance against experimentally evoked seizures and seizure-induced elemental anomalies of hippocampal formation. *Journal of Trace Elements in Medicine and Biology* **2017**, *42*, 50−58.
(36) Planeta, K.; Setkowicz, Z.; et al. Altered Elemental Distribution in Male Rat Brain Tissue as a Predictor of Glioblastoma Multiforme Growth—Studies Using SR-XRF Microscopy. *Int. J. Mol. Sci.* **2022**, *23*, 703.
(37) Simon, R.; Buth, G.; et al. The X-ray-fluorescence facility at ANKA, Karlsruhe: Minimum detection limits and micro probe capabilities. *Nucl. Instrum Methods Phys. Res. B* **2003**, *199*, 554−558.
(38) Bae, H.-G.; Kim, T. K.; et al. White matter and neurological disorders. *Arch Pharm. Res.* **2020**, *43*, 920−931.
(39) Safaiyan, S.; Besson-Girard, S.; Kaya, T.; Cantuti-Castelvetri, L.; Liu, L.; Ji, H.; Schifferer, M.; Gouna, G.; Usifo, F.; Kannaiyan, N.; Fitzner, D.; Xiang, X.; Rossner, M. J.; Brendel, M.; Gokce, O.; Simons, M.; et al. White matter aging drives microglial diversity. *Neuron* **2021**, *109*, 1100−1117.
(40) McKenzie, I. A.; Ohayon, D.; et al. Motor skill learning requires active central myelination. *Science* **2014**, *346* (1979), 318−322.
(41) Kister, A.; Kister, I. Overview of myelin, major myelin lipids, and myelin-associated proteins. *Front Chem.* **2023**, *10*, No. 1041961.
(42) Chrast, R.; Saher, G.; et al. Lipid metabolism in myelinating glial cells: lessons from human inherited disorders and mouse models. *J. Lipid Res.* **2011**, *52*, 419−434.
(43) Saab, A. S.; Nave, K.-A. Myelin dynamics: protecting and shaping neuronal functions. *Curr. Opin Neurobiol* **2017**, *47*, 104−112.
(44) Crawford, A. H.; Chambers, C.; et al. Remyelination: The True Regeneration of the Central Nervous System. *J. Comp Pathol* **2013**, *149*, 242−254.

https://doi.org/10.1021/acschemneuro.4c00283
ACS Chem. Neurosci. 2024, 15, 3932−3944

(45) Filley, C. M.; Fields, R. D. White matter and cognition: making the connection. *J. Neurophysiol* **2016**, *116*, 2093−2104.
(46) Bells, S.; Lefebvre, J.; et al. White matter plasticity and maturation in human cognition. *Glia* **2019**, *67*, 2020−2037.
(47) Kawon, K.; Rugiel, M.; Setkowicz, Z.; Matusiak, K.; Kubala-Kukus, A.; Stabrawa, I.; Szary, K.; Rauk, Z.; Chwiej, J.; et al. Ketogenic diet influence on the elemental homeostasis of internal organs is gender dependent. *Sci. Rep* **2023**, *13*, 18448.
(48) Pintado-Sierra, M.; García-Álvarez, I.; et al. A comprehensive profiling of sulfatides in myelin from mouse brain using liquid chromatography coupled to high-resolution accurate tandem mass spectrometry. *Anal. Chim. Acta* **2017**, *951*, 89−98.
(49) Baba, H.; Ishibashi, T. The Role of Sulfatides in Axon−Glia Interactions. *Adv. Exp. Med. Biol.* **2019**, *1190*, 165−179.
(50) Takahashi, T.; Suzuki, T. Role of sulfatide in normal and pathological cells and tissues. *J. Lipid Res.* **2012**, *53*, 1437−1450.
(51) Eckhardt, M. The Role and Metabolism of Sulfatide in the Nervous System. *Mol. Neurobiol* **2008**, *37*, 93−103.
(52) Xiao, S.; Finkielstein, C. V.; et al. The Enigmatic Role of Sulfatides: New Insights into Cellular Functions and Mechanisms of Protein Recognition. *Adv. Exp. Med. Biol.* **2013**, 27−40.
(53) Marcus, J.; Honigbaum, S.; et al. Sulfatide is essential for the maintenance of CNS myelin and axon structure. *Glia* **2006**, *53*, 372−381.
(54) Honke, K.; Hirahara, Y.; et al. Paranodal junction formation and spermatogenesis require sulfoglycolipids. *Proc. Natl. Acad. Sci. U. S. A.* **2002**, *99*, 4227−4232.
(55) Georgieff, M. K. Nutrition and the developing brain: nutrient priorities and measurement. *Am. J. Clin. Nutr.* **2007**, *85*, 614S−620S.
(56) Beard, J. L.; Connor, J. R. Iron status and neural functioning. *Annu. Rev. Nutr* **2003**, *23*, 41−58.
(57) Rao, R.; Tkac, I.; et al. Perinatal Iron Deficiency Alters the Neurochemical Profile of the Developing Rat Hippocampus. *J. Nutr.* **2003**, *133*, 3215−3221.
(58) Beard, J. L.; Wiesinger, J. A.; et al. Pre- and Postweaning Iron Deficiency Alters Myelination in Sprague-Dawley Rats. *Dev Neurosci* **2003**, *25*, 308−315.
(59) Zhang, N.; Yu, X.; et al. New Insights into the Role of Ferritin in Iron Homeostasis and Neurodegenerative Diseases. *Mol. Neurobiol* **2021**, *58*, 2812−2823.
(60) Ward, R. J.; Zucca, F. A.; et al. The role of iron in brain ageing and neurodegenerative disorders. *Lancet Neurol* **2014**, *13*, 1045−1060.
(61) Chwiej, J.; Palczynska, M.; et al. Elemental changes of hippocampal formation occurring during postnatal brain development. *Journal of Trace Elements in Medicine and Biology* **2018**, *49*, 1−7.
(62) Solé, V. A.; Papillon, M.; et al. A multiplatform code for the analysis of energy-dispersive X-ray fluorescence spectra. *Spectrochim Acta Part B At Spectrosc* **2007**, *62*, 63−68.
(63) Mishra, P.; Pandey, C. M.; et al. Selection of appropriate statistical methods for data analysis. *Ann. Card Anaesth* **2019**, *22*, 297.
(64) Conover, W. J. *Practical Nonparametric Statistics*; John Wiley & Sons: New York, 1980.
(65) Paxinos, George; Watson, Charles. *The Rat Brain in Stereotaxic Coordinates*; Academic Press: San Diego, 1998.

https://doi.org/10.1021/acschemneuro.4c00283
ACS Chem. Neurosci. 2024, 15, 3932−3944

Supplementary Materials

Element changes occurring in brain point at the white matter abnormalities in rats exposed to the ketogenic diet during prenatal life

Marzena Rugiel[1#], Zuzanna Setkowicz[2#], Mateusz Czyzycki[3], Rolf Simon[3], Tilo Baumbach[3,4], Joanna Chwiej[1*]

[1] Faculty of Physics and Applied Computer Science, AGH University of Krakow, Al. Mickiewicza 30, 30-059 Krakow, Poland
[2] Institute of Zoology and Biomedical Research, Jagiellonian University, Gronostajowa 9, 30-387 Krakow, Poland
[3] Institute for Photon Science and Synchrotron Radiation, Karlsruhe Institute of Technology, Hermann-von-Helmholtz-Platz 1, D-76344 Eggenstein-Leopoldshafen, Germany
[4] Laboratory for Applications of Synchrotron Radiation, Karlsruhe Institute of Technology, Kaiserstr. 12, D-76131 Karlsruhe, Germany

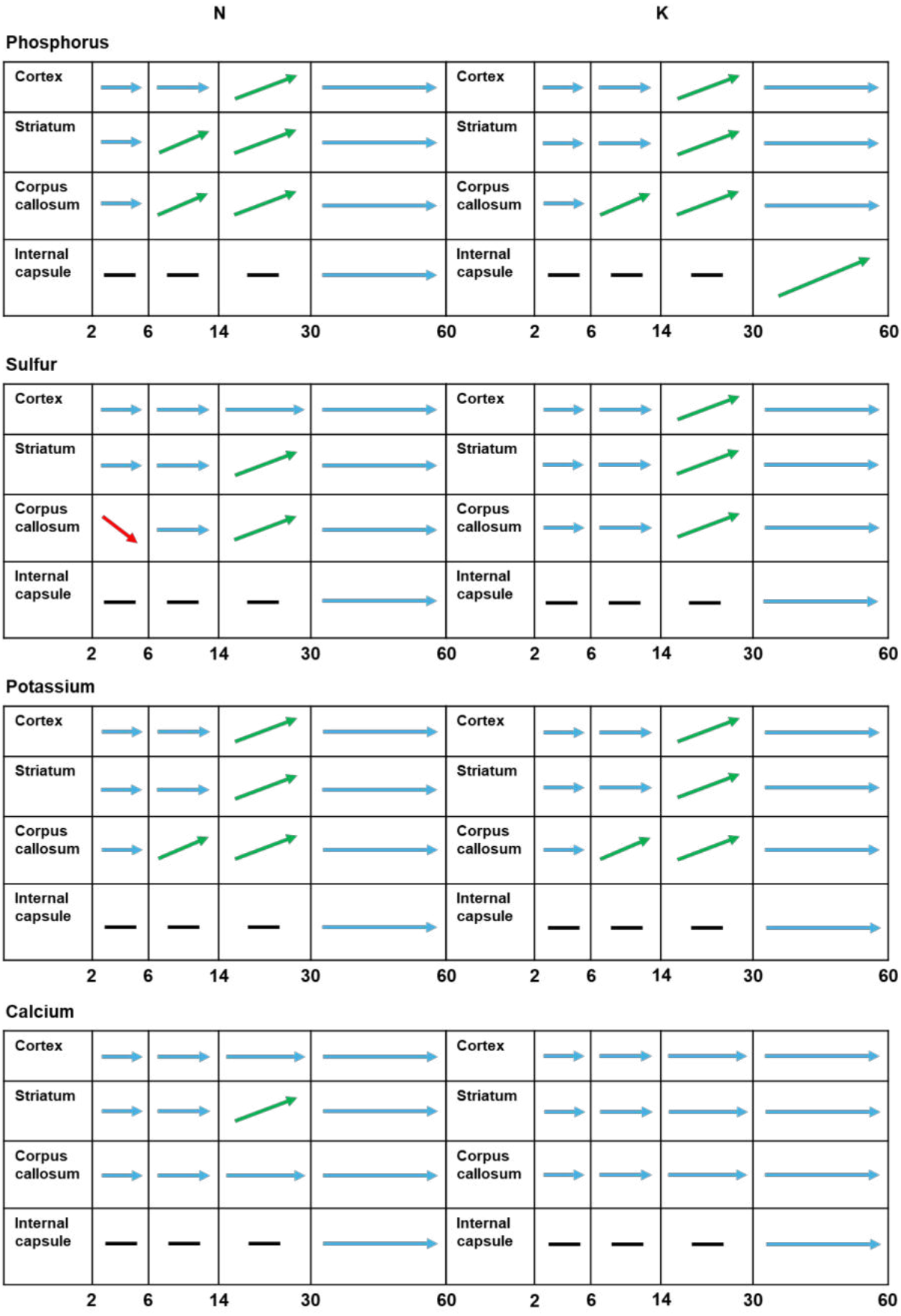
N
K
Phosphorus
Cortex
Striatum
Corpus callosum
Internal capsule
2
6
14
30
60
Sulfur
Potassium
Calcium

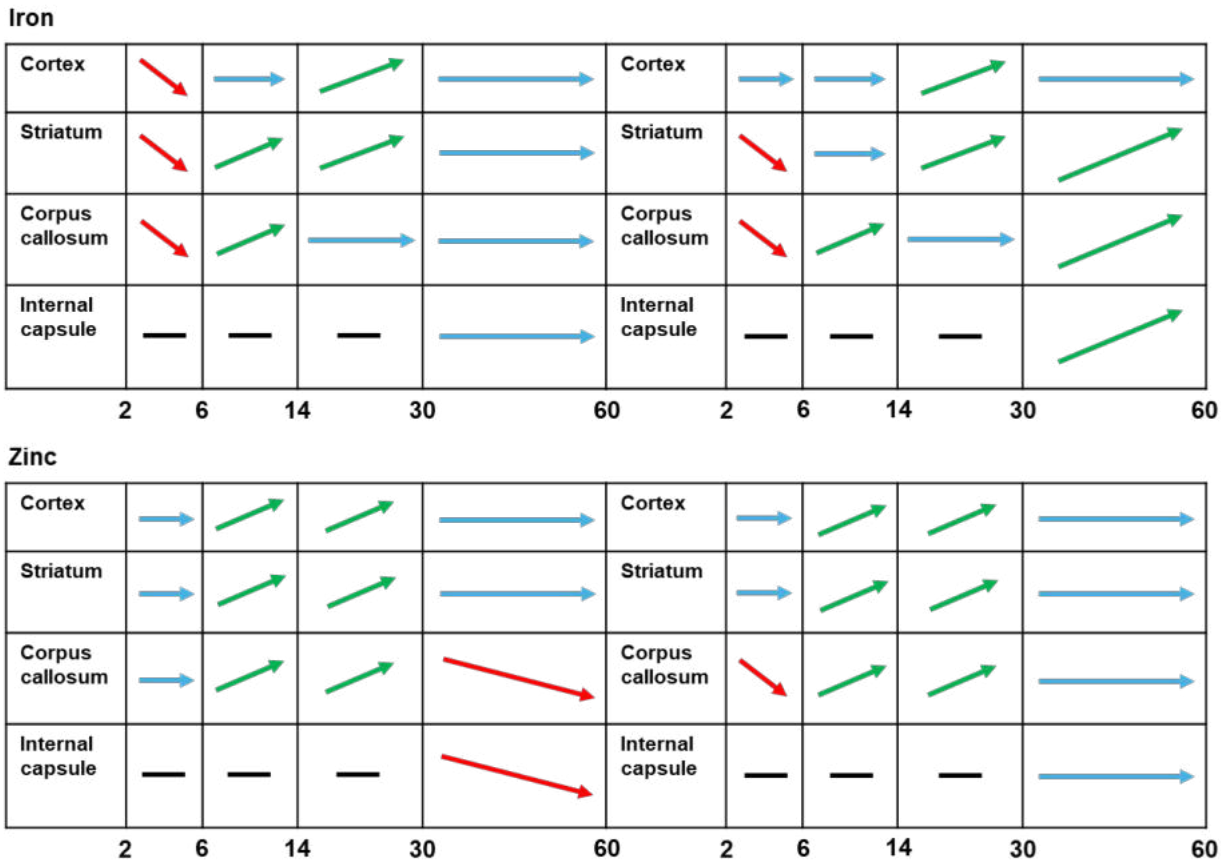

Figure S1. The dynamics of elemental changes (statistically significant differences in the elemental accumulation between the subsequent points of time) occurring in selected brain areas during postnatal development in the offspring of mothers fed during pregnancy with the ketogenic (K) or standard fodder (N). Statistically relevant increases of mass deposits of elements found for the examined periods were marked as the green sloping up arrows, whilst statistically relevant decreases as the sloping down red arrows. The blue arrow means no statistically significant differences between the subsequent points of time, and the black line indicates the lack of data enabling the performance of analysis for particular time period. The verification of the statistical significance of the observed differences was based on the Mann–Whitney *U* test (95% confidence level).

Fourier Transform Infrared Imaging Supported by Raman Spectroscopy Reveals Biochemical Changes in Adult Rat Brains Following Prenatal Exposure to a Ketogenic Diet

Marzena Rugiel[1#], Zuzanna Setkowicz [2#], Agnieszka Drozdz[1], Aleksandra Wilk[1], Zofia Brylowska[1], Joanna Chwiej[1*]

[1]AGH University of Krakow, Faculty of Physics and Applied Computer Science, al. Mickiewicza 30, 30-059 Krakow, Poland

[2]Jagiellonian University, Institute of Zoology and Biomedical Research, ul. Gronostajowa 9, 30-387 Krakow, Poland

# Contributed equally

* Corresponding author:

jchwiej@agh.edu.pl

Abstract

This study employed Fourier Transform Infrared (FTIR) and Raman microspectroscopy to investigate the long-term biochemical effects of prenatal exposure to a ketogenic diet (KD) on the developing rat brain. KD, high in fat and low in carbohydrates, shifts metabolism from glucose to ketone utilization and is widely used to treat drug-resistant epilepsy. Given its potential use in pregnant women, understanding KD impact on offspring neurodevelopment is critically important.

By combining the complementary strengths of FTIR and Raman microspectroscopy, this study enabled the detection of subtle biochemical changes within brain tissue of animals fed prenatally with KD. Spectroscopic analyses revealed region- and sex-dependent alterations, primarily involving metabolism of lipids and phosphate-containing compounds - key components of myelin and cellular membranes.

Most changes were observed in 60-day-old males prenatally exposed to KD. Creatine- and cholesterol-rich inclusions were detected in hippocampal and cortical regions, possibly reflecting maladaptive outcomes of altered energy metabolism and/or neuroadaptive mechanisms related to metabolic preconditioning. Furthermore, these males exhibited reductions in multiple lipid-associated FTIR parameters, which potentially reflecting disruptions in oligodendrocyte function or myelination dynamics.

While 30-day-old females from experimental group showed region-specific lipid decreases and elevated phosphate-related ratios, these changes largely normalized by 60 days, indicating developmental stabilization of metabolic effects after prenatal KD exposure. In contrast to males, females showed no creatine or cholesterol inclusions, likely reflecting sex-specific modulation. Estrogens regulate creatine metabolism, support mitochondrial and antioxidant function, and modulate lipid homeostasis, providing neuroprotection and mitigating metabolic disturbances.

Keywords:

FTIR microspectroscopy, Raman spectroscopy, biochemical analysis, ketogenic diet, creatine and cholesterol inclusions, prenatal exposure

Introduction

In the field of biomedical research, vibrational microspectroscopy techniques such as Fourier-transform infrared (FTIR) and Raman imaging have become increasingly valuable for probing the biochemical architecture of cells and tissues in a label-free, non-destructive manner [1–3]. These methods enable the spatially resolved detection of molecular alterations associated with physiological and pathological states, particularly in neurodegenerative diseases and brain tumors, where early biochemical disruptions often precede morphological changes [4–6].

FTIR microspectroscopy offers high spectral resolution and sensitivity to polar molecular vibrations, allowing precise quantification of major biochemical constituents such as lipids, proteins, and nucleic acids [1,2,7]. Its ability to identify secondary structures of proteins and monitor lipid peroxidation or aggregation phenomena has proven critical in models of Alzheimer's and Parkinson's diseases [8–11]. Nonetheless, the technique is susceptible to interference from water absorption, which can limit its utility in aqueous or live-cell environments [2,12]. Raman microscopy complements FTIR by targeting vibrational modes associated with changes in polarizability [12]. It provides excellent spatial resolution (often below 1 μm), making it particularly suitable for subcellular analysis and imaging of hydrated or live samples [3,13,14]. The capability of Raman spectroscopy/imaging to detect low-concentration metabolites, study protein misfolding, and assess oxidative stress markers has made it a powerful tool in neurological disease research [5,14,15]. Moreover, it has been found to be especially useful in analyzing the lipid composition of brain tissue [16–18]. However, limitations such as low signal intensity and potential fluorescence background may pose a problem in the correct interpretation of the data received and often require the use of various additional methods [2,12,14].

Importantly, the complementary nature of FTIR and Raman spectroscopy arises from their distinct selection rules: FTIR detects vibrational modes associated with changes in electrical dipole moment, whereas Raman is sensitive to variations in molecular polarizability [12,19]. As a consequence, some vibrational modes are active in both techniques, while others are exclusively observed in either FTIR or Raman spectra, depending on the nature of the molecular vibration [12]. By combining both approaches, it is possible to access a broader range of molecular vibrations, leading to more complete spectral characterization of biological specimens [1,7,19,20]. This dual-modality strategy enhances chemical specificity and improves the interpretation of complex vibrational spectra, particularly of cells and heterogeneous tissue samples where overlapping signals may obscure individual molecular contributions when using a single technique alone [1,7,19,20].

The aim of the present study is to employ FTIR and Raman microspectroscopy to investigate potential biochemical alterations in the brains of offspring born to mothers exposed to a ketogenic diet (KD) during the prenatal period. This approach was motivated by the need to better understand how maternal nutritional status, particularly under a high-fat, low-carbohydrate ketogenic regimen, may influence the development of the central nervous system in the progeny. KD, which induces a state of ketosis and shifts cellular energy metabolism from glucose to ketone bodies, is currently used as an alternative therapeutic strategy in drug-resistant epilepsy [21,22]. Given that this dietary approach could be considered for pregnant women suffering from refractory epilepsy, it is crucial to evaluate its potential long-term neurodevelopmental consequences. This study extends our previous work by addressing both age and sex as biological variables. Earlier analyses were limited to male offspring at early postnatal stages (days 2, 6, and 14). In the current investigation, we not only included female neonates at the corresponding developmental stages, thereby completing the early sex-based comparison, but also examined both male and female animals at postnatal days 30 and 60, which correspond to late juvenile and young adult stages. This broader experimental design

allowed for the assessment of long-term, sex-dependent biochemical effects of prenatal ketogenic exposure on brain tissue biomolecular composition.

Our earlier investigations revealed that prenatal exposure to KD leads to noticeable alterations in the regional biochemical profile of the developing rat brain, in comparison to offspring of mothers maintained on a standard diet [23]. In particular, 14-day-old juvenile rats born to KD-fed dams exhibited an elevated relative abundance of carbonyl groups-containing compounds, accompanied by a reduction in lipid levels and modifications in lipid structure within specific brain regions [23]. Furthermore, spectroscopic mapping of lipid-associated absorption bands indicated a reduced area of the internal capsule in these animals, suggesting potential delays or disruptions in myelination or axonal organization [23]. In addition, elemental mapping further indicated that prenatal ketogenic exposure may affect the cerebral distribution of key elements, notably phosphorus and sulfur [24]. In the oldest examined male rats, there was a marked reduction in the area of brain regions enriched in these elements, which correspond anatomically to white matter structures [24]. These findings suggest potential alterations in the composition of myelin-associated lipids, such as sphingomyelin and sulfatides, and may reflect compromised myelin integrity or disturbances in white matter organization [24].

Results

Chemical mapping performed for 30- and 60-days old rats

FTIR microspectroscopy was used for chemical mapping of whole-brain sections obtained from offspring prenatally exposed to either a ketogenic or a normal diet. A representative microscopic image of such a brain section, together with detailed anatomical structures including the cortex, white matter regions, and hippocampal cell layers, is presented in Figure 1.

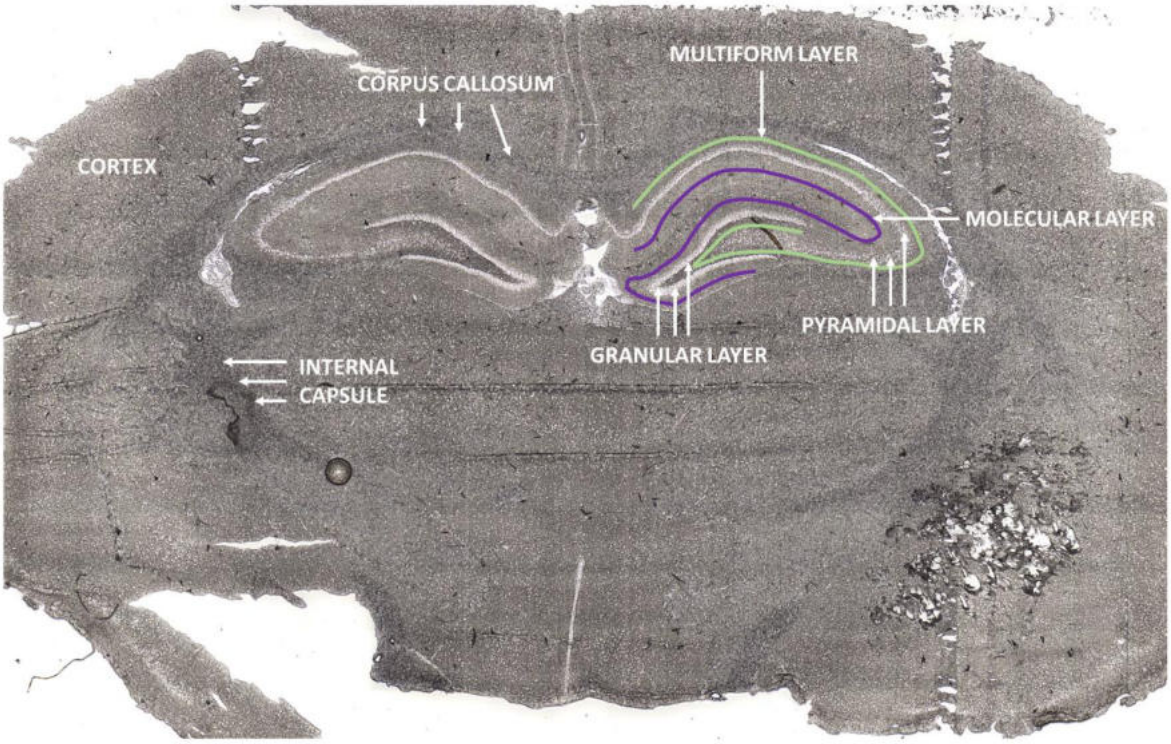

Fig. 1 The localization of areas of interest (cortex, structures of white matter: corpus callosum and internal capsule, and four cellular layers of hippocampal formation: granular, pyramidal, multiform and molecular) in the microscopic image of an exemplary brain slice taken from 60-days old rat.

Performing chemical mapping using FTIR spectroscopy, it was necessary to take into account possible variations in the thickness of examined tissue sections. Since the protein content in various regions of the rat brain remains relatively constant, the intensity of the amide I band was used as a normalization factor when calculating the relative content of the analyzed biomolecules.

In Figure 2 the results of chemical mapping of the absorption bands at 1395 cm^{-1} and 1304 cm^{-1} are shown. It has been proven in our previous studies that these absorption bands may serve as marker signals for the detection of creatine (CR) in biological samples [25–27], As one can see in this figure, no differences in the distribution of these bands between the control and experimental group were observed in case of 30-day-old males as well as 30- and 60-day-old females. Interesting result was, however, obtained for 60-day-old male rats, for which locally elevated signal from 1395 cm^{-1} and 1304 cm^{-1}, correlated with inclusions visible under the microscope, was observed in the hippocampal formation and cortex. Preliminary topographical analysis suggests that although these inclusions are observed in adult male rats prenatally exposed to both ketogenic and standard diets, their size, frequency of occurrence, and the corresponding IR signal may be higher in the offspring of KD-fed mothers. This tendency is illustrated by the data presented in Figures 3B and 3C, showing the results of chemical mapping of bands that may be attributed to creatine, obtained for all examined 60-day-old male rats.

To obtain the lipid profiles of the examined brain samples, relative levels of selected lipid absorption bands were analyzed. These included the lipid massif region (2800-3000 cm^{-1}), the band at 2924 cm^{-1} corresponding to saturated fatty acids, and the 1465 cm^{-1} band associated with lipids, cholesterol (CHL), and/or its esters (Figure 4). Additionally, the ratio of the bands at 2924 and 2955 cm^{-1} was examined to assess structural changes of lipids. No effect of prenatal diet on lipid distribution was observed in 30- and 60-day-old females or in 30-day-old males. However, certain differences were noted between 60-day-old males prenatally exposed to the standard diet versus the KD. In the latter group, elevated levels of the following intensity ratios were detected: 2800-3000 cm^{-1}/1658 cm^{-1}, 2924 cm^{-1}/1658 cm^{-1}, and 1465 cm^{-1}/1658 cm^{-1}. These locally increased values correlated with focal inclusions observed in the hippocampus and cortex. Notably, these inclusions appeared also in regions where high lipid accumulation is not typically expected, unlike, for example, in white matter, where lipids naturally occur in high abundances. The most prominent alterations were observed in the ratio of the bands at 1465 and 1658 cm^{-1}. Its higher intensities in brain tissue from adult males prenatally fed with KD colocalized with inclusions visible in microscopic images. These findings are presented in Figure 3D, which shows chemical maps of the 1465 cm^{-1}/1658 cm^{-1} ratio for all examined 60-day-old male rats.

Subsequently, absorption bands characteristic of phosphate-containing compounds (1080 and 1240 cm^{-1}) and carbonyl groups (1740 cm^{-1}) were analyzed relative to protein content (Figure 5). No visible differences in these band ratios were observed between the control and experimental groups across sexes and age groups (30 and 60 days). However, a slight overall decrease in the 1240 cm^{-1}/1658 cm^{-1} ratio was noted in 60-day-old males prenatally exposed to KD, when compared to their age-matched controls.

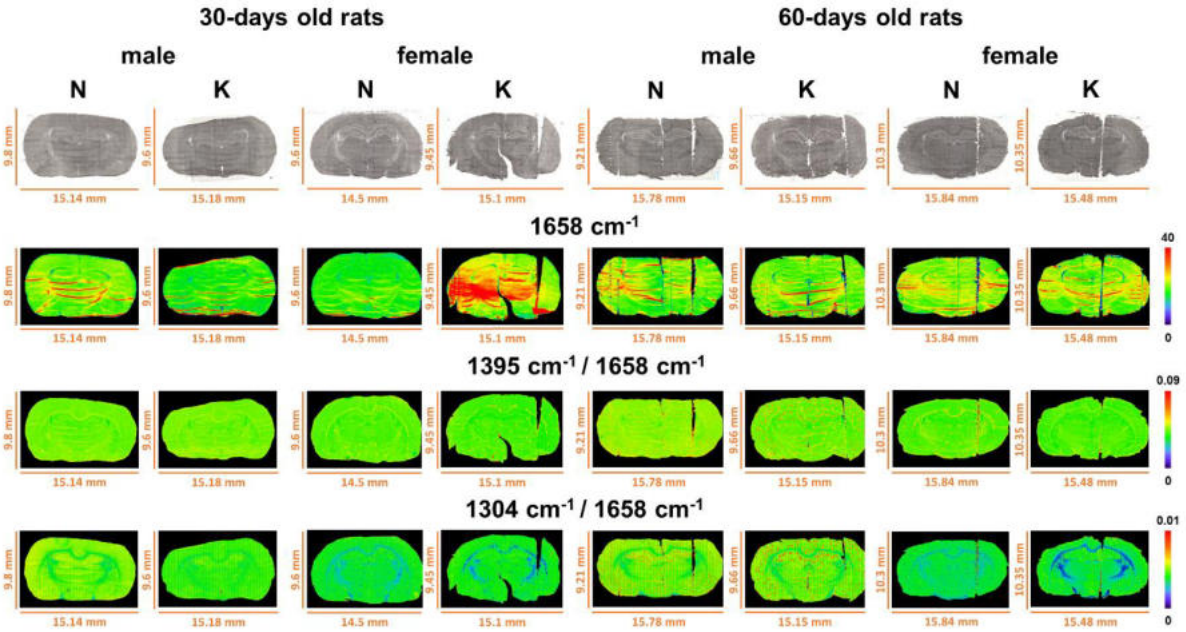

Fig. 2 Representative chemical maps illustrating the spatial distribution of the integrated area of the amide I band and the relative integrated areas of the IR bands at 1395 and 1304 cm^{-1} normalized to the amide I band. The maps were obtained for brain slices taken from male and female rats aged 30 and 60 days, prenatally exposed to either a ketogenic (K) or a normal (N) diet. The color scale represents intensity of the amide I band and band-area ratios relative to the amide I band, with black indicating the minimum value and red indicating the maximum value. Microscopic images of the analyzed tissues are shown in the top row.

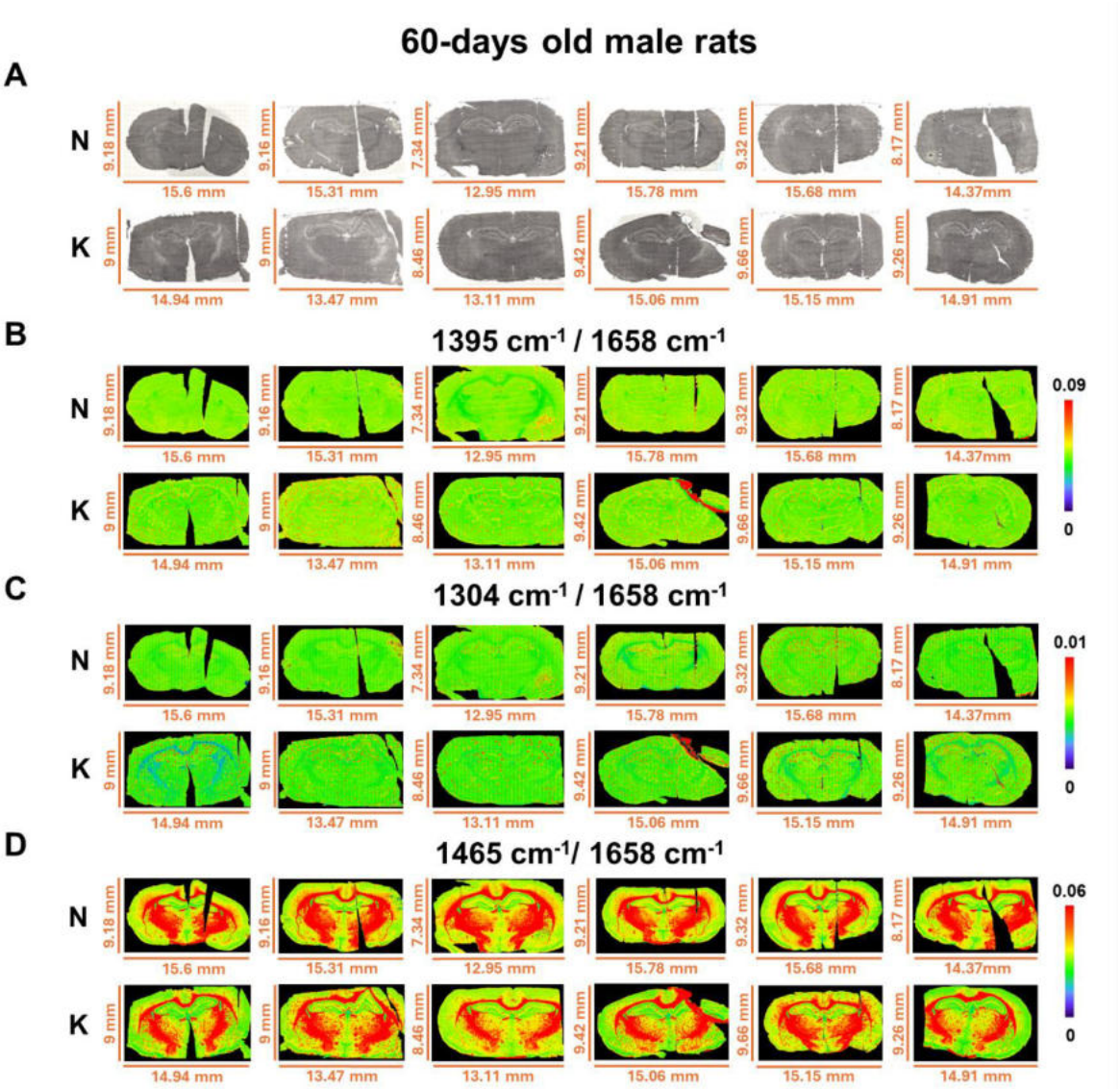

Fig. 3 Chemical maps obtained by FTIR microspectroscopy show distinct spatial patterns in the relative intensities of bands characteristic of Cr (1395 cm^{-1}/1658 cm^{-1} and 1304 cm^{-1}/1658 cm^{-1}, B and C), as well as CHL, its esters, and membrane lipids (1465 cm^{-1}/1658 cm^{-1}, D). These patterns indicate region-specific differences in their distribution in the brains of 60-day-old male rats prenatally exposed to a ketogenic (K) or normal (N) diet. The color scale represents band-area ratios relative to the amide I band, with black indicating the minimum value and red indicating the maximum value. Microscopic images of the analyzed tissue areas are displayed in the top row (A).

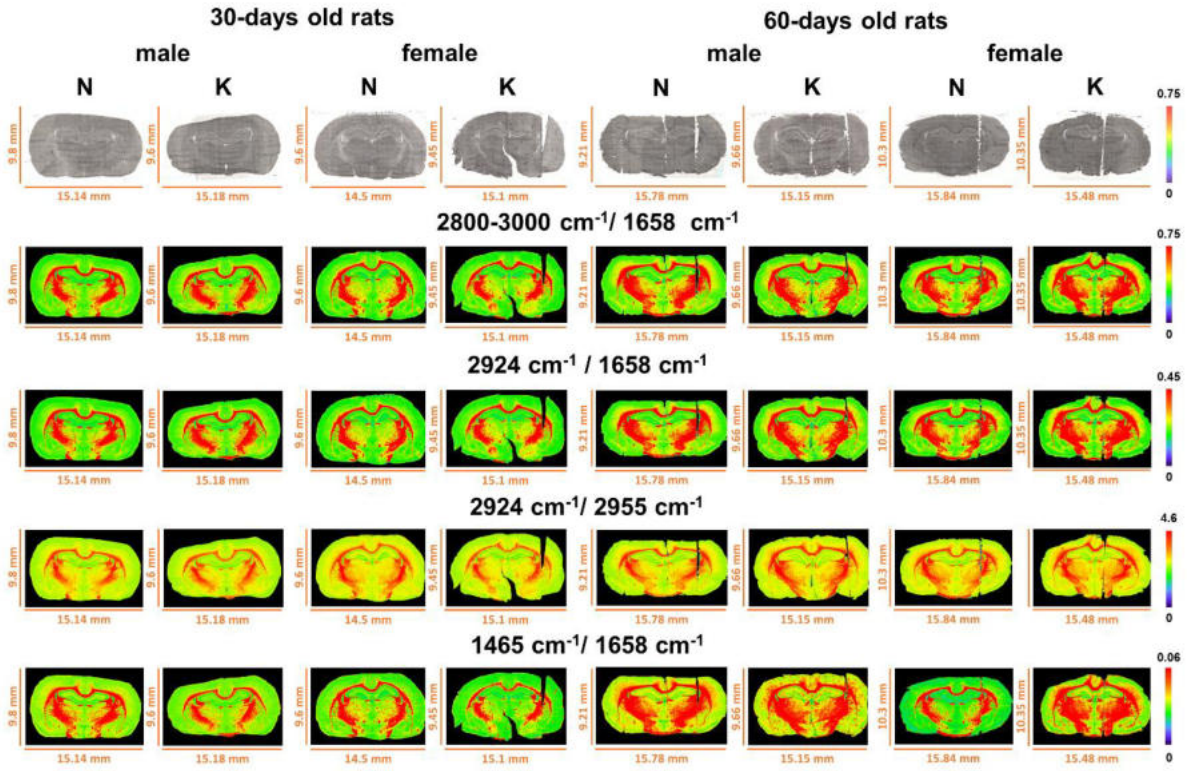

Fig. 4 Representative chemical maps illustrating the spatial distribution of the relative integrated areas of the IR bands at 2924 and 1465 cm^{-1} as well as the lipid massif region (2800-3000 cm^{-1}), normalized to the amide I band. Additionally, the maps showing the ratio of the bands at 2924 and 2955 cm^{-1} are presented. The maps were obtained for brain slices taken from male and female rats aged 30 and 60 days, prenatally exposed to either a ketogenic (K) or a normal (N) diet. The color scale represents band-area ratios relative to the amide I band, with black indicating the minimum value and red indicating the maximum value. Microscopic images of the analyzed tissues are shown in the top row.

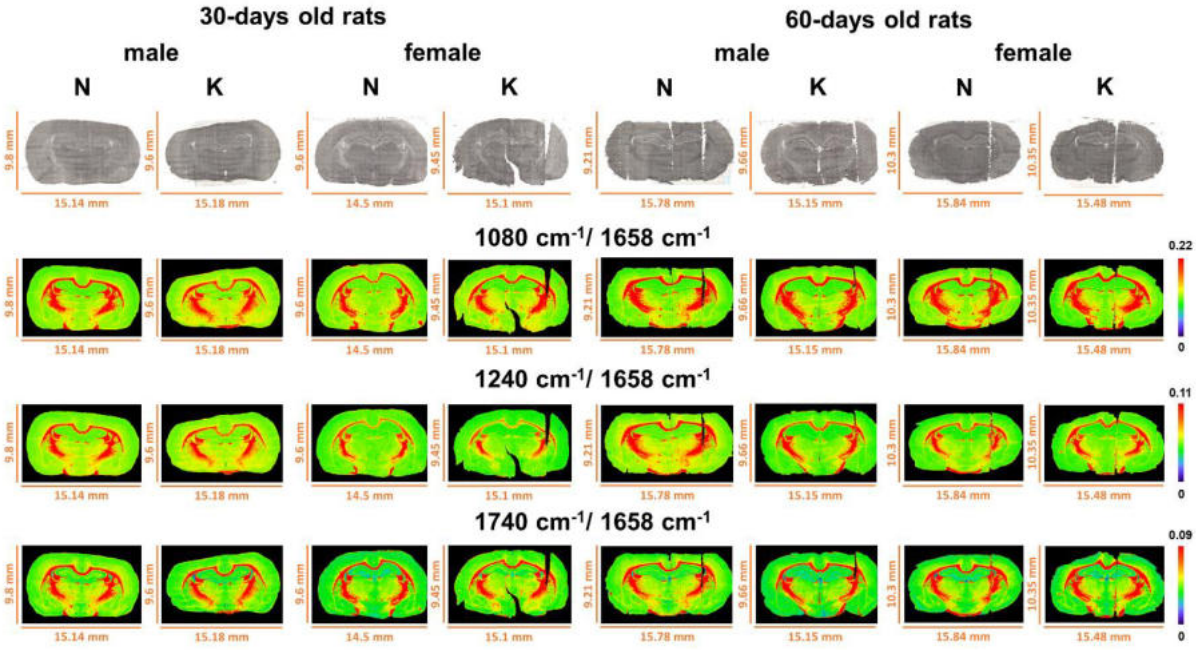

Fig. 5 Representative chemical maps illustrating the spatial distribution of the relative integrated areas of the IR bands at 1080, 1240 and 1740 cm^{-1}, normalized to the amide I band. The maps were obtained for brain slices taken from male and female rats aged 30 and 60 days, prenatally exposed to either a ketogenic (K) or a normal (N) diet. The color scale represents band-area ratios relative to the amide I band, with black indicating the minimum value and red indicating the maximum value. Microscopic images of the analyzed tissues are shown in the top row.

Confirmation of the presence of Cr and CHL inclusions

Chemical mapping of whole brain slices taken from 60-day-old males prenatally exposed to KD revealed the presence of focal areas characterized with the increased intensity of some of the examined IR bands. In the regions, located in the vicinity of the hippocampal formation and cortex, elevated absorption for bands which may originate from Cr (1395 cm^{-1} and 1304 cm^{-1}), as well as for lipid-associated bands, likely corresponding to CHL accumulation (1465 cm^{-1}) was noticed.

To confirm the presence of Cr within the inclusions visible under microscope, the IR and Raman spectra collected directly from the deposit were compared with the spectra of pure Cr and the ones recorded from the surrounding brain tissue. This is done, respectively, in Figure 6A and Figure 7A. As it is possible to notice from Figure 6A, IR bands characteristic for Cr and occurring at the wavenumbers of 1395 and 1304 cm^{-1} [25,28–30], were more pronounced in the spectrum obtained from the inclusion compared to the adjacent tissue, supporting the presence of localized Cr accumulation. The Raman spectrum of Cr contains a greater number of distinct bands, offering even more precise confirmation of its presence in the analyzed brain tissue. As shown in Figure 7A, these include prominent peaks at 830, 914, 980, 1055, and 1395 cm^{-1} [28,31,32].

A similar approach was applied for the confirmation of the presence of CHL within the selected inclusions found in brains of adult rats fed prenatally with KD. IR spectra of pure CHL, tissue-resident CHL inclusions, and the surrounding brain tissue are compared in Figure 6C. Characteristic CHL IR bands were observed at 1465 and 1378 cm^{-1} [33,34], however, the latter may overlap with other bands, including the Cr-associated band at 1395 cm^{-1}. In CHL inclusions, the relative intensity of these two bands shifted, with the 1465 cm^{-1} band becoming more dominant, whereas in normal tissue both bands remained at comparable levels. Additionally, an overall increase in absorbance was observed in the lipid massif region (2800-3000 cm^{-1}). In the Raman spectrum (Figure 7C), characteristic CHL bands were detected at 548, 700, and 2867 cm^{-1} [35–37]. Furthermore, Raman imaging using a 100× confocal objective revealed crystallized CHL within the brain tissue, exhibiting a distinctive plate-like morphology (Figure 7D).

In both cases, measurements of Cr and CHL inclusions, Raman microspectroscopy provides better confirmation, as it offers sub-micrometer spatial resolution and confocality, ensuring that the signal is collected almost exclusively from the inclusion itself, without interference from the surrounding tissue.

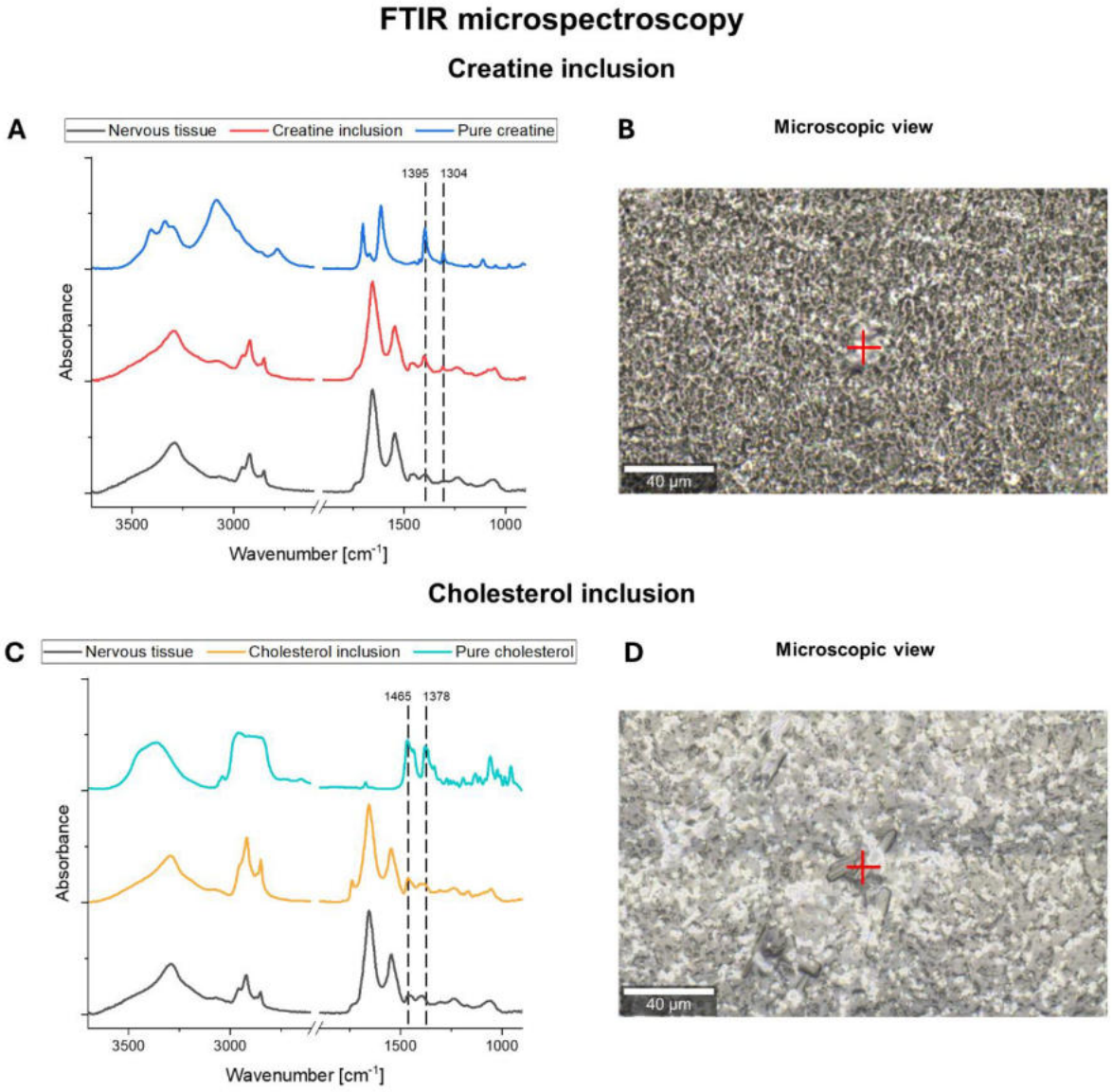

Fig. 6 (A) Comparison of baseline-corrected and vector-normalized IR spectra obtained from Cr inclusion, the surrounding nervous tissue, and pure Cr. (C) Analogical data obtained from CHL inclusion, surrounding tissue, and pure CHL. Absorption bands characteristic of Cr (1304 and 1395 cm^{-1}) and CHL (1378 and 1465 cm^{-1}) are indicated with black dashed lines. Corresponding microscopic images of the Cr and CHL inclusions identified within the nervous tissue are shown in panels (B) and (D), respectively.

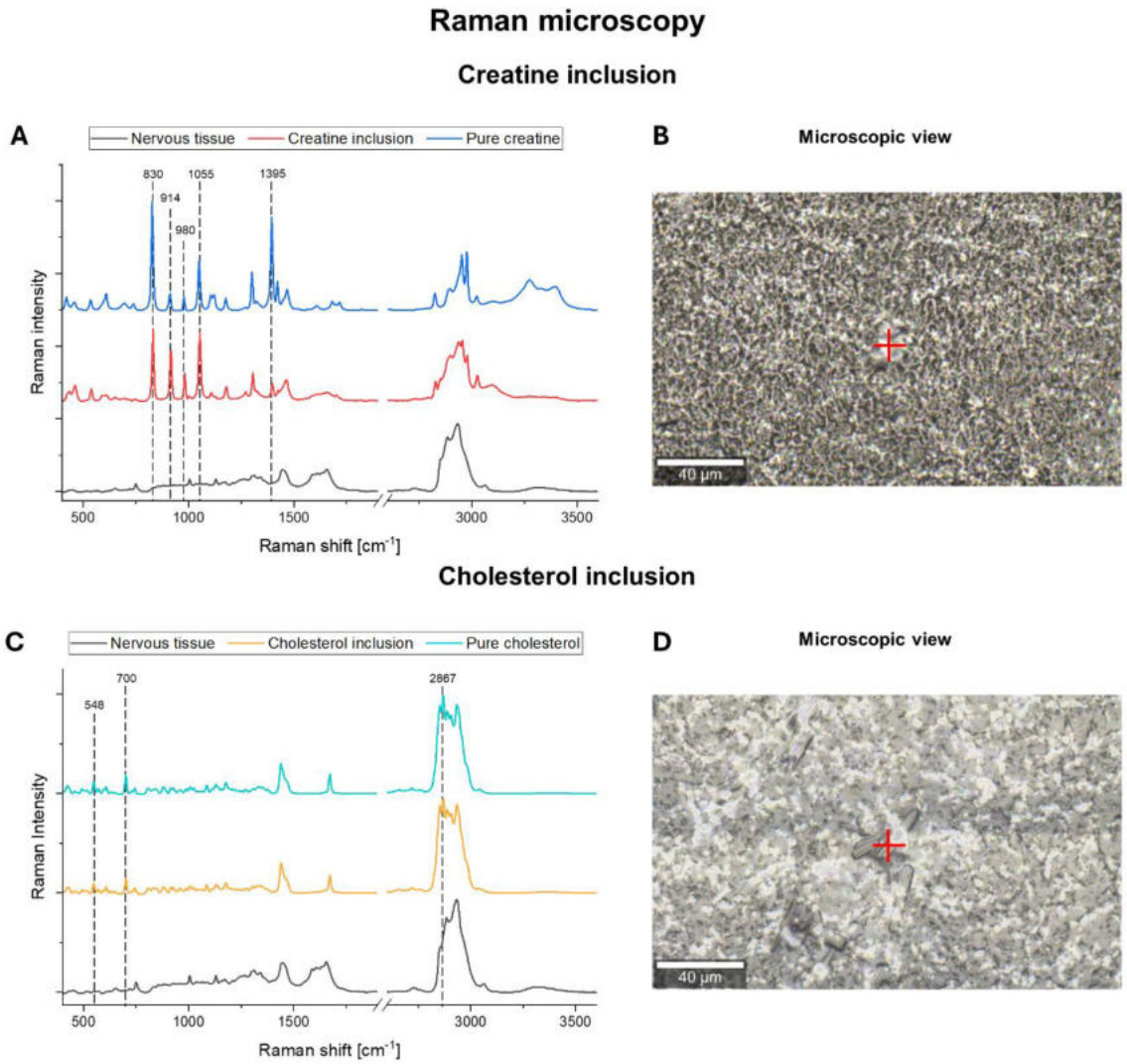

Fig. 7 (A) Comparison of baseline-corrected and vector-normalized Raman spectra obtained from Cr inclusion, the surrounding nervous tissue, and pure Cr. (C) Analogical data obtained from CHL inclusion, surrounding tissue, and pure CHL. Raman bands characteristic of Cr (830, 914, 980, 1055 and 1395 cm^{-1}) and CHL (548, 700 and 2867 cm^{-1}) are indicated with black dashed lines. Corresponding microscopic images of the Cr and CHL inclusions identified within the nervous tissue are shown in panels (B) and (D), respectively.

Quantitative analysis of Cr- and CHL-rich inclusions for 60-days old male rats

Quantitative analysis of Cr- and CHL-rich inclusions for adult male rats was performed using a custom image-processing workflow implemented in Python and MATLAB. First, red-blue false-color chemical maps corresponding to spectral bands characteristic for Cr and CHL were preprocessed in Python (OpenCV library). Images were converted to the RGB color space, and a binary mask was generated to remove the background. This involved morphological operations (dilation and closing), followed by contour filtering based on a minimum area threshold. The mask was then smoothed using a Gaussian filter and applied to isolate the tissue region of interest.

The preprocessed images were subsequently exported to MATLAB for segmentation and quantitative analysis. Inclusion detection was based on RGB thresholding. For Cr maps, pixels were classified as inclusions if they met the following criteria: R=194-255, G=0-109, and B=0-

152. For CHL maps, a modified threshold was applied based on the blue channel (B=0-182), while preserving the same processing workflow. Binary masks were then used to identify individual inclusions using connected component analysis, and their areas were determined.

For Cr, the analysis was performed for entire brain sections. For each section, the total area of inclusions and the relative inclusion area (expressed as a percentage of the total tissue area) were calculated. In contrast, due to the very high CHL signal observed in white matter regions, which dominated the overall intensity distribution and hindered reliable segmentation across the entire brain section, quantitative analysis was restricted to selected regions of interest, namely the hippocampal formation and cerebral cortex. Within these regions, the total area of inclusions and their relative contribution to the analyzed tissue area were determined.

In Table 1, a summary of the quantitative analysis of Cr- and CHL-rich inclusions is presented, together with the statistical evaluation of the results using the Mann-Whitney *U* test. As can be seen, the total and relative area of Cr inclusions tended to be higher in adult male rats prenatally subjected to KD. These differences, however, did not reach statistical significance (p=0.123 and p=0.331, respectively). In contrast, a clear and statistically significant increase in both the total and relative area of CHL-rich inclusions was observed in the ketogenic group, both in the cerebral cortex (p=0.001 for both parameters) and in the hippocampal formation (p=0.002 for total area and p=0.001 for relative area). Overall, these results indicate that prenatal exposure to KD is associated with a pronounced increase in CHL-rich inclusions, while the observed differences in Cr inclusions remain at the level of a non-significant trend.

Table 1 Absolute (px) and relative (%) area of Cr- and CHL-rich inclusions in adult male rat brains following prenatal exposure to ketogenic and standard diets

Creatine	**Ketogenic**	**Standard**
Total inclusion area [px] (p = 0.123)	9588 – 21454 (11466)*	4132 – 13472 (9782)
Relative inclusion area [%] (p = 0.331)	5.466 – 8.997 (6.294)	2.500 – 8.800 (5.974)
Cholesterol in cortex	**Ketogenic**	**Standard**
Total inclusion area [px] (p = 0.001)	1386 – 2002 (1544)	102 – 470 (248)
Relative inclusion area [%] (p = 0.001)	0.445 – 0.656 (0.521)	0.0433 – 0.241 (0.100)
Cholesterol in hippocampal formation	**Ketogenic**	**Standard**
Total inclusion area [px] (p = 0.002)	260 – 610 (518)	18 – 130 (24)
Relative inclusion area [%] (p = 0.001)	0.646 – 1.480 (1.265)	0.0453 – 0.369 (0.0925)

* Data are presented as ranges (minimum – maximum), with corresponding median values provided in parentheses.

Semi-quantitative analysis of regional biochemical changes following prenatal exposure to KD performed for 30- and 60-days old rats

In addition to the topographic analysis, which provided an overview of biochemical alterations in the brain resulting from prenatal exposure to KD, a more detailed semi-quantitative assessment was carried out for specific brain regions. These included the cortex, corpus callosum, internal capsule, and four hippocampal layers: granular, pyramidal, multiform, and molecular. The outcomes of these quantitative comparisons between the experimental groups (KM_30, KF_30, KM_60, and KF_60, where the number indicates postnatal age in days, M and F are male and female, respectively) and their respective control groups (NM_30, NF_30, NM_60, and NF_60) are presented as box-and-whisker plots in Figures 8-10.

In 30-day-old male rats statistically significant changes were observed mainly in the bands associated with lipids (Figure 9). Both the 2800-3000 cm^{-1}/1658 cm^{-1} and 2924 cm^{-1}/1658 cm^{-1} band intensity ratios were significantly lower in the hippocampal molecular layer of animals

prenatally exposed to the KD. A downward trend was noted also in the pyramidal layer and the internal capsule region. For the phosphate-related band (1240 cm^{-1}/1658 cm^{-1}), a significant increase was observed in the molecular layer of the hippocampal formation in the ketogenic group, while a similar upward trend was noted in the remaining analyzed brain regions (Figure 10).

The most pronounced KD induced biochemical alterations were observed in 60-day-old males. A statistically significant increase in the Cr-related band (1304 cm^{-1}/1658 cm^{-1}) was found in the corpus callosum and hippocampal multiform layer of animals prenatally exposed to high fat fodder (Figure 8). In other brain regions, except for the granular layer, a general upward trend of this band was also observed. The increase in intensity of Cr-associated bands in this group is consistent with the topographic maps, which showed the presence of Cr inclusion in the brain of animals from this experimental group. In the adult males prenatally fed with KD a significant increase of lipid-related bands (2800-3000 cm^{-1}/1658 cm^{-1}, 2924 cm^{-1}/1658 cm^{-1}, and 2924 cm^{-1}/2955 cm^{-1}) in the pyramidal layer of the hippocampal formation was detected (Figure 9). In the granular and multiform layers, similar upward trends were observed. The simultaneous increase in the 2800-3000 cm^{-1}/1658 cm^{-1} and 2924 cm^{-1}/2955 cm^{-1} ratios indicates enrichment in lipid components and a higher degree of chain ordering, which may reflect enhanced membrane stability in these regions. In contrast, the corpus callosum and hippocampal molecular layer exhibited statistically significant decreases in these lipid-related bands in the KM_60 group comparing to appropriate controls, with a downward trend noted in the cortex. The concurrent decrease in the 2800-3000 cm^{-1}/1658 cm^{-1} and 2924 cm^{-1}/2955 cm^{-1} ratios suggests a reduction in overall lipid content accompanied by shorter or more disordered hydrocarbon chains, indicative of increased membrane fluidity in these regions. The corpus callosum showed the greatest number of statistically significant biochemical changes, mainly decreases in lipid- and CHL-associated bands (1465 cm^{-1}/1658 cm^{-1}). These results may suggest lipids and/or CHL migration from this region, consistent with observation of CHL inclusions predominantly in the cortex and hippocampal formation and above-mentioned increased membrane fluidity. Across all investigated brain regions, except the internal capsule, decreases or downward trends were noted for phosphate-related bands (1240 cm^{-1}/1658 cm^{-1} and 1080 cm^{-1}/1658 cm^{-1}) (Figure 10). Conversely, the carbonyl-associated band (1740 cm^{-1}/1658 cm^{-1}) showed a significant increase in the granular layer and an upward trend in the pyramidal layer, while opposite trends were recorded in the remaining hippocampal layers, along with significant decreases in the corpus callosum and cortex.

In contrast to males, 30-day-old females exhibited more statistically significant changes than 60-day-old ones. In the younger females fed prenatally with KD, significant decreases were observed within the pyramidal layer, along with downward trends in the granular layer for the 2800-3000 cm^{-1}/1658 cm^{-1} and 2924 cm^{-1}/1658 cm^{-1} ratios (Figure 9). Additionally, alterations in the 2924 cm^{-1}/2955 cm^{-1} ratio indicated changes in lipid structure within these hippocampal layers. Significant increases or upward trends in phosphate-related parameters (1080 cm^{-1}/1658 cm^{-1} and 1240 cm^{-1}/1658 cm^{-1}) were also detected across all analyzed brain regions (Figure 10). These effects diminished with age, and, in contrast to males, 60-day-old females showed minimal differences between the control and experimental groups. Only a significant increase in the 2800-3000 cm^{-1}/1658 cm^{-1} band was noted in the pyramidal layer, accompanied by an upward trend in the multiform layer and cortex (Figure 9). This suggests a stronger prenatal KD effect in males compared to females.

Our previous studies have shown that white matter structures in male offspring of KD-fed mothers may be reduced compared with the offspring of mothers fed a normal diet. To verify this finding in the current study, the relative white matter area was determined for each animal compared to the whole brain section. This was done based on chemical maps representing the

ratio of the bands 2800-3000 cm^{-1}/1658 cm^{-1}. ImageJ software (version 1.52a) was used to estimate the white matter area and the whole brain section. The calculated relative areas were statistically evaluated using the Mann-Whitney *U* test to test for significance of differences between experimental animals and their respective controls. As can be seen in Figure 11, the statistical analysis performed showed that in 30- and 60-day-old males the relative white matter area determined on the basis of the intensity of the 2800-3000 cm^{-1}/1658 cm^{-1} band is significantly smaller in the experimental group.

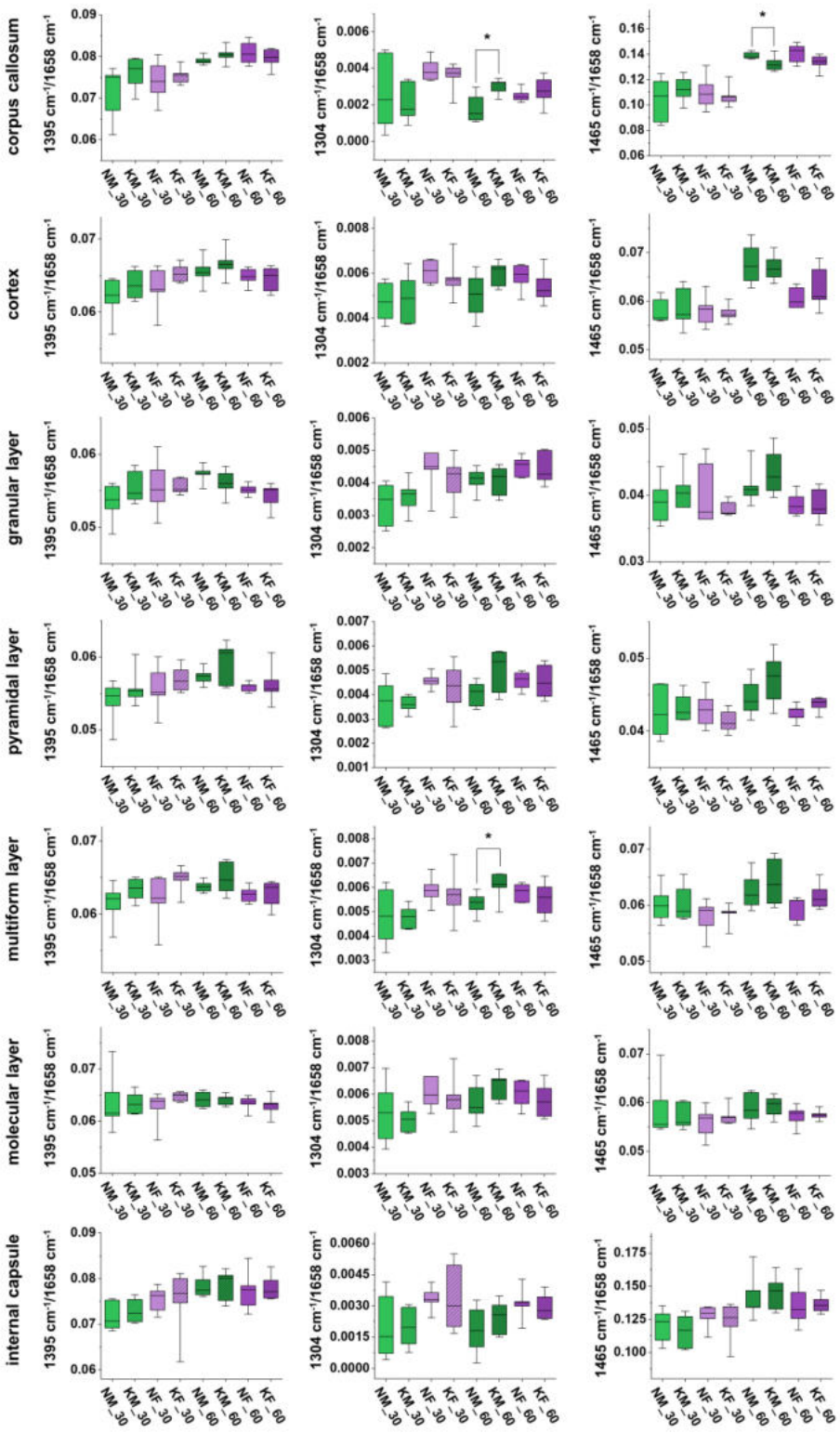

Fig. 8 Box-and-whisker plots illustrating the distribution of FTIR-derived biochemical parameters (ratios of integrated band areas: 1395 cm^{-1}/1658 cm^{-1}, 1304 cm^{-1}/1658 cm^{-1} and 1465 cm^{-1}/1658 cm^{-1}) across selected brain regions: the corpus callosum, cerebral cortex, internal capsule, and four hippocampal layers (granular, pyramidal, multiform, and molecular) for both experimental (K) and control (N) rat groups, including males (M) and females (F), at two postnatal developmental stages (30 and 60 days of age). Statistically significant differences between experimental and corresponding control groups (Mann-Whitney *U* test, $p < 0.05$) are indicated by an asterisk (*).

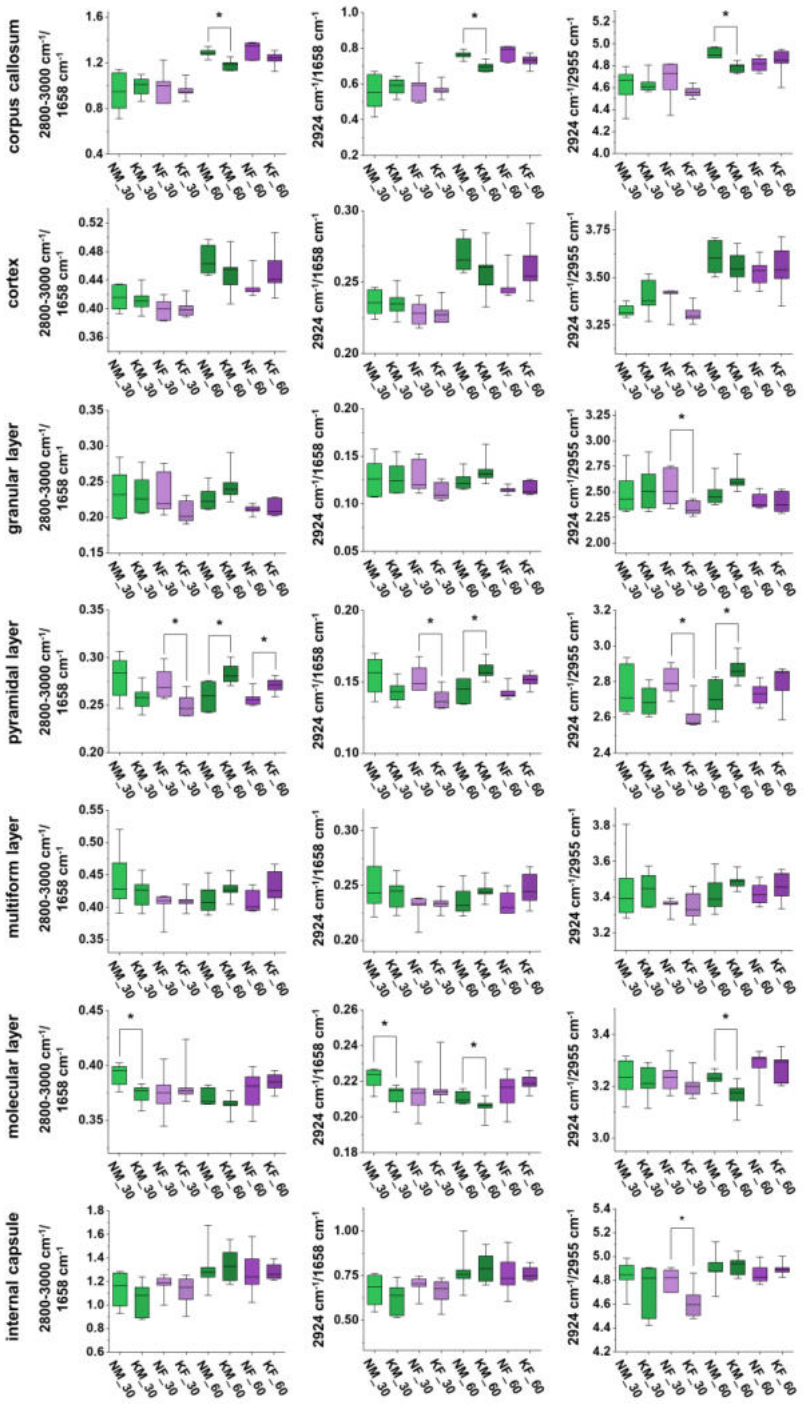

Fig. 9 Box-and-whisker plots illustrating the distribution of FTIR-derived biochemical parameters (ratios of integrated band areas: 2800-3000 cm^{-1}/1658 cm^{-1}, 2924 cm^{-1}/1658 cm^{-1} and 2924 cm^{-1}/2955 cm^{-1}) across selected brain regions: the corpus callosum, cerebral cortex, internal capsule, and four hippocampal layers (granular, pyramidal, multiform, and molecular) for both experimental (K) and control (N) rat groups, including males (M) and females (F), at two postnatal developmental stages (30 and 60 days of age). Statistically significant differences between experimental and corresponding control groups (Mann-Whitney *U* test, $p < 0.05$) are indicated by an asterisk (*).

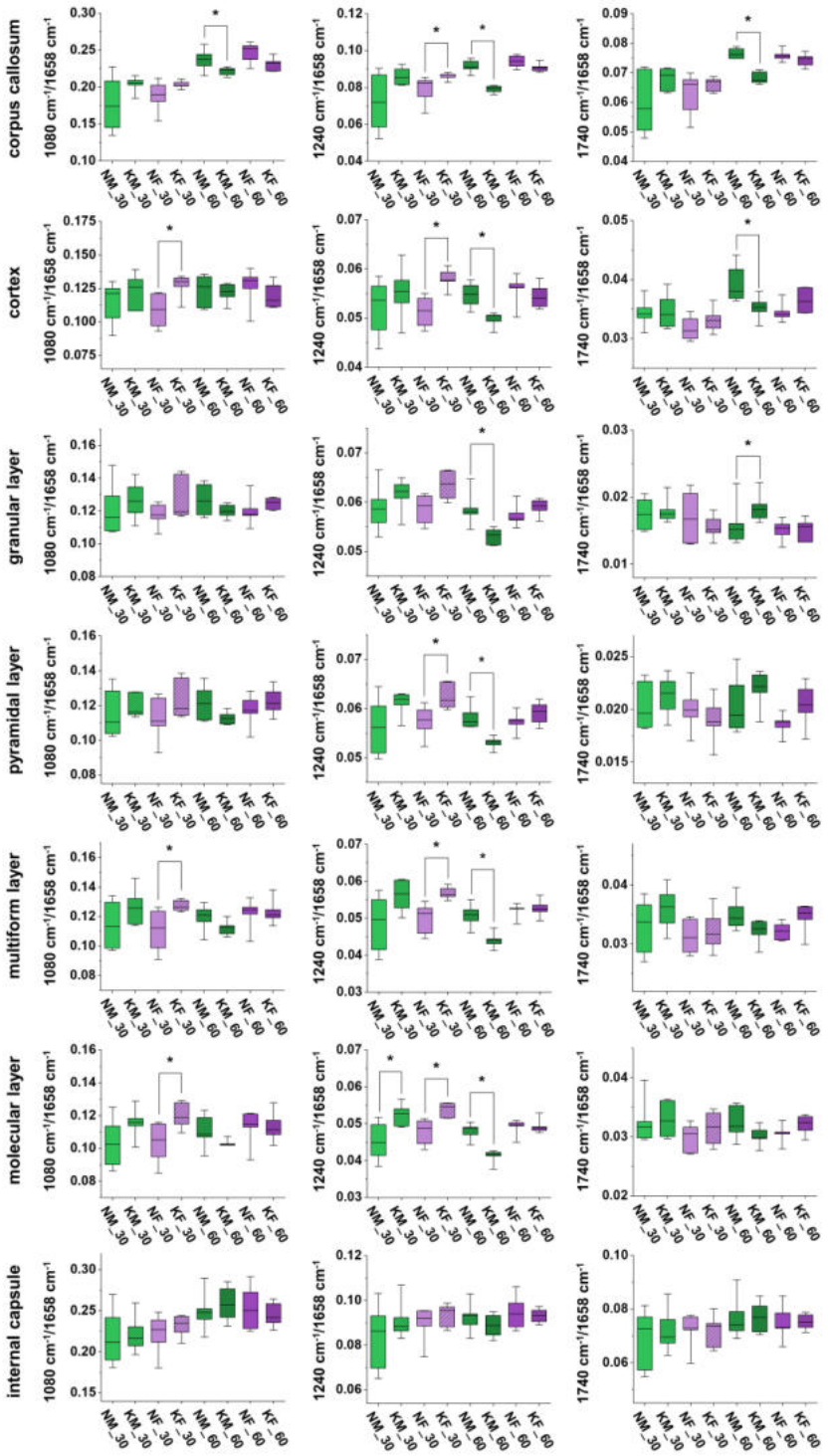

Fig. 10 Box-and-whisker plots illustrating the distribution of FTIR-derived biochemical parameters (ratios of integrated band areas: 1080 cm^{-1}/1658 cm^{-1}, 1240 cm^{-1}/1658 cm^{-1} and 1740 cm^{-1}/1658 cm^{-1}) across selected brain regions: the corpus callosum, cerebral cortex, internal capsule, and four hippocampal layers (granular, pyramidal, multiform, and molecular) for both experimental (K) and control (N) rat groups, including males (M) and females (F), at two postnatal developmental stages (30 and 60 days of age). Statistically significant differences between experimental and corresponding control groups (MannWhitney *U* test, $p < 0.05$) are indicated by an asterisk (*).

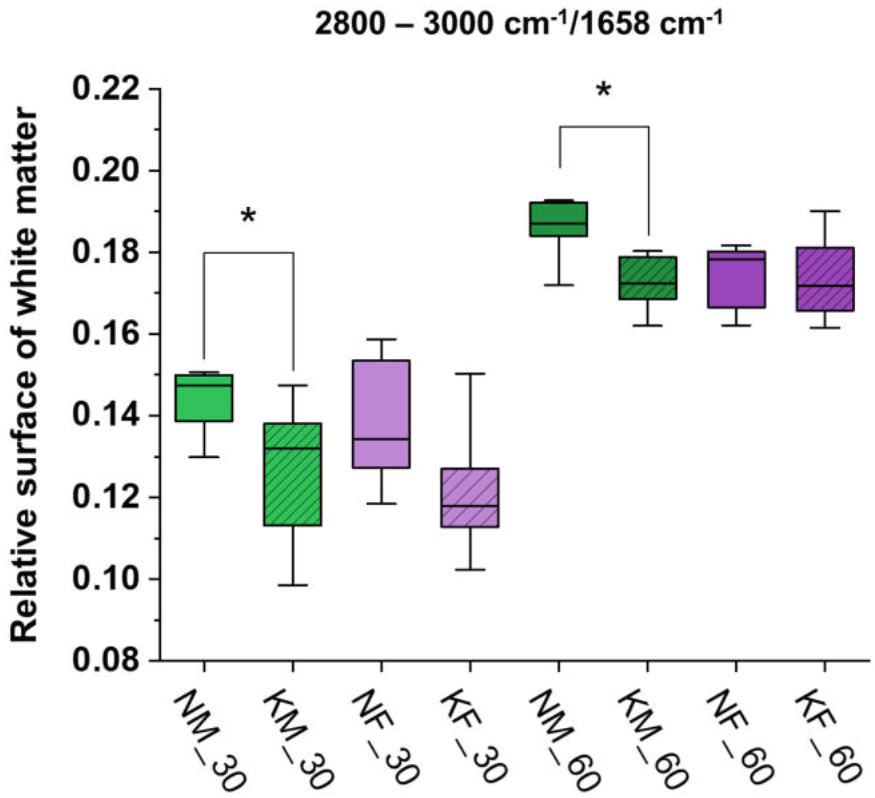

Fig. 11 Box-and-whisker plots illustrating the median, minimal, and maximal values of the relative sizes of the areas characterized by the increased intensity of 2800-3000 cm^{-1}/1658 cm^{-1} ratio corresponding to white matter for both experimental (K) and control (N) rat groups, including males (M) and females (F), at two postnatal developmental stages (30 and 60 days of age). Statistically significant differences between experimental and corresponding control groups (MannWhitney *U* test, $p < 0.05$) are indicated by an asterisk (*).

Chemical mapping and semi-quantitative analysis of regional biochemical changes following prenatal exposure to KD performed for 2-, 6- and 14- days old female rats

A similar analytical approach to that used for 30- and 60-day-old males and females was applied to 2-, 6-, and 14-day-old female offspring, which had not been previously examined. The corresponding chemical maps (Figures S1-S3) and box-and-whisker plots (Figures S4-S6) are provided in the supplementary materials. FTIR imaging using the ultrafast mapping system did not reveal major differences in Cr-associated bands (1395 cm^{-1}/1658 cm^{-1} and 1304 cm^{-1}/1658 cm^{-1}, Figure S1). However, further statistical analysis indicated a significant increase in the 1395 cm^{-1}/1658 cm^{-1} ratio in the molecular layer of prenatally exposed to KD 2-day-old females (Figure S4). When evaluating maps of lipid-associated bands, namely 2800-3000 cm^{-1}/1658 cm^{-1}, 2924 cm^{-1}/1658 cm^{-1}, 2924 cm^{-1}/2955 cm^{-1} and 1465 cm^{-1}/1658 cm^{-1}, in 14-day-old females, localized areas of elevated absorbance suggestive of lipid inclusions were observed (Figure S2). However, these inclusions appeared evenly distributed in both the control and experimental groups. Nevertheless, the intensity of above-mentioned lipid-associated bands seemed reduced in the white matter of animals prenatally exposed to KD. This observation was confirmed by statistical analysis, which showed a significant decrease in the 2924 cm^{-1}/2955 cm^{-1} and 1465 cm^{-1}/1658 cm^{-1} ratios in the corpus callosum of these animals compared to controls (Figures S4 and S5). In 2-day-old females from experimental group, a statistically significant reduction in lipid-related parameters was also found in the cortex (Figure S5). This effect appears to be transient, as no similar trends were observed in

older animals within this brain region. No major differences were observed in the bands associated with phosphate and carbonyl groups between experimental and control animals (Figure S3). However, statistical analysis revealed a significant decrease in the 1740 cm^{-1}/1658 cm^{-1} ratio in the cortex and hippocampal multiform layer of 2-day-old prenatally KD-exposed females (Figure S6).

Discussion

Given the increasing interest in the safety of KD use during pregnancy, it is essential to explore its potential impact on offspring, particularly regarding nervous system development. Building on our previous studies on the effects of prenatal KD exposure on offspring physiology, neurological status, and brain biochemistry [23,24,38], the present work extends this analysis to long-term and sex-dependent molecular alterations. FTIR tissue profiling was complemented by Raman spectroscopy to provide a comprehensive assessment of these changes.

One of the most remarkable findings of this study is the presence of well-defined focal inclusions composed of Cr and CHL in the brains of 60-day-old male rats whose mothers were exposed to KD during pregnancy. These inclusions were particularly abundant in the hippocampus and cortex - brain regions highly susceptible to metabolic perturbations and crucial for memory, learning, and sensory integration [39–41]. Although some inclusions of Cr were also observed in the control animals, their number, size, and signal intensity were clearly lower, suggesting that prenatal KD exposure significantly increases the likelihood of these metabolic anomalies.

Cr plays a central role in cellular energy homeostasis through the creatine/phosphocreatine/creatine kinase (Cr/PhCr/CK) system, which supports rapid ATP regeneration in tissues with high energy demands, such as the brain [25,42–44]. In contrast, CHL is a major structural lipid essential for membrane fluidity, mechanical stability, intracellular signaling, and myelin formation [35,45–48]. Given their key roles in energy metabolism and membrane organization, the accumulation of both Cr and CHL may reflect long-term disturbances in metabolic homeostasis and lipid handling induced by prenatal KD exposure.

In several cases, Cr and CHL deposits were observed in close proximity, suggesting that their accumulation may be at least partially metabolically linked. Both metabolites are closely related to cellular energy status and membrane homeostasis and may be influenced by nutrient availability and mitochondrial efficiency [49,50]. The high-fat, low-carbohydrate nature of KD shifts metabolism toward fatty acid oxidation and ketone body utilization [51,52], which may dysregulate both Cr turnover and lipid handling, thereby promoting their local deposition.

Despite this occasional co-localization, Cr and CHL inclusions were also found independently in several tissue regions, indicating that their accumulation may also occur through distinct mechanisms. In the case of Cr, its abnormal deposition may reflect altered biosynthesis impaired transport across the blood-brain barrier, or reduced utilization in energy-demanding cells such as neurons. In the context of KD, the metabolic shift toward enhanced fatty acid oxidation and ketone body utilization may dysregulate Cr homeostasis by affecting both its synthesis and transport. Furthermore, an imbalance between Cr and PhCr pools - driven by limited ATP availability or altered Cr kinase activity - could result in intracellular deposition of free Cr, possibly indicating impaired energy buffering or disrupted high-energy phosphate turnover. Similar disturbances in the Cr/PhCr ratio have been reported in the brain under metabolic stress, including seizure and hypoxia models [27,53]. On the other hand, the observed accumulation of free Cr - without parallel elevation in phosphorus signals - might reflect a compensatory response to metabolic stress. Elevated Cr levels could serve to support rapid ATP regeneration during transient energetic demand or act as a stabilizing factor for neuronal

membranes - a mechanism supported by evidence from *in vitro* studies showing Cr-mediated protection against oxidative stress and excitotoxic damage [54].

Disruption of neuronal CHL homeostasis has been linked to several neurodegenerative diseases, including Alzheimer's, Parkinson's, and Huntington's disease [55,56]. In particular, excessive CHL accumulation in mitochondria negatively affects their function by weakening key antioxidant systems, increasing reactive oxygen species, damaging cardiolipin, and impairing the formation of respiratory supercomplexes [50]. These disturbances promote oxidative stress and cell death, contributing to neurodegenerative and metabolic disorders [50]. As astrocytes and oligodendrocytes play key roles in maintaining cerebral CHL homeostasis [56,57], its accumulation in the brain may result from impaired lipid trafficking or dysregulated biosynthesis within glial cells. Since KD elevates circulating lipids and ketone bodies during a period of rapid fetal brain growth and myelination, excessive availability of lipid precursors may affect normal neurodevelopment.

Growing evidence suggests that *status epilepticus* (SE) can lead to significant disturbances in brain CHL homeostasis [58–60]. Following SE, an increase in CHL synthesis and a decrease in 24S-hydroxycholesterol levels have been observed, likely due to inhibition of CYP46A1, the key enzyme responsible for CHL metabolism in the brain [59]. This dysregulation results in neuronal CHL accumulation, which may promote excitotoxicity, neuronal loss, and spontaneous seizures [58,59]. Elevated levels of CHL precursors, such as desmosterol and lanosterol, further support the notion of upregulated CHL biosynthesis [59]. CHL plays a critical role in modulating ion channels and NMDA receptor activity, and its imbalance may perpetuate neuronal hyperexcitability through a vicious cycle of increased glutamate release and impaired reuptake [60]. These findings highlight CHL metabolism as a novel pathophysiological mechanism in epilepsy, positioning CYP46A1 and related pathways as promising targets for neuroprotective and antiseizure therapies [58–60].

On the other hand, the observed CHL accumulations might also reflect an adaptive cellular response to the metabolic conditions imposed by the ketogenic state. In the developing brain, CHL plays a crucial role in synaptogenesis, membrane stabilization, myelin formation, and lipid raft formation [47,61,62]. In response to KD-induced lipid influx, glial cells - particularly astrocytes and oligodendrocytes - may upregulate CHL synthesis and storage *via* lipid droplet formation as a compensatory mechanism to buffer excess lipids and preserve membrane homeostasis. Both excess and deficiency of CHL can adversely affect brain function, leading to impaired synaptic plasticity, neurodegenerative changes, and developmental abnormalities, which further underscores its essential role in brain homeostasis [62–66].

Our previous studies on the long-term effects of KDs and models of epilepsy suggest that such dietary interventions may induce structural, biochemical and elemental adaptations in the brain that resemble those observed after epileptic discharges [25–27,29,67,68]. Specifically, it was demonstrated that high-fat, low-carbohydrate diets with higher ketogenic ratios (KR), such as 9:1, result in increased accumulation of Cr and PhCr inclusions in the CA3 and dentate gyrus (DG) areas of the hippocampus [25]. These alterations, observed using synchrotron-based FTIR microspectroscopy, were similar to those reported in animal models following chemically induced seizures. Such findings support the notion that KD may precondition the brain by inducing adaptive responses that modify its susceptibility to future insults, including seizures. Accordingly, the observed CHL accumulation may also reflect a similar neuroadaptive mechanism rather than being solely pathological, potentially priming the nervous system for altered excitability or metabolic stress. This is consistent with the broader concept of metabolic preconditioning and suggests that KD may modulate lipid homeostasis as part of its protective or regulatory effects on neuronal function.

The lack of similar findings in female animals suggests a role of sex-specific factors. Female rats may benefit from higher baseline levels of neuroprotective hormones such as estrogens, which are known to modulate lipid metabolism, mitochondrial function, and antioxidant defense systems [69–74]. Sex hormones play a regulatory role in Cr metabolism, with estrogens and progesterone influencing both Cr kinase activity and the expression of enzymes involved in endogenous synthesis, such as arginine-glycine aminotransferase [75]. Notably, females typically exhibit substantially lower Cr stores than males, reflecting sex-specific differences in Cr homeostasis [75]. Estrogen also exerts a protective effect on lipid metabolism by supporting reverse CHL transport, enhancing hepatic uptake and metabolism of CHL, and inhibiting hepatic CHL biosynthesis [76]. Experimental models consistently demonstrate estrogen's CHL-lowering and anti-atherogenic potential [76]. Furthermore, estrogens contribute to neuroprotection by modulating membrane lipid composition and signaling, particularly through estrogen receptors embedded in CHL-rich lipid rafts, which are critical for neuronal signal transduction and membrane homeostasis [65]. Through these mechanisms, estrogens may help maintain lipid balance in neuronal membranes and protect against neurodegenerative processes.

It is therefore possible that the protective effects of estrogens render the CHL- and Cr-related adaptive mechanisms less necessary in females. On the other hand, estrogens may also modulate the neuroprotective potential of the diet itself through their effects on CHL and Cr metabolism. Thus, the sex-dependent pattern observed in this study likely reflects a combination of hormonal, genetic, and epigenetic mechanisms shaping the long-term impact of prenatal metabolic exposure. Given the observed alterations in CHL metabolism, it is also plausible that CHL itself may exert neuroprotective effects, potentially enhancing resilience to neurological insults such as epileptic seizures. Accordingly, evaluating the response of offspring from KD-fed dams to pilocarpine-induced seizures represents a promising direction for future studies, with particular attention to sex differences in metabolic and neuroprotective responses.

Prenatal KD exposure led to region-specific, age-dependent, and sex-dependent biochemical alterations in the developing brain, with the most pronounced changes observed in 60-day-old males. These included increased Cr-related ratios and decreased lipid-associated parameters, particularly in white matter regions and hippocampal structures, suggesting disturbances in energy metabolism, membrane organization, and possibly myelination [24]. In contrast, female offspring exhibited more transient changes, predominantly at 30 days of age, with relative stabilization by day 60. This further supports the presence of sex-dependent developmental responses to prenatal metabolic exposure.

Conclusions

Altogether, the data suggests that prenatal exposure to KD induces subtle yet widespread changes in brain biochemistry and structural maturation, particularly affecting lipid metabolism and phosphate-containing compounds - key elements of myelin and cellular membranes. A notable finding was the presence of distinct Cr and CHL-rich inclusions in hippocampal and cortical regions in 60-days old male rats. These accumulations raise important questions about their biological significance: whether they represent maladaptive consequences of altered energy and/or lipid metabolism, or rather a form of metabolic preconditioning - a neuroadaptive response priming the brain for future stress, in line with previous observations from epilepsy models. The possibility that such changes may serve protective or regulatory roles, especially in the context of neuronal excitability and membrane stabilization, warrants further investigation. Additionally, the effects appear to be modulated by developmental stage and sex, possibly reflecting differential hormonal influences -particularly the neuroprotective role of

estrogens in females. These sex-specific patterns might influence both the extent of biochemical changes and their functional consequences. The observed molecular alterations could have long-term implications for white matter integrity and hippocampal-dependent functions such as learning and memory. Therefore, extended longitudinal, behavioral and mechanistic studies are essential to clarify the adaptive versus pathological nature of these findings and to better assess the safety and developmental outcomes of maternal KD exposure. What is more further studies incorporating additional histological and molecular approaches would be required to confirm these interpretations.

Materials and methods

Animals

All experimental procedures were approved by the First Local Ethical Committee for Animal Experiments in Krakow (Permit no. 122/2015) and conducted in accordance with national and international regulations on animal welfare as well as the ARRIVE guidelines for reporting animal research. Subjects were obtained from the Laboratory of Experimental Neuropathology, Institute of Zoology and Biomedical Research, Jagiellonian University (Krakow, Poland). The study included male and female Wistar rats at five distinct postnatal stages: postnatal day (P) 2, P6, P14, P30, and P60 (n=6 per group).

Pregnant females were assigned at gestational day 0 to either a ketogenic diet (KD, experimental groups) or a standard laboratory diet (ND, control groups). Initially, 17 dams were included in the KD group and 13 dams in the ND group. A subset of dams (6 per dietary condition) was sacrificed at postnatal day 2 for FTIR analyses, and their offspring were not included in subsequent postnatal assessments. The present study focuses on two groups of offspring derived from the remaining dams: ND (n=7 litters) and KDND (n=6 litters, offspring of dams exposed prenatally to KD and switched to ND at PP2). Importantly, the group of dams maintained on KD throughout lactation (KD, n=5 litters) was not included in the analyses presented in this manuscript. Prenatal dietary intervention did not affect litter structure, including the male-to-female ratio. Detailed protocols concerning dietary regimen, animal handling, and housing conditions have been previously described [23,38].

In our earlier study [23], biochemical analyses of brain tissue samples from male offspring at P2, P6, and P14 were performed. The present investigation extends those findings by incorporating age-matched female neonates at the same developmental stages. Furthermore, to assess potential long-term consequences of prenatal dietary intervention, the study design was expanded to include both male and female offspring at later developmental stages (P30 and P60), corresponding to late juvenile and young adult periods, respectively.

Sample preparation

On the 2nd, 6th, 14th, 30th and 60th day of postnatal life (depending on the group) the rats were anesthetized with Morbital (Biowet) and perfused intracardially with physiological saline solution. The brains were removed, deeply frozen in liquid nitrogen and cut with a cryomicrotome into slices with a thickness of 12 μm. From each brain the slice containing the dorsal part of the hippocampal formation was taken and placed on CaF_2 slide.

Ketogenic and standard Diet

The mothers of rats belonging to experimental groups received a KD enriched with long-chain fatty acids (EF R/M, 80% fat; ssniff GmbH), while those of control animals were maintained on a standard laboratory chow (Labofeed; Morawski). The content of main nutrients in both fodders specified by the manufacturers, along with the elemental composition, previously determined *via* total reflection X-ray fluorescence (TXRF), have been detailed in our earlier publications [23,77] and summarized in Table S1 of the Supplementary materials.

FTIR and Raman measurements

The measurements with FTIR microspectroscopy were conducted at the Laboratory of Atomic and Molecular Biospectroscopy, Faculty of Physics and Applied Computer Science, AGH University of Krakow (Krakow, Poland). They were performed in transmission mode using a Thermo Scientific Nicolet iN10 MX infrared microscope (Thermo Fisher Scientific, USA) equipped with a ceramic IR source. Whole-brain sections were analyzed utilizing an ultrafast mapping system integrated with a linear array of mercury cadmium telluride (MCT) detectors, providing a spatial resolution of approximately 25 μm. Additionally, 100 individual spectra from selected regions of interest (Figure 1) were acquired using a single-point MCT detector. Spectral data were collected for the wavenumber range of 4000-900 cm^{-1} with a resolution of 8 cm^{-1}, averaging 32 scans per sample and corresponding background spectrum. Data acquisition and spectral processing were carried out using OMNIC Picta software (version 8.1).

Complementary Raman measurements were also conducted at the Laboratory of Atomic and Molecular Biospectroscopy. They were performed using a WITec Alpha300R confocal Raman microscope (WITec GmbH, Germany) equipped with a 532 nm laser, a 100× air objective (Zeiss EC Epiplan-Neofluar, NA=0.9), and a UHTS 300 spectrometer featuring a 600 grooves/mm grating. A thermoelectrically cooled, high-sensitivity CCD detector was used for spectra acquisition. Raman measurements were performed to confirm the presence of creatine (Cr) and cholesterol (CHL) within the inclusions that were previously detected in chemical maps obtained by FTIR microspectroscopy. Both tissue inclusions and standard samples of Cr and CHL were measured using a 10 mW laser power, with 10 accumulations and an integration time of 3 s.

Spectral and topographic biochemical analysis

FTIR microspectroscopy was utilized to examine the spatial patterns of key biological macromolecules in brain tissue. Using OMNIC Picta software (version 8.1) two-dimensional chemical maps showing the distributions of the intensities or ratios of intensities of selected infrared bands were created. Band intensity was calculated as the area under a curve after previous trapezoidal baseline correction. For the spectral region between 2800 and 3000 cm^{-1} - commonly referred to as the lipid massif - due to the overlapping of bands we assessed not individual band intensities but the total integrated absorbance over the entire region. Trapezoidal baseline correction was also applied in this case.

For spectral, semi-quantitative and further statistical analysis, all individual spectra acquired with the point-MCT detector from a given brain region and animal were averaged. Semi-quantitative comparisons were performed by calculating the integrated areas of selected absorption bands or their intensity ratios.

The initial preprocessing of the Raman spectra, conducted using the WITec Project Plus 5.1 software, involved cosmic rays removal and background subtraction. Further preprocessing, including vector normalization and peaks identification, was done using OriginPro 2023 software (version 10.0.0.154).

An overview of the IR and Raman bands and band ratios analyzed in this study were showed in Table 2.

Table 2 Examined IR and Raman bands with corresponding assignments [25,28–31,35,78–81]

FTIR microspectroscopy		
Wavenumber [cm^{-1}]	**Band assignment**	**Compound/group**
1658	amide I	proteins, reference band
1395	$\delta_s(CH_3)$, ν(C–N)	Cr (guanidino group)
1304	ν(C–N), δ(N–H)	Cr (guanidino group)
2800-3000	$\nu(CH_2)$, $\nu(CH_3)$	lipids
2924	$\nu_{as}(CH_2)$	lipids
2955	$\nu_{as}(CH_3)$	lipids and proteins
1465	$\delta(CH_2)$, $\delta_{as}(CH_3)$	lipids, CHL and its esters
1080	$\nu_s(PO_2^-)$	phosphate-containing compounds (nucleic acids, phospholipids)
1240	$\nu_{as}(PO_2^-)$	phosphate-containing compounds (nucleic acids, phospholipids)
1740	ν(C=O)	carbonyl-containing compounds (phospholipids, cholesterol esters)
Raman microscopy		
Raman shift [cm^{-1}]	**Band assignment**	**Compound/group**
830	τ(C=N), δ(N–C=N)	Cr (guanidino group), marker band
914	ν(C–C)	Cr, marker band
980	$\rho(CH_2)$	Cr, marker band
1055	ν(C–N)	Cr (amino group), marker band
1395	$\delta(CH_3)$	Cr (N-methyl group), marker band
548	δ(C–H)	CHL, marker band
700	δ(C=C)	CHL, marker band
2867	$\nu_s(CH_2)$	CHL, marker band

Statistical analysis

Seven predefined brain regions of interest (ROIs) were analyzed for each animal using FTIR microspectroscopy, including the cortex, corpus callosum, internal capsule, and four hippocampal cellular layers (Figure 1). Within each ROI, 100 spectra were collected from randomly selected measurement points using a point MCT detector. The spectra obtained from each ROI for a given animal were subsequently averaged to yield a single representative mean spectrum per region. Consequently, each animal was characterized by seven mean spectra corresponding to the analyzed ROIs. Based on these mean spectra, the absolute and/or relative intensities of selected bands (listed in Table 1) were calculated. Statistical significance of differences in the measured biochemical parameters between rats prenatally exposed to a ketogenic diet and control animals at the corresponding postnatal stage was assessed using the non-parametric Mann-Whitney *U* test. All statistical analyses were performed using OriginPro 2023 software (version 10.0.0.154), with the significance level set at 5%.

The Mann-Whitney *U* test was also applied to evaluate differences in the relative area of the internal capsule between the experimental and corresponding control groups.

Limitations of the study

We acknowledge that the investigators were not blinded during image acquisition and subsequent data analysis, which constitutes a limitation of the present study. This may introduce the possibility of observer-related bias during image interpretation. However, all analyses were performed using the same predefined procedures and criteria across all experimental groups to ensure methodological consistency.

Author information:

Corresponding Author

Joanna Chwiej - AGH University of Krakow, Faculty of Physics and Applied Computer Science, Al. Mickiewicza 30, 30-059 Krakow, Poland;
Orcid: https://orcid.org/0000-0002-3792-7876;

Email: jchwiej@agh.edu.pl

Authors

Marzena Rugiel - AGH University of Krakow, Faculty of Physics and Applied Computer Science, Al. Mickiewicza 30, 30-059 Krakow, Poland
Zuzanna Setkowicz - Jagiellonian University, Institute of Zoology and Biomedical Research, Gronostajowa 9, 30-387 Krakow, Poland
Agnieszka Drozdz - AGH University of Krakow, Faculty of Physics and Applied Computer Science, Al. Mickiewicza 30, 30-059 Krakow, Poland
Aleksandra Wilk - AGH University of Krakow, Faculty of Physics and Applied Computer Science, Al. Mickiewicza 30, 30-059 Krakow, Poland
Zofia Brylowska - AGH University of Krakow, Faculty of Physics and Applied Computer Science, Al. Mickiewicza 30, 30-059 Krakow, Poland
Joanna Chwiej - AGH University of Krakow, Faculty of Physics and Applied Computer Science, Al. Mickiewicza 30, 30-059 Krakow, Poland

Author Contribution

M.R. and Z.S. equally contributed to this work.
M.R. performed conceptualization, methodology, investigation, validation, writing original draft; Z.S. performed methodology, resources, investigation; A.D. performed methodology, investigation, validation, writing original draft; A.W. performed methodology, investigation, reviewing manuscript; Z.B. performed methodology, investigation, validation; J.C. performed conceptualization, methodology, validation, resources, supervision, writing original draft, corresponding author.

Notes:

The authors declare no competing financial interest.

Acknowledgements:

This work was partially financed by: (1) the Ministry of Science and Higher Education of Poland, (2) the statutory research fund no. N18/DBW/000018 of the Laboratory of Experimental Neuropathology (Institute of Zoology and Biomedical Research, Jagiellonian University) and (3) the funds granted to the AGH University of Krakow in the frame of the "Excellence Initiative - Research University" project (Action 4: A system of university grants for research carried out with the participation of doctoral students and young scientists, PL-Joanna Chwiej).

The presented results were obtained using WITec Alpha300R Raman microscope bought in frame of the “Excellence Initiative-Research University” Project granted to AGH UST.

Supporting information:

Table S1: Composition of normal and ketogenic diets. Figure S1: Representative chemical maps showing spatial distributions of the amide I band intensity and selected band-area ratios in brain sections of 2-, 6-, and 14-day-old female offspring prenatally exposed to ketogenic or standard diet. Figure S2: Representative FTIR chemical maps illustrating the distribution of lipid-related compounds and selected spectral parameters in brain sections of 2-, 6-, and 14-day-old female offspring prenatally exposed to ketogenic or standard diet. Figures S3-S5: Box-and-whisker plots of selected spectral parameters for 2-, 6-, and 14-day-old female offspring prenatally exposed to ketogenic or standard diet.

References

(1) Mclean, A.; Veettil, T. C. P.; Giergiel, M.; Wood, B. R. Evolution of Vibrational Biospectroscopy: Multimodal Techniques and Miniaturisation Supported by Machine Learning. *Vib. Spectrosc.* 2024, *133*, 103708. https://doi.org/10.1016/j.vibspec.2024.103708.

(2) Kannan, S.; Callery, E. L.; Rowbottom, A. W. Vibrational Biospectroscopy in the Clinical Setting: Exploring the Impact of New Advances in the Field of Immunology. *Journal of Spectroscopy* 2023, *2023*, 1–16. https://doi.org/10.1155/2023/5557441.

(3) Gomes da Costa, S.; Richter, A.; Schmidt, U.; Breuninger, S.; Hollricher, O. Confocal Raman Microscopy in Life Sciences. *Morphologie* 2019, *103* (341), 11–16. https://doi.org/10.1016/j.morpho.2018.12.003.

(4) Caine, S.; Heraud, P.; Tobin, M. J.; McNaughton, D.; Bernard, C. C. A. The Application of Fourier Transform Infrared Microspectroscopy for the Study of Diseased Central Nervous System Tissue. *Neuroimage* 2012, *59* (4), 3624–3640. https://doi.org/10.1016/j.neuroimage.2011.11.033.

(5) Ranasinghe, J. C.; Wang, Z.; Huang, S. Raman Spectroscopy on Brain Disorders: Transition from Fundamental Research to Clinical Applications. *Biosensors (Basel).* 2022, *13* (1), 27. https://doi.org/10.3390/bios13010027.

(6) Lilo, T.; Morais, C. L. M.; Shenton, C.; Ray, A.; Gurusinghe, N. Revising Fourier-Transform Infrared (FT-IR) and Raman Spectroscopy towards Brain Cancer Detection. *Photodiagnosis Photodyn. Ther.* 2022, *38*, 102785. https://doi.org/10.1016/j.pdpdt.2022.102785.

(7) Leng, H.; Chen, C.; Chen, C.; Chen, F.; Du, Z.; Chen, J.; Yang, B.; Zuo, E.; Xiao, M.; Lv, X.; Liu, P. Raman Spectroscopy and FTIR Spectroscopy Fusion Technology Combined with Deep Learning: A Novel Cancer Prediction Method. *Spectrochim. Acta A Mol. Biomol. Spectrosc.* 2023, *285*, 121839. https://doi.org/10.1016/j.saa.2022.121839.

(8) Mordechai, S.; Shufan, E.; Porat Katz, B. S.; Salman, A. Early Diagnosis of Alzheimer’s Disease Using Infrared Spectroscopy of Isolated Blood Samples Followed by Multivariate Analyses. *Analyst* 2017, *142* (8), 1276–1284. https://doi.org/10.1039/C6AN01580H.

(9) Vaz, M.; Soares Martins, T.; Leandro, K.; de Almeida, L. P.; da Cruz e Silva, O. A. B.; Nunes, A.; Henriques, A. G. Fourier Transform Infrared Spectroscopy Analysis as a

Tool to Address Aβ Impact on Extracellular Vesicles. *Molecules* 2025, *30* (2), 258. https://doi.org/10.3390/molecules30020258.

(10) Wang, X.; Wu, Q.; Li, C.; Zhou, Y.; Xu, F.; Zong, L.; Ge, S. A Study of Parkinson's Disease Patients' Serum Using FTIR Spectroscopy. *Infrared Phys. Technol.* 2020, *106*, 103279. https://doi.org/10.1016/j.infrared.2020.103279.

(11) Araki, K.; Yagi, N.; Ikemoto, Y.; Yagi, H.; Choong, C.-J.; Hayakawa, H.; Beck, G.; Sumi, H.; Fujimura, H.; Moriwaki, T.; Nagai, Y.; Goto, Y.; Mochizuki, H. Synchrotron FTIR Micro-Spectroscopy for Structural Analysis of Lewy Bodies in the Brain of Parkinson's Disease Patients. *Sci. Rep.* 2015, *5* (1), 17625. https://doi.org/10.1038/srep17625.

(12) Lin, S.-Y.; Li, M.-J.; Cheng, W.-T. FT-IR and Raman Vibrational Microspectroscopies Used for Spectral Biodiagnosis of Human Tissues. *Journal of Spectroscopy* 2007, *21* (1), 1–30. https://doi.org/10.1155/2007/278765.

(13) Eberhardt, K.; Stiebing, C.; Matthäus, C.; Schmitt, M.; Popp, J. Advantages and Limitations of Raman Spectroscopy for Molecular Diagnostics: An Update. *Expert Rev. Mol. Diagn.* 2015, *15* (6), 773–787. https://doi.org/10.1586/14737159.2015.1036744.

(14) Chen, C.; Qi, J.; Li, Y.; Li, D.; Wu, L.; Li, R.; Chen, Q.; Sun, N. Applications of Raman Spectroscopy in the Diagnosis and Monitoring of Neurodegenerative Diseases. *Front. Neurosci.* 2024, *18*. https://doi.org/10.3389/fnins.2024.1301107.

(15) Manciu, F. S.; Lee, K. H.; Durrer, W. G.; Bennet, K. E. Detection and Monitoring of Neurotransmitters—A Spectroscopic Analysis. *Neuromodulation: Technology at the Neural Interface* 2013, *16* (3), 192–199. https://doi.org/10.1111/j.1525-1403.2012.00502.x.

(16) Kochan, K.; Chrabaszcz, K.; Szczur, B.; Maslak, E.; Dybas, J.; Marzec, K. M. IR and Raman Imaging of Murine Brains from Control and ApoE/LDLR −/− Mice with Advanced Atherosclerosis. *Analyst* 2016, *141* (18), 5329–5338. https://doi.org/10.1039/C6AN00107F.

(17) Amharref, N.; Beljebbar, A.; Dukic, S.; Venteo, L.; Schneider, L.; Pluot, M.; Manfait, M. Discriminating Healthy from Tumor and Necrosis Tissue in Rat Brain Tissue Samples by Raman Spectral Imaging. *Biochimica et Biophysica Acta (BBA) - Biomembranes* 2007, *1768* (10), 2605–2615. https://doi.org/10.1016/j.bbamem.2007.06.032.

(18) Krafft, C.; Neudert, L.; Simat, T.; Salzer, R. Near Infrared Raman Spectra of Human Brain Lipids. *Spectrochim. Acta A Mol. Biomol. Spectrosc.* 2005, *61* (7), 1529–1535. https://doi.org/10.1016/j.saa.2004.11.017.

(19) Perez-Guaita, D.; Kochan, K.; Martin, M.; Andrew, D. W.; Heraud, P.; Richards, J. S.; Wood, B. R. Multimodal Vibrational Imaging of Cells. *Vib. Spectrosc.* 2017, *91*, 46–58. https://doi.org/10.1016/j.vibspec.2016.07.017.

(20) Gassner, C.; Adegoke, J. A.; Patel, S. K.; Sharma, V. J.; Kochan, K.; Burrell, L. M.; Raman, J.; Wood, B. R. Improved Tissue Preparation for Multimodal Vibrational Imaging of Biological Tissues. *Clinical Spectroscopy* 2022, *4*, 100021. https://doi.org/10.1016/j.clispe.2022.100021.

(21) D'Andrea Meira, I.; Romão, T. T.; Pires do Prado, H. J.; Krüger, L. T.; Pires, M. E. P.; da Conceição, P. O. Ketogenic Diet and Epilepsy: What We Know So Far. *Front. Neurosci.* 2019, *13*. https://doi.org/10.3389/fnins.2019.00005.

(22) McDonald, T. J. W.; Cervenka, M. C. Ketogenic Diet Therapies for Seizures and Status Epilepticus. *Semin. Neurol.* 2020, *40* (06), 719–729. https://doi.org/10.1055/s-0040-1719077.

(23) Rugiel, M.; Setkowicz-Janeczko, Z.; Kosiek, W.; Rauk, Z.; Kawon, K.; Chwiej, J. Does Ketogenic Diet Used in Pregnancy Affect the Nervous System Development in Offspring?─FTIR Microspectroscopy Study. *ACS Chem. Neurosci.* 2023, *14* (15), 2775–2791. https://doi.org/10.1021/acschemneuro.3c00331.

(24) Rugieł, M.; Setkowicz, Z.; Czyzycki, M.; Simon, R.; Baumbach, T.; Chwiej, J. Element Changes Occurring in Brain Point at the White Matter Abnormalities in Rats Exposed to the Ketogenic Diet During Prenatal Life. *ACS Chem. Neurosci.* 2024, *15* (21), 3932–3944. https://doi.org/10.1021/acschemneuro.4c00283.

(25) Skoczen, A.; Setkowicz, Z.; Janeczko, K.; Sandt, Ch.; Borondics, F.; Chwiej, J. The Influence of High Fat Diets with Different Ketogenic Ratios on the Hippocampal Accumulation of Creatine – FTIR Microspectroscopy Study. *Spectrochim. Acta A Mol. Biomol. Spectrosc.* 2017, *184*, 13–22. https://doi.org/10.1016/j.saa.2017.04.085.

(26) Dulinska, J.; Setkowicz, Z.; Janeczko, K.; Sandt, C.; Dumas, P.; Uram, L.; Gzielo-Jurek, K.; Chwiej, J. Synchrotron Radiation Fourier-Transform Infrared and Raman Microspectroscopy Study Showing an Increased Frequency of Creatine Inclusions in the Rat Hippocampal Formation Following Pilocarpine-Induced Seizures. *Anal. Bioanal. Chem.* 2012, *402* (7), 2267–2274. https://doi.org/10.1007/s00216-011-5488-z.

(27) Kutorasinska, J.; Setkowicz, Z.; Janeczko, K.; Sandt, C.; Dumas, P.; Chwiej, J. Differences in the Hippocampal Frequency of Creatine Inclusions between the Acute and Latent Phases of Pilocarpine Model Defined Using Synchrotron Radiation-Based FTIR Microspectroscopy. *Anal. Bioanal. Chem.* 2013, *405* (23), 7337–7345. https://doi.org/10.1007/s00216-013-7191-8.

(28) Dulinska, J.; Setkowicz, Z.; Janeczko, K.; Sandt, C.; Dumas, P.; Uram, L.; Gzielo-Jurek, K.; Chwiej, J. Synchrotron Radiation Fourier-Transform Infrared and Raman Microspectroscopy Study Showing an Increased Frequency of Creatine Inclusions in the Rat Hippocampal Formation Following Pilocarpine-Induced Seizures. *Anal. Bioanal. Chem.* 2012, *402* (7), 2267–2274. https://doi.org/10.1007/s00216-011-5488-z.

(29) Chwiej, J.; Skoczen, A.; Janeczko, K.; Kutorasinska, J.; Matusiak, K.; Figiel, H.; Dumas, P.; Sandt, C.; Setkowicz, Z. The Biochemical Changes in Hippocampal Formation Occurring in Normal and Seizure Experiencing Rats as a Result of a Ketogenic Diet. *Analyst* 2015, *140* (7), 2190–2204. https://doi.org/10.1039/C4AN01857E.

(30) Gallant, M.; Rak, M.; Szeghalmi, A.; Del Bigio, M. R.; Westaway, D.; Yang, J.; Julian, R.; Gough, K. M. Focally Elevated Creatine Detected in Amyloid Precursor Protein (APP) Transgenic Mice and Alzheimer Disease Brain Tissue. *Journal of Biological Chemistry* 2006, *281* (1), 5–8. https://doi.org/10.1074/jbc.C500244200.

(31) Gangopadhyay, D.; Sharma, P.; Singh, S. K.; Singh, P.; Tarcea, N.; Deckert, V.; Popp, J.; Singh, R. K. Raman Spectroscopic Approach to Monitor the in Vitro Cyclization of Creatine→creatinine. *Chem. Phys. Lett.* 2015, *618*, 225–230. https://doi.org/10.1016/j.cplett.2014.11.021.

(32) Moreira, L. P.; Rocco, D. D. F. M.; da Silva, A. G.; Pacheco, M. T. T.; Silveira, L. Detecting Creatine Excreted in the Urine of Swimming Athletes by Means of Raman Spectroscopy. *Lasers Med. Sci.* 2020, *35* (2), 455–464. https://doi.org/10.1007/s10103-019-02843-z.

(33) Gupta, U.; Singh, VivekK.; Kumar, V.; Khajuria, Y. Spectroscopic Studies of Cholesterol: Fourier Transform Infra-Red and Vibrational Frequency Analysis. *Materials Focus* 2014, *3* (3), 211–217. https://doi.org/10.1166/mat.2014.1161.

(34) Ha, B. J.; Park, S. Classification of Gallstones Using Fourier-Transform Infrared Spectroscopy and Photography. *Biomater. Res.* 2018, *22* (1). https://doi.org/10.1186/s40824-018-0128-8.

(35) Czamara, K.; Majzner, K.; Pacia, M. Z.; Kochan, K.; Kaczor, A.; Baranska, M. Raman Spectroscopy of Lipids: A Review. *Journal of Raman Spectroscopy* 2015, *46* (1), 4–20. https://doi.org/10.1002/jrs.4607.

(36) Simeral, M. L.; Demers, S. M. E.; Sheth, K.; Hafner, J. H. A Raman Spectral Marker for the Iso-octyl Chain Structure of Cholesterol. *Analytical Science Advances* 2024, *5* (1–2). https://doi.org/10.1002/ansa.202300057.

(37) Zhou, Y.; Xu, Y.; Hou, X.; Xia, D. Raman Analysis of Lipids in Cells: Current Applications and Future Prospects. *J. Pharm. Anal.* 2025, *15* (4), 101136. https://doi.org/10.1016/j.jpha.2024.101136.

(38) Kosiek, W.; Rauk, Z.; Szulc, P.; Cichy, A.; Rugieł, M.; Chwiej, J.; Janeczko, K.; Setkowicz, Z. Ketogenic Diet Impairs Neurological Development of Neonatal Rats and Affects Biochemical Composition of Maternal Brains: Evidence of Functional Recovery in Pups. *Brain Struct. Funct.* 2022, *227* (3), 1099–1113. https://doi.org/10.1007/s00429-021-02450-1.

(39) Preston, A. R.; Eichenbaum, H. Interplay of Hippocampus and Prefrontal Cortex in Memory. *Current Biology* 2013, *23* (17), R764–R773. https://doi.org/10.1016/j.cub.2013.05.041.

(40) Shapiro, M. L.; Riceberg, J. S.; Seip-Cammack, K.; Guise, K. G. Functional Interactions of Prefrontal Cortex and the Hippocampus in Learning and Memory. In *Space,Time and Memory in the Hippocampal Formation*; Springer Vienna: Vienna, 2014; pp 517–560. https://doi.org/10.1007/978-3-7091-1292-2_19.

(41) Bartsch, T. The Hippocampus in Neurological Disease. In *The Clinical Neurobiology of the Hippocampus*; Oxford University Press, 2012; pp 200–222. https://doi.org/10.1093/acprof:oso/9780199592388.003.0011.

(42) Bonilla, D. A.; Kreider, R. B.; Stout, J. R.; Forero, D. A.; Kerksick, C. M.; Roberts, M. D.; Rawson, E. S. Metabolic Basis of Creatine in Health and Disease: A Bioinformatics-Assisted Review. *Nutrients* 2021, *13* (4), 1238. https://doi.org/10.3390/nu13041238.

(43) Singh, S.; Dash, A. K. Creatine Monohydrate; 2009; pp 1–35. https://doi.org/10.1016/S1871-5125(09)34001-7.

(44) Colas, C.; Banci, G.; Martini, R.; Ecker, G. F. Studies of Structural Determinants of Substrate Binding in the Creatine Transporter (CreaT, SLC6A8) Using Molecular Models. *Sci. Rep.* 2020, *10* (1), 6241. https://doi.org/10.1038/s41598-020-63189-z.

(45) Guo, J.; Chen, S.; Zhang, Y.; Liu, J.; Jiang, L.; Hu, L.; Yao, K.; Yu, Y.; Chen, X. Cholesterol Metabolism: Physiological Regulation and Diseases. *MedComm (Beijing).* 2024, *5* (2). https://doi.org/10.1002/mco2.476.

(46) Zampelas, A.; Magriplis, E. New Insights into Cholesterol Functions: A Friend or an Enemy? *Nutrients* 2019, *11* (7), 1645. https://doi.org/10.3390/nu11071645.

(47) Harris J. Robin. *Cholesterol Binding and Cholesterol Transport Proteins:*; Harris, J. R., Ed.; Springer Netherlands: Dordrecht, 2010; Vol. 51. https://doi.org/10.1007/978-90-481-8622-8.

(48) Cortes, V. Physiological and Pathological Implications of Cholesterol. *Frontiers in Bioscience* 2014, *19* (3), 416. https://doi.org/10.2741/4216.

(49) Arazi, H.; Eghbali, E.; Suzuki, K. Creatine Supplementation, Physical Exercise and Oxidative Stress Markers: A Review of the Mechanisms and Effectiveness. *Nutrients* 2021, *13* (3), 869. https://doi.org/10.3390/nu13030869.

(50) Goicoechea, L.; Conde de la Rosa, L.; Torres, S.; García-Ruiz, C.; Fernández-Checa, J. C. Mitochondrial Cholesterol: Metabolism and Impact on Redox Biology and Disease. *Redox Biol.* 2023, *61*, 102643. https://doi.org/10.1016/j.redox.2023.102643.

(51) Alharbi, A.; Al-Sowayan, N. S. The Effect of Ketogenic-Diet on Health. *Food Nutr. Sci.* 2020, *11* (04), 301–313. https://doi.org/10.4236/fns.2020.114022.

(52) McDonald, T. J. W.; Cervenka, M. C. Lessons Learned from Recent Clinical Trials of Ketogenic Diet Therapies in Adults. *Curr. Opin. Clin. Nutr. Metab. Care* 2019, *22* (6), 418–424. https://doi.org/10.1097/MCO.0000000000000596.

(53) Kekelidze, T.; Khait, I.; Togliatti, A.; Benzecry, J. M.; Wieringa, B.; Holtzman, D. Altered Brain Phosphocreatine and ATP Regulation When Mitochondrial Creatine Kinase Is Absent. *J. Neurosci. Res.* 2001, *66* (5), 866–872. https://doi.org/10.1002/jnr.10060.

(54) Genius, J.; Geiger, J.; Bender, A.; Möller, H.-J.; Klopstock, T.; Rujescu, D. Creatine Protects against Excitoxicity in an In Vitro Model of Neurodegeneration. *PLoS One* 2012, *7* (2), e30554. https://doi.org/10.1371/journal.pone.0030554.

(55) Djelti, F.; Braudeau, J.; Hudry, E.; Dhenain, M.; Varin, J.; Bièche, I.; Marquer, C.; Chali, F.; Ayciriex, S.; Auzeil, N.; Alves, S.; Langui, D.; Potier, M.-C.; Laprevote, O.; Vidaud, M.; Duyckaerts, C.; Miles, R.; Aubourg, P.; Cartier, N. CYP46A1 Inhibition, Brain Cholesterol Accumulation and Neurodegeneration Pave the Way for Alzheimer's Disease. *Brain* 2015, *138* (8), 2383–2398. https://doi.org/10.1093/brain/awv166.

(56) Vance, J. E.; Hayashi, H. Formation and Function of Apolipoprotein E-Containing Lipoproteins in the Nervous System. *Biochimica et Biophysica Acta (BBA) - Molecular and Cell Biology of Lipids* 2010, *1801* (8), 806–818. https://doi.org/10.1016/j.bbalip.2010.02.007.

(57) Molina-Gonzalez, I.; Holloway, R. K.; Jiwaji, Z.; Dando, O.; Kent, S. A.; Emelianova, K.; Lloyd, A. F.; Forbes, L. H.; Mahmood, A.; Skripuletz, T.; Gudi, V.; Febery, J. A.; Johnson, J. A.; Fowler, J. H.; Kuhlmann, T.; Williams, A.; Chandran, S.; Stangel, M.; Howden, A. J. M.; Hardingham, G. E.; Miron, V. E. Astrocyte-Oligodendrocyte Interaction Regulates Central Nervous System Regeneration. *Nat. Commun.* 2023, *14* (1), 3372. https://doi.org/10.1038/s41467-023-39046-8.

(58) Hanin, A.; Roussel, D.; Lecas, S.; Baudin, P.; Navarro, V. Repurposing of Cholesterol-Lowering Agents in Status Epilepticus: A Neuroprotective Effect of Simvastatin. *Epilepsy & Behavior* 2023, *141*, 109133. https://doi.org/10.1016/j.yebeh.2023.109133.

(59) Hanin, A.; Baudin, P.; Demeret, S.; Roussel, D.; Lecas, S.; Teyssou, E.; Damiano, M.; Luis, D.; Lambrecq, V.; Frazzini, V.; Decavèle, M.; Plu, I.; Bonnefont-Rousselot, D.; Bittar, R.; Lamari, F.; Navarro, V. Disturbances of Brain Cholesterol Metabolism: A New Excitotoxic Process Associated with Status Epilepticus. *Neurobiol. Dis.* 2021, *154*, 105346. https://doi.org/10.1016/j.nbd.2021.105346.

(60) Wheless, J. W.; Rho, J. M. Role of Cholesterol in Modulating Brain Hyperexcitability. *Epilepsia* 2025, *66* (1), 33–46. https://doi.org/10.1111/epi.18174.

(61) Hussain, G.; Wang, J.; Rasul, A.; Anwar, H.; Imran, A.; Qasim, M.; Zafar, S.; Kamran, S. K. S.; Razzaq, A.; Aziz, N.; Ahmad, W.; Shabbir, A.; Iqbal, J.; Baig, S. M.; Sun, T.

Role of Cholesterol and Sphingolipids in Brain Development and Neurological Diseases. *Lipids Health Dis.* 2019, *18* (1), 26. https://doi.org/10.1186/s12944-019-0965-z.

(62) Shin, K. C.; Ali Moussa, H. Y.; Park, Y. Cholesterol Imbalance and Neurotransmission Defects in Neurodegeneration. *Exp. Mol. Med.* 2024, *56* (8), 1685–1690. https://doi.org/10.1038/s12276-024-01273-4.

(63) Martin, M. G.; Ahmed, T.; Korovaichuk, A.; Venero, C.; Menchón, S. A.; Salas, I.; Munck, S.; Herreras, O.; Balschun, D.; Dotti, C. G. Constitutive Hippocampal Cholesterol Loss Underlies Poor Cognition in Old Rodents. *EMBO Mol. Med.* 2014, *6* (7), 902–917. https://doi.org/10.15252/emmm.201303711.

(64) Martin, M.; Dotti, C. G.; Ledesma, M. D. Brain Cholesterol in Normal and Pathological Aging. *Biochimica et Biophysica Acta (BBA) - Molecular and Cell Biology of Lipids* 2010, *1801* (8), 934–944. https://doi.org/10.1016/j.bbalip.2010.03.011.

(65) Marin, R.; Diaz, M. Estrogen Interactions With Lipid Rafts Related to Neuroprotection. Impact of Brain Ageing and Menopause. *Front. Neurosci.* 2018, *12*. https://doi.org/10.3389/fnins.2018.00128.

(66) Peri, A.; Benvenuti, S.; Luciani, P.; Deledda, C.; Cellai, I. Membrane Cholesterol as a Mediator of the Neuroprotective Effects of Estrogens. *Neuroscience* 2011, *191*, 107–117. https://doi.org/10.1016/j.neuroscience.2011.03.011.

(67) Chwiej, J.; Patulska, A.; Skoczen, A.; Janeczko, K.; Ciarach, M.; Simon, R.; Setkowicz, Z. Elemental Changes in the Hippocampal Formation Following Two Different Formulas of Ketogenic Diet: An X-Ray Fluorescence Microscopy Study. *JBIC Journal of Biological Inorganic Chemistry* 2015, *20* (8), 1277–1286. https://doi.org/10.1007/s00775-015-1306-y.

(68) Chwiej, J.; Winiarski, W.; Ciarach, M.; Janeczko, K.; Lankosz, M.; Rickers, K.; Setkowicz, Z. The Role of Trace Elements in the Pathogenesis and Progress of Pilocarpine-Induced Epileptic Seizures. *JBIC Journal of Biological Inorganic Chemistry* 2008, *13* (8), 1267–1274. https://doi.org/10.1007/s00775-008-0411-6.

(69) Klinge, C. M. Estrogenic Control of Mitochondrial Function. *Redox Biol.* 2020, *31*, 101435. https://doi.org/10.1016/j.redox.2020.101435.

(70) Arnold, S.; Victor, M. B.; Beyer, C. Estrogen and the Regulation of Mitochondrial Structure and Function in the Brain. *J. Steroid Biochem. Mol. Biol.* 2012, *131* (1–2), 2–9. https://doi.org/10.1016/j.jsbmb.2012.01.012.

(71) Klinge, C. M. Estrogens Regulate Life and Death in Mitochondria. *J. Bioenerg. Biomembr.* 2017, *49* (4), 307–324. https://doi.org/10.1007/s10863-017-9704-1.

(72) Rettberg, J. R.; Yao, J.; Brinton, R. D. Estrogen: A Master Regulator of Bioenergetic Systems in the Brain and Body. *Front. Neuroendocrinol.* 2014, *35* (1), 8–30. https://doi.org/10.1016/j.yfrne.2013.08.001.

(73) Palmisano, B. T.; Zhu, L.; Stafford, J. M. Role of Estrogens in the Regulation of Liver Lipid Metabolism; 2017; pp 227–256. https://doi.org/10.1007/978-3-319-70178-3_12.

(74) Knopp, R. H.; Zhu, X. Multiple Beneficial Effects of Estrogen on Lipoprotein Metabolism. *J. Clin. Endocrinol. Metab.* 1997, *82* (12), 3952–3954. https://doi.org/10.1210/jcem.82.12.4472.

(75) Smith-Ryan, A. E.; Cabre, H. E.; Eckerson, J. M.; Candow, D. G. Creatine Supplementation in Women's Health: A Lifespan Perspective. *Nutrients* 2021, *13* (3), 877. https://doi.org/10.3390/nu13030877.

(76) Palmisano, B. T.; Zhu, L.; Stafford, J. M. Role of Estrogens in the Regulation of Liver Lipid Metabolism; 2017; pp 227–256. https://doi.org/10.1007/978-3-319-70178-3_12.

(77) Kawon, K.; Rugiel, M.; Setkowicz, Z.; Matusiak, K.; Kubala-Kukus, A.; Stabrawa, I.; Szary, K.; Rauk, Z.; Chwiej, J. Ketogenic Diet Influence on the Elemental Homeostasis of Internal Organs Is Gender Dependent. *Sci. Rep.* 2023, *13* (1), 18448. https://doi.org/10.1038/s41598-023-45611-4.

(78) Movasaghi, Z.; Rehman, S.; ur Rehman, Dr. I. Fourier Transform Infrared (FTIR) Spectroscopy of Biological Tissues. *Appl. Spectrosc. Rev.* 2008, *43* (2), 134–179. https://doi.org/10.1080/05704920701829043.

(79) Malek, K.; Wood, B. R.; Bambery, K. R. FTIR Imaging of Tissues: Techniques and Methods of Analysis; 2014; pp 419–473. https://doi.org/10.1007/978-94-007-7832-0_15.

(80) Kochan, K.; Chrabaszcz, K.; Szczur, B.; Maslak, E.; Dybas, J.; Marzec, K. M. IR and Raman Imaging of Murine Brains from Control and ApoE/LDLR −/− Mice with Advanced Atherosclerosis. *Analyst* 2016, *141* (18), 5329–5338. https://doi.org/10.1039/C6AN00107F.

(81) Morisaki, S.; Ota, C.; Matsuda, K.; Kaku, N.; Fujiwara, H.; Oda, R.; Ishibashi, H.; Kubo, T.; Kawata, M. Application of Raman Spectroscopy for Visualizing Biochemical Changes during Peripheral Nerve Injury *in Vitro* and *in Vivo*. *J. Biomed. Opt.* 2013, *18* (11), 116011. https://doi.org/10.1117/1.JBO.18.11.116011.

TOC Graphic

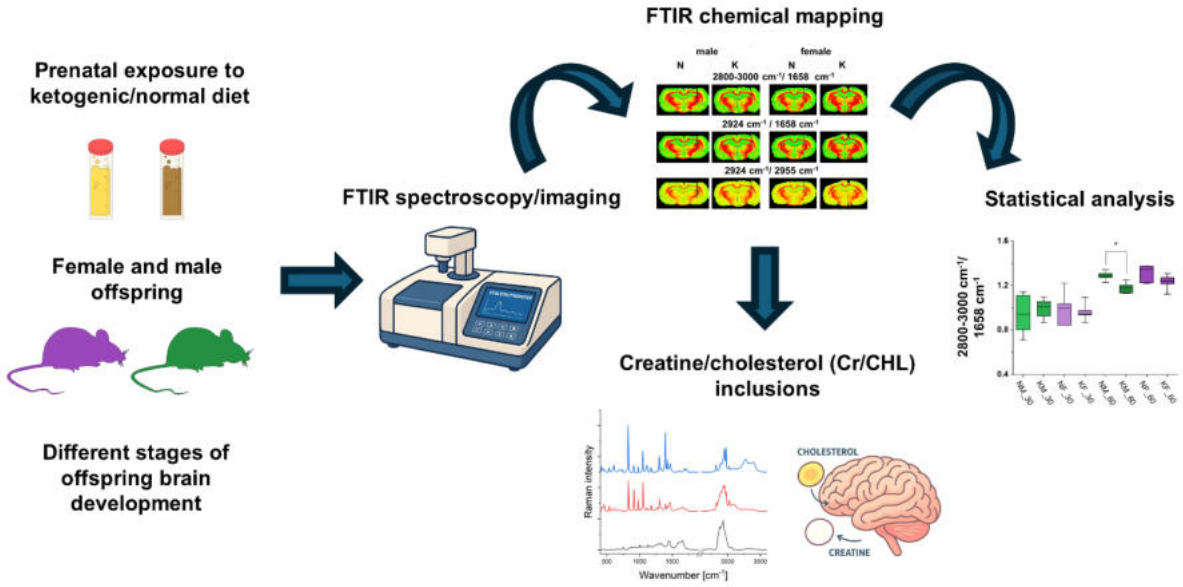
FTIR chemical mapping
Prenatal exposure to ketogenic/normal diet
male
female
N
K
N
K
2800-3000 cm⁻¹/ 1658 cm⁻¹
2924 cm⁻¹ / 1658 cm⁻¹
2924 cm⁻¹/ 2955 cm⁻¹
FTIR spectroscopy/imaging
Statistical analysis
Female and male offspring
2800-3000 cm⁻¹/ 1658 cm⁻¹
Creatine/cholesterol (Cr/CHL) inclusions
Raman intensity
Wavenumber [cm⁻¹]
CHOLESTEROL
CREATINE
Different stages of offspring brain development

Supplementary materials

Fourier Transform Infrared Imaging Supported by Raman Spectroscopy Reveals Biochemical Changes in Adult Rat Brains Following Prenatal Exposure to a Ketogenic Diet

Marzena Rugiel[1#], Zuzanna Setkowicz [2#], Agnieszka Drozdz[1], Aleksandra Wilk[1], Zofia Brylowska[1], Joanna Chwiej[1*]

[1]AGH University of Krakow, Faculty of Physics and Applied Computer Science, al. Mickiewicza 30, 30-059 Krakow, Poland

[2]Jagiellonian University, Institute of Zoology and Biomedical Research, ul. Gronostajowa 9, 30-387 Krakow, Poland

# Contributed equally

* Corresponding author:

jchwiej@agh.edu.pl

Table S1 The composition of a normal and ketogenic diet

Nutrient	**Normal diet***	**Ketogenic diet***
Lipids	10	79
Carbohydrates	60	1
Proteins	30	8
Others	0	12
*The content of main nutrients (% of the dry mass) of normal and ketogenic diet given by the manufacturer.		
Element	**Normal diet****	**Ketogenic diet****
P	11500 (530)	8900 (1700)
S	5080 (650)	2290 (560)
K	13800 (24000)	13500 (2300)
Ca	17900 (2800)	14000 (3000)
Fe	540 (160)	330 (220)
Cu	20.1 (5.9)	4.8 (1.6)
Zn	137 (36)	147 (14)
Se	0.68 (0.29)	< DL
** Median of element concentrations [µg/g] with interquartile ranges (Q3-Q1, given in brackets), obtained from TXRF measurements of 6 samples (200 mg) taken from initially homogenized fodder.		

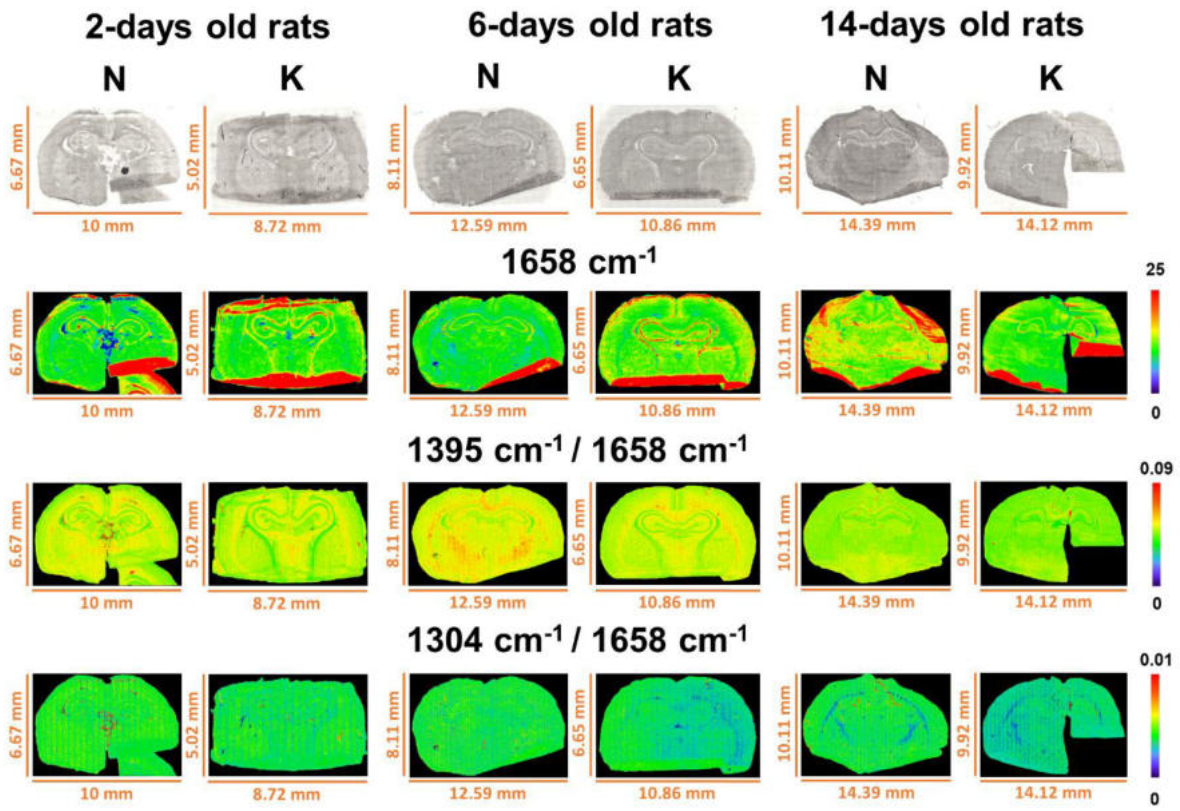

Fig. S1 Representative chemical maps illustrating the spatial distribution of the integrated area of the amide I band and the relative integrated areas of the IR bands at 1395 and 1304 cm^{-1}, normalized to the amide I band. The maps were obtained for brain slices taken from female rats aged 2, 6, and 14 days, prenatally exposed to either a ketogenic (K) or a normal (N) diet. The color scale represents intensity of the amide I band and band-area ratios relative to the amide I band, with black indicating the minimum value and red indicating the maximum value. Microscopic images of the analyzed tissues are shown in the top row.

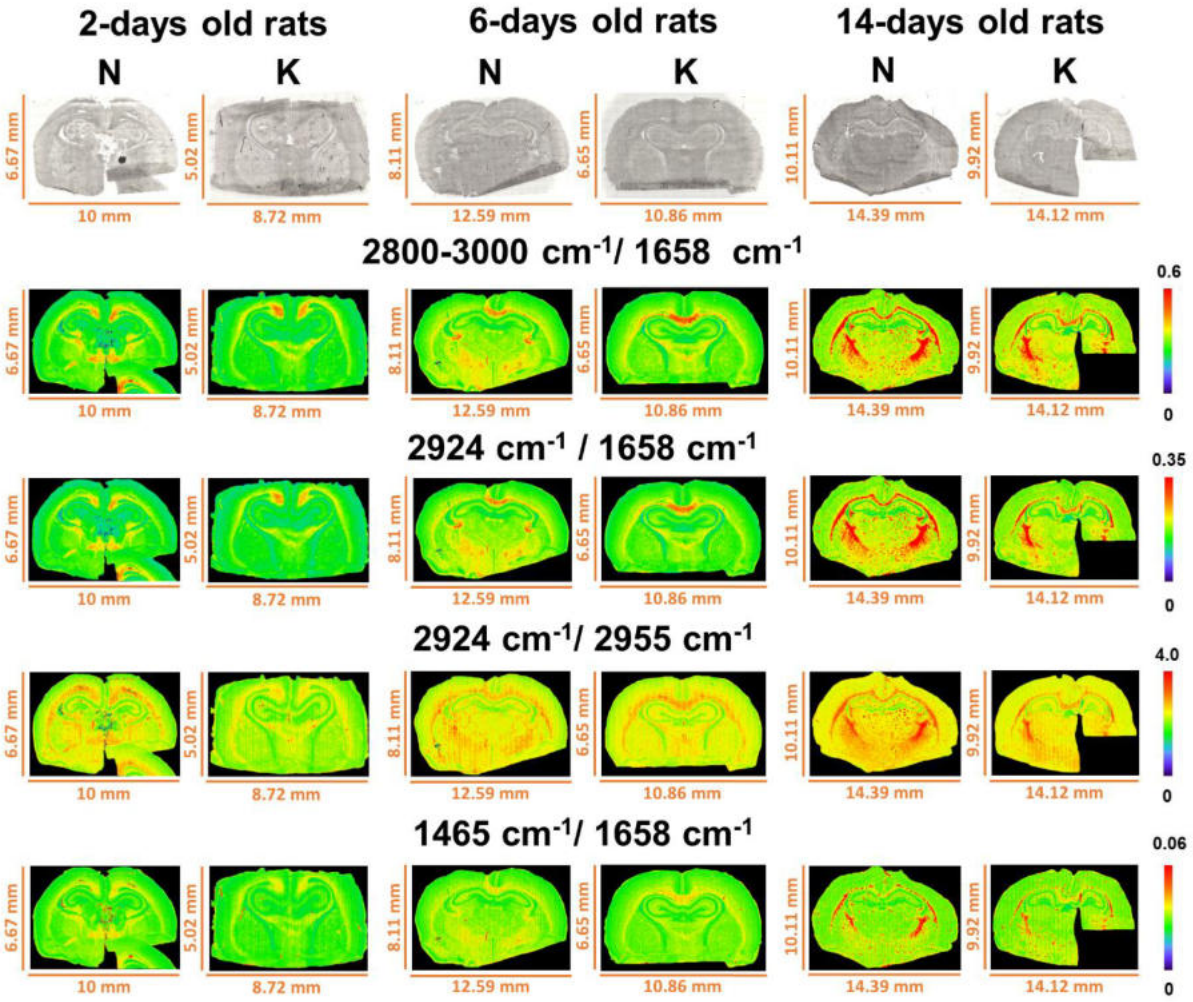

Fig. S2 Representative chemical maps illustrating the spatial distributions of the relative integrated areas of the IR bands at 2924 and 1465 cm^{-1} as well as the lipid massif region (2800-3000 cm^{-1}), normalized to the amide I band. Additionally, the maps showing the ratio of the bands at 2924 and 2955 cm^{-1} are presented. The maps were obtained for brain slices taken from female rats aged 2, 6, and 14 days, prenatally exposed to either a ketogenic (K) or a normal (N) diet. The color scale represents band-area ratios relative to the amide I band, with black indicating the minimum value and red indicating the maximum value. Microscopic images of the analyzed tissues are shown in the top row.

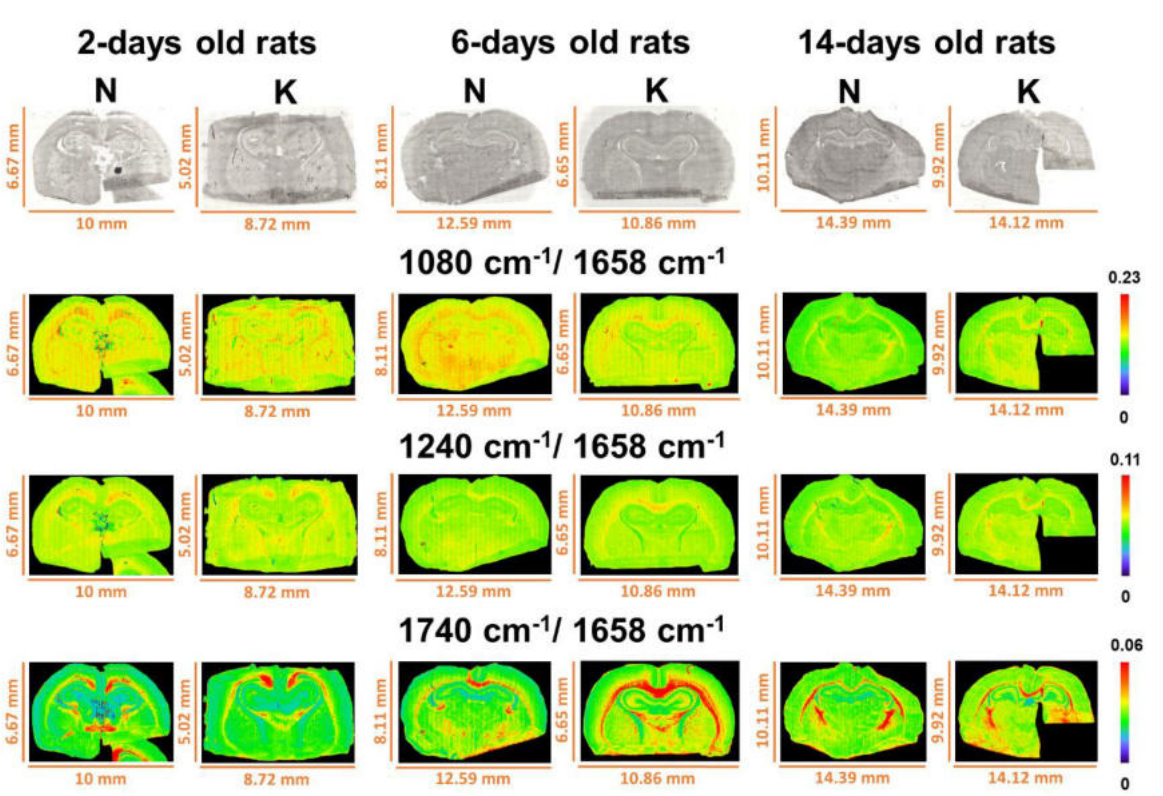

Fig. S3 Representative chemical maps illustrating the spatial distributions of the relative integrated areas of the IR bands at 1080, 1240 and 1740 cm^{-1}, normalized to the amide I band. The maps were obtained for brain slices taken from female rats aged 2, 6 and 14 days, prenatally exposed to either a ketogenic (K) or a normal (N) diet. The color scale represents band-area ratios relative to the amide I band, with black indicating the minimum value and red indicating the maximum value. Microscopic images of the analyzed tissues are shown in the top row.

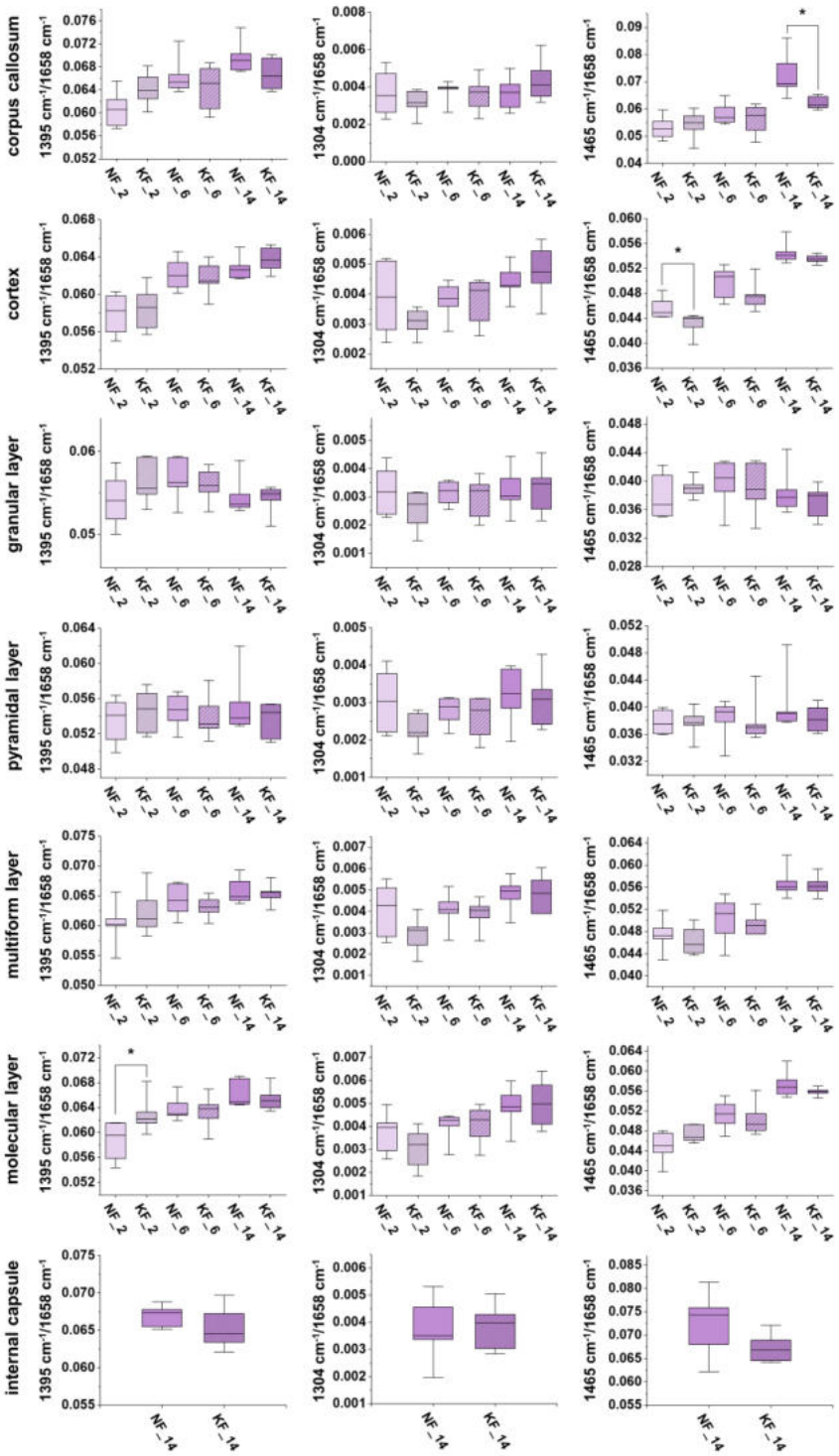

Fig. S4 Box-and-whisker plots illustrating the distribution of FTIR-derived biochemical parameters (ratios of integrated band areas: 1395 cm^{-1}/1658 cm^{-1}, 1304 cm^{-1}/1658 cm^{-1} and 1465 cm^{-1}/1658 cm^{-1}) across selected brain regions: the corpus callosum, cerebral cortex, internal capsule, and four hippocampal layers (granular, pyramidal, multiform, and molecular) for both experimental (K) and control (N) rat groups, including females (F), at three postnatal developmental stages (2, 6 and 14 days of age). Statistically significant differences between experimental and corresponding control groups (Mann-Whitney *U* test, $p < 0.05$) are indicated by an asterisk (*).

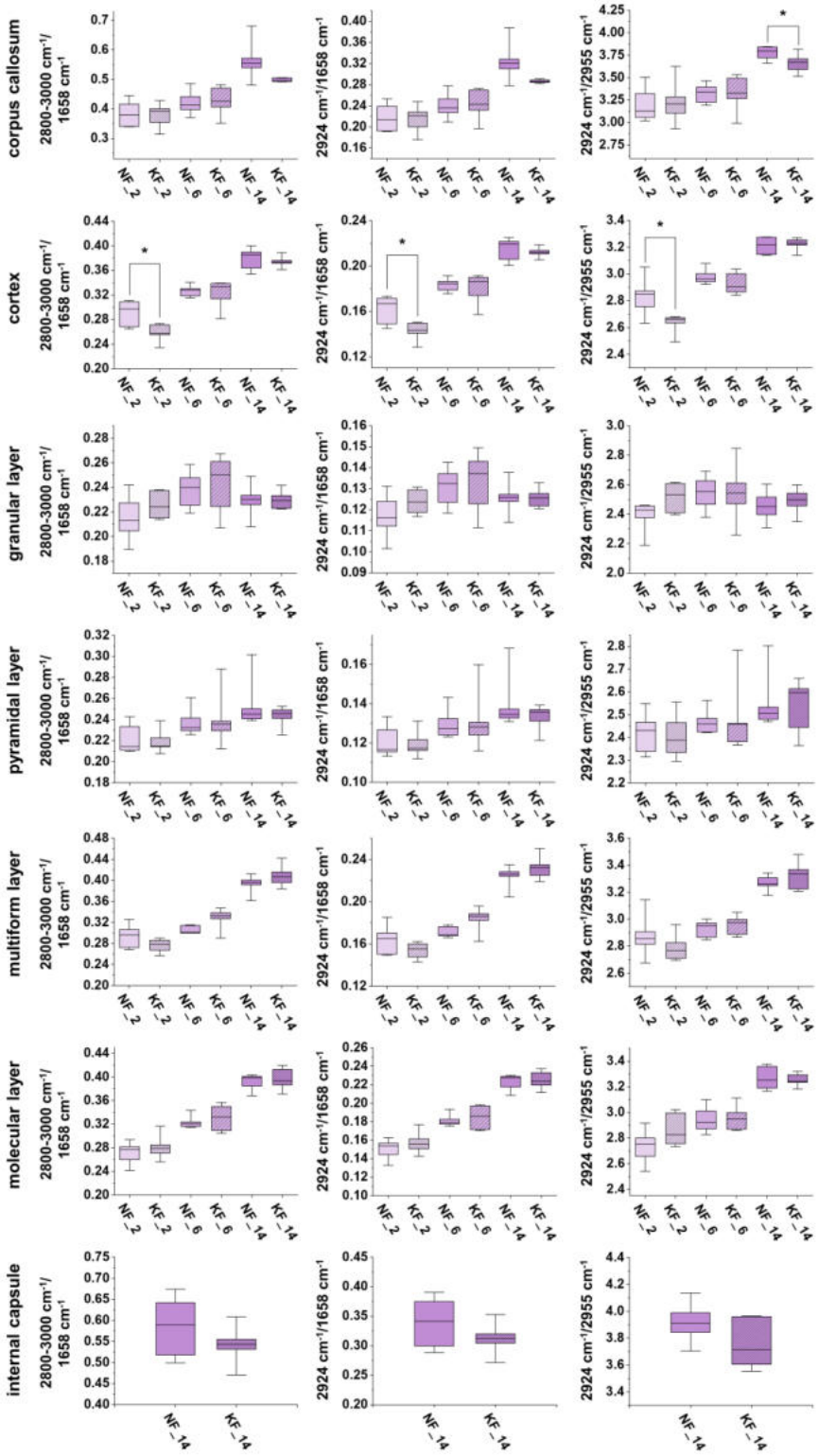

Fig. S5 Box-and-whisker plots illustrating the distribution of FTIR-derived biochemical parameters (ratios of integrated band areas: 2800-3000 cm^{-1}/1658 cm^{-1}, 2924 cm^{-1}/1658 cm^{-1} and 2924 cm^{-1}/2955 cm^{-1}) across selected brain regions: the corpus callosum, cerebral cortex, internal capsule, and four hippocampal layers (granular, pyramidal, multiform, and molecular) for both experimental (K) and control (N) rat groups, including females (F), at three postnatal developmental stages (2, 6 and 14 days of age). Statistically significant differences between experimental and corresponding control groups (Mann–Whitney *U* test, $p < 0.05$) are indicated by an asterisk (*).

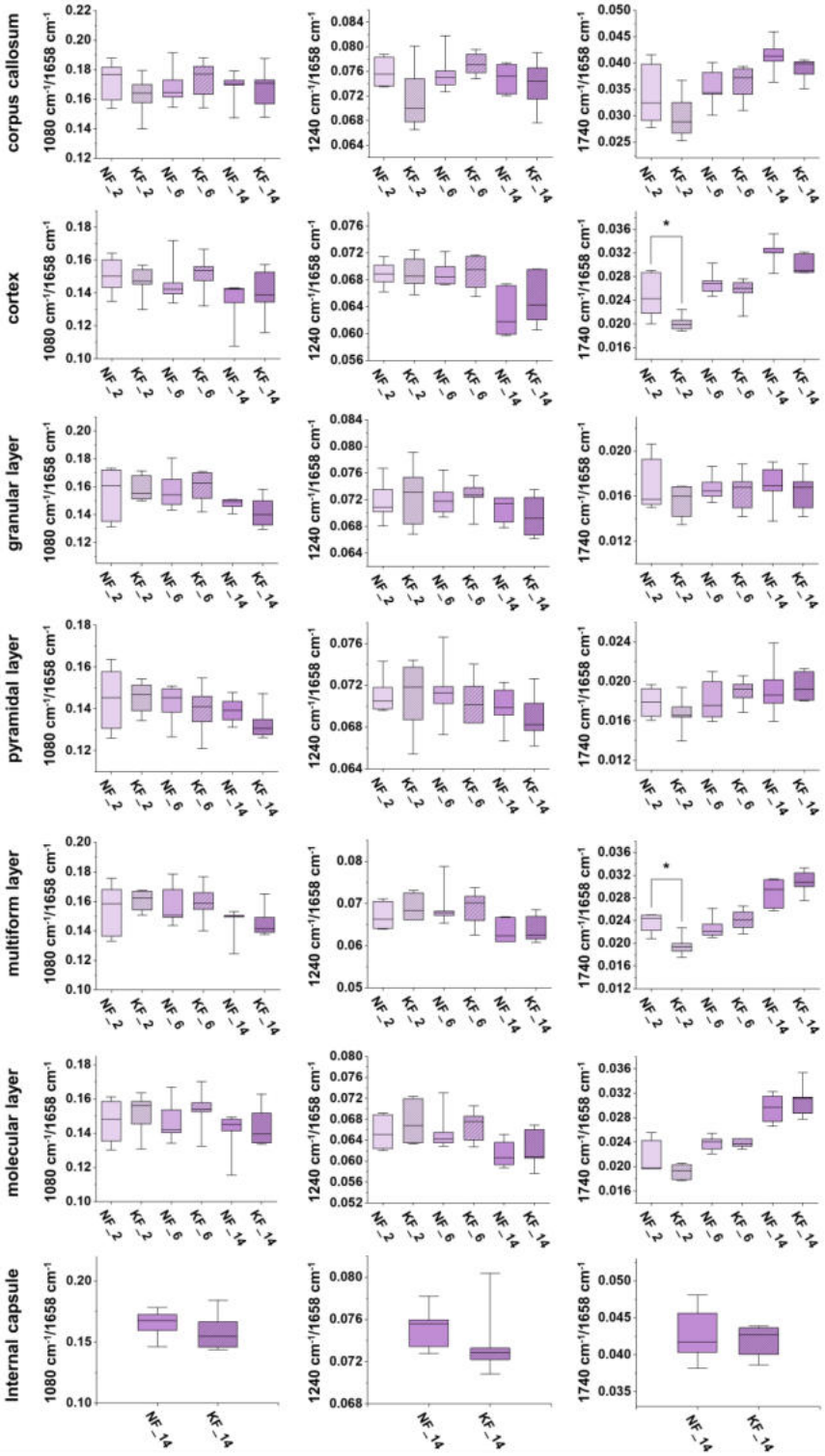

Fig. S6 Box-and-whisker plots illustrating the distribution of FTIR-derived biochemical parameters (ratios of integrated band areas: 1080 cm^{-1}/1658 cm^{-1}, 1240 cm^{-1}/1658 cm^{-1} and 1740 cm^{-1}/1658 cm^{-1}) across selected brain regions: the corpus callosum, cerebral cortex, internal capsule, and four hippocampal layers (granular, pyramidal, multiform, and molecular) for both experimental (K) and control (N) rat groups, including females (F), at three postnatal developmental stages (2, 6 and 14 days of age). Statistically significant differences between experimental and corresponding control groups (Mann-Whitney *U* test, $p < 0.05$) are indicated by an asterisk (*).